Dégradation chimique et mécanique de l'alumine en phase aqueuse : mécanisme et inhibition en conditions ambiantes et hydrothermales

Jane Abi Aad

Université Pierre et Marie Curie

ED 397

Laboratoire de Réactivité de Surface

UMR 7197 CNRS

Dégradation chimique et mécanique de l'alumine en phase aqueuse : mécanisme et inhibition en conditions ambiantes et hydrothermales

par Jane Abi Aad

Thèse de doctorat de Physique et Chimie des Matériaux

Dirigée par M. Xavier Carrier et M. Éric Marceau

Soutenance prévue le 4 novembre 2016

Devant un jury composé de :

M. Sébastien Royer, Professeur, Université Lille 1	**Rapporteur**
M. Jean-François Hochepied, Chargé de Recherche, Mines Paris Tech	**Rapporteur**
Mme Corinne Chanéac, Professeur, UPMC	**Examinatrice**
M. Didier Tichit, Directeur de Recherche, ENS de Montpellier	**Examinateur**
M. Xavier Carrier, Professeur, UPMC,	**Directeur de thèse**
M. Éric Marceau, Maître de Conférences, Université de Lille 1	**Directeur de thèse**
M. Fabrice Diehl, Ingénieur de Recherche, IFPEN	**Examinateur**
M. Mathieu Michau, Ingénieur de Recherche, IFPEN	**Examinateur**

Remerciements

Les remerciements sont rédigés à la fin des trois ans de recherche. C'est à ce moment-là qu'on se rend compte de l'importance des gens qui nous entouraient au cours de cette période et sans qui, l'élaboration de ce manuscrit n'aurait pas été possible. Je souhaite profiter de cette opportunité pour leur adresser toutes ma reconnaissance.

Je tiens dans un premier temps à remercier mes encadrants de thèse, qui se sont investis énormément dans ce projet. Leurs compétences scientifiques et leur réactivité ont été précieuses.

Merci à Xavier Carrier pour sa bonne humeur et son optimisme qu'il a réussi à maintenir tout au long de mon travail. J'ai apprécié profondément sa patience et ses compétences pédagogiques qui ont poussé plus loin ma curiosité scientifique. Merci de m'avoir responsabilisée sur l'achat de l'appareil de test, ceci a ajouté plus d'expériences sur mon profil. Merci pour son dévouement, son soutien au cours de ces trois ans de thèse et ses encouragements qui m'ont aidée à avancer, même durant les périodes les plus dures.

Je remercie Éric Marceau pour sa rigueur, sa disponibilité malgré la distance, et pour le partage de ses idées. J'ai réussi à travers ses qualités à améliorer mes compétences organisationnelles, à développer ma prise de recul, et à enrichir mes connaissances scientifiques. Je lui suis très reconnaissante de m'avoir tirée vers le haut en m'aidant à combler mes lacunes et en s'investissant pour moi, en plus du projet.

Je remercie mes encadrants à l'IFPEN, Fabrice Diehl pour sa réactivité, son aide inconditionnelle et ses encouragements durant les périodes où j'en ai eu besoin (avant les congrès, avant la rédaction de la thèse et des articles…). Merci à Mathieu Michau pour ses conseils sur mon projet professionnel, et en particulier pour le mot « bravo » qui remonte le moral et aide à avancer. Merci à M. Philippe Courty pour le partage de ses connaissances bibliographiques ainsi que pour ses conseils scientifiques et son expérience intéressante.

Merci bien sûr à IFPEN, particulièrement à Denis Guillaume, directeur de la division Catalyse et Séparation, et Tivadar Cseri, chef du groupe Catalyse par les Métaux et Solides Acido-Basiques, de m'avoir accueillie et soutenue financièrement pendant cette thèse. Merci également à Claire-Marie Pradier, directrice du LRS jusqu'en septembre 2014, et Hélène Pernot, qui lui a succédé à ce poste, pour m'avoir accueillie au sein du Laboratoire de Réactivité de Surface (LRS).

Je tiens à remercier Sébastien Royer et Jean-François Hochepied pour avoir accepté d'être les rapporteurs de cette thèse et à Corinne Chanéac et Didier Tichit, pour avoir accepté de juger ce travail.

J'adresse mes plus sincères remerciements à Maya Boutros qui est devenue une amie très précieuse. Je n'aurai jamais pu effectuer cette expérience sans son dévouement professionnel et son aide.

Merci à Adrien Berliet pour son implication dans ce projet, son investissement, sa disponibilité, ses conseils scientifiques et techniques. Merci pour m'avoir formée sur l'utilisation de l'autoclave ainsi que pour son effort sur les autres manips qu'on a mises au point ensemble. Merci à Etienne Girel qui a préparé les solides stabilisés par le silicium.

Merci à Antoine Fécant et Sylvie Maury pour leurs sourires, leurs encouragements et les bons moments qu'on a passés à Tromsø. Une pensée à tous mes collègues à l'IFPEN, en particulier à Nadia, pour sa gentillesse inestimable.

Merci à toute l'équipe au laboratoire LRS :

- Vincent Losinho, pour son aide à gérer l'autoclave durant le déménagement. Merci de m'avoir prêté tes outils et d'être intervenu sur l'appareil avant et après le déplacement,
- Cyril Domingos, de m'avoir aidée à monter en compétences sur certaines techniques de caractérisation,
- Sandra Casale, pour la partie microscopie et pour son sourire qui transmet des ondes positives,
- Annie Mettendorff, Sabine Meme et Sonia Mbarek pour leur gentillesse et leur bienveillance,
- Junior et sa famille pour leur gentillesse, leur sourire, les déjeuners chez eux et surtout pour Léonie,
- Tous les permanents, qui ont réussi à créer une belle ambiance au laboratoire.

Merci à tous mes collègues, thésards, post-docs ou stagiaires. Une pensée particulière à Camella, Manel, Chyrine, Tesnim, Zhao, Xiaojing, Antoine H., Claire, Kim, Laetitia, Olfa, Marie Nour, Cédric, Noémie, Miao, Mariem (et à tous ceux que j'ai oubliés). Merci à Marie pour les pauses café et pour avoir toujours demandé de mes nouvelles. Marc, un des meilleurs collègues de bureau souvent absents, pour m'avoir toujours écoutée et pour être si attentionné. Sarah D.G. pour son énergie, son temps, ses petites pensées (même le soir ou le WE), et pour la bonne ambiance qu'elle crée partout ! Et un énorme merci à Marwa et Sarah, pour leur amitié ! Merci pour les moments inoubliables qu'on a vécus ensemble ainsi que pour les sourires et les rires qu'on a partagés. Sarah, merci pour avoir pris des risques en t'aventurant avec moi (Catacombes, Karmeliet, coiffeur…), tu es vraiment ma blonde jumelle ! Et Marwa, merci pour m'avoir écoutée et supportée quand je te racontais les plus petits détails de ma vie, je suis sûre que ça va te manquer !

J'adresse un énorme merci à mes amis que j'ai rencontrés à Paris et qui m'ont aidé. J'en garde de très beaux souvenirs. Je pense aussi à deux amies d'enfance, Nisrine et Nancy, qui m'ont soutenue et qui étaient toujours à l'écoute.

Ces remerciements ne seraient pas complets sans une pensée pour Kaïs. Merci pour ton soutien, ton aide et tes conseils. Merci pour avoir cru en moi (et de continuer à le faire), pour m'avoir supportée durant les mauvaises périodes et pour avoir partagé les meilleurs moments avec moi. Merci de me porter bonheur !

Mes dernières pensées iront vers ma famille. Je remercie tout d'abord ma sœur Chimène pour sa patience, son sourire et sa présence toujours malgré la distance. Mon frère Charbel, pour la fierté qu'il me porte et pour tous ses messages pour prendre de mes nouvelles. Et enfin pour ma mère Dalal et mon père Antoine pour TOUT ! Les mots me manquent et ne seront jamais suffisants pour exprimer ma reconnaissance et mes remerciements pour eux. J'espère que je serai toujours à la hauteur, auprès d'eux et qu'ils seront toujours fiers de moi.

Merci à ce merveilleux pays qu'est la France ! Merci Paris pour m'aider à oublier les moments difficiles traversés pendant la thèse et pour me donner la chance de profiter pleinement de la vie !

Sommaire

Introduction générale 1

I. Etude Bibliographique 11

I.1. (Oxy)hydroxydes d'aluminium 11

I.1.1. Nature chimique des (oxy)hydroxydes d'aluminium 11

I.1.2. Structure des (oxy)hydroxydes d'aluminium 12

I.1.3. Conditions de formation des (oxy)hydroxydes d'aluminium en solution 14

I.1.4. Conclusion 16

I.2. Transformations des alumines en présence d'eau (température ambiante et température élevée) 17

I.2.1. Rappel sur les oxydes d'aluminium 17

I.2.2. Effet du pH à température ambiante 20

I.2.3. Effet de la température 26

I.2.4. Influence du temps de traitement à température constante 29

I.2.5. Effet de l'hydratation sur la texture et la structure de surface 32

I.2.6. Mécanisme de formation 33

I.2.7. Conclusion 34

I.3. Influence des espèces supportées sur la transformation de l'alumine dans l'eau 35

I.3.1. Métaux supportés 35

I.3.2. Introduction d'hétéroatomes sur le support 38

I.3.3. Molécules organiques 44

I.3.4. Conclusion 47

I.4. Conclusion et démarche de la thèse 48

I.5. Références 50

II. Chemical weathering and physical attrition of alumina in aqueous suspension at ambient pressure: a mechanistic study. 61

II.1. Préambule 61

II.2. Introduction 63

II.3. Materials and methods 65

II.4. Results 68

II.4.1. Identification of the hydration products 68

II.4.2. pH evolution 69

II.4.3. Liquid-phase aluminum concentration 70

II.4.4. Evolution and location of hydroxide phases 73

II.4.5. Formation of hydroxide polymorphs from γ-Al_2O_3 as a function of time 76

II.4.6. Alumina polymorphs hydration 79

II.5. Conclusion 81

II.6. References 83

II.7. Supplementary information 87

II.7.1. Quantitative analysis by TGA and XRD 90

II.8. Annex – Acidic medium 97

II.8.1. Nitric acid 97

II.8.2. Acetic acid 98

II.8.3. Conclusion 103

II.8.4. References 103

III. Chemical weathering of alumina in aqueous phase in hydrothermal conditions and influence of organic additives 109

III.A. Chemical weathering of alumina in aqueous suspension in hydrothermal conditions... 109

III.A.1. Introduction 109

III.A.2. Materials and methods 110

III.A.3. Hydrothermal ageing of alumina polymorphs 112

III.A.4. Mechanism of hydration in hydrothermal conditions for γ-Al_2O_3 115

III.A.5. Conclusion 123

III.B. Influence of organic additives on alumina chemical weathering in aqueous phase under hydrothermal conditions 125

III.B.1. Introduction 125

III.B.2. Effect of organic molecules on boehmite formation 126

III.B.3. Interaction of sorbitol with γ-Al_2O_3 upon hydrothermal treatment 129

III.B.4. Evidence for a dissolution step and role of polyols 134

III.B.5. Conclusion 143

III.C. Conclusion 145

III.D. Annex to chapter III – part A 147

III.E. References 150

IV. Inhibition of chemical weathering of γ-Al_2O_3 by inorganic dopants in hydrothermal conditions 157

IV.1. Preamble 157

IV.2. Introduction 160

IV.3. Results and Discussion 161

IV.3.1. Effect of dopants and calcination temperature on chemical weathering of γ-Al_2O_3–isomolar systems 163

IV.3.2. Effect of calcination treatment: spinel and hydrotalcite formation 165
IV.3.3. Kinetic of boehmite formation 169
IV.3.4. Effect of calcination and weathering on specific surface area 170
IV.3.5. Effect of specific surface area on chemical weathering of γ-Al_2O_3 172
IV.3.6. Role of dopants – surface study 176
IV.3.7. Effect of dopant loadings on boehmite formation 181
IV.3.8. Role of dopants - Liquid-state aluminum concentration 182
IV.4. Conclusions 184
IV.5. Experimental section 185
IV.5.1. Sample preparation 185
IV.5.2. Ageing tests in hydrothermal conditions 186
IV.5.3. Characterization techniques 186
IV.6. Acknowledgments 187
IV.7. Keywords 187
IV.8. References 187
IV.9. Supplementary information 193
IV.9.1. Qualitative analysis by XRD and TGA 193
IV.9.2. Additional figures and tables mentioned in the text 197
IV.9.3. References 201
Conclusion générale 205

Introduction générale

Introduction générale

Les alumines de transition, de formule chimique Al_2O_3, et particulièrement l'une d'entre elles, l'alumine γ, sont largement employées comme catalyseurs ou comme supports de catalyseurs hétérogènes dans l'industrie chimique et pétrolière. L'alumine γ y est couramment utilisée en raison, notamment, de sa surface spécifique élevée, de sa grande stabilité thermique, de son excellente résistance mécanique et de son coût de production modéré.[1] Parmi ces réactions, certaines se déroulent dans des conditions relativement agressives pour des oxydes métalliques,[2–4] notamment en présence d'eau à haute température (>100°C). Nous pouvons citer à titre d'exemple les réactions de transformation des molécules biosourcées en conditions hydrothermales, comme le reformage de matériaux lignocellulosiques pour la production de H_2, pour lesquelles l'eau constitue le solvant,[3–5] ou encore les réactions de synthèse d'hydrocarbures sur catalyseurs au fer ou au cobalt supporté sur alumine, telle que la réaction de Fischer-Tropsch (FT), pour laquelle l'eau constitue un produit de réaction comme le montre l'équation suivante:

$$(2n+1)\ H_2 + n\ CO \rightarrow C_nH_{(2n+2)} + n\ H_2O$$

Le procédé FT, découvert en Allemagne en 1923 par Frantz Fischer et Hans Tropsch, regroupe un ensemble de réactions catalytiques permettant d'obtenir une large gamme de molécules hydrocarbonées (paraffines, oléfines, dérivés oxygénés...) à partir du gaz de synthèse CO/H_2[6,7] conduisant à des distillats moyens alternatifs à ceux produits par raffinage pétrolier.[7,8] En outre, un des intérêts majeurs de ce procédé est que le gaz de synthèse peut être produit à partir d'une matière première variée, gaz naturel, charbon ou biomasse.[9] Ce procédé a suscité un regain d'intérêt ces dernières décennies car il devient un procédé économiquement viable par rapport au raffinage du pétrole pour la production d'hydrocarbures, et il fournit des produits propres (sans soufre ni molécules aromatiques) et hautement valorisables.

En conditions FT, la température et la pression totale élevées (~ 200-230°C, ~ 20 bar), la pression partielle de l'eau (~ 4,5 bar) ainsi que la présence de faibles quantités de produits oxygénés de type acides carboxyliques, conduisent à une *érosion* (usure chimique) de l'alumine γ,[10] support de la phase catalytiquement active.

Par ailleurs, la synthèse FT, par exemple dans le cas du procédé Gasel® proposé commercialement par Axens et développé par l'IFPEN, est mise en œuvre dans un réacteur slurry à colonne à bulles (SBCR) en présence d'un milieu triphasique : réactifs et produits gazeux, hydrocarbures liquides, catalyseur solide, auxquels on peut ajouter l'eau susceptible de se condenser au sein du catalyseur. Dans ces conditions, la quantité importante de catalyseur par réacteur (plusieurs centaines de tonnes pour une unité de capacité de 30000 barils/jour), la vitesse des particules (supérieure à plusieurs m/s) ainsi que la granulométrie du catalyseur (~20 à 200 microns) sont les facteurs menant à une *attrition* (usure physique) du support du catalyseur liée aux chocs des grains de catalyseur entre eux ou contre le réacteur.

En raison de ces deux phénomènes d'érosion (chimique) et d'attrition (physique), le délitement de l'alumine γ a comme conséquence une baisse d'activité catalytique et une création de fines (de taille de quelques dizaines de nanomètres à quelques microns) qui, entrainées par l'écoulement des effluents, peuvent provoquer le bouchage des filtres du réacteur. Ceci contribue à la diminution des performances du réacteur et à la surconsommation de catalyseur pour maintenir la productivité de l'unité.

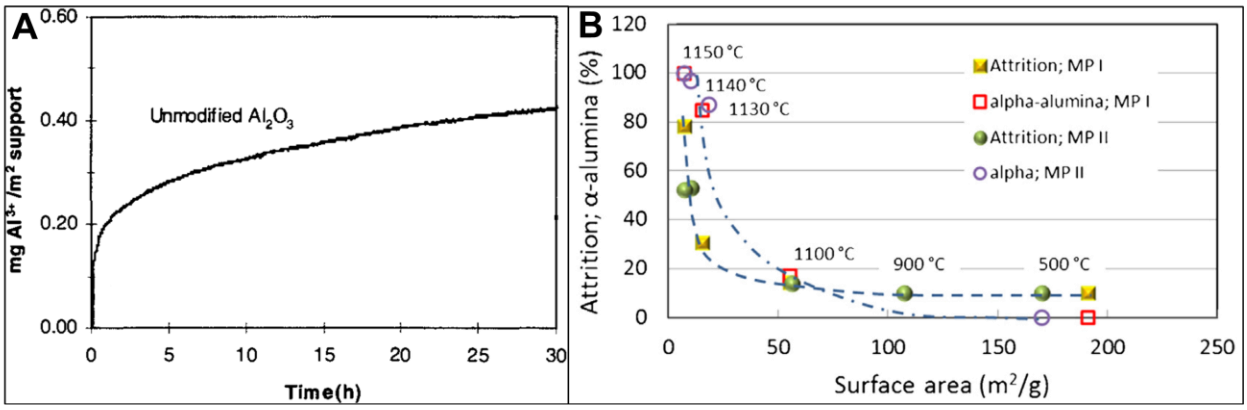

Figure 1. (A) Dissolution de l'alumine γ en fonction du temps[11] et (B) niveau d'attrition (en %) des particules pour deux alumines γ (MPI (en jaune) et MPII (en vert)) calcinées à températures croissantes et contenant des quantités croissantes d'alumine α (rouge et violet) (données obtenues par un équipement de type ASTM modifié pour tester l'attrition[12]).[13] Ces deux tests d'usure chimique et physique respectivement ont été conduits dans des études ayant pour application la synthèse FT.

A titre d'exemple de ces deux phénomènes, la Figure 1-A montre la libération d'aluminium au cours du temps indiquant la dissolution du support, conséquence de l'érosion de l'alumine γ. La Figure 1-B montre, elle, que même l'utilisation d'alumines ayant une résistance mécanique plus élevée, comme l'alumine α, n'est pas suffisante pour éviter l'attrition du support du catalyseur en conditions FT : symboles jaunes (niveau d'attrition pour le premier catalyseur) et verts (niveau d'attrition pour le second catalyseur).[13]

Chimiquement parlant, il est constaté que la dégradation des alumines, dans ces conditions d'exposition à l'eau à température élevée, s'accompagne d'une réaction d'hydratation, conduisant à la formation d'oxyhydroxydes d'aluminium,[10,11] qui induit un changement structural et textural du matériau : $Al_2O_3 + H_2O \rightarrow 2\ Al(OOH)$.

La réaction d'hydratation de l'alumine a été découverte dès 1957 par Tertian et Papée (Péchiney).[14] Elle a ensuite fait l'objet de nombreux travaux parmi lesquels on peut citer le travail de Franck *et al*. en 1984 (IFP),[15] et plus récemment Carrier *et al*. en 2007.[16] Cette transformation des alumines dans l'eau est également connue pour se produire à température ambiante ou sous conditions douces (i.e. pression atmosphérique). La nature des produits issus de cette réaction dépend de plusieurs facteurs, comme le pH et le couple pression/température. A température ambiante elle conduit à des hydroxydes $Al(OH)_3$: $Al_2O_3 + 3\ H_2O \rightarrow 2\ Al(OH)_3$.

Limiter la dégradation de l'alumine en phase aqueuse ne peut se faire que par l'intermédiaire d'une compréhension fondamentale des mécanismes de dégradation évoqués plus haut, dégradation chimique, *érosion* (en anglais *chemical weathering*), et dégradation mécanique, *attrition*. Malgré l'importance de ces problématiques, peu d'études systématiques ont été publiées sur le sujet. Dans un second temps, il convient de définir des stratégies pour inhiber la dégradation de l'alumine et développer, à terme, des supports aluminiques dotés d'une résistance mécanique et chimique accrues sous conditions hydrothermales. La littérature propose des pistes, via le dopage de l'alumine par des ions métalliques et par des hétéroatomes, mais la raison pour laquelle ces dopants stabilisent l'alumine est encore peu abordée.

Le projet de recherche présenté dans ce manuscrit vise donc à expliciter les mécanismes d'hydratation de l'alumine et à rationaliser le rôle des dopants, en identifiant si possible les sites

de surface de l'oxyde où débute le processus de dégradation. Les conditions expérimentales de la réaction FT (température, pression, milieu triphasique), ou encore la présence de mélanges de molécules (réactifs, impuretés) dans les réactions liées à la transformation de la biomasse, rendent complexe la mise en œuvre d'un suivi de la dégradation de l'alumine dans des conditions réelles de réaction. Pour mener à bien cette étude fondamentale, nous serons donc amenés à définir des conditions opératoires modèles, qui permettront de comparer et de découpler l'influence de différents paramètres expérimentaux, et de suivre plus simplement l'évolution du matériau.

Ce présent manuscrit débutera par une étude bibliographique sur les processus d'hydratation de l'alumine. A l'issue de cette étude, nous dégagerons un plan détaillé de la thèse basé sur les différentes conditions opératoires que nous serons amenés à mettre en œuvre.

Références

(1) Euzen, P.; Raybaud, P.; Krokidis, X.; Toulhoat, H.; Le Loarer, J.-L.; Jolivet, J.-P.; Froidefond, C. Alumina. In *Handbook of Porous Solids*; Schüth, F., Kenneth, Weitkamp, J., Eds.; Wiley-VCH Verlag GmbH, 2008; pp 1591–1677.

(2) Wu, K.; Wu, Y.; Chen, Y.; Chen, H.; Wang, J.; Yang, M. Heterogeneous Catalytic Conversion of Biobased Chemicals into Liquid Fuels in the Aqueous Phase. *ChemSusChem* **2016**, *9*, 1355–1385.

(3) Xiong, H.; Pham, H. N.; Datye, A. K. Hydrothermally Stable Heterogeneous Catalysts for Conversion of Biorenewables. *Green Chem.* **2014**, *16*, 4627–4643.

(4) Sádaba, I.; López Granados, M.; Riisager, A.; Taarning, E. Deactivation of Solid Catalysts in Liquid Media: The Case of Leaching of Active Sites in Biomass Conversion Reactions. *Green Chem.* **2015**, *17*, 4133–4145.

(5) Valenzuela, M. B.; Jones, C. W.; Agrawal, P. K. Batch Aqueous-Phase Reforming of Woody Biomass. *Energy Fuels* **2006**, *20*, 1744–1752.

(6) Inderwildi, O. R.; Jenkins, S. J.; King, D. A. Fischer-Tropsch Mechanism Revisited: Alternative Pathways for the Production of Higher Hydrocarbons from Synthesis Gas. *J. Phys. Chem. C* **2008**, *112*, 1305–1307.

(7) Brady, R. C., III; Pettit, R. Mechanism of the Fischer-Tropsch Reaction. The Chain Propagation Step. *J. Am. Chem. Soc.* **1981**, *103*, 1287–1289.

(8) Biloen, P.; Helle, J. N.; Sachtler, W. M. H. Incorporation of Surface Carbon into Hydrocarbons during Fischer-Tropsch Synthesis: Mechanistic Implications. *J. Catal.* **1979**, *58*, 95–107.

(9) Schulz, H. Short History and Present Trends of Fischer–Tropsch Synthesis. *Appl. Catal. A Gen.* **1999**, *186*, 3–12.

(10) Boyer, C.; Gazarian, J.; Lecocq, V.; Maury, S.; Forret, A.; Schweitzer, J. M.; Souchon, V. Development of the Fischer-Tropsch Process: From the Reaction Concept to the Process Book. *Oil Gas Sci. Technol. – Rev. D'IFP Energ. Nouv.* **2016**, *71*, 44.

(11) Van de Loosdrecht, J.; Barradas, S.; Caricato, E. A.; Van Berge, P. J.; Visagie, J. L. Support Modification of Cobalt Based Slurry Phase Fischer-Tropsch Catalysts. *Preprints of Symposia - American Chemical Society, Division of Fuel Chemistry* **2000**, *45*, 587–591.

(12) Rytter, E.; Skagseth, T. H.; Wigum, H.; Sincadu, N. Enhanced Strength of Alumina Based Co Fischer-Tropsch Catalyst. Brevet WO 2005072866, 2005.

(13) Rytter, E.; Holmen, A. On the Support in Cobalt Fischer–Tropsch synthesis—Emphasis on Alumina and Aluminates. *Catal. Today* **2016**, *275*, 11–19.

(14) Tertian, R.; Papee, D. Thermal and Hydrothermal Transformations of Alumina. *J. Chim. Phys. Phys.-Chim. Biol.* **1958**, *55*, 341–353.

(15) Franck, J. P.; Freund, E.; Quéméré, E. Textural and Structural Changes in Transition Alumina Supports. *J. Chem. Soc., Chem. Commun.* **1984**, 629–630.

(16) Carrier, X.; Marceau, E.; Lambert, J.-F.; Che, M. Transformations of γ-Alumina in Aqueous Suspensions. *J. Colloid Interface Sci.* **2007**, *308*, 429–437

Chapitre I

Etude Bibliographique

I. Etude Bibliographique 11

I.1. (Oxy)hydroxydes d'aluminium 11

I.1.1. Nature chimique des (oxy)hydroxydes d'aluminium 11

I.1.2. Structure des (oxy)hydroxydes d'aluminium 12

I.1.3. Conditions de formation des (oxy)hydroxydes d'aluminium en solution 14

I.1.4. Conclusion 16

I.2. Transformations des alumines en présence d'eau (température ambiante et température élevée) 17

I.2.1. Rappel sur les oxydes d'aluminium 17

I.2.2. Effet du pH à température ambiante 20

I.2.3. Effet de la température 26

I.2.4. Influence du temps de traitement à température constante 29

I.2.5. Effet de l'hydratation sur la texture et la structure de surface 32

I.2.6. Mécanisme de formation 33

I.2.7. Conclusion 34

I.3. Influence des espèces supportées sur la transformation de l'alumine dans l'eau 35

I.3.1. Métaux supportés 35

I.3.2. Introduction d'hétéroatomes sur le support 38

I.3.3. Molécules organiques 44

I.3.4. Conclusion 47

I.4. Conclusion et démarche de la thèse 48

I.5. Références 50

I. Etude Bibliographique

Ce chapitre présente un bilan de la littérature sur l'hydratation de l'alumine entrainant la formation d'oxyhydroxydes ou d'hydroxydes d'aluminium. Nous commencerons par décrire la structure de ces composés et leurs conditions de formation en solution. Nous résumerons ensuite ce qui est connu des transformations de l'alumine en milieu aqueux et des paramètres expérimentaux dont dépend l'hydratation. La troisième partie présentera enfin l'influence d'espèces supportées, telles que des phases actives (particules métalliques), des éléments dopants (comme le silicium ou le zirconium) et des molécules organiques (comme le sorbitol ou le glycérol), sur l'hydratation de l'alumine et sur la possibilité d'inhiber ce phénomène.

I.1. (Oxy)hydroxydes d'aluminium

I.1.1. Nature chimique des (oxy)hydroxydes d'aluminium

Les hydroxydes $Al(OH)_3$ et oxy-hydroxydes AlOOH d'aluminium servent à la production d'oxydes d'aluminium utilisés comme supports de catalyseurs, céramiques techniques, condensateurs, substrats pour les circuits intégrés, etc.[1–4] Ils présentent un polymorphisme avec des structures cristallines différentes, et des phases plus ou moins bien cristallisées. Les phases les plus courantes peuvent être classées en deux catégories :

1- Les trihydroxydes d'aluminium dont la formule est $Al(OH)_3$: principalement la gibbsite (γ-$Al(OH)_3$) et la bayerite (α-$Al(OH)_3$).

2- Les oxyhydroxydes d'aluminium dont la formule est AlOOH : la boehmite (γ-AlOOH) et le diaspore (α-AlOOH).

D'autres phases peuvent être ajoutées à cette liste, telle la pseudoboehmite, dont le degré de cristallinité est faible et qui diffère de la boehmite AlOOH par un rapport $n=H_2O/Al_2O_3$ élevé (boehmite : n compris entre 1 et 1,4 ; pseudoboehmite n>1,4).[5] La nordstrandite est un trihydroxyde d'aluminium $Al(OH)_3$ dont la structure est proche de celle de la bayerite et de la gibbsite, mais dont l'abondance est faible.[6,7] Elle est connue pour être le minéral le moins stable parmi les polymorphes d'hydroxydes d'aluminium. Ogorodova *et al.*[8] ont calculé l'enthalpie de transition

nordstrandite → gibbsite à 25°C et ont trouvé une valeur négative (-14,1 ± 3,6 kJ) indiquant une plus grande stabilité de la gibbsite par rapport à la nordstrandite. Des calculs montrant une plus grande solubilité de la bayerite par rapport à la gibbsite indiquent en outre que la gibbsite est le produit le plus stable thermodynamiquement.[9,10]

I.1.2. Structure des (oxy)hydroxydes d'aluminium

Les hydroxydes d'aluminium sont construits à partir de plans structurés AB composés de couches [hydroxyle – aluminium – hydroxyle]. Ces plans forment des feuillets non chargés[5,6] reliés entre eux par des liaisons hydrogène faibles. Les ions aluminium occupent les 2/3 des sites octaédriques au sein des feuillets.

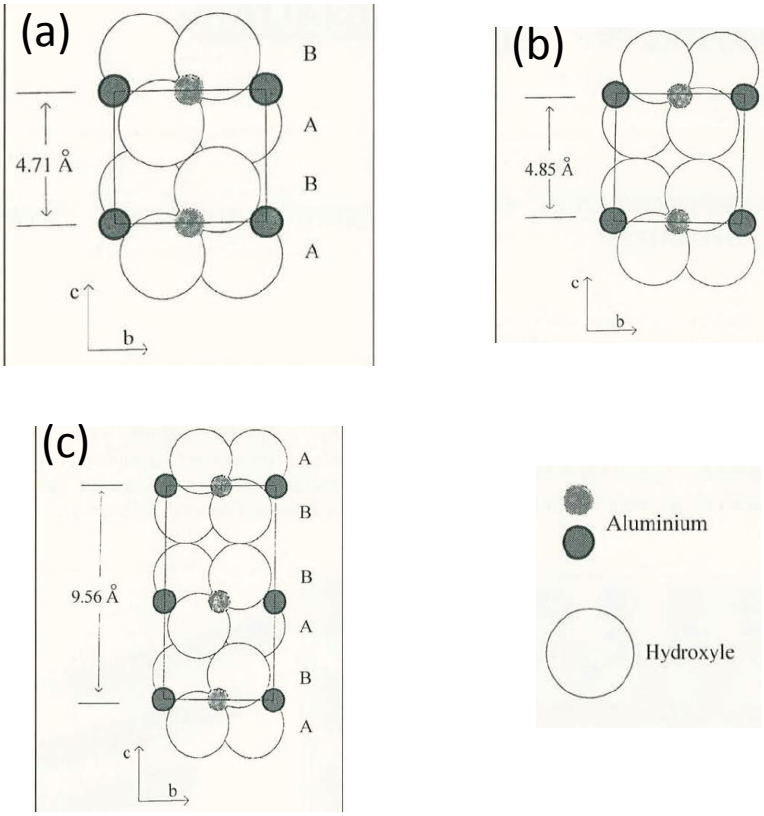

Figure 1. Séquence d'empilement des feuillets pour les différents hydroxydes d'aluminium. (a) bayerite, (b) gibbsite et (c) nordstrandite.[11]

Dans la bayerite, les feuillets empilés sont identiques et exactement superposés (empilement de type AB AB AB) (Figure 1.a). Dans le cas de la gibbsite, les feuillets sont décalés selon un axe 2_1

(AB BA AB BA) (Figure 1.b), ce qui conduit à un empilement des ions OH^- les uns au-dessus des autres et à une augmentation du paramètre de maille c. La structure de la nordstrandite est une combinaison des deux arrangements précédents. Saalfeld et Jarchow[11] ont affiné la structure de cette dernière en indiquant que le type d'empilement des couches s'effectue alternativement d'abord sur le mode AB AB identique à celui de la bayerite puis AB BA identique à celui de la gibbsite, dans une maille de paramètre c double (Figure 1.c).

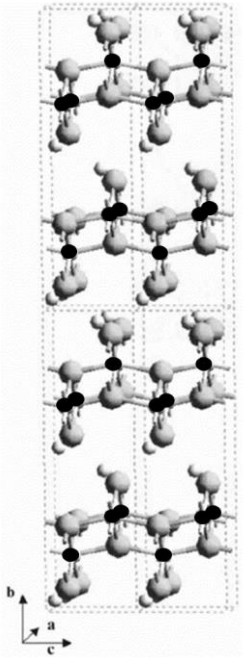

Figure 2. Structure de la boehmite γ-AlOOH. Grandes boules foncées: oxygène, petites boules noires : aluminium et petites boules blanches: hydrogène.[5]

La structure de la boehmite peut être décrite par un arrangement suivant l'axe b de couches ondulées comprenant deux couches Al-O-Al terminées par des groupes OH et entretenant des liaisons hydrogène les unes avec les autres (Figure 2). Chaque atome d'aluminium est localisé dans un environnement octaédrique déformé d'atomes d'oxygène. Ces octaèdres partagent la moitié de leurs arêtes et construisent des chaînes linéaires en respectant la stœchiométrie AlOOH tout au long de l'axe a. Ces chaînes sont reliées le long de l'axe c pour former les couches ondulées. Ceci résulte en une structure approximativement cubique compacte à l'intérieur de chaque couche et moins compacte entre les couches. La structure de la boehmite orthorhombique est formée des couches de même type que celles dans FeOCl.[12,13]

La pseudo-boehmite est une boehmite nanocristalline dans laquelle un excès d'eau est localisé sur les arêtes des nanocristallites. Elle est de plus faible cristallinité.

I.1.3. Conditions de formation des (oxy)hydroxydes d'aluminium en solution

Les hydroxydes d'aluminium sont généralement obtenus en solution aqueuse par précipitation à partir de sels d'aluminium. Cette précipitation et le type de phases produites dépendent de plusieurs facteurs expérimentaux, notamment le pH du milieu et la température.

Par exemple, Jolivet *et al.*[14] ont synthétisé une boehmite par précipitation d'$Al(NO_3)_3$ à un pH compris entre 8 et 11. Le vieillissement dans ce cas est réalisé pendant plus de 2 semaines et à 100°C, ce qui favorise la formation de boehmite (Figure 3-A). Au contraire, pour un vieillissement de 12 h à température ambiante, Du *et al.*[15] ont montré que la bayerite $Al(OH)_3$ est favorisée en conditions basiques (Figure 3-B, pH>7) tandis que les pH neutres favorisent la phase boehmite AlOOH.

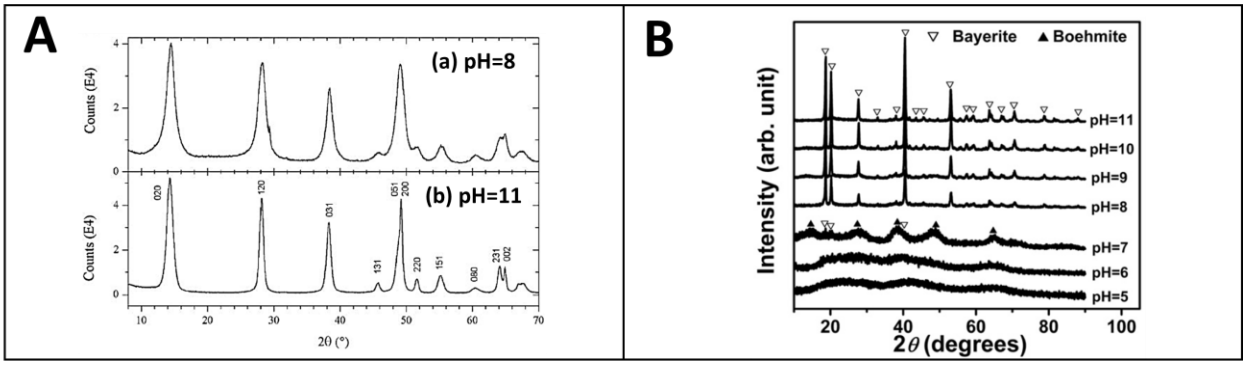

Figure 3. (A) Diffractogrammes de RX des particules de boehmite synthétisées à : (a) pH=8, (b) pH=11 et vieillies durant 2 semaines à 100°C,[14] et (B) Diffractogrammes de RX des hydroxydes d'aluminium précipités à différentes valeurs de pH avec un vieillissement de 12 h à température ambiante.[15]

La présence d'autres phases en fonction du pH est démontrée par Lefèvre *et al.*[16] en étudiant les diffractogrammes X des particules obtenues par une précipitation à pH basique (9,4-10,8, échantillons notés U94 à U108) à 70°C et conduisant majoritairement à la formation de bayerite. La Figure 4 montre que la synthèse conduit aussi à des quantités minimes d'autres phases

cristallines : gibbsite pour les valeurs de pH les plus basses et nordstrandite pour les valeurs de pH supérieures à 10.

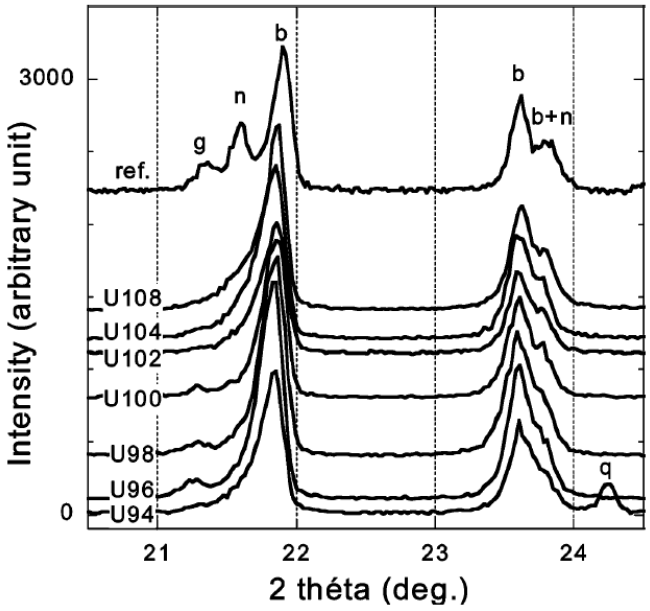

Figure 4. Diffractogrammes de rayons X des solides obtenus par précipitation à 70°C pour différentes valeurs de pH (9,4-10,8, i.e. U94 à U108). L'échantillon U94 est mélangé avec du quartz comme référence interne (q). Les diffractogrammes sont comparés à un diffractogramme de référence formé d'un mélange de gibbsite (g), nordstrandite (n) et bayerite (b).[16]

Ces résultats ont été vérifiés dans la littérature [12,13] et résumés dans la Figure 5 par Euzen et al.[5] Cette figure montre que la précipitation à des températures inférieures à 100°C peut conduire, suivant le pH du milieu, aux hydroxydes d'aluminium suivants: gibbsite si le pH est inférieur à 7, pseudoboehmite nanocristalline (1- 2 nm) si le pH est compris entre 7 et 9, bayerite si le pH est supérieur à 9. A des températures plus élevées (supérieures à 100ºC) il n'y a que la phase boehmite hautement cristallisée qui est formée quelle que soit la valeur de pH. La nordstrandite, qui est rarement rapportée dans la littérature, a été synthétisée par quelques auteurs dans des conditions proches de celles de formation de la bayerite[17] ou même encore dans des milieux plus basiques (pH>13).[18]

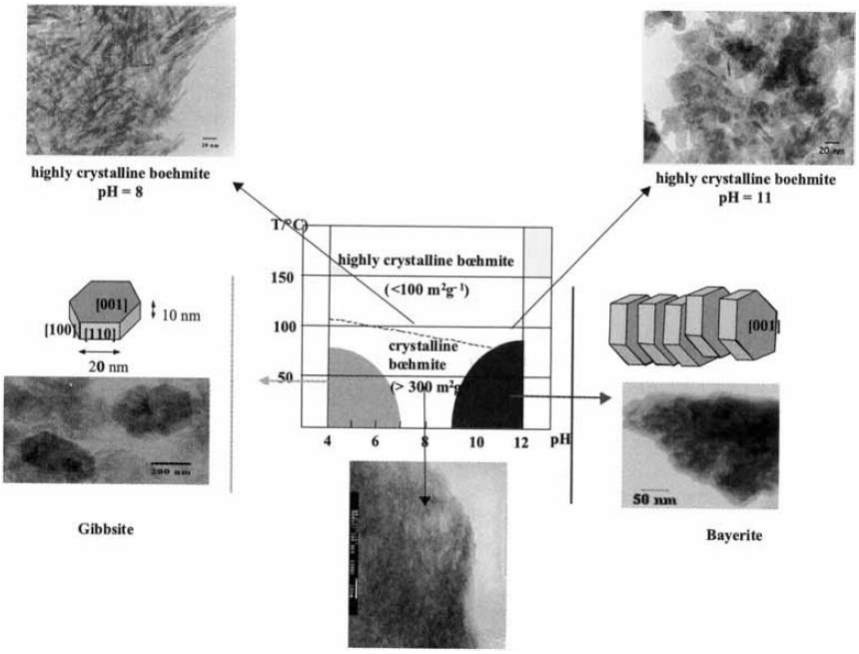

Figure 5. Diagramme de phase pH-température des (oxy)hydroxydes d'aluminium.[5]

I.1.4. Conclusion

Les trois polymorphes d'hydroxydes d'aluminium : bayerite, gibbsite et nordstrandite sont constitués d'octaèdres $[Al(OH)_6]$ agencés en feuillets dont l'empilement varie : empilement de type (AB AB AB) pour la bayerite, (AB BA AB BA) pour la gibbsite tandis que la nordstrandite est une combinaison de ces deux empilements.

La boehmite, oxyhydroxyde de formule AlOOH, est formée par des doubles couches Al-O-Al ondulées terminées par des groupes OH et liées par des liaisons hydrogène.

La stabilité thermodynamique relativement élevée pour la gibbsite comparée à la bayerite n'est pas le facteur déterminant la nature des phases qui précipitent en solution. La nature des hydroxydes et des oxyhydroxydes d'aluminium précipités est influencée principalement par le pH et la température. En dessous de 100°C, un pH acide favorise plutôt la formation de gibbsite et un pH basique favorise la bayerite. A température plus élevée (au-dessus de 100°C) la formation de boehmite hautement cristallisée est favorisée.

La section suivante explorera la transformation des alumines en présence d'eau sous différentes conditions expérimentales.

I.2. Transformations des alumines en présence d'eau (température ambiante et température élevée)

De nombreuses études de la littérature[9,19–28] ont montré que les alumines, en présence d'eau liquide, peuvent subir une transformation menant à la formation de phases hydroxydes et/ou oxyhydroxydes d'aluminium. Nous nommerons ces transformations "hydratation" au sens large, sans préjuger du mécanisme de formation de ces phases (hydratation de surface, dissolution-reprécipitation, dissolution/croissance…) puisque ce dernier n'est pas connu avec précision et qu'il est peu discuté dans la littérature. En présence d'alumine, la nature des phases hydroxydes et/ou oxyhydroxydes, leur structure, leur morphologie et la cinétique de leur formation dépendent de différents facteurs, comme le pH, la température et le temps de vieillissement. Nous détaillerons ces paramètres dans la suite de ce chapitre.

I.2.1. Rappel sur les oxydes d'aluminium

L'alumine la plus concernée par les études de la littérature est l'alumine gamma dont les surfaces spécifiques varient entre 150 et 450 m²/g. Néanmoins, l'alumine delta (dont les surfaces spécifiques sont plus faibles, 100-150 m²/g) a aussi été étudiée.[20] En guise d'introduction à cette partie, un résumé sur les caractéristiques des principales formes d'alumines va être tout d'abord présenté.

L'alumine existe sous plusieurs polymorphes, depuis les alumines de transition de structure cubique, quadratique ou monoclinique, métastables, qui existent sur différentes gammes de température, jusqu'à la forme stable à haute température, le corindon α-Al_2O_3 de structure hexagonale.[5,6,17] Les alumines de transition sont obtenues par des traitements thermiques à différentes températures, à partir des hydroxydes (gibbsite, bayerite) ou oxyhydroxydes (boehmite, diaspore) d'aluminium. La structure et la morphologie de ces alumines dépendent du précurseur utilisé. Sept alumines de transition existent et sont identifiées par des lettres grecques : γ, δ, θ, κ, χ, η et ρ. Le diagramme de filiation est présenté dans la Figure 6.[5]

L'alumine γ est produite par déshydratation de la boehmite dans la gamme de température 400-700°C. L'alumine δ est produite à partir de l'alumine gamma par calcination dans une gamme de température de 800-950°C. L'alumine θ peut être formée à 950-1100°C selon deux voies : (a) par déshydratation de boehmite selon la filiation γ → δ → θ ou (b) par déshydratation de bayerite selon la filiation η → θ (Figure 6).

Les caractéristiques principales de la transition γ → δ → θ → α sont présentées sur la Figure 7. La filiation γ → δ → θ évolue sous forme d'un frittage progressif de nature textural. En effet, l'empilement cubique compact des ions oxygène de l'alumine γ est préservé jusqu'à l'alumine θ en raison de la nature topotactique de la transformation. La migration des ions aluminium vers un arrangement plus régulier et la déshydroxylation progressive sont les deux forces motrices de cette évolution vers l'alumine θ quasi déshydroxylée. Le nombre des lacunes cationiques diminue quand l'occupation des sites tétraédriques augmente au détriment des sites octaédriques.

La transformation θ → α se fait au contraire par une réorganisation complète de la structure puisque le réseau des ions oxygène adopte une symétrie hexagonale. Cette transformation induit une diminution de la surface spécifique et une forte densification du matériau. Une taille critique du noyau θ-Al_2O_3 est nécessaire pour que cette transformation commence (mécanisme de nucléation-croissance). Ceci explique par ailleurs pourquoi la diaspore (AlOOH), qui cristallise dans le système hexagonal, se transforme directement en α-Al_2O_3 à des températures basses, autour de 500°C.[5]

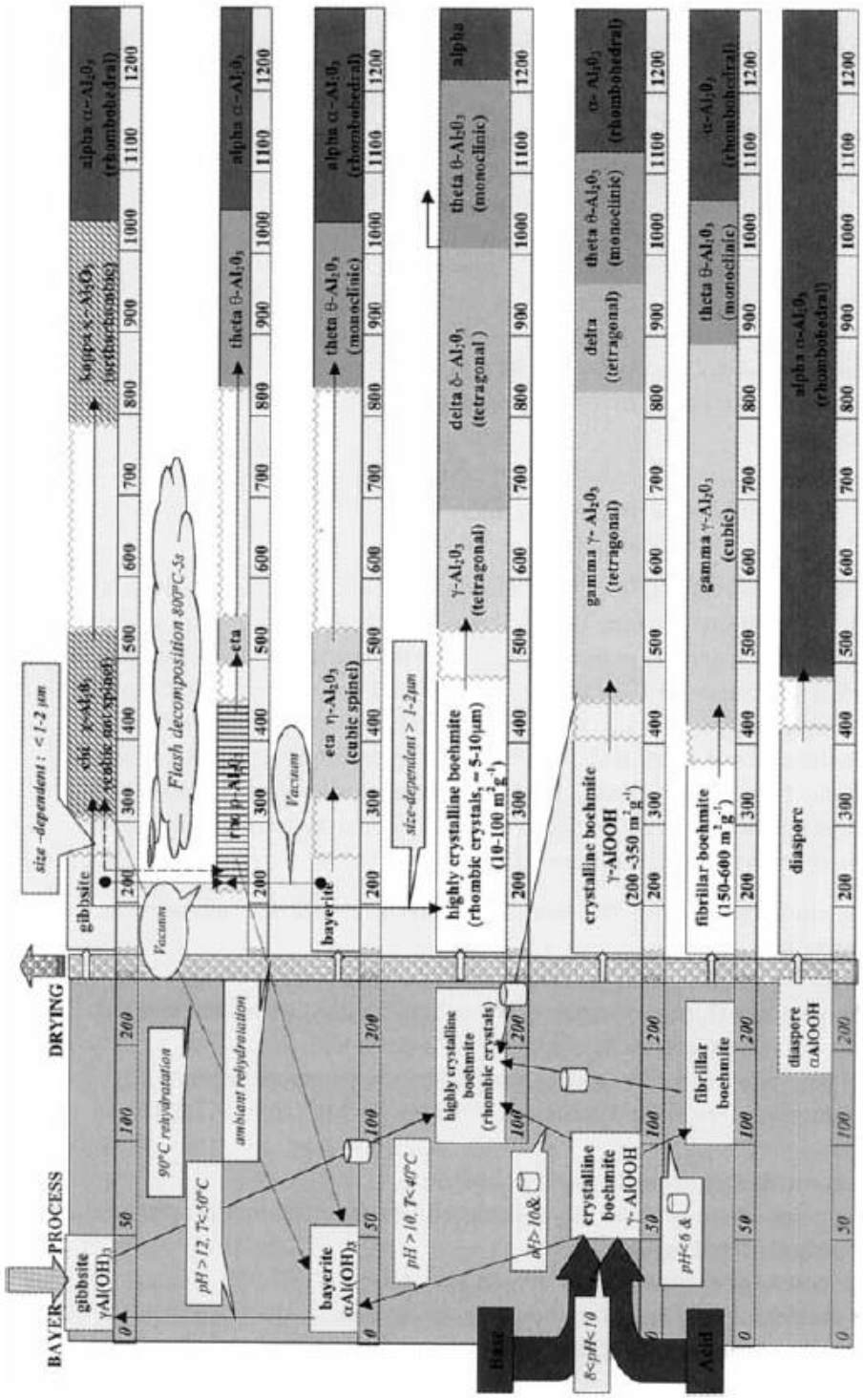

Figure 6. Les filiations des alumines de transition. Sur le côté gauche, les transformations des alumines en présence de l'eau en fonction de la température et du pH. Les nombres dans les barres horizontales sont les températures en °C. ⛁ *indique les transformations en conditions hydrothermales.*[5]

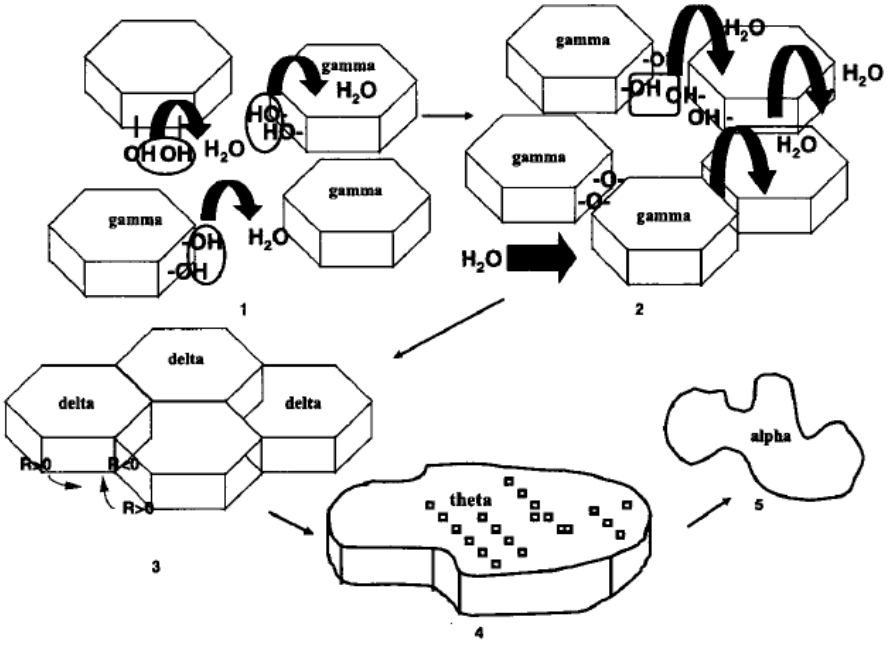

Figure 7. Schéma simplifié de la transition $\gamma \rightarrow \delta \rightarrow \theta \rightarrow \alpha$: 1: déshydroxylation de γ-Al_2O_3 ; 2 : formation de ponts Al-O-Al entre plaquettes ; 3: $\gamma \rightarrow \delta$-$Al_2O_3$; 4 : évolution vers θ-Al_2O_3 avec formations des lacunes ; 5 : transformation en α-Al_2O_3. [5]

I.2.2. Effet du pH à température ambiante

L'étude de l'hydratation de l'alumine en fonction des différents paramètres expérimentaux sera abordée dans ce qui suit. A température ambiante, la nature des phases hydroxydes et/ou oxyhydroxydes d'aluminium formées par hydratation des alumines en solution aqueuse dépend en premier lieu du pH du milieu. Carrier *et al*.[9] ont montré qu'en travaillant à température ambiante à un pH acide (pH=5), la formation de gibbsite est dominante par rapport à la bayerite. Aux pH neutres et basiques (jusqu'à pH=11), il y a, au contraire, prédominance de la bayerite (Figure 8). Ces deux polymorphes peuvent être discriminés par diffraction des RX sur la base des raies (001) à 2θ = 18,2° pour la gibbsite et 18,8° pour la bayerite, en lien avec la différence de distance basale entre les deux structures.

La prédominance de gibbsite en milieu acide et de bayerite en milieu basique a aussi été démontrée par Roelofs et Vogelsberger[20] par spectroscopie Raman (Figure 9). L'alumine gamma a été mise en suspension dans l'eau à 25°C, puis le pH a été ajusté en ajoutant un volume adéquat de solutions d'HCl ou de KOH, et la solution a été laissée sous agitation. La bayerite a pu être identifiée par les

3 bandes Raman à 3426, 3547 et 3655 cm^{-1} avec un épaulement à 3455 cm^{-1} sur la bande intense à 3426 cm^{-1}, et la gibbsite par les 3 bandes à 3364, 3523 et 3619 cm^{-1}.[29,30] Ces bandes correspondent aux vibrations d'élongation des hydroxyles.

Il faut aussi noter que pour de faibles valeurs de pH (inférieures à 4) aucune formation d'hydroxyde cristallisé n'est identifiée en accord avec les résultats de Carrier *et al*.[9] (Figure 8).

La spectroscopie infrarouge confirme aussi les conclusions précédentes (Figure 10). Dans ce cas, la bayerite est identifiée par 4 bandes à 3425, 3460, 3550 et 3655 cm^{-1} et la gibbsite par 3 bandes à 3380, 3525 et 3625 cm^{-1}.

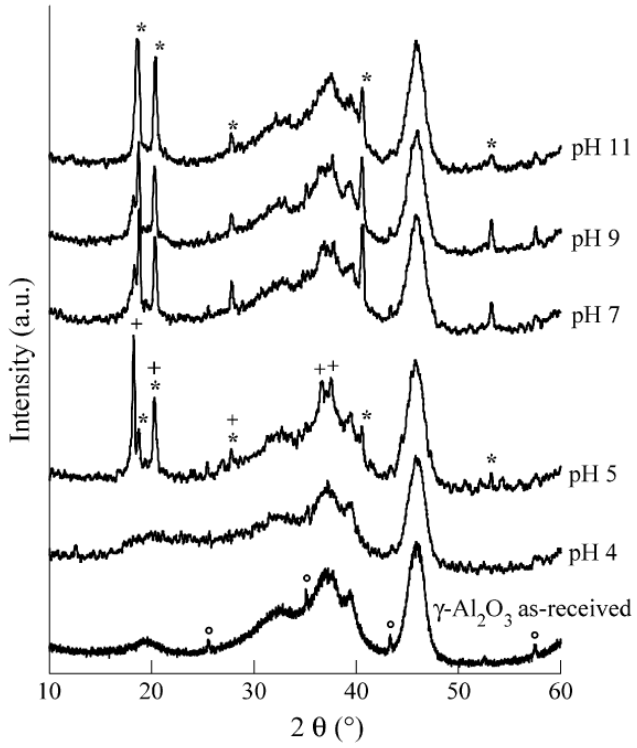

Figure 8. Diffractogrammes de RX d'une alumine gamma mise en contact avec de l'eau liquide durant 168h, sous agitation continue, à température ambiante et à des valeurs de pH différentes. Les suspensions sont filtrées et séchées à l'air à température ambiante. (o) traces de corindon, (+) gibbsite et (*) bayerite.[9]

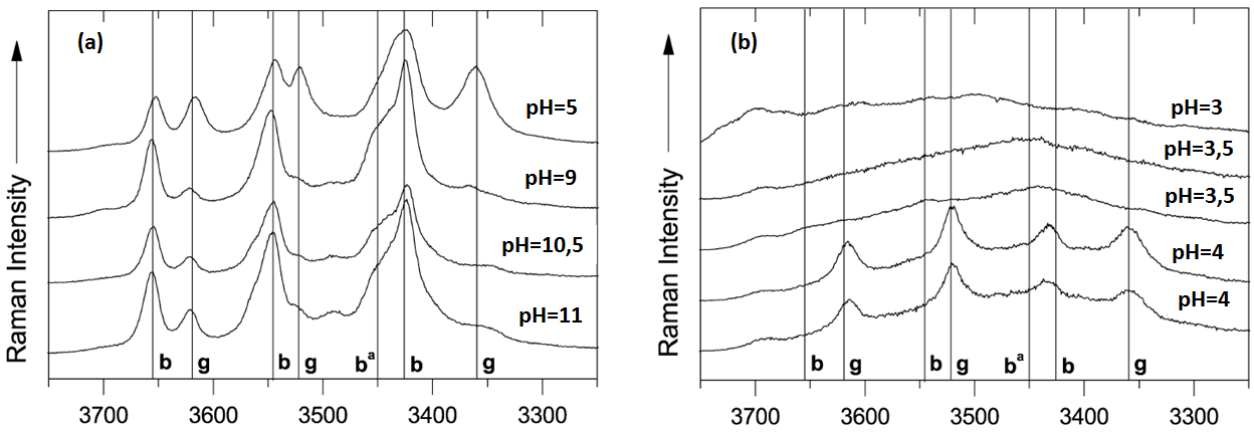

Figure 9 (adaptée). Spectres Raman de l'alumine gamma en suspension dans l'eau sur une table à secousses à 25°C pour différentes valeurs de pH. b: bayerite, g: gibbsite.[20] Les quatre échantillons notés pH 3.5 et pH 4 correspondent à des tests de reproductibilités. Spectres obtenus sur une poudre séchée à 110°C après un lavage visant à éliminer les molécules et les ions adsorbés.

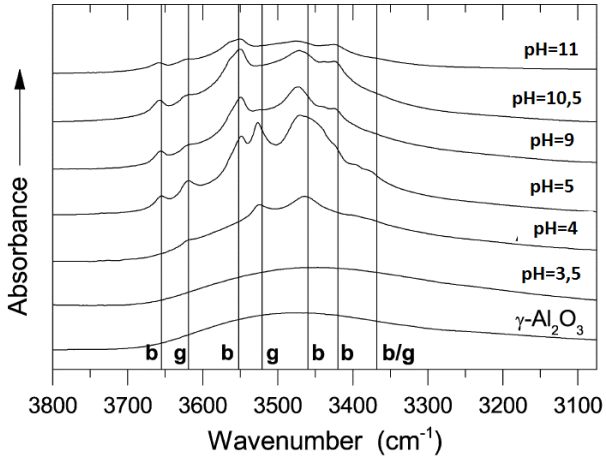

Figure 10 (adaptée). Spectres IR de l'alumine gamma en contact avec l'eau sur une table à secousses à 25°C à différentes valeurs de pH. b: bayerite, g: gibbsite.[20] Spectres obtenus sur une poudre séchée à 110°C après un lavage visant à éliminer les molécules et les ions adsorbés.

La tendance générale décrite dans les exemples précédents se retrouve dans de nombreux travaux et le Tableau 1 regroupe la nature des phases obtenues dans plusieurs études en précisant le domaine de pH utilisé pour l'hydratation de l'alumine (alumine γ le plus fréquemment, mais aussi δ et η). La formation de gibbsite est donc plutôt favorisée en milieu acide, et la bayerite en milieu neutre ou basique en bonne cohérence avec les résultats de précipitation en solution (Figure 5).

Carrier *et al.*[9] ont postulé la formation de phases amorphes d'hydroxydes d'aluminium à pH très acide (pH≤ 4).

Tableau 1. Nature des phases hydroxydes d'aluminium formées par mise en suspension d'une alumine dans l'eau en fonction du pH à température ambiante.

pH	Phase obtenue	Référence
≤4	Phases amorphes d'hydroxyde d'aluminium	Carrier *et al.*[9] (γ) Franck *et al.*[31] (γ) Roelofs et Vogelsberger[20] (γ)
5	Gibbsite (majoritaire) et bayerite (minoritaire)	Carrier *et al.*[9] (γ) Roelofs et Vogelsberger[20] (γ)
7	Bayerite (majoritaire) et gibbsite (minoritaire)	Carrier *et al.*[9] (γ)
8,5	Bayerite	Franck *et al.*[31] (γ) Lefèvre *et al.*[21] (γ)
9	Bayerite (majoritaire) et gibbsite (minoritaire)	Laiti *et al.*[32] (γ) Roelofs et Vogelsberger[20] (γ) Carrier *et al.*[9] (γ)
10	Bayerite	Roelofs et Vogelsberger[20] (γ) Carrier *et al.*[9] (γ)
11	Bayerite	Roelofs et Vogelsberger[20] (γ) Carrier *et al.*[9] (γ)

En revanche, certains résultats de la littérature ne confirment pas la tendance décrite dans les études précédentes (Tableau 2) et sont détaillés ci-dessous.

Tableau 2. Nature des phases hydroxydes et oxyhydroxydes d'aluminium formées par mise en suspension d'une alumine dans l'eau en fonction du pH à température ambiante: quelques exceptions.

pH	Phase obtenue	Référence
« acide, basique ou neutre »	Bayerite	Dyer *et al.*[31] (γ)
12	Gibbsite	Franck *et al.*[32] (γ)
« acide, basique ou neutre »	Bayerite (sans agitation) Boehmite (avec agitation)	Chen *et al.*[33] (η)

Franck *et al.*[31] ont identifié par DRX de la gibbsite après mise en suspension d'une alumine à pH fortement basique (pH = 12) à température ambiante pendant près de 23 jours (Tableau 3).

Tableau 3. Conditions de traitement d'une alumine et type de phase obtenue dans l'étude menée par Franck et al.[31]

	1	2	3
Milieu	H_2O	NH_4OH	NH_4OH
pH	7	8,5	12
Température (°C)	137	27	27
Pression (Bar)	3	1	1
Temps (h)	6	550	550
Phase	Alumine γ_c + boehmite	Alumine γ_c + bayerite	Alumine γ_c + gibbsite

L'identification de gibbsite à pH très basique par Franck *et al.*[31] est intéressante puisque cela est en accord avec la plus grande stabilité thermodynamique de cette phase. En effet, Carrier *et al.*[9] ont montré que les hydroxydes sont moins solubles en suspension aqueuse, donc plus stables que l'alumine γ. La solubilité minimum se situe entre pH 6 et 7. L'hydratation de l'alumine γ est donc une conséquence de son instabilité thermodynamique par rapport aux hydroxydes. En outre, la Figure 11 montre clairement une plus grande stabilité thermodynamique de la gibbsite par rapport à la bayerite. Le polymorphe gibbsite devrait donc être favorisé thermodynamiquement sur l'ensemble du domaine de pH, lors de l'hydratation d'une alumine γ. Les résultats précédents (Tableau 2) montrent que ce n'est pas le cas et que la thermodynamique ne doit donc pas contrôler entièrement la formation des polymorphes d'hydroxydes sur toute la gamme de pH puisque la bayerite le plus souvent est dominante à pH élevé.

Les résultats de Franck *et al.*[31] semblent néanmoins suggérer qu'à pH très élevé, la stabilité thermodynamique de la gibbsite l'emporte tout de même sur la métastabilité cinétique de la bayerite.

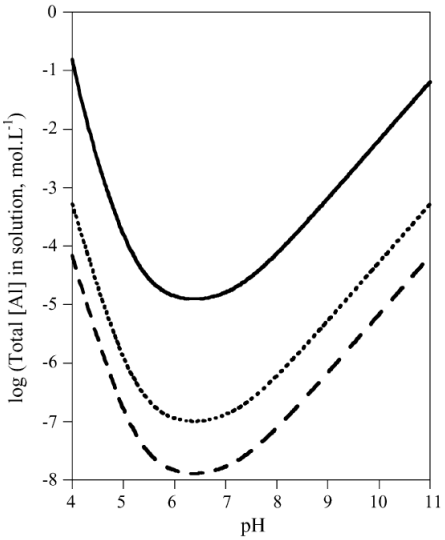

Figure 11. Profils de solubilité pour l'alumine gamma (ligne continue), bayerite (ligne en pointillés), gibbsite (ligne en tirets).Concentration (échelle log) d'Al (III) dissous en fonction du pH.[9]

Dyer *et al.*[34] ont identifié de la bayerite par spectroscopie Raman pour des suspensions aqueuses d'alumine γ «acides, neutres et basiques» sans plus de précision sur le pH. Ils n'ont trouvé effectivement aucun changement spectral significatif en IR ou en Raman en variant le pH du milieu. L'absence d'impact du pH est cependant à relativiser car pour ces séries d'expériences, l'alumine γ est hydratée durant 4 mois en suspension aqueuse, puis le pH est uniquement ajusté à la suite de ce temps long et la suspension est laissée équilibrée pendant 12 h. L'absence de changements majeurs aux pH «acides, neutres et basiques» n'est donc pas surprenante, puisque la durée d'hydratation sans ajustement de pH est très longue comparée au temps où le pH est contrôlé.

De manière surprenante, Zhang *et al.*[35] n'observent par DRX la formation d'aucune phase à pH neutre et identifient de la boehmite à pH acide et basique.

Les résultats de Chen *et al.*[33] sont aussi instructifs car ils pointent l'effet d'un paramètre très souvent négligé : l'agitation du milieu. Dans cette étude, l'agitation ou non d'une suspension d'alumine à température ambiante durant 24 h permet d'orienter la nature du polymorphe formé. Sans agitation, de la bayerite est formée tandis qu'avec agitation, de la boehmite est obtenue. Il existe très peu d'études qui mentionnent ce point et il est difficile de l'expliquer avec les

connaissances actuelles (augmentation locale de température ? effet de l'attrition ?) mais c'est un paramètre que nous choisirons d'examiner dans notre travail.

I.2.3. Effet de la température

a) Aspect structural

La température d'hydratation influence également la nature des phases (oxy)hydroxydes d'aluminium formées. La température n'est cependant pas à considérer seule car dans bien des cas il s'agit de traitements en conditions hydrothermales. Température (>100°C), pression totale et pression partielle de l'eau sont alors à prendre en compte globalement.

Une synthèse globale de la littérature (Tableau 4) amène à conclure que l'hydratation d'une alumine conduit, très majoritairement, à la formation de bayerite et gibbsite pour une hydratation réalisée à température ambiante. Au contraire, un oxyhydroxyde de type boehmite est obtenu pour des températures d'hydratation plus élevées (entre 50 et 200°C).

Certains travaux rapportent des résultats qui ne rentrent pas dans le cadre général décrit ci-dessus. En effet, de la bayerite a parfois été identifiée après hydratation au-dessus de la température ambiante : à 60°C[34] et à 100°C.[20] D'autre part, Roelofs et Vogelsberger[20] notent la disparition en DRX des raies correspondant à une phase bayerite en travaillant à une température de 350°C sans qu'une phase de type boehmite soit identifiée.

On peut donc constater que les paramètres expérimentaux (pH, température, pression…) jouent un rôle sur la nature de la phase formée, ce qui est en accord à nouveau avec la Figure 5 de la section I.1.3. Une phase cristalline de type boehmite est souvent mise en évidence à haute température quand le pH est neutre. Rares sont les études faites dans des conditions de pH non neutres. Il existe cependant trop peu d'études où les paramètres pH et température sont étudiés conjointement pour aller plus loin dans cette interprétation.

On peut aussi à nouveau noter que les travaux de Chen *et al*.[33] sont les seuls à décrire la formation de boehmite à température ambiante dans des conditions d'agitation particulières (agitation continue durant 24 h).

Tableau 4. Nature des phases hydroxydes et oxyhydroxydes d'aluminium formées par mise en suspension d'une alumine dans l'eau pour différentes températures d'hydratation.

Température d'hydratation	Phase (oxy)hydroxyde d'aluminium obtenue	Référence
25°C	Bayerite et/ou gibbsite (suivant le pH)	Franck *et al.*[31] (γ) Carrier *et al.*[9] (γ) Lefèvre *et al.*[21] (γ) Roelofs et Volgesberger[20] (γ) Chen *et al.*[33] (η) Laiti *et al.*[32] (γ) Dyer *et al.*[34] (δ)
50-500°C	Boehmite	Franck *et al.*[31] (γ) Jun-Cheng *et al.*[36] (γ) Mironenko *et al.*[37] (γ) Ravenelle *et al.*[38] (γ) Zhang *et al.*[35] (γ) Zhou *et al.*[39] (γ) De Vlieger *et al.*[40] (γ) Elliott *et al.*[41] (γ, δ, η) El Doukkali *et al.*[42] (γ) Li *et al.*[25] (γ) Tan et *al.*[28] (γ)

b) Aspect quantitatif

La température d'hydratation joue un rôle aussi sur la cinétique de formation des phases hydroxydes et oxyhydroxydes et donc sur la quantité d'hydroxydes d'aluminium produits lors de cette hydratation. A titre d'exemple, les résultats de Dyer *et al.*[34] ont montré qu'en augmentant la température à 60°C la quantité de bayerite produite (et identifiée par DRX) est plus importante qu'à 20°C alors que la durée d'hydratation est plus courte (10 jours au lieu de 4 mois, Figure 12).

Le même type d'effet cinétique est observé lors de la formation de boehmite en conditions hydrothermales (Tableau 5). Mironenko *et al.*[37] ont en effet montré qu'en faisant varier la température du traitement hydrothermal de 50°C à 200°C durant 3 h, le pourcentage de boehmite formée, estimé à partir de la réflexion (002) en diffraction des RX, augmente de 5 à 100%.

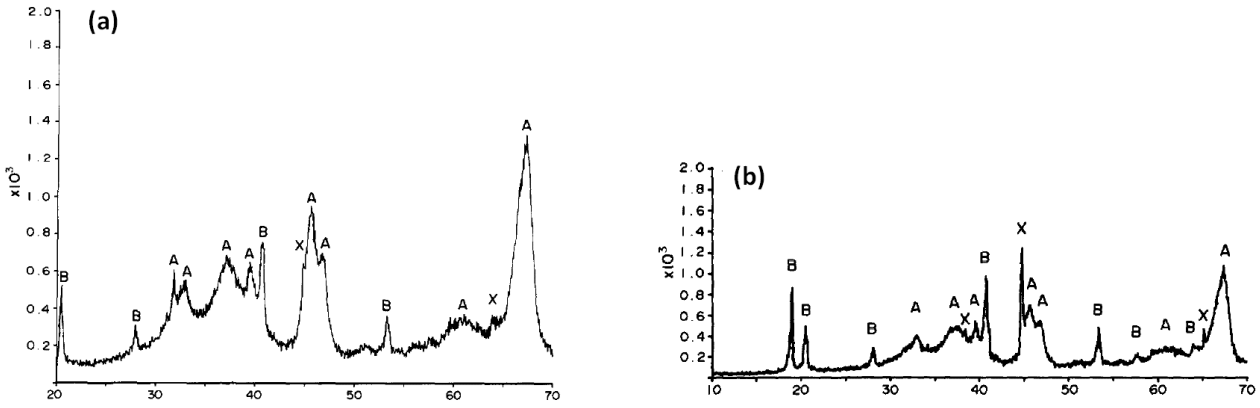

Figure 12. Diffractogrammes de RX d'une alumine δ mise en suspension dans l'eau sous agitation (a) à 20°C durant 4 mois et (b) à 60°C durant 10 jours (pH non précisé).[34] A : alumine, B : bayerite et X : pics de référence de l'aluminium. N.B. Dyer et al.[34] ont indiqué qu'ils travaillent avec une alumine γ, mais les diffractogrammes de RX montrent qu'il s'agit plutôt d'une alumine δ.

Tableau 5. Effet de la température de traitement hydrothermal (en autoclave) d'une alumine γ en phase aqueuse sur la quantité de boehmite formée (le rapport des phases solide et liquide est maintenu constant à 1:25 (wt)).[37]

Température de traitement hydrothermal (°C)	Durée de traitement hydrothermal (h)	Quantité de boehmite formée (%)
50	3	5
120	3	9
150	3	24
200	3	100

Cette augmentation a été aussi validée par les travaux de Koichumanova *et al.*[43] Une étude IR ATR *in situ* a été menée sur une alumine γ qui a subi un traitement sous eau à 40 bar à des températures allant de 150°C à 230°C (Figure 13). L'intensité de la bande en IR à 1064 cm^{-1} correspondant aux modes vibrationnels de déformation des OH de la phase boehmite[44–48] augmente avec la température. Il a été conclu, en traçant l'intégration des pics en IR à 1064 cm^{-1} en fonction du temps

de traitement, que la vitesse apparente de la formation de la boehmite augmente avec la température.

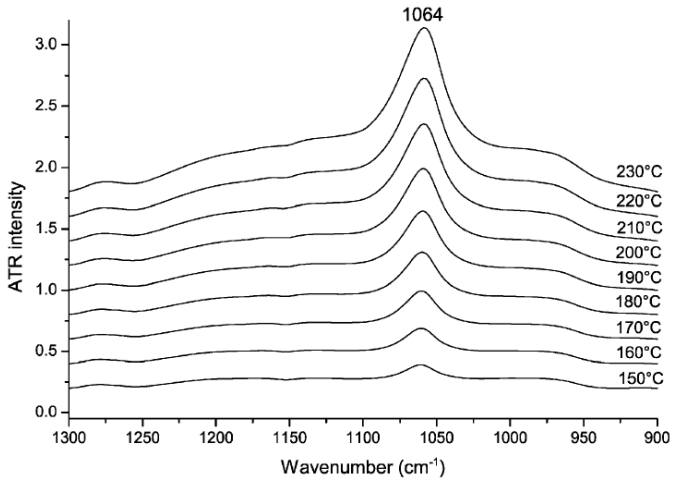

Figure 13. Spectres IR ATR d'une alumine γ ayant subi un chauffage par paliers de 30 min à chaque température allant de 150°C à 230°C sous 40 bar et un débit de 1 mL.min^{-1} H_2O.[43]

I.2.4. Influence du temps de traitement à température constante

A l'image de la température, le temps est bien évidemment un facteur décisif pour la quantité d'hydroxyde d'aluminium formée lors de l'hydratation de l'alumine. Dans cette section, une synthèse des résultats de la littérature sur la formation des phases $Al(OH)_3$ ou AlOOH en fonction du temps pour une température donnée va être présentée.

Lefèvre *et al.* [21] ont ainsi montré par des analyses MEB qu'à température ambiante, la quantité de bayerite produite augmente fortement entre 2 semaines et 6 mois d'hydratation (Figure 14). Les clichés MEB de la Figure 14 montrent qu'un mécanisme de nucléation/croissance se produit à la surface de l'alumine. De même, Koichumanova *et al.*[43] ont montré que la quantité de boehmite formée à 230°C augmente entre 30 et 310 min mais avec une vitesse de formation plus lente avec le temps. Les auteurs suggèrent donc que cette vitesse de formation dépend de la quantité d'alumine disponible.

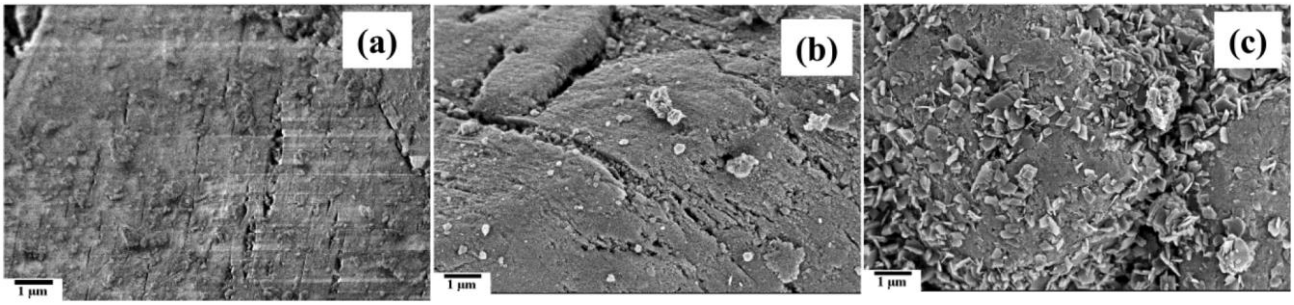

Figure 14. Clichés MEB d'une alumine γ : (a) à l'état initial puis ayant subi une hydratation en solution à température ambiante sous agitation durant : (b) 2 semaines et (c) 6 mois.[21]

Ravenelle *et al.*[38] ont confirmé cet effet du temps de traitement en suivant par RMN ^{27}Al et DRX l'hydratation d'une alumine γ à 200°C en conditions hydrothermales. Ils ont montré que les pics correspondant à l'aluminium en coordinence tétraédrique (70 ppm) disparaissent en 10 h alors que ceux en position octaédrique (8 ppm) sont toujours présents. Ceci montre la transformation quantitative de l'alumine γ en boehmite puisque seule l'alumine γ possède des aluminiums en coordinence tétraédrique (Figure 15.a). La transformation totale de l'alumine γ en boehmite est aussi mise en évidence par DRX (Figure 15.b).

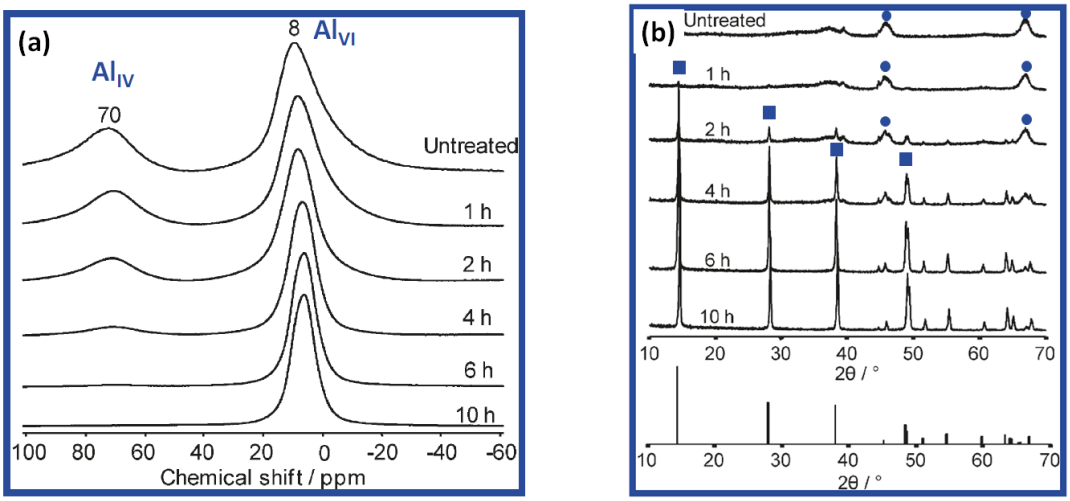

Figure 15 (adaptée). Hydratation à 200°C sous agitation continue dans un autoclave d'une alumine γ et caractérisation : (a) par RMN (b) diffraction des RX .[38] ● *γ-Al$_2$O$_3$ et* ■ *AlOOH.*

L'apparition de différentes phases (oxy)hydroxydes avec le temps peut se faire parallèlement ou successivement. Pour Jun-Cheng *et al.*[36] (conditions hydrothermales, Figure 16.a) l'apparition de boehmite et de $Al(OH)_3$ (les auteurs n'ont pas fait la différence entre les polymorphes, mais les diffractogrammes de RX suggèrent la présence conjointe de bayerite et gibbsite) est simultanée au cours du temps. Au contraire, Lefèvre *et al.*[21] ont montré la formation intermédiaire d'une phase amorphe à température ambiante (Figure 16.b, 10 jours) avec prédominance de bayerite. Ces observations suggèrent l'existence de mécanismes d'hydratation différents qui peuvent être liés aux conditions expérimentales mises en œuvre dans les deux cas : traitement hydrothermal d'une part et hydratation à température ambiante d'autre part.

La taille des particules d'(oxy)hydroxydes d'aluminium formées varie aussi avec le temps de vieillissement (Figure 14 à température ambiante et Figure 17 en conditions hydrothermales). En conditions hydrothermales, quelques cristallites de boehmite sous forme de plaquettes ayant une épaisseur d'environ 20 nm apparaissent sur la surface de l'alumine γ suite à un traitement à 140°C pendant 1 h et la taille de ces nanocristallites croît clairement avec le temps (Figure 17(3-5)).

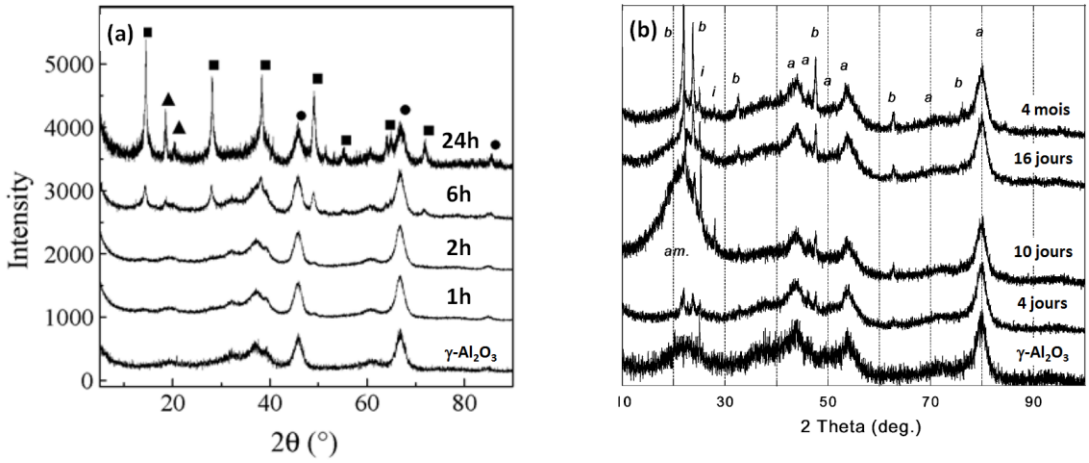

Figure 16 (adaptée). (a) Diffractogrammes de RX d'une alumine γ qui a subi : (a) un traitement hydrothermal à 140°C[36] et (b) une hydratation à température ambiante sous agitation[21] durant différents temps de traitement. ● alumine γ, ■ boehmite et ▲ $Al(OH)_3$. a: alumine, b: bayerite, i: impureté et am: phase amorphe.

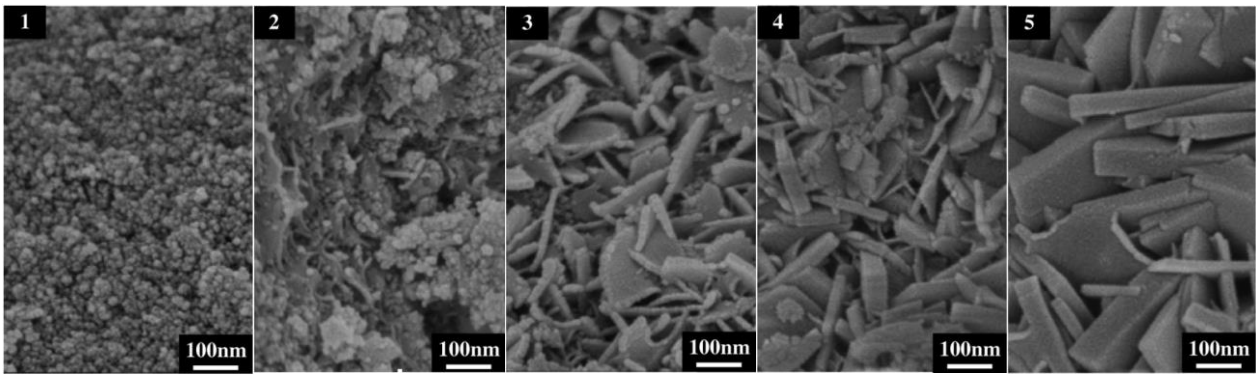

Figure 17. Clichés MEB d'une alumine gamma à l'état initial (1) puis ayant subi un traitement hydrothermal à 140°C sous agitation durant : (2) 1 h, (3) 2 h, (4) 6 h et (5) 24 h.[36]

Ces différents résultats montrent que l'hydratation d'une phase de type alumine γ est continue au cours du temps et que cette hydratation peut conduire à la disparition totale de l'oxyde initial en quelques heures dans des conditions sévères (conditions hydrothermales pour une température de l'ordre de 200°C).

I.2.5. Effet de l'hydratation sur la texture et la structure de surface

Il existe peu de travaux qui étudient en détail les conséquences texturales et structurales de l'hydratation de l'alumine. Néanmoins il existe quelques données qui concernent l'aspect textural[20,35,38,49] (évolution de la surface spécifique et du volume poreux) mais rarement des données qui concernent la modification de la structure de surface.

Certains travaux[20,38,49] ont montré une augmentation de la surface spécifique globale du matériau durant les premières heures d'hydratation d'une alumine γ (environ 14% en 2 h à 200°C en conditions hydrothermales,[38] Figure 18). Cette augmentation peut être expliquée par la formation de phases hydroxydes/oxyhydroxydes d'aluminium qui sont souvent constituées de nanoparticules déposées sur la surface de l'alumine.[35] Ces nanoparticules peuvent donc créer de la surface supplémentaire sans diminuer sensiblement la surface initiale de l'alumine.

Pour un temps d'hydratation plus long, la croissance des néophases hydroxydes/oxyhydroxydes peut conduire à une couverture de la surface initiale de l'oxyde et à une diminution de la porosité du support alumine et donc de sa surface spécifique sans que la surface développée par les néophases hydratées puisse compenser cette baisse (Figure 18).

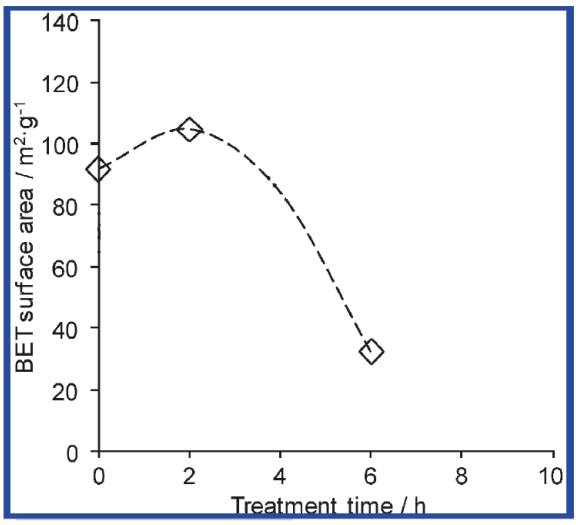

Figure 18 (adaptée). Variation de la surface spécifique mesurée par physisorption de N_2 pour une alumine γ traitée en phase aqueuse en conditions hydrothermales à 200°C en fonction du temps du traitement (agitation continue, 0,5g de solide dans 30 mL d'eau ionisée).[38]

I.2.6. Mécanisme de formation

L'étude du mécanisme de formation des (oxy)hydroxydes d'aluminium par hydratation de l'alumine est très rare dans la littérature. Cependant, quelques auteurs proposent un mécanisme de dissolution-précipitation des hydroxydes qui se formeraient indépendamment de la surface de l'alumine selon un processus de nucléation/croissance.[9,38] Mukhambetov et Lamberov[49] introduisent une complexité supplémentaire en suggérant que ce mécanisme dépend de la porosité. D'après ces auteurs,[49] le mécanisme de « dissolution/précipitation » (ainsi nommé par les auteurs) serait dominant dans les macropores (>500 nm) alors que dans les mésopores (~10 nm) une hydratation de surface aurait lieu de la surface vers le cœur du matériau.

Carrier *et al.*[9] ont démontré ce mécanisme de dissolution-précipitation à partir d'analyses des phases liquide et solide lors du vieillissement d'une alumine en phase aqueuse à pH basique (Figure 19). Il a ainsi été montré que la concentration de l'aluminium en phase liquide augmente régulièrement par dissolution (aucun hydroxyde n'est détecté au début de l'expérience) tandis que cette concentration diminue après 10 h et les particules d'hydroxydes cristallisées commencent à grossir (précipitation). Ainsi, après quelques jours, un plateau correspondant à la solubilité de la bayerite est atteint impliquant que la transformation continue de l'alumine en hydroxydes d'aluminium via sa dissolution a atteint un état stationnaire. Cette idée a été reprise par

Koichumanova *et al.*[43] sans que ces auteurs puissent clairement discriminer une simple hydratation de surface et un mécanisme de dissolution-précipitation.

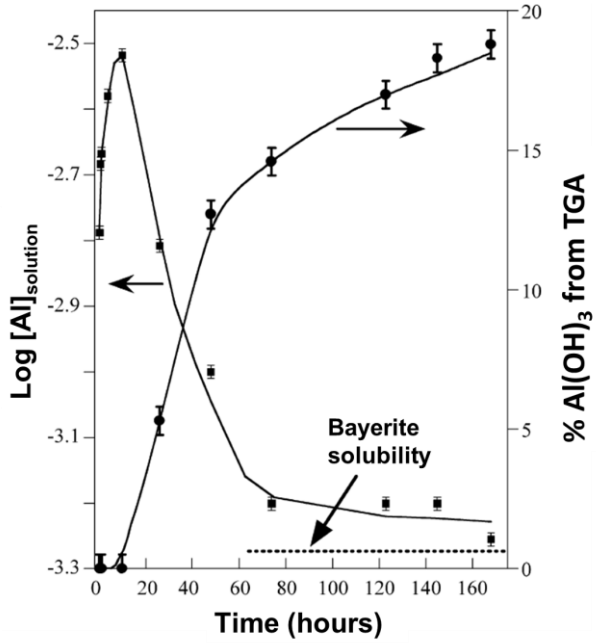

Figure 19. Comparaison de l'évolution de la quantité de bayerite (cercles) déterminée par ATG avec la concentration de l'aluminium dans les filtrats (carrés) en fonction du temps après suspension à pH=11 pour différentes durées.[9]

Lefèvre *et al.*[21] ont aussi avancé que ce mécanisme de dissolution-précipitation est cohérent avec la disparition de la phase amorphe formée intermédiairement lors de l'hydratation de l'alumine γ en conditions ambiantes et visible sur les diffractogrammes de la Figure 16.b (10 jours notamment).

I.2.7. Conclusion

L'hydratation de l'alumine en phase aqueuse conduit à la formation de néophases hydroxydes ($Al(OH)_3$) et/ou oxyhydroxydes (AlOOH). La quantité de phases formées, leur nature et la taille des particules dépendent de plusieurs facteurs parmi lesquels le pH, la température et le temps de vieillissement apparaissent majeurs. Dans la majorité des cas, à température ambiante, l'obtention de gibbsite (majoritaire à pH acide) et de bayerite (majoritaire ou seule, à pH neutre ou basique) est distinguée. La bayerite semble être sous contrôle cinétique car le polymorphe le plus stable est la gibbsite dans toute la gamme de pH. A température élevée (conditions hydrothermales), la formation et la prédominance de boehmite est observée dans une large gamme de pH. La surface

spécifique de l'alumine augmente durant les premières heures d'hydratation due à la formation de petites particules d'(oxy)hydroxydes d'aluminium, et elle diminue pour un temps d'hydratation plus long en raison de la croissance de ces dernières qui peuvent bloquer la porosité.

De manière attendue, en augmentant le temps d'hydratation ou la température, la quantité de phases (oxy)hydroxydes d'aluminium produites augmente. Mais on note peu d'études dans lesquelles temps *et* températures sont variés de façon systématique. Le mécanisme de formation des (oxy)hydroxydes d'aluminium lors de la mise en suspension de l'alumine est supposé être de type dissolution-précipitation, mais globalement, le mécanisme de formation de ces phases est peu étudié. Egalement, l'effet de la surface spécifique ou de la cristallinité de l'alumine sur sa réactivité vis-à-vis de l'eau est peu traité dans la littérature. Enfin, contrairement à la dégradation de type chimique (érosion), la dégradation de type mécanique *(attrition)* est rarement considérée dans la littérature académique.

I.3. Influence des espèces supportées sur la transformation de l'alumine dans l'eau

Nous avons vu que l'alumine subit des transformations quand elle est mise en contact avec l'eau, et ce peut être aussi le cas de catalyseurs de type métaux supportés sur alumine placés dans les mêmes conditions, ce qui a généralement des conséquences néfastes sur l'activité catalytique. Ainsi, plusieurs équipes ont cherché à éviter la transformation de l'alumine en néophases hydratées en ajoutant à sa surface des éléments métalliques ou non, ou des composés organiques. Ce chapitre traitera donc de l'influence des espèces supportées, inorganiques ou organiques, sur l'hydratation de l'alumine.

I.3.1. Métaux supportés

Ravenelle *et al.*[38] ont étudié la cinétique de transformation de l'alumine γ en boehmite et celle de catalyseurs supportés au Ni ou au Pt. Ils ont montré que dans l'eau à 200°C l'alumine γ se convertit totalement en boehmite en 6 à 10 h à une vitesse initiale de 0,10 $mol.h^{-1}$. Au contraire, les catalyseurs à base de Ni et Pt supportés sur cette même alumine γ se convertissent à des vitesses initiales plus faibles (0,03-0,05 $mol.h^{-1}$) (Figure 20). Les cinétiques de transformation sont

initialement similaires pour les deux catalyseurs mais la conversion finale en boehmite est de 73% pour Ni/γ-Al_2O_3 et seulement 60% pour Pt/γ-Al_2O_3 après 10h de traitement.

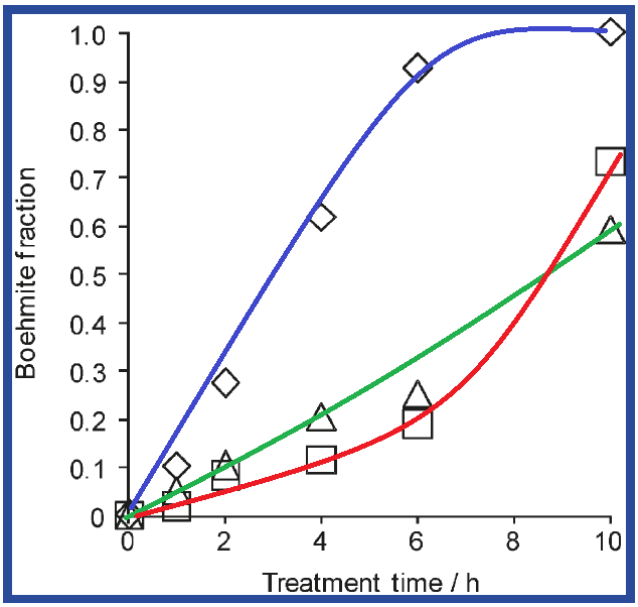

Figure 20.Cinétique de formation de boehmite durant un traitement hydrothermal sous agitation constante à 200°C à partir : i) d'une alumine pure (losanges) et ii) de catalyseurs 1 wt% Pt/γ-Al_2O_3 (triangles) et 1 wt% Ni/γ-Al_2O_3 (carrés).[38] .

La présence de particules métalliques limite donc l'hydratation de l'alumine malgré des taux de couverture faible : une teneur de 1 wt % en particules de Pt couvre seulement ~2% de la surface spécifique totale de l'alumine γ alors qu'une teneur similaire en Ni couvre ~5,5% de la surface spécifique disponible. Des analyses RMN ^{1}H suggèrent que le nickel s'associe à toutes les espèces OH de surface alors que le Pt s'associerait seulement aux OH de surface basiques (groupements OH résonant à -0,4 ppm, simplement coordinés à un Al). Comme le catalyseur à base de Pt montre une vitesse de formation de boehmite la plus faible, il est supposé que les groupements OH basiques jouent un rôle important dans l'hydratation de l'alumine.[38] Ces résultats et hypothèses sont confirmés par Koichumanova *et al.*[43] qui confirment la disparition d'un épaulement à -0,1 ppm en RMN ^{1}H pour le catalyseur Pt/γ-Al_2O_3 (Figure 21) correspondant aux groupements OH simplement coordinées selon Knœzinger et Ratnasamy.[50] Ce catalyseur présente aussi l'énergie d'activation la plus élevée pour la formation de boehmite.

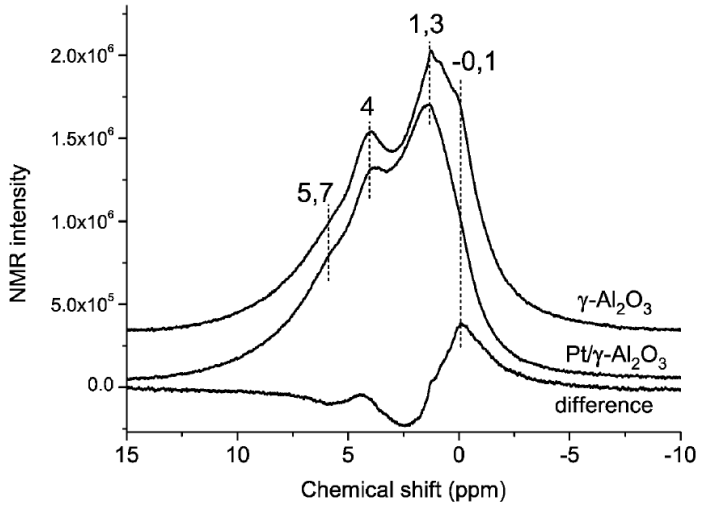

Figure 21. Spectres RMN ^{1}H de γ-Al_2O_3 et Pt/γ-Al_2O_3 et spectre différence.[43]

En revanche, les travaux de Li et al.[51] suggèrent que la présence de particules de Ni n'affecte pas l'hydratation de γ-Al_2O_3 pour un catalyseur 17 wt% Ni/γ-Al_2O_3 (préparé à partir de $Ni(NO_3)_2.6H_2O$ réduit sous H_2 à 450°C) ayant subi un traitement hydrothermal sous pression autogène et sous agitation dans la gamme de température 90-150°C. Ils ont montré la formation de boehmite dès 110°C et dès 8 h à cette température. Un résultat similaire a été trouvé mais en présence de ruthénium dans les travaux de Ketchie *et al.*[52]. En outre, l'hydrolyse du support induit aussi une agglomération des particules de Ru, ce qui suggère fortement que l'alumine γ n'est pas un support approprié pour la conversion de la biomasse en phase aqueuse. Néanmoins, ces deux travaux[51,52] ne comparent pas la dégradation du catalyseur dans l'eau à celle d'une alumine pure. Il est donc difficile de confirmer leurs affirmations.

Un autre paramètre à prendre en compte est le choix du sel métallique utilisé pour introduire le métal. Pour des catalyseurs Pt/γ-Al_2O_3 préparés à partir de H_2PtCl_6 (noté Pt-Cl) et $H_2Pt(OH)_6$ (noté Pt-OH), 60 et 93% de conversion de l'alumine en boehmite sont observés, respectivement après un traitement de 10 h dans l'eau à 200°C (Figure 22).[53] La plus faible transformation en boehmite pour Pt-Cl est expliquée par un échange entre les ions chlorures et les OH de surface les plus basiques qui, comme on l'a vu précédemment, ont été supposés impliqués dans l'hydratation de l'alumine. Cependant, une quantité significative d'aluminium dissous est détectée dans la solution quand le catalyseur Pt-Cl est traité dans l'eau à 200°C. Ravenelle *et al.*[53] supposent que ceci serait

dû au pH plus acide de la solution, ce qui peut aussi expliquer l'inhibition de la formation de boehmite car un milieu acide limite la précipitation des (oxy)hydroxydes en augmentant leur solubilité.

Ces différents résultats (parfois contradictoires) suggèrent que la préparation du catalyseur métallique supporté (type de précurseur, dispersion de la phase métallique…) est un paramètre important pour maîtriser l'hydratation du support. Ce lien est pourtant rarement étudié dans les publications sur le sujet.

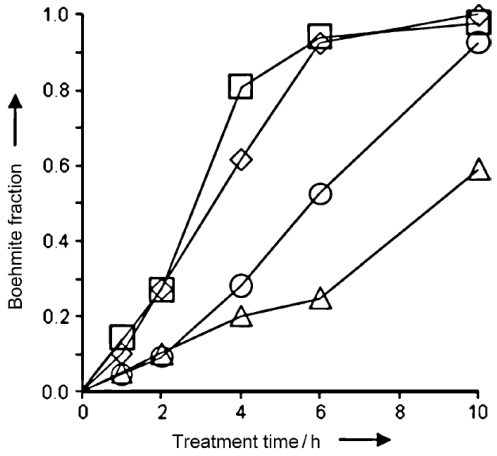

Figure 22. Cinétique de formation de boehmite durant un traitement hydrothermal à 200°C de : i) ◊ γ-Al_2O_3, ○ Pt-OH, △ Pt-Cl et □ Pt-com (catalyseur commercial Pt/γ-Al_2O_3 Alfa Aesar).[53]

I.3.2. Introduction d'hétéroatomes sur le support

Certains travaux ont visé à diminuer ou à inhiber l'hydratation de l'alumine en introduisant sur ou dans le support des ions métalliques ou des hétéroatomes qui ne correspondent pas à une phase active.

Ainsi, Wang et *al.*[54] suggèrent que le zirconium se comporte comme un stabilisant de l'alumine. A titre d'exemple, l'introduction de Zr au cours de la synthèse d'une alumine mésoporeuse (par l'intermédiaire d'oxychlorure de zirconium) améliore sa résistance hydrothermale puisque la structuration ordonnée des mésopores est maintenue suite à un traitement hydrothermal à 100°C durant 6 h[54] (Figure 23(b)). Des pics de diffraction à bas angles sont toujours observés pour l'échantillon contenant du Zr après traitement hydrothermal (Zr/Al = 0.2 noté HT) alors qu'aucun

pic n'est observé pour l'alumine ne contenant pas de Zr (Zr/Al = 0 noté HT). Les résultats de physisorption (Figure 24) ont aussi validé une amélioration de la résistance hydrothermale de l'alumine modifiée. La courbe de distribution de taille des pores de cette dernière reste étroite après traitement HT et le volume total des pores diminue seulement de 19,6%. Au contraire, la distribution de taille de pores de l'alumine exempte de Zr présente une distribution très large indiquant une inhomogénéité des mésopores due à l'hydrolyse des liaisons Al-O-Al durant le processus de traitement hydrothermal.

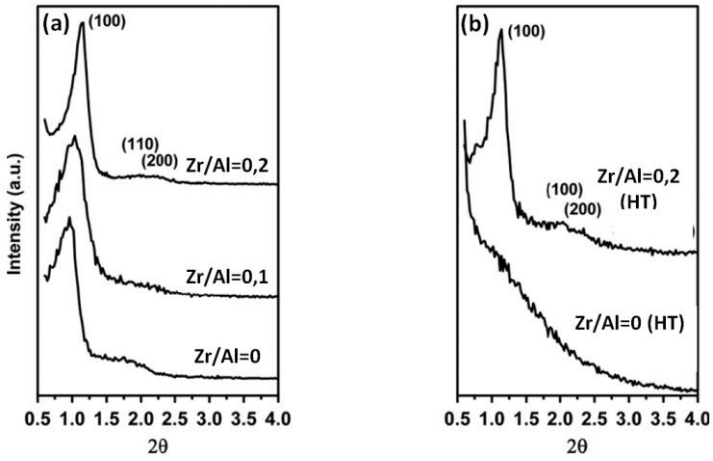

Figure 23 (adaptée). (a) Diffractogrammes de RX d'alumines mésoporeuses dopées au Zr et calcinées à 550°C durant 5h et (b) ayant subi un traitement hydrothermal à 100°C durant 6 h.[54]

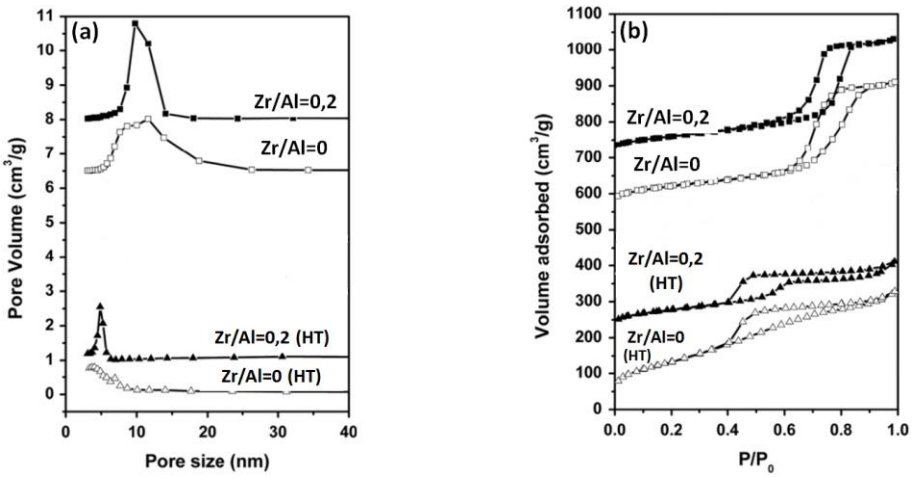

Figure 24 (adaptée). (a) Courbes de distribution de taille des pores et (b) isothermes de physisorption pour des alumines mésoporeuses dopées ou non au Zr, calcinées à 550°C durant 5 h et ayant subi un traitement hydrothermal à 100°C durant 6 h (notées HT).[54]

Il a été montré par ailleurs que les aluminophosphates sont plus stables qu'une alumine γ après traitement thermique sous vapeur d'eau (appelé traitement hydrothermal dans la publication).[55] La surface spécifique d'un aluminophosphate (échantillon nommé AP, préparé par neutralisation d'une solution de nitrate d'aluminium et d'acide phosphorique à pH=8 puis calcination à 500°C) diminue de 5% seulement suite à un traitement à 750°C durant 48h sous vapeur d'eau alors que celle de l'alumine diminue de 40% (Figure 25(a)). La distribution de taille des pores de l'échantillon AP reste aussi étroite et centrée autour d'un diamètre de 70 Å après traitement à 750°C durant 24 h alors que celle d'Al_2O_3 est plus large et se déplace vers les tailles des pores les plus grandes suite à un traitement similaire. Ceci a été expliqué par la présence d'espèces chimiques en coordinence tétraédrique ($AlPO_4$) qui augmenteraient la stabilité hydrothermale.[55]

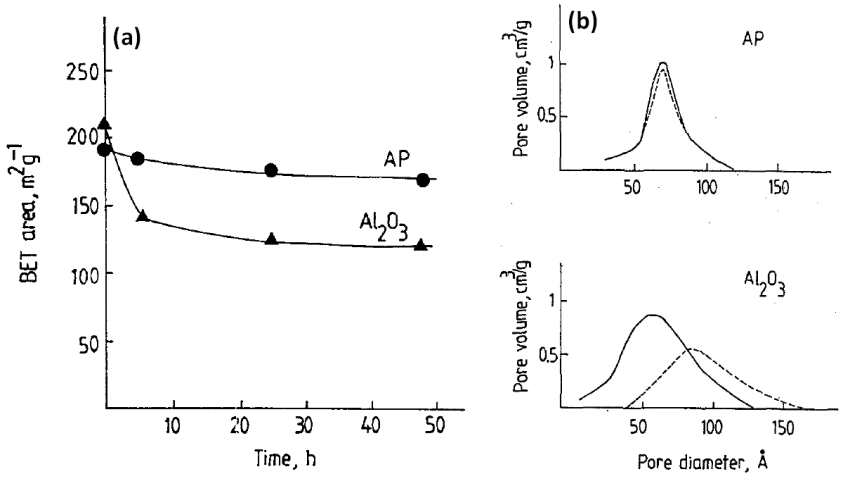

Figure 25. Influence d'un traitement thermique sous vapeur d'eau à 750°C durant 48h pour une Al_2O_3 γ et un aluminophosphate sur : (a) la surface BET en fonction du temps et (b) la distribution de taille des pores ,avant (ligne continue) et après (ligne discontinue) traitement sous vapeur d'eau.[55] AP : aluminophosphate. Le traitement est fait dans un four avec un débit d'eau de 2,5 mL/min

Ha *et al.*[56] ont également ajouté du phosphore (sous forme de phosphates) comme stabilisant pour l'alumine. Les spectres IR de la Figure 26 montrent que seul le catalyseur Co/Al_2O_3 ne contenant pas de phosphore (noté P(0)) est partiellement transformé en boehmite sous conditions hydrothermales (120h à 230°C). Pour cet échantillon les bandes IR larges à 3319 et 3103 cm^{-1} sont attribuées aux vibrations d'élongation symétriques et asymétriques des OH de la boehmite.[57] Les auteurs attribuent les bandes proches de 1100-1170 cm^{-1} pour les catalyseurs contenant du P aux vibrations d'élongation P-O du tétraèdre PO_4^{3-} indiquant la formation de la phase $AlPO_4$ (réputée

insoluble) sur la surface.[58,59,60] Sa présence, comme il a été montré précédemment, contribue à améliorer la résistance hydrothermale de l'alumine.

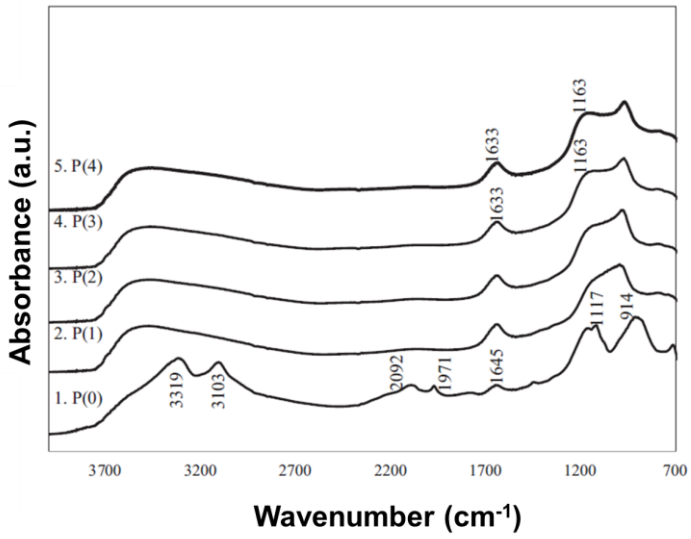

Figure 26. Spectres IR de catalyseurs Co/γ-Al_2O_3 dopés par des ions phosphate ayant subi un traitement hydrothermal à 230°C sous agitation durant 120h. Les catalyseurs sont nommés P(x) où x représente la teneur massique en phosphore.[56]

Les travaux de Stanislaus *et al.*[61] confirment l'étude précédente puisque les diffractogrammes de RX de la Figure 27 montrent que les alumines dopées au phosphore ainsi qu'au fluor ne subissent pas de transformation en boehmite dans des conditions hydrothermales. Les auteurs postulent (sans justification) que l'adsorption de vapeur d'eau sur les lacunes anioniques de l'alumine et l'hydroxylation immédiate en boehmite soient inhibées par la présence des ions F^- et PO_4^{3-}. F^- et PO_4^{3-} interagiraient avec les groupements OH et rempliraient de même quelques lacunes anioniques durant l'imprégnation. Ainsi, d'après ces auteurs, la présence de lacunes anioniques et de groupements hydroxyles spécifiques jouerait un rôle primordial dans la transformation de l'alumine γ en boehmite.

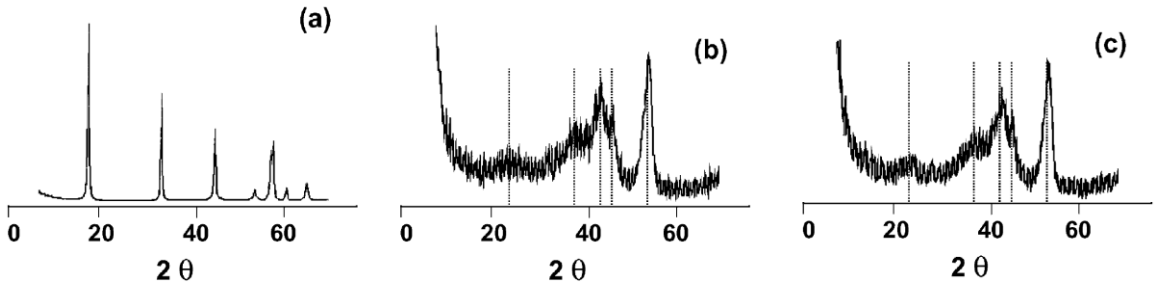

Figure 27 (adaptée). Diffractogrammes de RX de différentes alumines suite à un traitement hydrothermal à 300°C. (a) alumine γ, (b) alumine γ dopée au 2% P et (c) alumine γ dopée au 2% F.[61]

L'alumine peut aussi être stabilisée en conditions hydrothermales en favorisant les liaisons Al-O-Si au lieu de Al-OH.[28,62,63] Van de Loosdrecht *et al.*[62] (Sasol) ont montré qu'en greffant du silicium sur l'alumine en utilisant le TEOS (tetraethylorthosilicate) comme précurseur, Si réagit avec les groupements hydroxyles de la surface de l'alumine. Les trois groupements éthoxy qui restent sont décomposés thermiquement durant une étape de calcination à 500°C sous air. La Figure 28 montre que la dissolution de l'alumine est inhibée par la présence de Si en surface, comme le prouve la quantification des ions Al^{3+} produits au cours du temps. Une autre étude[64] a montré que le dopage par du silicium par coprécipitation d'une solution de nitrate d'aluminium et de $Na_2SiO_3.9H_2O$ stabilise l'alumine et évite la formation des hydroxydes d'aluminium sous conditions douces (90°C). Cette stabilisation est expliquée par les auteurs par la réaction du Si avec les hydroxydes de surface.

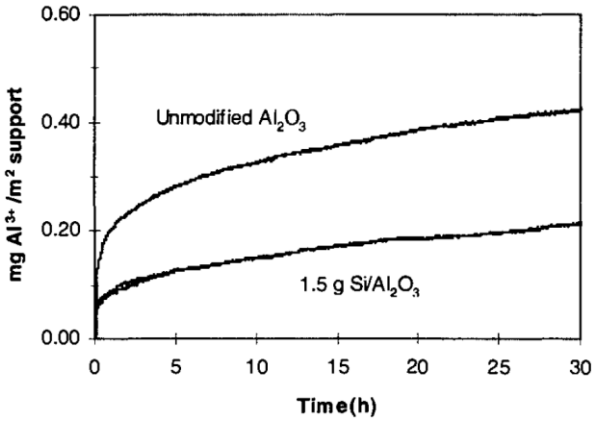

Figure 28. Analyse quantitative de la dissolution d'une alumine et d'une alumine modifiée par Si en conditions de synthèse Fischer-Tropsch (220°C et 20 bar sous agitation).[62]

Enfin, un brevet récent de Chevron[65] montre que l'alumine stabilisée par des ions métalliques aussi variés que l'yttrium (Y), le niobium (Nb), le molybdène (Mo), l'étain (Sn), l'antimoine (Sb) et leurs mélanges, présente une meilleure stabilité hydrothermale que l'alumine pure. Les résultats DRX (Figure 29) montrent que suite à un test hydrothermal dans un autoclave à 220°C sous 370 psig (~25 bar) durant 2 h, l'alumine pure s'est complètement transformée en boehmite alors que l'alumine dopée par Mo (Mo/γ-Al_2O_3) présente toujours les pics d'alumine γ initiaux. Les auteurs montrent aussi que le volume poreux du support stabilisé varie dans une moindre mesure par rapport à l'alumine pure.

Deux autres brevets de Chevron[66,67] montrent des résultats allant dans le même sens en balayant largement le tableau périodique pour les dopants utilisés : le vanadium (V) ou le zinc (Zn), seul ou en présence d'autres éléments comme le magnésium (Mg), le phosphore (P), le titane (Ti), le vanadium (V), le chrome (Cr), le cobalt (Co), le gallium (Ga), le germanium (Ge), le molybdène (Mo), le tungstène (W) ou le praséodyme (Pr).

Ces résultats montrent qu'il est difficile, dans l'état actuel des connaissances, de conférer une spécificité particulière aux différents dopants utilisés.

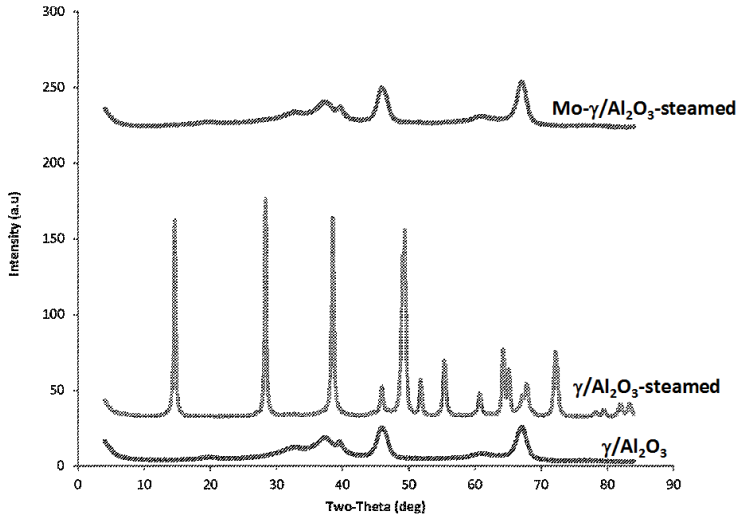

Figure 29 (adaptée). Diffractogrammes de RX de γ-Al_2O_3 et de Mo-γ/Al_2O_3 ayant subi un traitement hydrothermal à 220°C sous 25 bar durant 2 h.[65]

I.3.3. Molécules organiques

La présence de molécules organiques dans le milieu aqueux et/ou adsorbées sur l'alumine semble enfin utile pour réduire la formation des phases (oxy)hydroxydes d'aluminium par hydratation de l'alumine.

Pour un catalyseur Pt/Al_2O_3 exposé à des alcools (glycérol et sorbitol) en solution aqueuse en conditions hydrothermales, la prévention de formation de boehmite a été attribuée à la formation d'une couche hydrocarbonée provenant de la déshydratation et condensation des alcools et qui augmenterait l'hydrophobicité de la surface du catalyseur.[68] Cette hypothèse est d'ailleurs reprise par d'autres auteurs.[23]

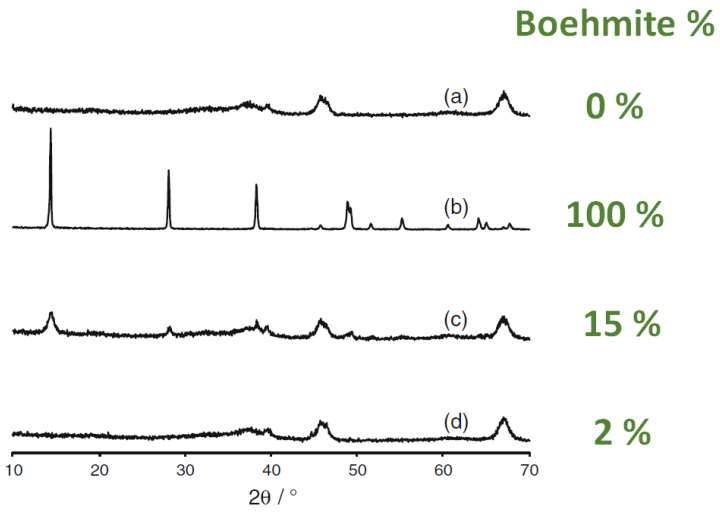

Figure 30 (adaptée). Diffractogrammes de RX de catalyseurs 1 wt % Pt/Al_2O_3 (a) non traité (état initial) et ayant subi un traitement hydrothermal à 225°C durant 10h dans (b) l'eau et des solutions avec : (c) 5 wt% glycérol et (d) 5 wt % sorbitol. La quantification de la boehmite formée est fondée sur une combinaison linéaire des spectres RMN ^{27}Al de l'alumine pure et de la boehmite pure.[68]

L'effet inhibiteur augmente avec l'augmentation de longueur de la chaine carbonée : la quantité de boehmite formée sur le catalyseur traité dans le glycérol (C_3) est supérieure à celle formée dans le catalyseur traité avec du sorbitol (C_6) (Figure 30). Ravenelle et al.[68] propose d'expliquer ceci par le nombre de groupements hydroxyles vicinaux, qui déterminerait la force d'adsorption des alcools avec les groupements hydroxyles de surface et donc la quantité de couche carbonée formée en surface. Ceci est confirmé par les analyses élémentaires effectuées (4,3% de dépôt carboné formé

avec le sorbitol et 2,5% avec le glycérol). Cette interprétation semble confirmée par d'autres travaux.[61,69,70]

Dans le même ordre d'idée, Jongerius *et al.*[71] ont montré que la vanilline et le gaïacol stabilisent plus l'alumine que le phénol, l'anisole et le benzaldéhyde. Ceci serait dû au nombre plus élevé de fonctions contenant de l'oxygène capables de se coordiner aux aluminiums insaturés sur le support empêchant ainsi les molécules d'eau d'y accéder. Un catalyseur 1wt% Pt/γ-Al_2O_3 traité en présence de lignine a montré une inhibition totale de formation de boehmite grâce à la forte interaction entre cette macromolécule hautement fonctionnalisée et hydrophobe et la surface du support, prévenant ainsi l'hydratation de la surface.[71]

Un travail similaire a été réalisé par Pham *et al.*[72] qui ont déposé une couche de carbone sur la surface de l'alumine γ par pyrolyse de sucres simples comme le glucose à 400°C. La couverture de la surface de l'alumine par la couche carbonée est prouvée par FTIR (diminution du nombre de groupements hydroxyles de surface). Après un traitement hydrothermal à 200°C durant 12 h, ils ont montré que la morphologie et la surface spécifique de leur support modifié sont préservées alors que la surface spécifique d'une alumine non couverte par la couche de carbone a diminué de 70%. Par DRX, ils ont confirmé que le support γ-Al_2O_3 est toujours présent et n'est pas transformé en boehmite. A nouveau, l'hypothèse d'une stabilisation par augmentation de l'hydrophobicité de surface est avancée.

La couverture d'un catalyseur CuO/Al_2O_3 avec du PTFE (polytétrafluoroéthylène) (par immersion du catalyseur dans une solution de fibres de PTFE et du tensioactif Triton X-100) augmente de même l'hydrophobicité de la surface et empêche par suite la formation des hydroxydes (Figure 31).[73] La présence de ce film hydrophobe réduit le contact direct de l'oxyde avec le milieu aqueux, tout en permettant aux réactifs de diffuser et de réagir sur le catalyseur.

Il a aussi été suggéré que la présence de molécules organiques peut modifier la cristallinité de la boehmite formée. Stanislaus et al.[61] ont tout d'abord montré qu'en présence de phénol (25%) ou d'acide acétique (25%) dans l'eau l'augmentation de la taille des pores de l'alumine après traitement hydrothermal était limitée (Figure 32 (a) et (b)) en accord avec une transformation incomplète en boehmite (Figure 33). Par ailleurs, la largeur à mi-hauteur des pics de boehmite

formée en présence de phénol et d'acide acétique (Figure 33) suggère une faible cristallinité pour cette dernière. Dans le cas de l'acide acétique, on peut également supposer que la boehmite ne cristallise pas en milieu trop acide. Toutefois ceci n'est pas validé pour le cas du phénol.

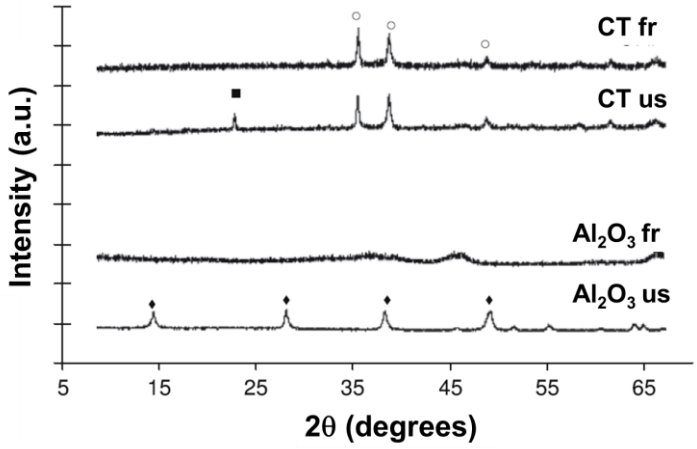

Figure 31. Diffractogrammes de RX d'une γ-Al_2O_3, avant (fr) et après (us) utilisation, catalyseur au cuivre recouvert de PTFE (CT), avant (fr) et après (us) utilisation. Réacteur à ruissellements (trickle bed reactor) à une pression de 7 atm en O_2, 140°C, débit de l'eau 1 mL/min. Catalyseurs utilisés dans des expériences successives jusqu'à 80h. (○ : CuO ; ■ $Cu(C_2O_4)\cdot 0{,}4H_2O$; ◆ boehmite).[73]

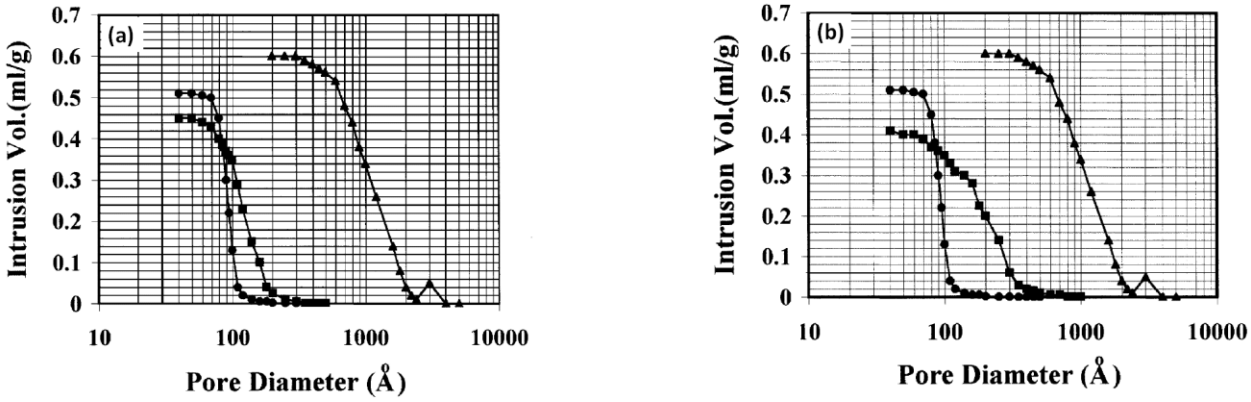

Figure 32. Effet (a) du phénol et (b) de l'acide acétique sur la taille des pores d'une alumine γ suite à un traitement hydrothermal à 300°C. ● Alumine γ non traitée, ▲ traitée sous conditions hydrothermales dans l'eau pure et ■ traitée sous conditions hydrothermales avec 25% de phénol ou d'acide acétique dans l'eau.[61]

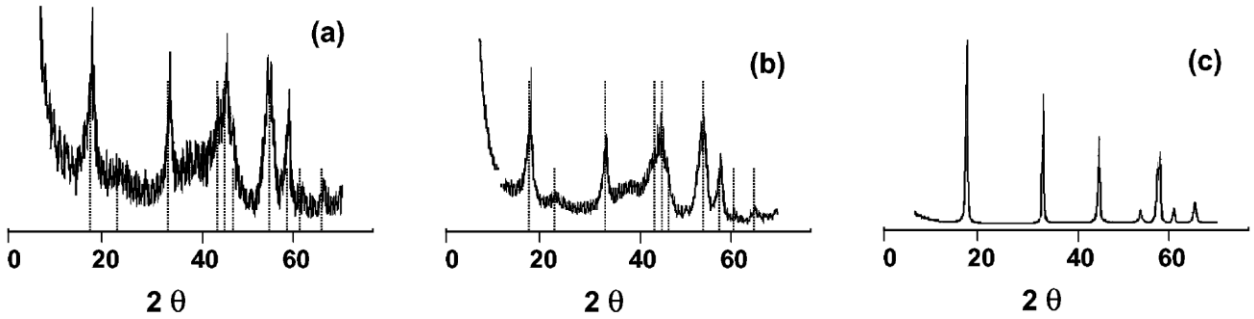

Figure 33 (adaptée). Diffractogrammes de RX d'une alumine suite à un traitement hydrothermal à 300°C en présence de (a) 25% de phénol dans l'eau, (b) 25% d'acide acétique dans l'eau et (c) de l'eau pure.[61]

I.3.4. Conclusion

Les travaux antérieurs rapportés dans la littérature ont montré que la présence de métaux supportés (Ni, Pt, Co…) utilisés comme phase active ainsi que de stabilisants comme Cl, P, F, Si, Zr…, ajoutés avec le précurseur métallique peuvent limiter la transformation de l'alumine (gamma principalement) en (oxy)hydroxyde d'aluminium en présence d'eau. Il est le plus souvent proposé que ces hétéroatomes se fixent sur les groupes réactifs du support (hydroxyles probablement) et les OH basiques de surface sont le plus souvent invoqués. Néanmoins, la plupart des travaux sur le sujet se contentent de balayer un spectre de candidats potentiels sans apporter de rationalisation à leur action.

Par ailleurs, il a aussi été montré que la présence de molécules organiques (de type polyols le plus souvent) permettait aussi d'améliorer la stabilité hydrothermale de l'alumine en se liant à sa surface. Il a ainsi été proposé que la décomposition de ces molécules organiques formait des couches carbonées qui augmentaient l'hydrophobicité de l'alumine et donc sa résistance hydrothermale.

Les études précédentes ont caractérisé principalement la phase solide c'est à dire le support stabilisé et ayant subi une hydratation. On peut cependant regretter que l'étude de la phase liquide permettant de discuter d'une éventuelle dissolution de l'alumine soit rarement rapportée. Cette étude sera donc partie intégrante de notre projet.

I.4. Conclusion et démarche de la thèse

L'amélioration de la résistance hydrothermale des supports à base d'alumine utilisés pour la réaction Fischer-Tropsch ainsi que pour la conversion de la biomasse est un enjeu majeur pour le développement de catalyseurs plus performants. Pour optimiser les performances chimiques et mécaniques de ces supports, il faut comprendre les mécanismes d'érosion (chimique) au niveau moléculaire et d'attrition (physique) au niveau microscopique afin de pouvoir rationaliser l'effet et le rôle des dopants dans leur dégradation. Ces résultats doivent permettre d'identifier et localiser les sites ou les faces responsables de la réactivité de l'alumine avec l'eau.

Il est à ce jour bien connu que l'alumine *s'hydrate* quand elle est en contact avec l'eau, c'est à dire que sa mise en suspension dans l'eau liquide conduit à la formation d'hydroxydes/oxyhydroxydes ($Al(OH)_3$/AlOOH). Le principal mécanisme de formation postulé implique des phénomènes de dissolution-précipitation. La nature des phases qui se forment, leur taille/morphologie, ainsi que leur quantité dépendent de paramètres expérimentaux tels que le pH, le temps et la température. A température ambiante, un pH acide (~5) favorise la formation de gibbsite alors qu'à un pH neutre ou basique (~7-11) c'est la bayerite qui est majoritaire. La gibbsite est pourtant le produit le plus stable thermodynamiquement sur toute la gamme de pH. Un pH fortement acide (pH< 4) inhibe la précipitation des hydroxydes et/ou favorise la formation d'une phase hydroxyde amorphe. Pour des températures supérieures à 100°C (conditions hydrothermales), la seule phase formée (à de rares exceptions près) est un oxyhydroxyde de type boehmite.

Dans le but de limiter la transformation de l'alumine en (oxy)hydroxydes dans l'eau, l'ajout de métaux, de stabilisants inorganiques et de molécules organiques au support a été proposé dans la littérature. Il a été suggéré que l'inhibition de l'hydratation de l'alumine peut être reliée à la substitution des OH basiques de surface, à la formation de liaisons ion métallique-hydroxyles de surface ou enfin à l'augmentation de l'hydrophobicité de la surface.

L'enjeu principal de ce travail est donc de préciser le mécanisme de formation des phases (oxy)hydroxydes, de déterminer le rôle des dopants et d'identifier les sites responsables de l'hydratation de l'alumine dans l'eau.

Le chapitre II fera la synthèse des expériences d'hydratation (appelées aussi vieillissement) de différentes alumines de transition (γ, δ, θ) dans des conditions douces (température ambiante ou 70°C) afin de mettre en évidence les effets séparés ou conjoints de la température, du temps de contact de l'alumine avec l'eau et de l'agitation. Ces conditions douces ont été choisies car aucune étude *systématique* de l'hydratation/dissolution de l'alumine dans l'eau n'a été conduite dans la littérature, malgré les nombreux travaux rapportés sur ce sujet (section I.2).

Le chapitre III sera divisé en deux parties. La partie A se concentrera sur les tests de vieillissement en conditions hydrothermales (autoclave sous pression) effectués sur une alumine pure. Il est à noter que les tests seront réalisés en présence d'une phase aqueuse majoritaire, donc dans des conditions d'hydratation modèles non comparables aux conditions réelles de synthèse Fischer-Tropsch. Pour cela, un couple température/pression a été défini afin d'éviter une dégradation complète de l'alumine et de pouvoir suivre les mécanismes se produisant et menant à son hydratation. Les résultats obtenus en conditions douces auront fourni des guides pour interpréter ceux obtenus en conditions hydrothermales. La partie B sera dédiée à l'étude de l'effet inhibiteur de molécules organiques (glycérol, butanol, xylitol, sorbitol, mannitol et heptane) ajoutées préalablement dans le milieu aqueux dans le but de comprendre leur mode d'action sur la réduction de l'hydratation de l'alumine et leur spécificité.

Enfin, le chapitre IV sera consacré à la compréhension du rôle de quatre inhibiteurs inorganiques d'hydratation de l'alumine : Mg, Zr, Ni et Si. Les résultats obtenus permettront de préciser la réactivité des différentes faces de l'alumine γ.

Dans l'ensemble de ce travail, la nature des phases hydroxydes formées ainsi que leur quantité ont été étudiées par DRX et ATG. La morphologie de ces phases ainsi que leur localisation ont été observées par microscopie électronique (MEB et MET). La spectroscopie IR a été mise en œuvre afin de préciser la nature chimique de la surface du support et tenter d'identifier les sites responsables de l'érosion. Le suivi de la concentration des ions aluminium en phase liquide a enfin été réalisé par ICP ou par fluorescence X.

I.5. Références

(1) Ahn, K. Y.; Forbes, L. Methods, Systems, and Apparatus for Atomic-Layer Deposition of Aluminum Oxides in Integrated Circuits, Brevet US 20030207032 A1, 2003.

(2) Korotkikh, S. M.; Babushkin, V. V. Electrolyte for Aluminum Oxide Capacitors, Brevet SU 1061182 A1, 1983.

(3) Wang, L.; Lu, C.; Chen, S.; Wu, H.; Meng, X. Preparation Method of Aluminum Oxide Porous Foamed Ceramic Sound-Absorbing Material, Brevet CN 105565783 A 2016.

(4) Xu, Y.; Ye, T.; Qiu, S.; Ning, S.; Gong, F.; Liu, Y.; Li, Q. High Efficient Conversion of CO_2-Rich Bio-Syngas to CO-Rich Bio-Syngas Using Biomass Char: A Useful Approach for Production of Bio-Methanol from Bio-Oil. *Bioresour. Technol.* **2011**, *102*, 6239–6245.

(5) Euzen, P.; Raybaud, P.; Krokidis, X.; Toulhoat, H.; Le Loarer, J.-L.; Jolivet, J.-P.; Froidefond, C. Alumina. In *Handbook of Porous Solids*; Schüth, F., Kenneth, Weitkamp, J., Eds.; Wiley-VCH Verlag GmbH, 2008; pp 1591–1677.

(6) Wefers, K.; Misra, C. *Oxides and Hydroxides of Aluminum*; Alcoa Laboratories, 1987.

(7) Papee, D.; Tertian, R.; Biais, R. Constitution of Gels and Crystalline Hydrates of Alumina. *Bull. Soc. Chim. Fr.* **1958**, 1301–1310.

(8) Ogorodova, L. P.; Kiseleva, I. A.; Sokolova, E. L.; Vigasina, M. F.; Kabalov, Y. K. Thermochemical Study of Polymorphic Modifications of $Al(OH)_3$: Gibbsite and Nordstrandite. *Geochem. Int.* **2012**, *50*, 90–94.

(9) Carrier, X.; Marceau, E.; Lambert, J.-F.; Che, M. Transformations of γ-Alumina in Aqueous Suspensions. *J. Colloid Interface Sci.* **2007**, *308*, 429–437.

(10) Digne, M.; Sautet, P.; Raybaud, P.; Toulhoat, H.; Artacho, E. Structure and Stability of Aluminum Hydroxides: A Theoretical Study. *J. Phys. Chem. B* **2002**, *106*, 5155–5162.

(11) Saalfeld, H.; Jarchow, O. Crystal Structure of Nordstrandite, Aluminum Hydroxide. *Neues Jahrb. Fuer Mineral. Abh.* **1968**, *109*, 185–191.

(12) Inoue, M.; Kondo, Y.; Inui, T. An Ethylene Glycol Derivative of Boehmite. *Inorg. Chem.* **1988**, *27*, 215–221.

(13) Bujoli, B.; Rouxel, J.; Palvadeau, P. In: Pillared Layered Structures, I. V. Mitchell (Ed.), Elsevier Applied Science, London, New York. **1993**, 79–90.

(14) Jolivet, J.-P.; Froidefond, C.; Pottier, A.; Chanéac, C.; Cassaignon, S.; Tronc, E.; Euzen, P. Size Tailoring of Oxide Nanoparticles by Precipitation in Aqueous Medium. A Semi-Quantitative Modelling. *J. Mater. Chem.* **2004**, *14*, 3281-3288.

(15) Du, X.; Wang, Y.; Su, X.; Li, J. Influences of pH Value on the Microstructure and Phase Transformation of Aluminum Hydroxide. *Powder Technol.* **2009**, *192*, 40–46.

(16) Lefèvre, G.; Pichot, V.; Fédoroff, M. Controlling Particle Morphology during Growth of Bayerite in Aluminate Solutions. *Chem. Mater.* **2003**, *15*, 2584–2592.

(17) Aldcroft, D.; Bye, G. C. Crystallization Processes in Aluminum Hydroxide Gels: Formation and Thermal Decomposition of Nordstrandite. *Sci. Ceram.* **1967**, *3*, 75–94.

(18) Lipin, V. A. A New Technique for Synthesis of Nordstrandite. *Russ. J. Appl. Chem. Transl. Zhurnal Prikl. Khimii* **2001**, *74*, 184–187.

(19) Tertian, R.; Papee, D. Thermal and Hydrothermal Transformations of Alumina. *J. Chim. Phys. Phys.-Chim. Biol.* **1958**, *55*, 341–353.

(20) Roelofs, F.; Vogelsberger, W. Dissolution Kinetics of Nanodispersed γ-Alumina in Aqueous Solution at Different pH: Unusual Kinetic Size Effect and Formation of a New Phase. *J. Colloid Interface Sci.* **2006**, *303*, 450–459.

(21) Lefèvre, G.; Duc, M.; Lepeut, P.; Caplain, R.; Fédoroff, M. Hydration of γ-Alumina in Water and Its Effects on Surface Reactivity. *Langmuir* **2002**, *18*, 7530–7537.

(22) Lange, J.-P. Renewable Feedstocks: The Problem of Catalyst Deactivation and Its Mitigation. *Angew. Chem. Int. Ed.* **2015**, *54*, 13186–13197.

(23) Xiong, H.; Pham, H. N.; Datye, A. K. Hydrothermally Stable Heterogeneous Catalysts for Conversion of Biorenewables. *Green Chem.* **2014**, *16*, 4627–4643.

(24) Koichumanova, K.; Vikla, A. K. K.; de Vlieger, D. J. M.; Seshan, K.; Mojet, B. L.; Lefferts, L. Towards Stable Catalysts for Aqueous Phase Conversion of Ethylene Glycol for Renewable Hydrogen. *ChemSusChem* **2013**, *6*, 1717–1723.

(25) Li, G.; Liu, Y.; Tang, Z.; Liu, C. Effects of Rehydration of Alumina on Its Structural Properties, Surface Acidity, and HDN Activity of Quinoline. *Appl. Catal. A Gen.* **2012**, *437-438*, 79–89.

(26) Sádaba, I.; López Granados, M.; Riisager, A.; Taarning, E. Deactivation of Solid Catalysts in Liquid Media: The Case of Leaching of Active Sites in Biomass Conversion Reactions. *Green Chem* **2015**, *17*, 4133–4145.

(27) Luo, N.; Fu, X.; Cao, F.; Xiao, T.; Edwards, P. P. Glycerol Aqueous Phase Reforming for Hydrogen Generation over Pt Catalyst – Effect of Catalyst Composition and Reaction Conditions. *Fuel* **2008**, *87*, 3483–3489.

(28) Tan, J.; Cui, J.; Ding, G.; Deng, T.; Zhu, Y.; Li, Y. Efficient Aqueous Hydrogenation of Levulinic Acid to γ-Valerolactone over a Highly Active and Stable Ruthenium Catalyst. *Catal Sci Technol* **2016**, *6*, 1469–1475.

(29) Rzhevskii, A. M.; Ribeiro, F. H. UV Raman Spectroscopic Study of Hydrogen Bonding in Gibbsite and Bayerite between 93 and 453 K. *J. Raman Spectrosc.* **2001**, *32*, 923–928.

(30) Ruan, H. D.; Frost, R. L.; Kloprogge, J. T. Comparison of Raman Spectra in Characterizing Gibbsite, Bayerite, Diaspore and Boehmite. *J. Raman Spectrosc.* **2001**, *32*, 745–750.

(31) Franck, J. P.; Freund, E.; Quéméré, E. Textural and Structural Changes in Transition Alumina Supports. *J. Chem. Soc. Chem. Commun.* **1984**, 629–630.

(32) Laiti, E.; Persson, P.; Öhman, L.-O. Balance between Surface Complexation and Surface Phase Transformation at the Alumina/water Interface. *Langmuir* **1998**, *14*, 825–831.

(33) Chen, Y.; Hyldtoft, J.; Jacobsen, C. J.; Nielsen, O. F. NIR FT Raman Spectroscopic Studies of H-Al2O3 and Mo/η-Al_2O_3 Catalysts. *Spectrochim. Acta. A. Mol. Biomol. Spectrosc.* **1995**, *51*, 2161–2169.

(34) Dyer, C.; Hendra, P. J.; Forsling, W.; Ranheimer, M. Surface Hydration of Aqueous γ-Al_2O_3 Studied by Fourier Transform Raman and Infrared spectroscopy—I. Initial Results. *Spectrochim. Acta Part Mol. Spectrosc.* **1993**, *49*, 691–705.

(35) Zhang, J.; Chen, J.; Ren, J.; Sun, Y. Chemical Treatment of γ-Al_2O_3 and Its Influence on the Properties of Co-Based Catalysts for Fischer–Tropsch Synthesis. *Appl. Catal. A Gen.* **2003**, *243*, 121–133.

(36) Jun-Cheng, L.; Lan, X.; Feng, X.; Zhan-Wen, W.; Fei, W. Effect of Hydrothermal Treatment on the Acidity Distribution of γ-Al_2O_3 Support. *Appl. Surf. Sci.* **2006**, *253*, 766–770.

(37) Mironenko, R. M.; Belskaya, O. B.; Talsi, V. P.; Gulyaeva, T. I.; Kazakov, M. O.; Nizovskii, A. I.; Kalinkin, A. V.; Bukhtiyarov, V. I.; Lavrenov, A. V.; Likholobov, V. A. Effect of γ-Al_2O_3 Hydrothermal Treatment on the Formation and Properties of Platinum Sites in Pt/γ-Al_2O_3 Catalysts. *Appl. Catal. A Gen.* **2014**, *469*, 472–482.

(38) Ravenelle, R. M.; Copeland, J. R.; Kim, W.-G.; Crittenden, J. C.; Sievers, C. Structural Changes of γ-Al_2O_3-Supported Catalysts in Hot Liquid Water. *ACS Catal.* **2011**, *1*, 552–561.

(39) Zhou, Y.; Fu, H.; Zheng, X.; Li, R.; Chen, H.; Li, X. Hydrogenation of Methyl Propionate over Ru–Pt/AlOOH Catalyst: Effect of Surface Hydroxyl Groups on Support and Solvent. *Catal. Commun.* **2009**, *11*, 137–141.

(40) De Vlieger, D. J. M.; Chakinala, A. G.; Lefferts, L.; Kersten, S. R. A.; Seshan, K.; Brilman, D. W. F. Hydrogen from Ethylene Glycol by Supercritical Water Reforming Using Noble and Base Metal Catalysts. *Appl. Catal. B Environ.* **2012**, *111-112*, 536–544.

(41) Elliott, D. C.; Sealock Jr, L. J.; Baker, E. G. Chemical Processing in High-Pressure Aqueous Environments. 2. Development of Catalysts for Gasification. *Ind. Eng. Chem. Res.* **1993**, *32*, 1542–1548.

(42) El Doukkali, M.; Iriondo, A.; Cambra, J. F.; Arias, P. L. Recent Improvement on H_2 Production by Liquid Phase Reforming of Glycerol: Catalytic Properties and Performance, and Deactivation Studies. *Top. Catal.* **2014**, *57*, 1066–1077.

(43) Koichumanova, K.; Sai Sankar Gupta, K. B.; Lefferts, L.; Mojet, B. L.; Seshan, K. An in Situ ATR-IR Spectroscopy Study of Aluminas under Aqueous Phase Reforming Conditions. *Phys. Chem. Chem. Phys.* **2015**, *17*, 23795–23804.

(44) Ram, S. Infrared Spectral Study of Molecular Vibrations in Amorphous, Nanocrystalline and $AlO(OH)\cdot\alpha H_2O$ Bulk Crystals. *Infrared Phys. Technol.* **2001**, *42*, 547–560.

(45) Tunega, D.; Pašalić, H.; Gerzabek, M. H.; Lischka, H. Theoretical Study of Structural, Mechanical and Spectroscopic Properties of Boehmite (γ-AlOOH). *J. Phys. Condens. Matter* **2011**, *23*, 404201.

(46) Dickie, S. A.; McQuillan, A. J. In-Situ Infrared Spectroscopic Studies of Adsorption Processes on Boehmite Particle Films: Exchange of Surface Hydroxyl Groups Observed upon Chelation by Acetylacetone. *Langmuir* **2004**, *20*, 11630–11636.

(47) Kiss, A. B.; Keresztury, G.; Farkas, L. Raman and IR Spectra and Structure of Boehmite (γ-AlOOH). Evidence for the Recently Discarded D172h Space Group. *Spectrochim. Acta Mol. Spectrosc.* **1980**, *36*, 653-658.

(48) Raybaud, P.; Digne, M.; Iftimie, R.; Wellens, W.; Euzen, P.; Toulhoat, H. Morphology and Surface Properties of Boehmite (γ-AlOOH): A Density Functional Theory Study. *J. Catal.* **2001**, *201*, 236–246.

(49) Mukhambetov, I. N.; Lamberov, A. A. Effect of Hydrothermal Treatment on the Structure and Acid Properties of the Surface of Molded Gamma-Aluminum Oxide. *Russ. J. Appl. Chem.* **2014**, *87*, 676–683.

(50) Knözinger, H.; Ratnasamy, P. Catalytic Aluminas: Surface Models and Characterization of Surface Sites. *Catal. Rev.* **1978**, *17*, 31–70.

(51) Li, H.; Xu, Y.; Gao, C.; Zhao, Y. Structural and Textural Evolution of Ni/γ-Al_2O_3 Catalyst under Hydrothermal Conditions. *Catal. Today* **2010**, *158*, 475–480.

(52) Ketchie, W. C.; Maris, E. P.; Davis, R. J. In-Situ X-Ray Absorption Spectroscopy of Supported Ru Catalysts in the Aqueous Phase. *Chem. Mater.* **2007**, *19*, 3406–3411.

(53) Ravenelle, R. M.; Diallo, F. Z.; Crittenden, J. C.; Sievers, C. Effects of Metal Precursors on the Stability and Observed Reactivity of Pt/γ-Al_2O_3 Catalysts in Aqueous Phase Reactions. *ChemCatChem* **2012**, *4*, 492–494.

(54) Wang, X.; Pan, D.; Guo, M.; He, M.; Niu, P.; Li, R. Facile Synthesis of Highly Ordered Mesoporous Alumina with High Thermal and Hydrothermal Stability Using Zirconia as Promoter. *Mater. Lett.* **2013**, *97*, 27–30.

(55) Chen, Y.-W.; Lin, C.-S.; Hsu, W.-C. Hydrothermal Stability of Aluminophosphate Catalyst Supports. *Catal. Lett.* **1989**, *3*, 99–102.

(56) Ha, K.-S.; Jung, G.-I.; Woo, M.-H.; Jun, K.-W.; Bae, J. W. Effects of Phosphorus and Saccharide on Size, Shape, and Reducibility of Fischer–Tropsch Catalysts for Slurry Phase and Fixed-Bed Reactions. *Appl. Catal. A Gen.* **2013**, *453*, 358–369.

(57) Zhang, J.; Chen, J.; Ren, J.; Sun, Y. Chemical Treatment of γ-Al_2O_3 and Its Influence on the Properties of Co-Based Catalysts for Fischer-Tropsch Synthesis. *Appl. Catal. A Gen.* **2003**, *243*, 121–133.

(58) Bae, J. W.; Kim, S.-M.; Lee, Y.-J.; Lee, M.-J.; Jun, K.-W. Enhanced Fischer-Tropsch Activity on Co/P-Al_2O_3 Catalyst: Effect of Phosphorous Content. *Catal. Commun.* **2009**, *10*, 1358–1362.

(59) Chary, K. V. R.; Kishan, G.; Ramesh, K.; Kumar, C. P.; Vidyasagar, G. Synthesis, Characterization, and Catalytic Properties of Vanadium Oxide Catalysts Supported on $AlPO_4$. *Langmuir* **2003**, *19*, 4548–4554.

(60) Bautista, F. M.; Campelo, J. M.; Garcia, A.; Luna, D.; Marinas, J. M.; Romero, A. A.; Colon, G.; Navio, J. A.; Macias, M. Structure, Texture, Surface Acidity, and Catalytic Activity of $AlPO_4$-ZrO_2 (5-50 Wt% ZrO_2) Catalysts Prepared by a Sol-Gel Procedure. *J. Catal.* **1998**, *179*, 483–494.

(61) Stanislaus, A.; Al-Dolama, K.; Absi-Halabi, M. Preparation of a Large Pore Alumina-Based HDM Catalyst by Hydrothermal Treatment and Studies on Pore Enlargement Mechanism. *J. Mol. Catal. Chem.* **2002**, *181*, 33–39.

(62) Van de Loosdrecht, J.; Barradas, S.; Caricato, E. A.; Van Berge, P. J.; Visagie, J. L. Support Modification of Cobalt Based Slurry Phase Fischer-Tropsch Catalysts. *Preprints of Symposia - American Chemical Society, Division of Fuel Chemistry* **2000**, *45*, 587–591.

(63) Keyvanloo, K.; Hecker, W. C.; Woodfield, B. F.; Bartholomew, C. H. Highly Active and Stable Supported Iron Fischer–Tropsch Catalysts: Effects of Support Properties and SiO_2 Stabilizer on Catalyst Performance. *J. Catal.* **2014**, *319*, 220–231.

(64) Li, S.; Chen, H.; Shen, J. Preparation of Highly Active and Hydrothermally Stable Nickel Catalysts. *J. Colloid Interface Sci.* **2015**, *447*, 68–76.

(65) Jothimurugesan, K. Stable Support for Fischer-Tropsch Catalyst. Brevet WO 2016/039861 Al, 2016.

(66) Jothimurugesan, K. Support For Fischer-Tropsch Catalyst Having Improved Activity. Brevet US 9,233,358 BI, 2016.

(67) Jothimurugesan, K.; Muraoka, M. Support For Fischer-Tropsch Catalyst Having Improved Activity. Brevet WO 2016/039862 Al, 2016.

(68) Ravenelle, R. M.; Copeland, J. R.; Pelt, A. H.; Crittenden, J. C.; Sievers, C. Stability of Pt/γ-Al_2O_3 Catalysts in Model Biomass Solutions. *Top. Catal.* **2012**, *55*, 162–174.

(69) Copeland, J. R.; Shi, X.-R.; Sholl, D. S.; Sievers, C. Surface Interactions of C_2 and C_3 Polyols with γ-Al_2O_3 and the Role of Coadsorbed Water. *Langmuir* **2013**, *29*, 581–593.

(70) Copeland, J. R.; Santillan, I. A.; Schimming, S. M.; Ewbank, J. L.; Sievers, C. Surface Interactions of Glycerol with Acidic and Basic Metal Oxides. *J. Phys. Chem. C* **2013**, *117*, 21413–21425.

(71) Jongerius, A. L.; Copeland, J. R.; Foo, G. S.; Hofmann, J. P.; Bruijnincx, P. C. A.; Sievers, C.; Weckhuysen, B. M. Stability of Pt/γ-Al_2O_3 Catalysts in Lignin and Lignin Model Compound Solutions under Liquid Phase Reforming Reaction Conditions. *ACS Catal.* **2013**, *3*, 464–473.

(72) Pham, H. N.; Anderson, A. E.; Johnson, R. L.; Schmidt-Rohr, K.; Datye, A. K. Improved Hydrothermal Stability of Mesoporous Oxides for Reactions in the Aqueous Phase. *Angew. Chem. Int. Ed.* **2012**, *51*, 13163–13167.

(73) Massa, P.; Ivorra, F.; Haure, P.; Fenoglio, R. Optimized Wet-Proofed CuO/Al_2O_3 Catalysts for the Oxidation of Phenol Solutions: Enhancing Catalytic Stability. *Catal. Commun.* **2009**, *10*, 1706–1710.

Chapitre II

Chemical weathering and physical attrition of alumina in aqueous suspension at ambient pressure: a mechanistic study

II. Chemical weathering and physical attrition of alumina in aqueous suspension at ambient pressure: a mechanistic study. 61

II.1. Préambule 61

II.2. Introduction 63

II.3. Materials and methods 65

II.4. Results 68

II.4.1. Identification of the hydration products 68

II.4.2. pH evolution 69

II.4.3. Liquid-phase aluminum concentration 70

II.4.4. Evolution and location of hydroxide phases 73

II.4.5. Formation of hydroxide polymorphs from γ-Al_2O_3 as a function of time 76

II.4.6. Alumina polymorphs hydration 79

II.5. Conclusion 81

II.6. References 83

II.7. Supplementary information 87

II.7.1. Quantitative analysis by TGA and XRD 90

II.8. Annex – Acidic medium 97

II.8.1. Nitric acid 97

II.8.2. Acetic acid 98

II.8.3. Conclusion 103

II.8.4. References 103

II. Chemical weathering and physical attrition of alumina in aqueous suspension at ambient pressure: a mechanistic study.

II.1. Préambule

L'alumine subit une dégradation chimique et physique (érosion et attrition, respectivement) quand elle est exposée à un milieu aqueux (Chapitre I). Une étude systématique de l'hydratation de l'alumine dans une suspension aqueuse sera présentée ici afin d'expliquer les mécanismes conduisant à la dégradation de l'alumine.

Des traitements d'hydratation de différentes alumines de transition (γ, δ, θ et des mélanges de ces phases) ont été effectués sous conditions douces (pression atmosphérique, température ambiante ou 70°C) afin de mettre en évidence le rôle de la température, du temps de contact entre l'alumine et l'eau et de l'agitation sur la dégradation de l'alumine.

Les études quantitatives et qualitatives par différentes techniques de caractérisation (DRX, ATG, MEB, ICP-OES ...) nous ont permis de suivre l'évolution du matériau. Ceci nous conduira à proposer un mécanisme global pour l'hydratation de l'alumine dans ces conditions.

Ces résultats sont présentés sous la forme d'une publication scientifique rédigée en anglais.

Chemical weathering and physical attrition of alumina in aqueous suspension at ambient pressure: a mechanistic study.

Jane Abi Aad,[a,b] Sandra Casale,[a] Philippe Courty,[b] Mathieu Michau,[b] Fabrice Diehl,[b] Eric Marceau*,[a,c] Xavier Carrier* [a]

[a] Sorbonne Universités, UPMC Univ Paris 06, CNRS, Laboratoire de Réactivité de Surface, F-75005, Paris, France

[b] IFP Energies nouvelles, BP3, Rond-Point de l'échangeur de Solaize, F-69360 Solaize, France

[c] Univ. Lille, CNRS, Centrale Lille, ENSCL, Univ. Artois, UMR 8181 - UCCS - Unité de Catalyse et Chimie du Solide, F-59000 Lille, France.

KEYWORDS: alumina, hydration mechanism, dissolution, precipitation, aluminum hydroxide, chemical weathering, catalysis

ABSTRACT: Transition aluminas rank among the main supports used for heterogeneous catalysts. Their stability when contacted with an aqueous phase is a key issue for catalytic processes, as their hydration can be strongly detrimental to their physico-chemical and mechanical properties. As a consequence, the design of more stable alumina supports relies on a better understanding of the mechanisms leading to their chemical and physical degradation, by weathering and attrition, respectively. It is shown here that when suspended in water at atmospheric pressure and at temperatures up to 70°C, all transition aluminas (from γ to θ) transform into $Al(OH)_3$ polymorphs (bayerite, gibbsite and nordstrandite), though to different extents. A quantitative study of the aluminum concentration in solution and of the amount of hydroxides formed through time demonstrates that Al_2O_3 hydration occurs via a two-step dissolution / heterogeneous precipitation process, with nucleation of $Al(OH)_3$ starting on the surface of the alumina grains and followed by particle growth. The grains become more fragile because of chemical weathering; the ensuing mechanical degradation by attrition, in turn, brings the weathering process to completion. The nature of the main hydroxide polymorph is a function of aluminum concentration and ageing time: first the kinetic product, bayerite, forming from aluminum supersaturated solutions, then nordstrandite and eventually gibbsite, the most thermodynamically stable hydroxide, during the steady-state stage of precipitation. Increasing crystallinity and decreasing specific surface area of alumina lead to a reduced amount of hydroxides formed, which can be explained both by a thermodynamic and kinetic control of alumina dissolution.

II.2. Introduction

Transition aluminas are the predominant oxide supports used in heterogeneous catalysis.[1] Within this family of oxides, γ-alumina exhibits the most interesting properties such as a high specific surface area, thermal stability and mechanical resistance.[1] It is thus used in a wide range of catalytic applications, not only in the gas phase, but also in aqueous phases, for water depollution[2], for aldol condensation[3] or for the processing of biosourced molecules.[4,5] Water is essential here as a green solvent.[5] Catalysts are also exposed to water coming from the biomass and released during the process.

However, it has been repeatedly shown that γ-Al_2O_3 does not remain chemically inert when contacted with an aqueous phase: it undergoes *chemical degradation (*or *weathering)* into hydroxides ($Al(OH)_3$) and/or oxy-hydroxides (AlOOH) phases.[6–8] This degradation process, in combination with *physical degradation* (or *attrition*), may trigger leaching of the active phase, and is the source of fine particles that may cause plugging problems while operating in continuous reactors, as is also encountered under the harsh conditions of the Fischer-Tropsch synthesis when it is carried out in slurry bubble column reactors.[9] This explains why denser supports, such as α-Al_2O_3 or ZrO_2, have been explored for reactions taking place in hydrothermal conditions,[10] despite their lower specific surface area. A better understanding of the mechanism leading to alumina *hydration* (a term we will use in a generic sense to cover the formation of hydroxides whatever their nature and origin) is thus a definite prerequisite for the development of more stable catalysts both in an aqueous phase and in continuous or slurry reactors.

Though there is broad experimental evidence of the hydration of γ-alumina in aqueous solution, the genesis of the hydration products and, secondly, the preferential formation of one hydration product over the other, are not fully explained yet. In particular, while boehmite γ-AlOOH is clearly favored in hydrothermal conditions,[7,11–15] the nature of the γ-alumina hydration products seems to highly depend on experimental conditions at lower temperatures and ambient pressure. Carrier *et al*.[6] have postulated the formation of an amorphous aluminum hydroxide phase at very low pH (below 4). At acidic pH, the formation of gibbsite tends to predominate, whereas at basic pH, bayerite is the major phase.[6,11,16–19] The formation of hydration products is also thermally activated.[8] Dyer *et al.* showed that the amount of bayerite formed at 60°C is larger than at 20°C while hydration time is shorter (10 days instead of 4 months).[20] The ageing time in water has also an effect on the growth of hydroxide particles.[13] This was demonstrated by Lefèvre *et al.*[17] who have shown that the amount of bayerite formed after ageing alumina at room temperature strongly increases between 2 weeks and 6 months. Only very few studies have mentioned an effect of stirring on alumina hydration. Chen *et al*.[21] have reported that when a η-Al_2O_3 suspension is stirred at room temperature for 24 h, stirring may guide the nature of the polymorph formed: bayerite is formed in static conditions and boehmite in stirred conditions. Finally, most hydration studies have

been carried out on γ-Al_2O_3 and the influence of the type of alumina polymorph on the hydration process has been overlooked so far.

The fact that at least four experimental parameters (pH, temperature, ageing time and stirring), often varied independently, influence the transformation of alumina in water may explain why only a few studies have proposed a mechanism to account for alumina hydration. While it has been assumed that hydroxide particles are formed through a dissolution-precipitation mechanism followed by nucleation/growth,[16,17] Carrier *et al*.[6] proposed two mechanisms that may well occur in parallel: i) surface hydration through hydrolysis of Al-O bonds or ii) dissolution of γ-Al_2O_3 and subsequent precipitation proved by the observation of independent hydroxide particles after ageing.

Our goal is to bring a complete view of the evolution of alumina suspensions in heated water, by investigating both the liquid phase and the evolution of the microstructure of the solids. In the present work, γ-Al_2O_3 and other alumina polymorphs have been subjected to ageing treatments at 70°C, which will allow us to systematically explore the physico-chemical parameters responsible for their chemical degradation (weathering) and for their physical degradation (attrition) in stirred suspension. A quantitative evaluation by X-ray diffraction and thermogravimetric analysis of the amount of hydroxide formed after ageing has been complemented with scanning electron microscopy measurements and liquid-phase Al elemental analysis, to allow us to propose a comprehensive mechanism for alumina hydration in these conditions.

II.3. Materials and methods

Five transition aluminas were obtained by calcination of a commercial boehmite powder (Sasol Pural® SB3 SCCa, Na: 20 ppm, Si: 50 ppm, Fe: 60 ppm and Ti: 60 ppm) in static air in a muffle furnace, with a heating rate of 10°C/min and a plateau at the calcination temperature of 12 h. The following transition aluminas were obtained at different calcination temperatures[1,22] and characterized by XRD (Figure 1) and N_2 physisorption:

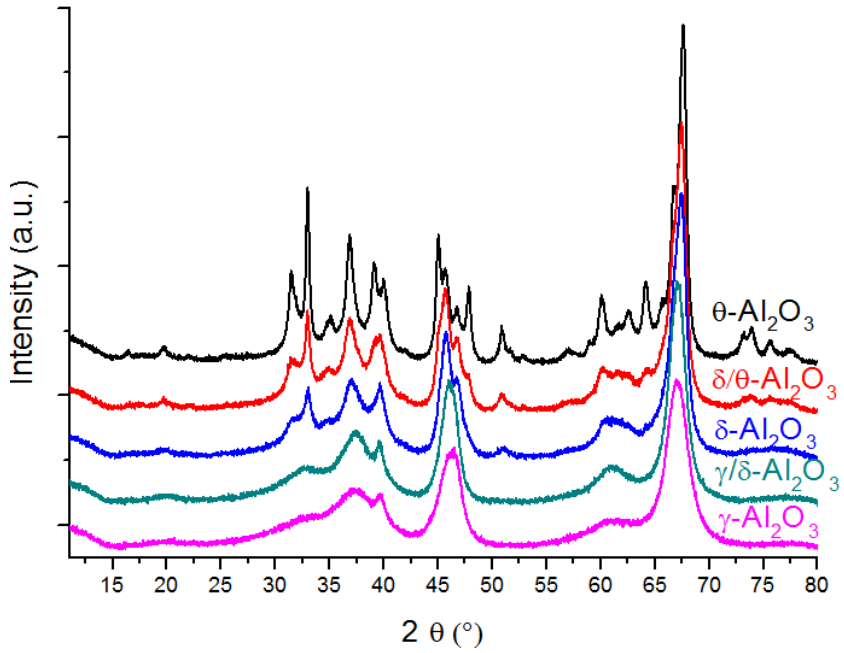

Figure 1. XRD patterns of transition aluminas obtained by calcination of boehmite at: 500°C (γ-Al_2O_3, pink, PDF No. 10-0425), 700°C (γ/δ-Al_2O_3, green), 850°C (δ-Al_2O_3, blue, PDF No. 16-0394), 900°C (δ/θ-Al_2O_3, red) and 1000°C (θ-Al_2O_3, black, PDF No. 23-1009).

- 500°C: γ-Al_2O_3 (238 m^2/g)
- 700°C: γ/δ-Al_2O_3 (183 m^2/g)
- 850°C: δ-Al_2O_3 (110 m^2/g)
- 900°C: δ/θ-Al_2O_3 (109 m^2/g)
- 1000°C: θ-Al_2O_3 (77 m^2/g)

γ/δ-Al_2O_3 and δ/θ-Al_2O_3 appear as mixtures between the γ and δ, and between the δ and θ polymorphs, respectively. The diagram of thermal transformation of transition aluminas is presented in the supplementary information (Figure S1). SEM images show that the morphology of the boehmite grains was conserved when it was thermally transformed into transition aluminas (Figure S2). Size of the grains is comprised between 40 and 80 μm. TEM pictures (not shown) provide evidence that at a smaller scale, the γ-Al_2O_3 grains consist of the agglomeration of 10-30 nm individual elongated nanoparticles, and the δ/θ-Al_2O_3 grains of significantly larger, 10-100 nm platelets.

For the ageing tests, the various alumina polymorphs were suspended in distilled water (initial pH: 5.8) with an oxide/water content of 0.6 g/30 mL, either at 25°C (for control experiments) or 70°C, under continuous magnetic stirring at 400 rpm (using a PTFE-coated magnetic bar). Experiments performed at 70°C were conducted in a round-bottomed flask equipped with a reflux condenser to avoid water evaporation. The filtrate was separated from the solid by centrifuging, followed by extraction using a syringe equipped with a filter of 0.2 µm porosity.

X-Ray diffraction patterns were recorded with a Bruker D8 Advanced diffractometer operated at 30 kV and 5 mA in the θ–2θ mode with Bragg–Brentano geometry using CuKα radiation (λ = 1.5418 Å). The diffractometer is equipped with a back monochromator and a scintillation detector. A scan rate of 0.5 step per second was used from 2θ = 10 to 80°.

Specific surface areas were determined by nitrogen physisorption (Brunauer-Emmett-Teller model (BET)), performed with a BELSORP-max analyzer from BelJapan, after degassing the samples for 1 night at 150°C.

Combined thermogravimetric and differential thermal analyses (TGA-DTA) were performed with a SDT Q600 TA instrument. The samples were heated in a flow of nitrogen (100 mL/min) at a heating rate of 10 °C/min.

SEM-FEG images were recorded with a Hitachi SU-70 Field Emission Gun Scanning Electron Microscope. The powder samples were fixed on an alumina SEM support with a carbon adhesive tape and observed without any metallization. Low accelerating voltage (1 kV) was used and the working distance was either about 3 or 15 mm. According to these experimental conditions, images were obtained by an “in Lens” secondary electron detector (SE-Upper). TEM-microtomy images were recorded with a JEOL JEM 1011 microscope at 1000 KV with a tungsten filament and with a Orius Gatan camera.

Liquid-phase elemental analysis of dissolved Al was performed by X-ray fluorescence (XRF) with a SPECTRO XEPOS analyzer from AMETEK materials analysis division and by ICP-OES with a Thermo Fischer Scientific iCAP series 6000.

II.4. Results

II.4.1. Identification of the hydration products

After ageing of the transition aluminas in liquid water at 25 or 70°C, the formation of aluminum hydroxides $Al(OH)_3$ was observed by XRD, in particular with reflections well visible between 2θ = 18 and 20° (Figure 2 for ageing at 70°C during 7 days (168 h), Figure S3 for ageing at 25°C during 25 days (600 h)). Two polymorphs were observed in all cases: gibbsite and bayerite, whose main characteristic peaks are located at 2θ = 18.2, 20.3, 27.9, 36.5, 37.3°, 52.2° and 53.9° for the former (PDF No. 33-18), and at 18.8, 20.3, 27.9, 40.5 and 53.2° for the latter (PDF No. 20-11). The formation of these hydroxides at 25 or 70°C under atmospheric pressure is consistent with previous reports[6,11,16–18] and with the thermodynamic instability of γ-Al_2O_3.[6] A third polymorph, seldom reported, nordstrandite, whose structure is intermediate between that of bayerite and gibbsite in terms of $Al(OH)_3$ layers stacking,[23] was also detected, with diffraction peaks at 2θ = 18.5, 44.7 and 47.74° (PDF No. 01-085-1049), but only when alumina was subjected to ageing treatments at 70°C.

Sections 3.2 to 3.5 will give a detailed description of the results obtained on γ-Al_2O_3, since it is the most reactive polymorph and also the most investigated in the literature due to its industrial applications. The hydration of γ-Al_2O_3 has been followed as a function of time at 70°C, with experiments done at 25°C mostly used as reference. It can be noted that pH measurements were carried out after cooling to room temperature, and that nitric acid was added after recovery of the liquid phase by filtration, in order to prevent $Al(OH)_3$ precipitation before elemental analysis of aluminum was performed. Characterization thus reflects the composition of the system once it has come back to room temperature, at the moment when separation between the solid and liquid phases takes place. The hydration of the other polymorphs will be detailed in section 3.6.

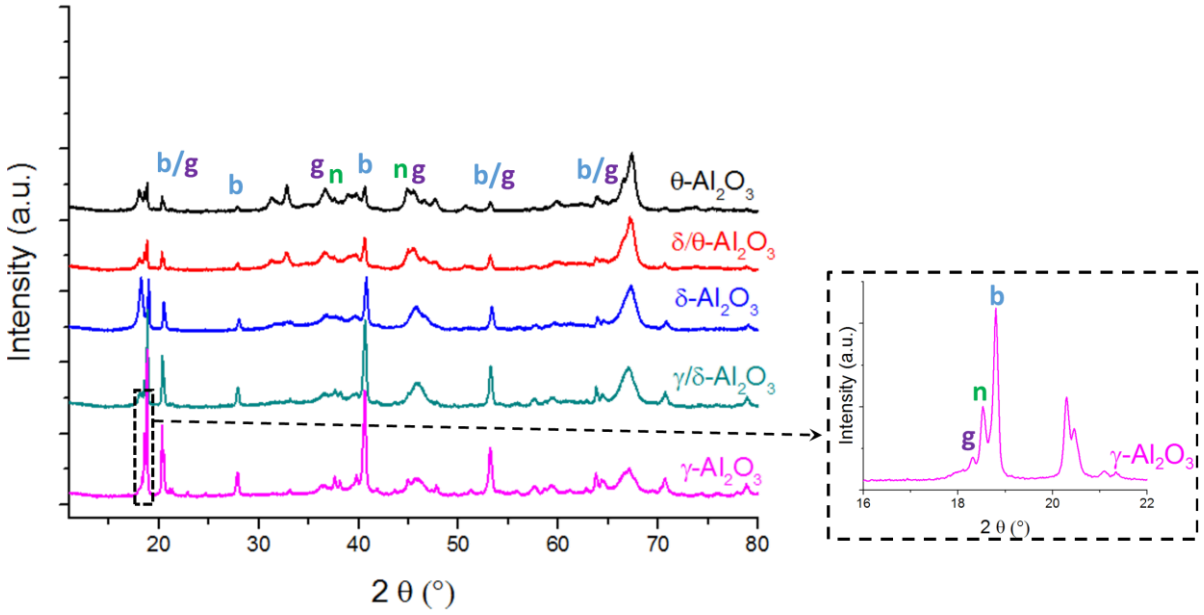

Figure 2. XRD patterns of γ-Al_2O_3 (pink), γ/δ-Al_2O_3 (green), δ-Al_2O_3 (blue), δ/θ-Al_2O_3 (red) and θ-Al_2O_3 (black) subjected to an ageing treatment in water at 70°C under stirring during 7 days (168 h) (0.6g/30 mL). g: gibbsite (PDF No. 33-18), n: nordstrandite (PDF No. 85-1049) and b: bayerite (PDF No. 20-11).

II.4.2. pH evolution

The pH of γ-Al_2O_3-water suspensions was measured after ageing under stirring at 25°C (open circles) and 70°C (filled circles), in order to better interpret the evolution of aluminum speciation (Figure 3). The pH of heated distilled water as a function of time is also given for comparison; the acidic pH results from the presence of dissolved hydrogenocarbonates. In contrast, the clear increase of pH at 25 and 70°C is directly linked to the hydration of γ-Al_2O_3. At 70°C, the pH increase to 8 during the first 2 h is followed by a slight decrease to 7, and then to a new increase to 8 after 24 h. The same pattern is observed at 25°C though it is delayed and less marked.

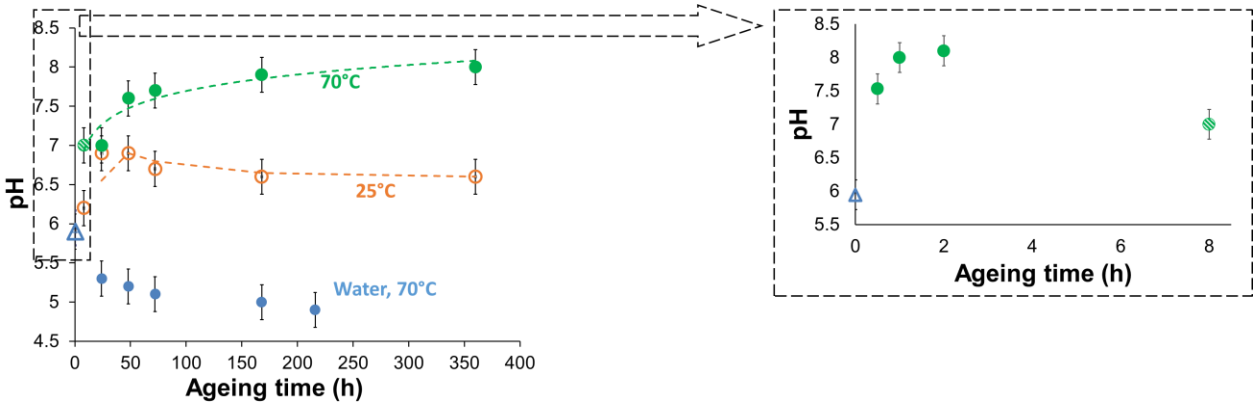

Figure 3. Variation of pH for γ-Al_2O_3-water suspensions (0.6 g/30 mL distilled water, atm. pressure) after an ageing treatment at 70°C (green filled circles) and at 25°C (orange open circles) during 15 days (360 h). pH of distilled water left at 70°C is shown with blue filled circles. Initial pH for all experiments is shown with an empty triangle (Δ). Note: all pHs were measured after cooling down the suspension to room temperature. Inset shows the pH evolution in the first hours for the ageing treatment at 70°C.

II.4.3. Liquid-phase aluminum concentration

Liquid-phase Al(III) concentrations were analyzed in the solutions obtained after filtration of the γ-Al_2O_3-water suspensions aged at 70°C. Al(III) concentrations were determined by XRF (short ageing times, ≤ 2 h) and ICP-OES (long ageing times, ≥ 8 h). Results are reported on Figure 4 along with the solubility curves of γ-Al_2O_3, bayerite and gibbsite. These curves were calculated with the ChemEQL software[24] by taking into account the aqueous phase equilibria implying monomeric species and some polymeric species of Al(III) ($Al_2(OH)_2^{4+}$ and $Al_3(OH)_4^{5+}$) in equilibrium with the solid phases. The Gibbs free energies of formation taken from the literature and listed in Table S1 were used for the different solid phases (bayerite, gibbsite and γ-alumina), while the equilibrium constants from the ChemEQL database (Martell and Smith, Stumm and Morgan) were used for the aqueous-phase species.

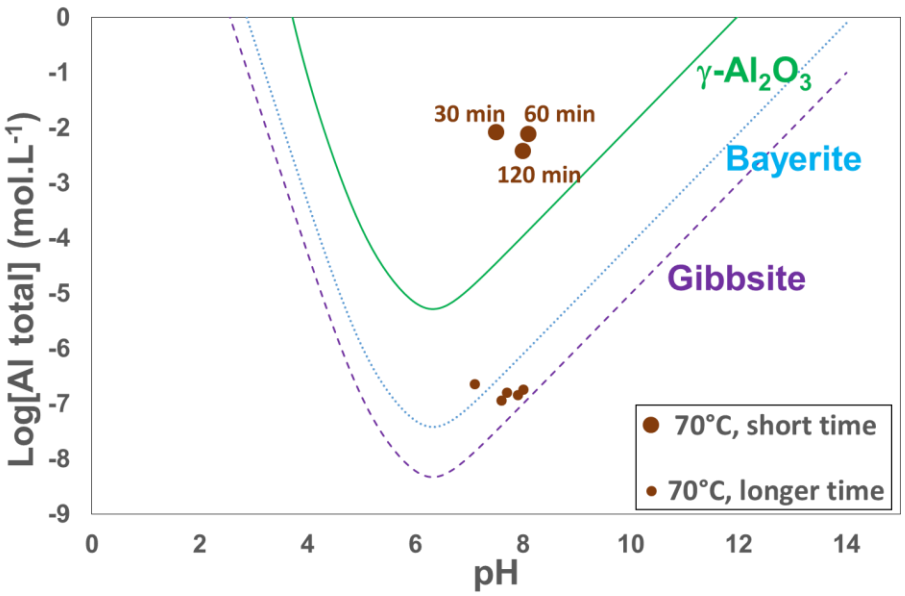

Figure 4. Calculated concentrations of Al(III) in solution (log scale) as a function of pH for γ-Al_2O_3 (solid green line), bayerite (dotted blue line), and gibbsite (dashed purple line). Experimental data points are shown as filled circles for suspensions aged at 70°C (short time ≤ 2 h, longer time ≥ 8 h) (0.6 g/30 mL for distilled water, atm. pressure).

By comparing the experimental Al(III) concentrations in solution obtained from ageing at 70°C with the different solubility curves, two major stages can be distinguished:

i. For short ageing times (≤2 h), values are consistent with γ-alumina solubility and supernatant liquors are supersaturated with respect to $Al(OH)_3$ precipitation. This tends to indicate that at this early stage *alumina dissolution* by reaction with water is the predominant phenomenon. Given the pH range (6 to 8) and the large difference in terms of orders of magnitude between the low amount of free OH^- ions, quantified by pH measurements *before* acidification of the supernatant liquor, and the high amount of Al^{3+} ions, quantified *after* acidification of the supernatant liquor, it is likely that aluminum is present in solution as $[Al(H_2O)_x(OH)_y]^{(3-y)-}$ complexes, oligomers of hydroxo complexes, or $Al(OH)_3$ colloids smaller than 200 nm, which corresponds to the porosity of the filter.

ii. For longer ageing times (≥8 h), dissolved Al(III) concentrations remain almost constant and they are consistent with $Al(OH)_3$ solubility. The existence of a pH plateau after 50 h tends to indicate that a steady-state is reached between the production and

consumption of OH^- ions. After a few hours of ageing, *hydroxide precipitation* regulates pH and Al concentration in solution.

This dissolution-precipitation mechanism is consistent with previous results from Carrier *et al.*[6] for experiments conducted in much more basic conditions (pH = 11) and from Lefèvre *et al.*[17] It is also in agreement with some concentration profiles as a function of ageing time given by Roelofs and Vogelbergers[16] in an intermediate pH range (5 to 10).

At short ageing times (up to 2 h), the pH and [Al(III)] peaks are thus interpreted as resulting from alumina dissolution

(1) $Al_2O_3 + 3\ H_2O = 6\ Al^{3+} + 3\ OH^-$

which at pH 6-8 yields a mixture of $[Al(H_2O)_x(OH)_y]^{(3-y)-}$ complexes. The larger pH increase observed at 70°C (up to a slightly basic pH) compared to 25°C (final pH close to neutrality) (Figure 3) is in agreement with a higher dissolution rate of alumina at 70°C. Additionally, the small size of the γ-Al_2O_3 units constituting the grains (10-30 nm, TEM) can be limited to the high Al(III) concentrations that exceed the solubility of alumina. Roelofs and Vogelbergers have demonstrated that due to a Kelvin effect, the solubility of nanoparticles is enhanced compared to the bulk material, their dissolution is also faster and easily leads to supersaturated solutions.[16,25]

The decrease of pH between 8 and 24 h, followed by a new increase and a plateau, is accompanied by a strong displacement of [Al(III)] from solution, toward the formation of solid hydroxide phases:

(2) $[Al(H_2O)_x(OH)_y]^{(3-y)-} + (3-y)\ OH^- = Al(OH)_{3\ (s)} + x\ H_2O$

or, more simply in the case of the neutral species predominant in solution

(3) $Al(OH)_{3\ (aq)} = Al(OH)_{3\ (s)}$

Depending on the degree of hydroxylation of the complex, reaction (2) releases or consumes OH^- ions, leading to an increase or decrease of pH. As the situation may be out-of-equilibrium or depend on adsorption or precipitation kinetics, rationalizing the variations of pH in the intermediate stage is quite difficult. However, the same pattern of pH variations has been documented by Hermans

and Geus[26] and Burattin *et al*.[27] during the deposition-precipitation of $Ni(OH)_2$ on silica. Hermans and Geus[26] have assigned the pH drop to a nucleation step, while the pH increase and plateau that occur next were interpreted as the sign of the hydroxide growth under steady-state conditions. By analogy, and keeping in mind that deposition-precipitation onto silica is more complex as it involves the transient formation of silicates, we can suggest that between 1 and 8 h, Al(III) species leave the supersaturated solution to adsorb on the surface (nucleation), and hydroxide growth follows.

II.4.4. Evolution and location of hydroxide phases

Figure 5 shows SEM micrographs at different magnifications of grains of the same batch of γ-Al_2O_3 hydrated at 70°C during 7 days (168 h), here *without stirring*. These static conditions were chosen so as to observe the formation of hydroxides in the absence of attrition, whose possible effect is discussed in the last paragraphs of this section. A new phase is visible all around the surface of the γ-Al_2O_3 grains in full agreement with the precipitation of $Al(OH)_3$.

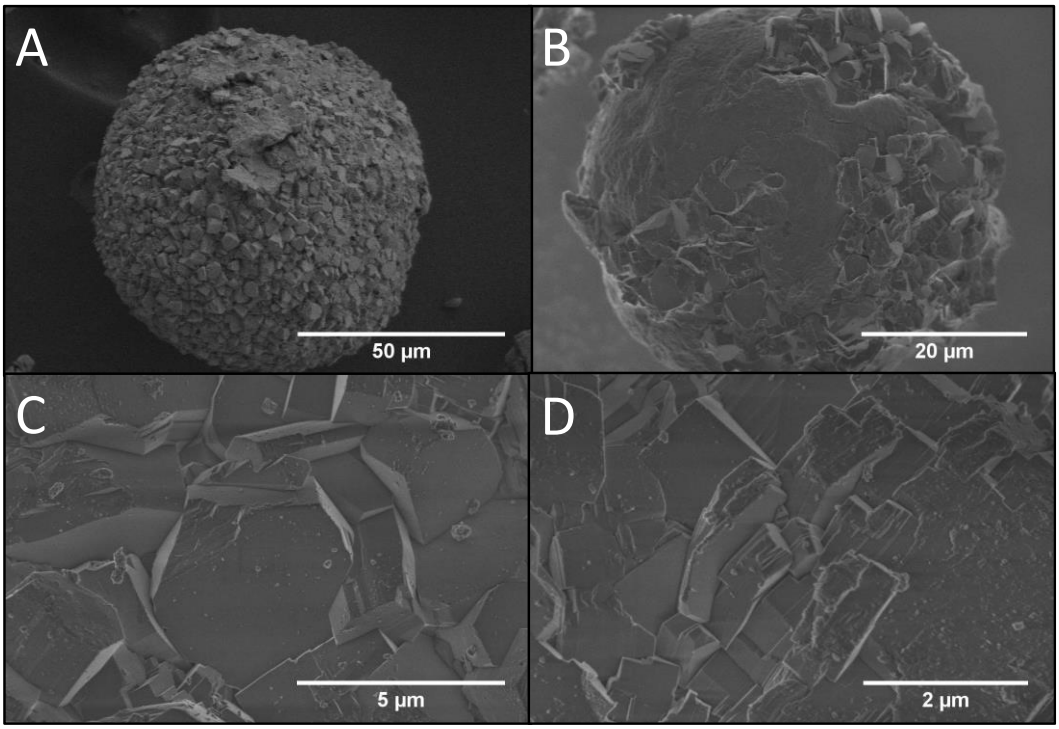

Figure 5. SEM images at different magnifications of γ-Al_2O_3 subjected to an ageing treatment at 70°C during 7 days (168 h) without stirring (0.6 g/30 mL of distilled water, atm. pressure).

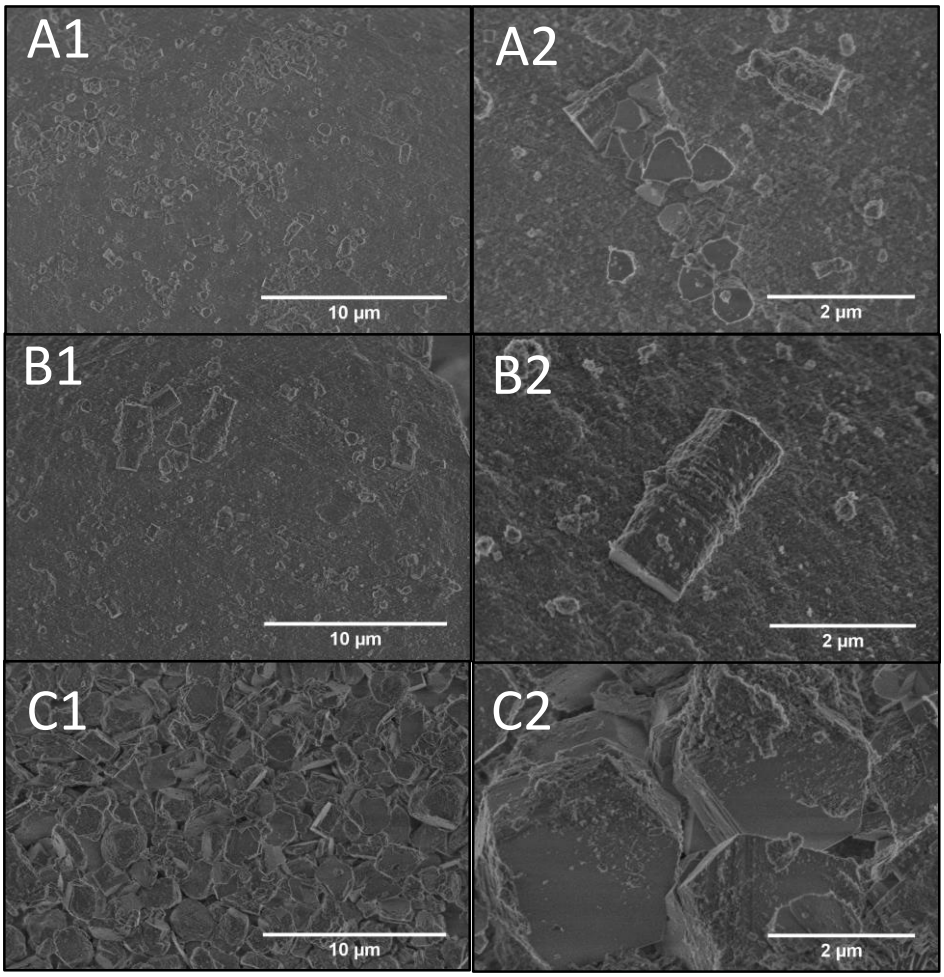

Figure 6. SEM images at different magnifications (series 1 and 2) of γ-Al_2O_3 subjected to an ageing treatment under stirring at 70°C during 2 h (series A), 8h (series B) and 7 days (168 h) (series C).

Figure 6 compares SEM images of γ-Al_2O_3 aged at 70°C during 2 h, 8 h and 7 days (168 h) *under stirring* (series A, B and C, respectively). At 2 h of ageing (Figure 6, series A), 100 to 1000 nm rod-like particles are visible on the surface of the alumina grains. Their elongated and symmetrical habit after 8 h (series B) is characteristic of bayerite.[28,29] As will be seen below, bayerite is clearly detected by XRD after ageing for 8 h; a very small diffraction peak corresponding to the basal distance of bayerite is visible after ageing for 2 h. Hydroxide growth at longer ageing time (7 days, series C) leads to large 2-5 µm $Al(OH)_3$ particles that have not conserved their rod shape. They are now platelet-like, in line with Figure 5, and have probably grown out of the germs. Hence, SEM demonstrates the *surface nucleation* of hydroxide particles and confirms that *heterogeneous precipitation* is followed by *crystal growth* from aluminum in solution by Ostwald ripening.

The influence of stirring on the microstructure of the grains will now be examined. When the γ-Al_2O_3-water suspensions are stirred with a magnetic bar, alumina grains ultimately burst due to the shearing of the magnetic bar as evidenced by the comparison between Figure S2 and Figure 7-A1 and 2. In order to evidence the possible links between mechanical attrition and chemical weathering, γ-Al_2O_3 was subjected to an ageing treatment at 70°C in stirred conditions during different times. At short ageing times (2 h, Figure 7-B1 and 2), SEM images do not exhibit any mechanical degradation. A higher magnification (Figure 7-B2) shows the small aluminum hydroxide particles that have started to form on the surface of the alumina. This indicates that chemical weathering starts before attrition.

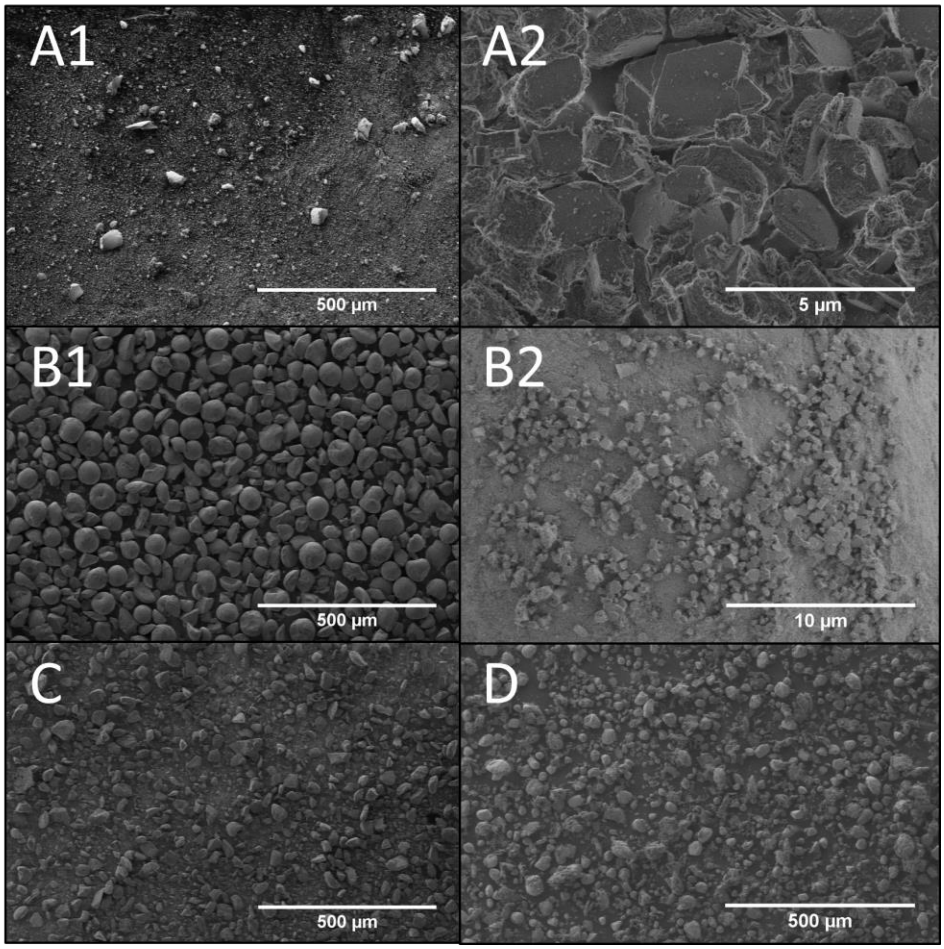

Figure 7. SEM images of γ-Al_2O_3 subjected to an ageing treatment at 70°C in stirred conditions during 7 days (168 h) in water (A1 and A2 at two different magnifications), 2 h in water (B1 and B2 at two different magnifications), 8 h in water (C) and at 25°C during 5 days in n-heptane (D).

In order to determine whether chemical degradation could enhance the effect of attrition by weakening the mechanical resistance of γ-Al_2O_3, ageing treatments were then performed at 70 °C during 8 h (Figure 7C) and at 25°C in a non-polar hydrocarbon solvent, i.e. n-heptane (Figure 7D), in which no sign of weathering and hydroxide precipitation was evidenced. Even if alumina grains burst in heptane because of the shearing of the magnetic bar, the extent of degradation due to attrition is already much higher after 8 h in water. Additionally, for a similar ageing time, it is seen by TGA and XRD (see the quantification procedure below) that the amount of hydroxides formed under stirring is more than twice that formed in static conditions. In conclusion, even if chemical weathering is not initiated by attrition, it makes alumina grains more fragile, and in turn, the increased degradation of alumina by attrition ultimately enhances its degradation by chemical weathering. Hence chemical weathering occurs before attrition but there is a strong interplay between chemical and mechanical degradation. In contrast with Chen *et al*.[21] though, no boehmite was detected by XRD under stirring and bayerite was always the main polymorph.

II.4.5. Formation of hydroxide polymorphs from γ-Al_2O_3 as a function of time

The total amount of hydroxides formed, whatever their crystallographic structure, after ageing γ-Al_2O_3 at 25 and 70°C between 8 h and 15 days (360 h) is presented as a function of time in Figure 8 (X-ray diffractograms are presented on Figure S4 and Figure S5, respectively). This evaluation relies on a quantitative analysis by TGA measurements, through the weight loss at 250°C corresponding to $Al(OH)_3$ dehydration (as explained in Carrier et al.[6]). Another analysis was also carried out to quantify each polymorph individually based on the characteristic XRD peaks of aluminum hydroxides (bayerite, gibbsite and nordstrandite) between 2θ=18 and 19° by comparison with reference mechanical mixtures (see supplementary information, Figures S6-8). Despite biases that could be expected from the possible influence of the particles habit on the diffraction lines width and intensity, a good agreement was found between TGA measurements and the total integration of the XRD basal peaks (Figure S7). This agreement also precludes the potential formation of a transient amorphous $Al(OH)_3$ phase in a large amount, as suggested by Lefèvre *et al*.[17] after a few days of ageing at 25°C, as it would remain undetected by XRD but quantified by TGA. Error bars in Figure 8 correspond to the standard deviation between TGA and XRD measurements.

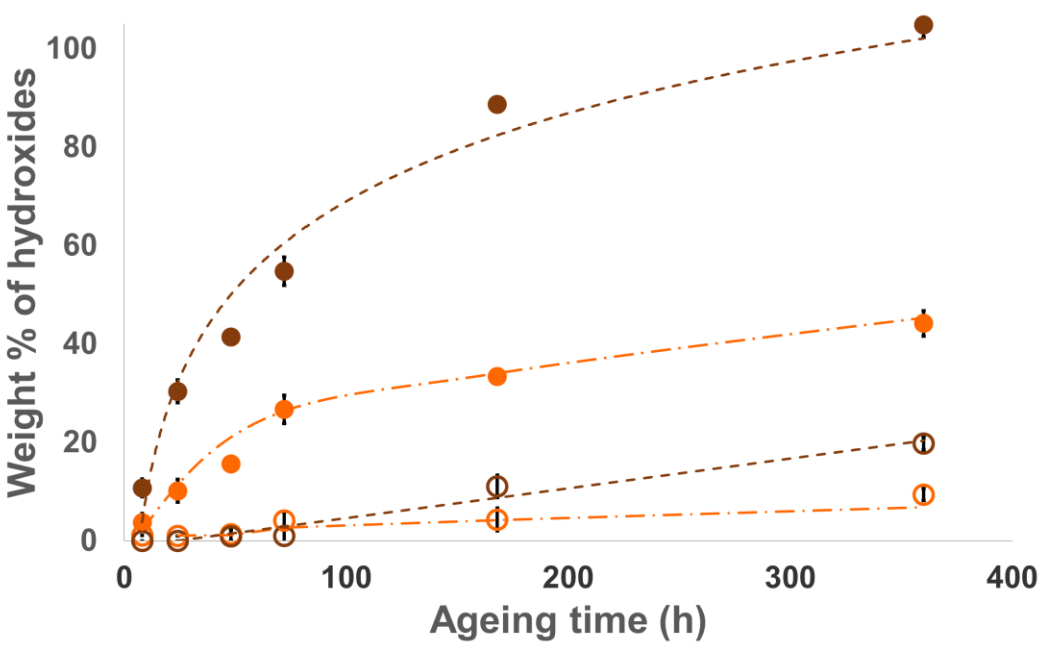

Figure 8. Variation of the amount of hydroxides formed after ageing γ-Al_2O_3 (brown) and δ/θ-Al_2O_3 (orange) in water under stirring at 70°C (filled circles) and 25°C (open circles) (0.6 g/30 mL, atm. pressure).

For both temperatures (25 and 70°C), the amount of hydroxides formed as a result of γ-Al_2O_3 hydration increases with ageing time, in agreement with SEM measurements. No plateau is reached whatever the temperature. The existence of a plateau as mentioned by Lefèvre *et al.*[17] may be more apparent after longer times of ageing (720 h, in their case). The temperature has a large impact on the initial rate of formation of $Al(OH)_3$ since the amount of hydroxides formed at short ageing times is clearly higher at 70°C, in line with Dyer *et al.*[20] This observation is also in full agreement with the higher dissolution rate at 70°C. Thereby, kinetic parameters such as time and temperature obviously play an important role in controlling Al_2O_3 hydration through dissolution-precipitation processes.

The detailed evolution of each $Al(OH)_3$ polymorph with time, based on an integration of the diffraction lines mentioned above (see decomposition on Figure S8), will now be described.

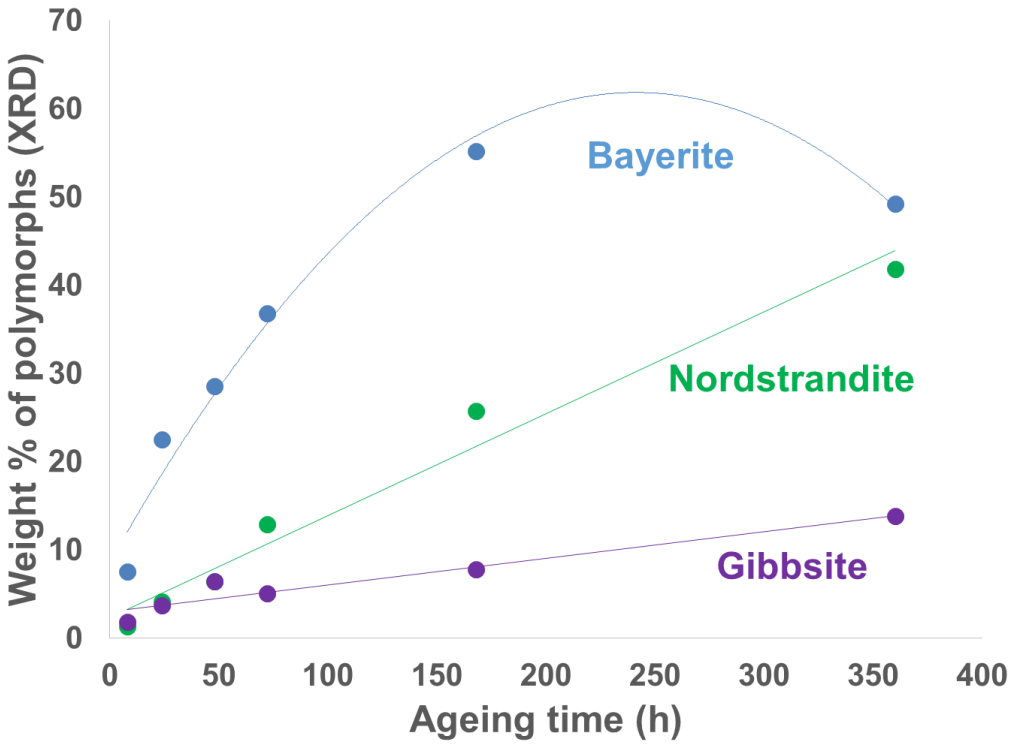

Figure 9. Variation of the amount of bayerite (blue), nordstrandite (green) and gibbsite (purple) after ageing γ-Al_2O_3 in water under stirring at 70°C (0.6 g/30 mL, atm. pressure).

Upon ageing at 70°C and up to 300 h (Figure 9), bayerite is the predominant polymorph. A low amount of gibbsite is detected at the beginning of the ageing period, and nordstrandite appears later. These results are consistent with the slightly basic pH (7 < pH < 8) reported in Figure 3 which has been reported to favor bayerite precipitation at the expense of gibbsite.[6,16,18] Table S1 and Figure 4 show that bayerite is less thermodynamically stable than gibbsite, the thermodynamically favored polymorph in agreement with MacDonald and Butler.[30] The formation of bayerite at the onset of the ageing period is under kinetic control and driven by the *fast surface dissolution* of γ-Al_2O_3 leading to high supersaturation. It has been noted too that for any ageing time, the bayerite-to-gibbsite ratio is higher in static conditions than under stirring. This can be explained by the absence of forced diffusion of aluminum ions outside the area surrounding the grains, and continuing supersaturation conditions where hydroxides form. In contrast, bayerite and gibbsite are formed in approximately the same proportions at 25°C, at a lower pH and with a lower dissolution rate of alumina (Figure S9).

Overtime at 70°C (>50 h), a progressive formation of nordstrandite and gibbsite (consistent with the platelet morphology seen on Figure 6, series C) is observed by XRD, ultimately at the expense of the bayerite fraction. It has been shown that nordstrandite is a polymorph favored at basic pH ($pH \geq 8$)[31,32], as is measured after 200 h of ageing, when the solubilization of the aluminum source and crystallization are both slow.[33] This evolution is consistent with a phase transformation in aqueous medium within the aluminum hydroxide series toward the thermodynamically stable phases via the following sequence bayerite (kinetic, metastable product) → nordstrandite → gibbsite (thermodynamic product), with a shift from a regime of fast solubilization of alumina to a steady-state regime of dissolution-precipitation.

The predominant formation of bayerite up to 300 h of ageing may have a consequence on the material physico-chemical properties if alumina has to be thermally regenerated after ageing. As bayerite transforms into η-Al_2O_3 instead of γ-Al_2O_3 (Figures S1 and S10), the regenerated alumina surface will not exhibit the same surface properties as the original grains.

II.4.6. Alumina polymorphs hydration

The total amount of hydroxide formed after alumina ageing was finally studied for a variety of alumina polymorphs: γ-Al_2O_3, γ/δ-Al_2O_3, δ-Al_2O_3, δ/θ-Al_2O_3 and θ-Al_2O_3. Results are plotted as a function of the specific surface area of the corresponding oxides in Figure 10. Ageing was performed at 25°C for 25 days (600 h) and 70°C for 7 days (168 h). The total amount of hydroxide clearly decreases with the specific surface area of the aluminas and the increase of alumina crystallinity.

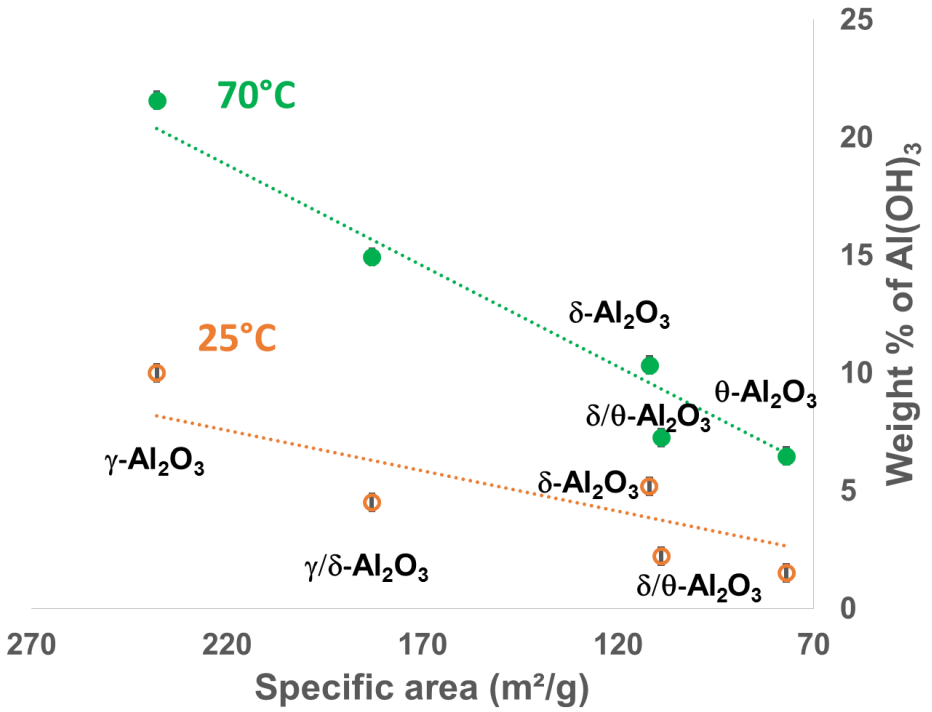

Figure 10. Variation of the total amount of hydroxides formed for different transition aluminas subjected to an ageing treatment at 70°C during 7 days (168 h) (filled circles) and 25°C during 25 days (600 h) (open circles) (0.6 g/30 mL of distilled water, atm. pressure). Dashed lines are drawn to guide the eye.

A kinetic study was carried out on δ/θ-Al_2O_3 since it is the alumina with the lowest specific surface area on which hydroxides could be quantified accurately at any ageing time. Figure 8 reports the evolution of hydroxide formation when δ/θ-Al_2O_3 is aged at 25 and 70°C. Results are comparable to those obtained on γ-Al_2O_3: the pH evolution is similar, nordstrandite is also detected at 70°C along with bayerite, and despite its expected higher density, δ/θ-Al_2O_3 also undergoes attrition upon chemical weathering in the same proportions as for γ-Al_2O_3. The amount of hydroxide formed upon ageing (Figure 8) is about twice lower than for γ-Al_2O_3, but follows the same trend. It can be noted that a similar ratio, close to 2, exists between the specific surface areas of the two alumina polymorphs. It can thus be supposed that the weathering process is mainly governed by the specific surface area of alumina. However, it should be reminded that an increase of alumina crystallinity, or in other terms an increasing stability of alumina, is also expected to affect the solubility of the oxide when contacted with water.[34] Moreover, the largest size of δ/θ-Al_2O_3 crystallites evidenced by TEM, compared to γ-Al_2O_3, would decrease the intensity of the Kelvin effect described in section 3.3. Hence, increasing crystallinity, increasing particle size and decreasing surface area,

three highly correlated parameters that cannot be disentangled, work against alumina dissolution and thus against alumina hydration, both from a thermodynamic and a kinetic point of view. Even if the change of solubility is small between 25 and 70°C, the increased hydroxide formation observed in Figure 10 at 70°C (compare filled circles and empty circles) can still be directly connected to an enhanced dissolution rate at this temperature.

II.5. Conclusion

The degradation of micrometer-sized grains of transition aluminas in heated aqueous suspensions at atmospheric pressure depends both on chemical factors (weathering) and physical factors (attrition), and follows a succession of irreversible stages. The key stage is *alumina dissolution* starting early, at short ageing times (≤2 h at 70 °C). After *nucleation* at the *surface* of the alumina grains, and for longer ageing times (≥8 h), *hydroxide precipitation* controls the Al concentration in solution through a steady-state crystal growth of large hydroxide particles (Ostwald ripening). Physical degradation (attrition) is also observed after a few hours, and comparison with an experiment carried out in n-heptane suggests that weathering in water has contributed to weakening the mechanical properties of the alumina grains and making them more fragile. In turn, the smaller grains resulting from the attrition process are more prone to weathering, and under stirring γ-Al_2O_3 is almost completely turned into hydroxides after 7 days at 70°C. Alumina hydration in aqueous suspensions is thus the result of dissolution and heterogeneous precipitation, with an amplification brought by attrition, rather than from a topotactic surface transformation of Al_2O_3 to aluminum hydroxides.

The whole process of alumina hydration and degradation thus derives from the initial dissolution step, which is driven both by thermodynamics and kinetics (instability of alumina with respect to water; Kelvin effect resulting in the faster and higher dissolution of alumina nanoparticles compared with a bulk material). The less transition alumina is crystallized, the smaller the alumina nanoparticles are, the higher the specific surface area is, and the more alumina dissolves; but all transition aluminas from γ-Al_2O_3 to θ-Al_2O_3 are observed to undergo hydration, to different extents.

The formation of hydration products at the onset of the process is under kinetic control, when bayerite precipitates from the supernatant solutions resulting from alumina dissolution and supersaturated with respect to $Al(OH)_3$ solubility. Bayerite is initially favored at higher temperatures, because of a higher dissolution rate of alumina. A thermodynamic control is postulated at longer times (several days), with amounts of nordstrandite and gibbsite (the thermodynamic product) that increase at the expense of bayerite. The speciation of aluminum hydroxides seems to be highly dependent on pH and concentrations in solution, which themselves depend on the kinetics of parallel and consecutive processes (alumina dissolution, aluminum adsorption, hydroxide growth). The nature and proportions of the various hydroxide polymorphs formed at a specific time for a specific alumina is difficult to predict, but the global trends follow what is known from the literature about $Al(OH)_3$ speciation when precipitated from aqueous solutions.

Inhibiting alumina degradation in heated aqueous suspensions thus means inhibiting its initial dissolution. If alumina is not stabilized, leaching could occur from the first hours in water, and the production of alumina and aluminum hydroxide fines in less than one day at 70°C, under the combined effects of weathering and attrition. Thermal regeneration of the material would also lead to a change of phases and properties, as bayerite decomposes in a transition alumina, η-Al_2O_3, that exhibits surface characteristics different from those of the initial γ-Al_2O_3 solid.

ASSOCIATED CONTENT

Supporting Information. A figure showing the thermal transformation of transition aluminas, SEM pictures of the starting aluminas, XRD patterns of transition aluminas aged at 25°C/25 days and of γ-Al_2O_3 aged at 25 and 70°C for different times and details of the quantitative analysis of hydroxides carried out with XRD and TGA. This material is available free of charge via the internet at http://pubs.acs.org.

AUTHOR INFORMATION

Corresponding Authors

* Eric Marceau: eric.marceau@univ-lille1.fr
* Xavier Carrier: xavier.carrier@upmc.fr

Author Contributions

The manuscript was written through contributions of all authors.

ACKNOWLEDGMENT

We gratefully acknowledge Dr. G. Lefèvre for help in ICP-OES analysis.

II.6. References

(1) Euzen, P.; Raybaud, P.; Krokidis, X.; Toulhoat, H.; Le Loarer, J.-L.; Jolivet, J.-P.; Froidefond, C. Alumina. In *Handbook of Porous Solids*; Schüth, F., Sing, K. S. W., Weitkamp, J., Eds.; Wiley-VCH Verlag GmbH, 2008; pp 1591–1677.

(2) Kasprzyk-Hordern, B. Chemistry of Alumina, Reactions in Aqueous Solution and Its Application in Water Treatment. *Adv. Colloid Interface Sci.* **2004**, *110*, 19–48.

(3) Zsolnai, D.; Mayer, P.; Szőri, K.; London, G. Pd/Al_2O_3-Catalysed Redox Isomerisation of Allyl Alcohol: Application in Aldol Condensation and Oxidative Heterocyclization Reactions. *Catal Sci Technol* **2016**, *6*, 3814–3820.

(4) Hu, J.; Yu, F.; Lu, Y. Application of Fischer–Tropsch Synthesis in Biomass to Liquid Conversion. *Catalysts* **2012**, *2*, 303–326.

(5) Wu, K.; Wu, Y.; Chen, Y.; Chen, H.; Wang, J.; Yang, M. Heterogeneous Catalytic Conversion of Biobased Chemicals into Liquid Fuels in the Aqueous Phase. *ChemSusChem* **2016**, *9*, 1355–1385.

(6) Carrier, X.; Marceau, E.; Lambert, J.-F.; Che, M. Transformations of γ-Alumina in Aqueous Suspensions. *J. Colloid Interface Sci.* **2007**, *308*, 429–437.

(7) Mironenko, R. M.; Belskaya, O. B.; Talsi, V. P.; Gulyaeva, T. I.; Kazakov, M. O.; Nizovskii, A. I.; Kalinkin, A. V.; Bukhtiyarov, V. I.; Lavrenov, A. V.; Likholobov, V. A. Effect of γ-Al_2O_3 Hydrothermal Treatment on the Formation and Properties of Platinum Sites in Pt/γ-Al_2O_3 Catalysts. *Appl. Catal. A Gen.* **2014**, *469*, 472–482.

(8) Koichumanova, K.; Sai Sankar Gupta, K. B.; Lefferts, L.; Mojet, B. L.; Seshan, K. An in Situ ATR-IR Spectroscopy Study of Aluminas under Aqueous Phase Reforming Conditions. *Phys. Chem. Chem. Phys.* **2015**, *17*, 23795–23804.

(9) Zhao, R.; Goodwin, J. G.; Oukaci, R. Attrition Assessment for Slurry Bubble Column Reactor Catalysts. *Appl. Catal. A Gen.* **1999**, *189*, 99–116.

(10) Elliott, D. C.; Sealock Jr, L. J.; Baker, E. G. Chemical Processing in High-Pressure Aqueous Environments. 2. Development of Catalysts for Gasification. *Ind. Eng. Chem. Res.* **1993**, *32*, 1542–1548.

(11) Franck, J. P.; Freund, E.; Quéméré, E. Textural and Structural Changes in Transition Alumina Supports. *J. Chem. Soc., Chem. Commun.* **1984**, 629–630.

(12) Ravenelle, R. M.; Copeland, J. R.; Kim, W.-G.; Crittenden, J. C.; Sievers, C. Structural Changes of γ-Al_2O_3-Supported Catalysts in Hot Liquid Water. *ACS Catal.* **2011**, *1*, 552–561.

(13) Jun-Cheng, L.; Lan, X.; Feng, X.; Zhan-Wen, W.; Fei, W. Effect of Hydrothermal Treatment on the Acidity Distribution of γ-Al_2O_3 Support. *Appl. Surf. Sci.* **2006**, *253*, 766–770.

(14) Zhou, Y.; Fu, H.; Zheng, X.; Li, R.; Chen, H.; Li, X. Hydrogenation of Methyl Propionate over Ru–Pt/AlOOH Catalyst: Effect of Surface Hydroxyl Groups on Support and Solvent. *Catal. Commun.* **2009**, *11*, 137–141.

(15) Zhang, J.; Chen, J.; Ren, J.; Sun, Y. Chemical Treatment of γ-Al_2O_3 and Its Influence on the Properties of Co-Based Catalysts for Fischer-Tropsch Synthesis. *Appl. Catal. A Gen.* **2003**, *243*, 121–133.

(16) Roelofs, F.; Vogelsberger, W. Dissolution Kinetics of Nanodispersed γ-Alumina in Aqueous Solution at Different pH: Unusual Kinetic Size Effect and Formation of a New Phase. *J. Colloid Interface Sci.* **2006**, *303*, 450–459.

(17) Lefèvre, G.; Duc, M.; Lepeut, P.; Caplain, R.; Fédoroff, M. Hydration of γ-Alumina in Water and Its Effects on Surface Reactivity. *Langmuir* **2002**, *18*, 7530–7537.

(18) Laiti, E.; Persson, P.; Öhman, L.-O. Balance between Surface Complexation and Surface Phase Transformation at the Alumina/water Interface. *Langmuir* **1998**, *14*, 825–831.

(19) Handjani, S.; Blanchard, J.; Marceau, E.; Beaunier, P.; Che, M. From Mesoporous Alumina to Pt/Al_2O_3 Catalyst: A Comparative Study of the Aluminas Synthesis in Aqueous Medium, Physicochemical Properties and Stability. *Microporous Mesoporous Mater.* **2008**, *116*, 14–21.

(20) Dyer, C.; Hendra, P. J.; Forsling, W.; Ranheimer, M. Surface Hydration of Aqueous γ-Al_2O_3 Studied by Fourier Transform Raman and Infrared spectroscopy—I. Initial Results. *Spectrochim. Acta Part Mol. Spectrosc.* **1993**, *49*, 691–705.

(21) Chen, Y.; Hyldtoft, J.; Jacobsen, C. J.; Nielsen, O. F. NIR FT Raman Spectroscopic Studies of η-Al_2O_3 and Mo/η-Al_2O_3 Catalysts. *Spectrochim. Acta. A. Mol. Biomol. Spectrosc.* **1995**, *51*, 2161–2169.

(22) Wefers, K.; Misra, C. *Oxides and Hydroxides of Aluminum*; Alcoa Laboratories, 1987.

(23) Saalfeld, H.; Jarchow, O. Crystal Structure of Nordstrandite, Aluminum Hydroxide. *Neues Jahrb. Fuer Mineral. Abh.* **1968**, *109*, 185–191.

(24) Muller, B. ChemEQL V2. 0. *Swiss Fed. Inst. Environ. Sci. Technol. Kastanienbaum SwitzerlandLinks* **1992**.

(25) Roelofs, F.; Vogelsberger, W.; Buntkowsky, G. Kinetic Size Effect During Dissolution of a Synthetic γ-Alumina. *Z. Phys. Chem.* **2008**, 222, p 1131-1153.

(26) Hermans, L. A. M.; Geus, J. W. Interaction Of Nickel Ions With Silica Supports During Deposition-Precipitation. In *Studies in Surface Science and Catalysis*; B. Delmon, P. G., P. Jacobs and G. Poncelet, Ed.; Elsevier, 1979, 3, pp 113–130.

(27) Burattin, P.; Che, M.; Louis, C. Molecular Approach to the Mechanism of Deposition-Precipitation of the Ni (II) Phase on Silica. *J. Phys. Chem. B* **1998**, *102*, 2722–2732.

(28) McHardy, W. J.; Thomson, A. P. Conditions for the Formation of Bayerite and Gibbsite. *Mineralogical Magazine*. 1971, pp 358–368.

(29) Van Straten, H. A.; De Bruyn, P. L. Precipitation from Supersaturated Aluminate Solutions II. Role of Temperature. *Journal of Colloid and lnterface Sci*. **1984**, 102 pp 260–277.

(30) MacDonald, D. D.; Butler, P. The Thermodynamics of the Aluminium—Water System at Elevated Temperatures. *Corros. Sci.* **1973**, *13*, 259–274.

(31) Aldcroft, D.; Bye, G. C. Crystallization Processes in Aluminum Hydroxide Gels: Formation and Thermal Decomposition of Nordstrandite. *Sci. Ceram.* **1967**, *3*, 75–94.

(32) Lipin, V. A. A New Technique for Synthesis of Nordstrandite. *Russ. J. Appl. Chem. Transl. Zhurnal Prikl. Khimii* **2001**, *74*, 184–187.

(33) Violante, A.; Huang, P. M. Formation Mechanism of Aluminum Hydroxide Polymorphs. *Clays Clay Miner.* **1993**, *41*, 590–597.

(34) Stumm, W. Reactivity at the Mineral-Water Interface: Dissolution and Inhibition. *Colloids Surf. Physicochem. Eng. Asp.* **1997**, *120*, 143–166.

Abstract Graphical:

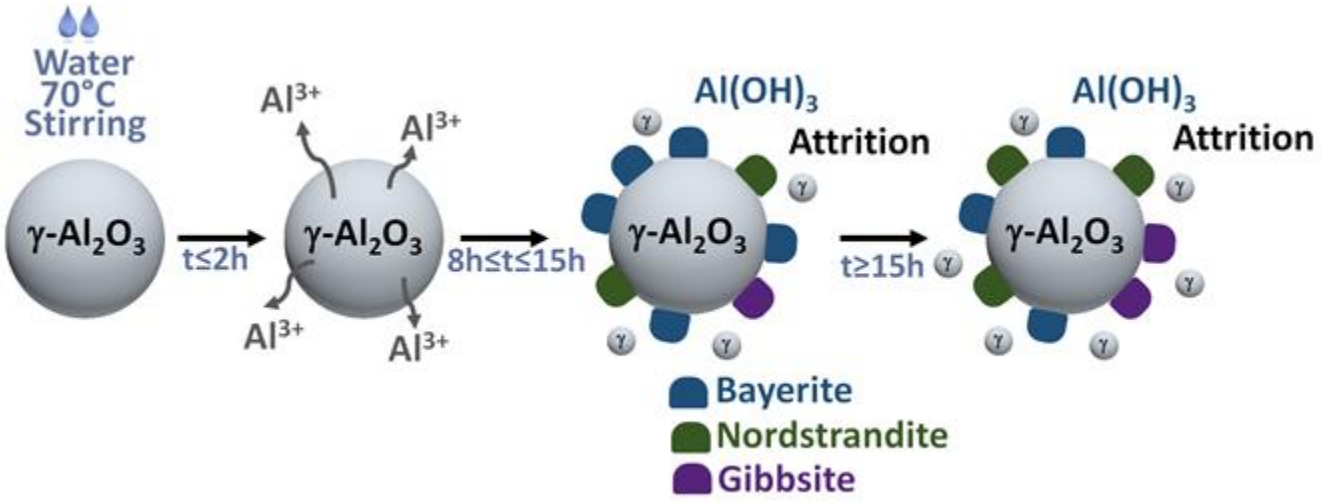

II.7. Supplementary information

Chemical weathering and physical attrition of γ-alumina in aqueous suspension at ambient pressure: a mechanistic study.

Jane Abi Aad,[a,b] Sandra Casale,[a] Philippe Courty, Mathieu Michau,[b] Fabrice Diehl,[b] Eric Marceau*,[a,c] Xavier Carrier*,[a]

[a] Sorbonne Universités, UPMC Univ Paris 06, CNRS, Laboratoire de Réactivité de Surface, F-75005, Paris, France

[b] IFP Energies nouvelles, BP3, Rond-Point échangeur de Solaize, F-69360 Solaize, France

[c] Univ. Lille, CNRS, Centrale Lille, ENSCL, Univ. Artois, UMR 8181 - UCCS - Unité de Catalyse et Chimie du Solide, F-59000 Lille, France.

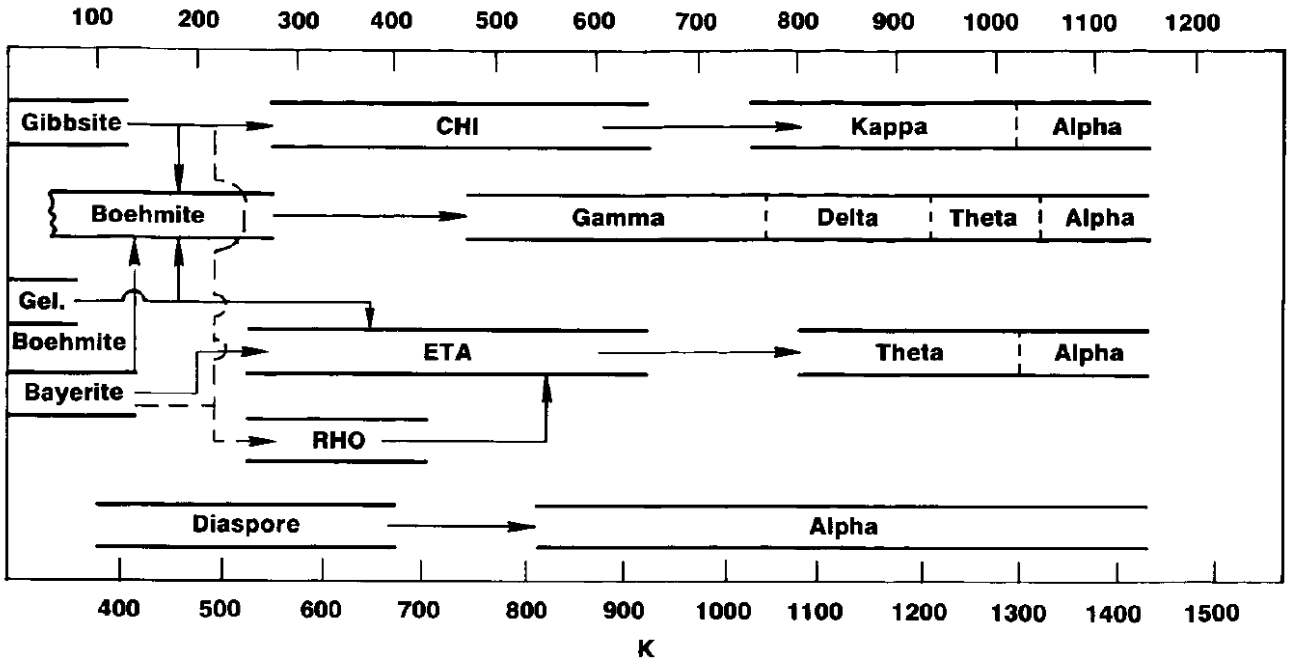

Figure S1. Thermal transformation sequences of transition aluminas. On the left part, aluminum (oxy)hydroxides and on the central and right parts, aluminum oxides.[1]

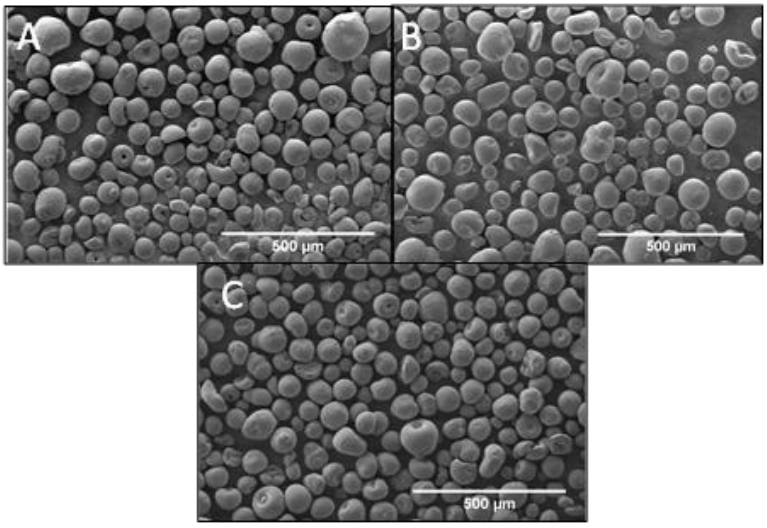

Figure S2. SEM images of: (A) boehmite Sasol Pural SB3, (B) γ-Al_2O_3 obtained by calcining the Pural SB3 at 500°C during 12 h and (C) δ/θ-Al_2O_3 obtained by calcining the Pural SB3 at 900°C during 12 h.

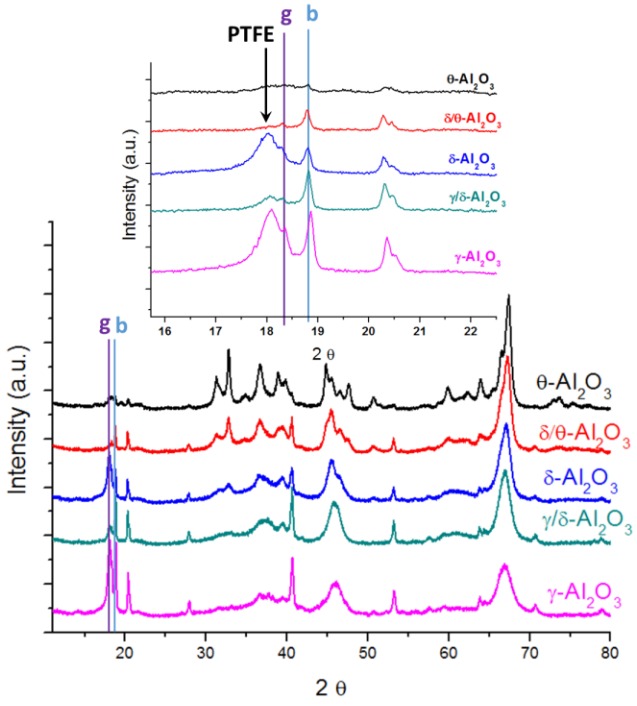

Figure S3. XRD patterns of γ-Al_2O_3 (pink), γ/δ-Al_2O_3 (green), δ-Al_2O_3 (blue), δ/θ-Al_2O_3 (red) and θ-Al_2O_3 (black) subjected to an ageing treatment in water at 25°C under magnetic stirring during 25 days (600 h) (0.6 g/30 mL). g: gibbsite (PDF No. 33-18) and b: bayerite (PDF No. 20-11).

Table S1. Free energies of formation of various aluminum species

Species	$\Delta_f G°$, 298 K (kJ.mol^{-1})	References
γ-Al_2O_3	-1564.2	Chen *et al.*[2]
$Al(OH)_3$ (bayerite)	-1149.8	Verdes *et al.*[3]
$Al(OH)_3$ (gibbsite)	-1154.9	Verdes *et al.*[3]
Al^{3+}	-487.7	Castet *et al.*[4]
$Al_3(OH)_4^{5+}$	-2332.2	Martell and Smith[5]
$Al_2(OH)_2^{4+}$	-1405.7	Martell and Smith[5]
$Al(OH)_4^-$	-1306.7	Stumm and Morgan[6]
$Al(OH)_2^+$	-904.3	Stumm and Morgan[6]
$Al(OH)^{2+}$	-696.3	Stumm and Morgan[6]

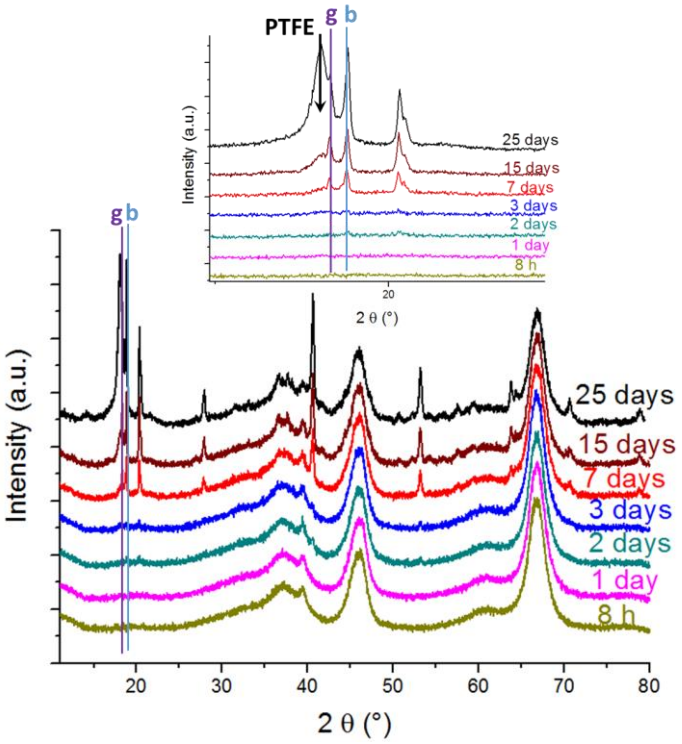

Figure S4. XRD patterns of γ-Al_2O_3 subjected to an ageing treatment in water at 25°C under magnetic stirring during 8 h (gold), 1 day (pink,) 2 days (green), 3 days (blue) and 7 days (red) (0.6 g/30 mL). g: gibbsite (PDF No. 33-18) and b: bayerite (PDF No. 20-11).

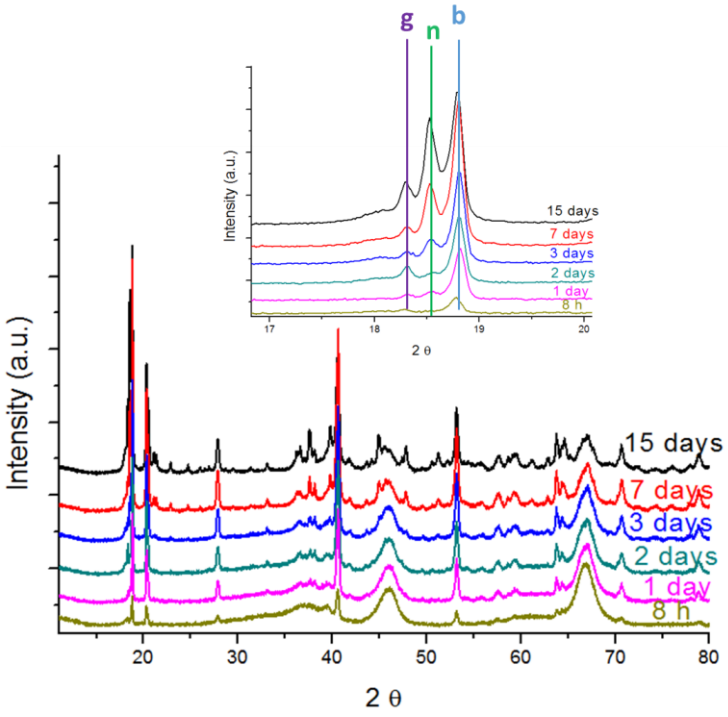

Figure S5. XRD patterns of γ-Al_2O_3 subjected to an ageing treatment in water at 70°C under magnetic stirring during 8 h (gold), 1 day (pink,) 2 days (green), 3 days (blue), 7 days (red) and 15 days (black) (0.6 g/30 mL).

II.7.1. Quantitative analysis by TGA and XRD

A calibration curve for XRD was created by preparing mechanical mixtures between a commercial bayerite (Sasol, 590100) and γ-alumina with weight ratios varying between 10 and 90% (the total mass of the mixture was constant and equal to 0.6 g). The integrated area of the characteristic XRD peak of bayerite (at 2θ=18.8°, (001), PDF No. 20-11) was then plotted as a function of the weight percentage of bayerite introduced in the mixture as shown on Figure S6. A linear correlation was found and the slope of the curve equal to 0.22 was found.

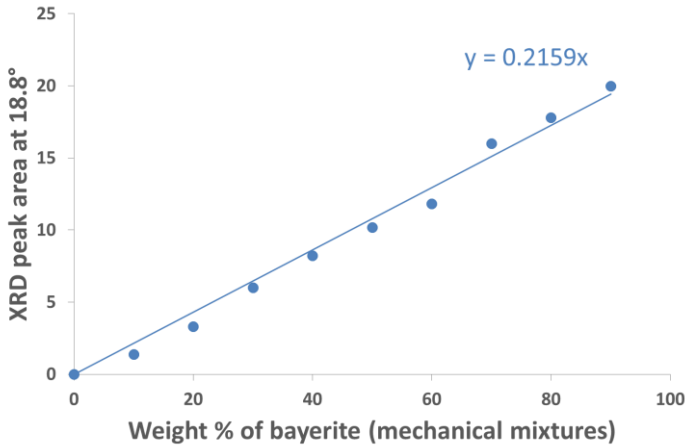

Figure S6. XRD peak intensity at 2θ=18.8° (bayerite) as a function of the weight % of bayerite in γ-Al_2O_3-bayerite mechanical mixtures.

Validation of this correlation was performed by comparing the $Al(OH)_3$ weight % derived from XRD with that obtained by TGA (taking into account the weight loss at 250°C corresponding to $Al(OH)_3$ dehydration as explained in Carrier et al.[7]). The series of γ-aluminas aged at 70°C was used for this purpose. Figure S7 shows the correlation between the weight percentages evaluated by XRD and TGA. A very good agreement is found between both techniques with a slope of about 1 for the linear correlation, which is validating the quantification by XRD using the peak assigned to the basal distance of bayerite.

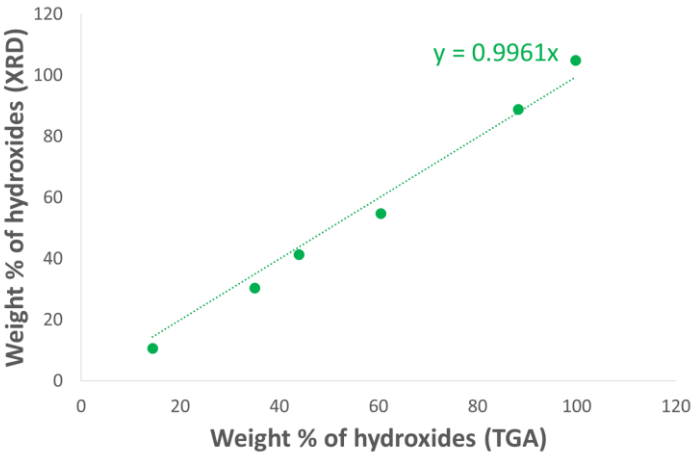

Figure S7. Weight percentage of hydroxide determined by XRD as a function of that determined by TGA for a series of γ-alumina aged at 70°C in water.

However, it should be added that the quantification by XRD may overestimate the hydroxide amount at high conversion of alumina, when the broad alumina peaks become less visible (see e.g. Figure S5-15 days). A larger error should be expected for the last point of the brown curve on Figure 8.

The amount of each hydroxide polymorph (gibbsite, bayerite, nordstrandite) formed after γ-Al_2O_3 ageing was evaluated by integration of the XRD basal peaks. An example of fitting using WinPLOTR is shown in the figure below (Figure S8). The integrated intensity was transposed to a weight % by using the correlation established for bayerite. This hypothesis was justified by the fact that the chemical composition of the layers of the three types of hydroxides (gibbsite, bayerite, nordstrandite) is identical.[1,8,9]

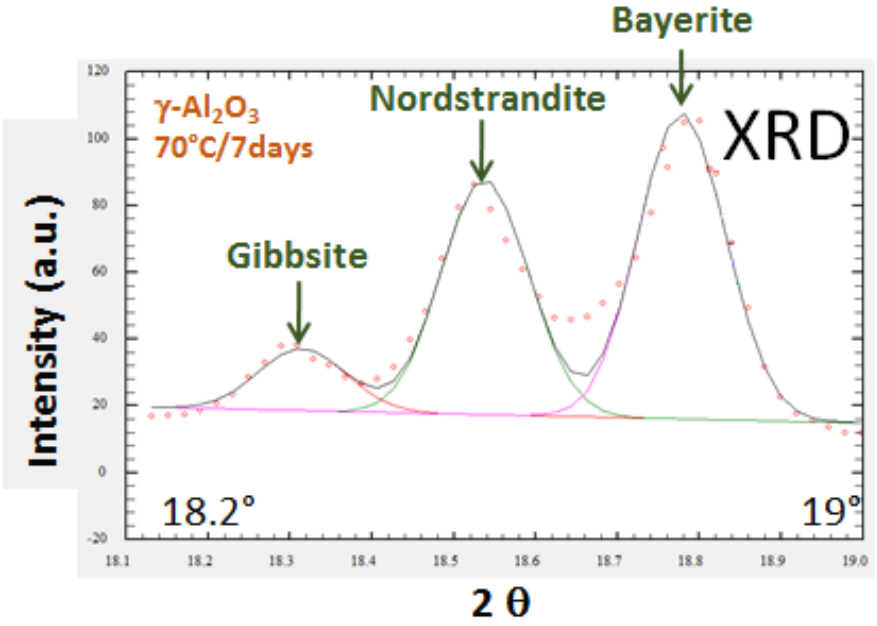

Figure S8. Fitting of the XRD peaks corresponding to hydroxide polymorphs: gibbsite, nordstrandite and bayerite formed after ageing γ-Al_2O_3 in water at 70°C during 7 days (0.6 g/30 mL, atm. pressure).

Another diffraction peak is visible on some diffractograms at long times of ageing, and has been assigned to PTFE resulting from the degradation of the magnetic bar. This degradation seemed to take place quite haphazardly. However we preferred not to use a magnetic bar coated with glass,

as it had been mentioned in the literature that siliceous species deposited on alumina could inhibit its dissolution, and thus perturb the investigation of alumina weathering. The presence of the PTFE XRD peak could especially make the quantification of gibbsite difficult. In the few cases when the gibbsite peak was not clearly visible (for δ-Al_2O_3 on Figure 2 for example), we estimated the amount of gibbsite from the gibbsite/nordstrandite or gibbsite/bayerite ratio measured on aluminas subjected to similar ageing treatments. As gibbsite is most often the minor phase, we believe that the error of the global quantification of hydroxides is not large.

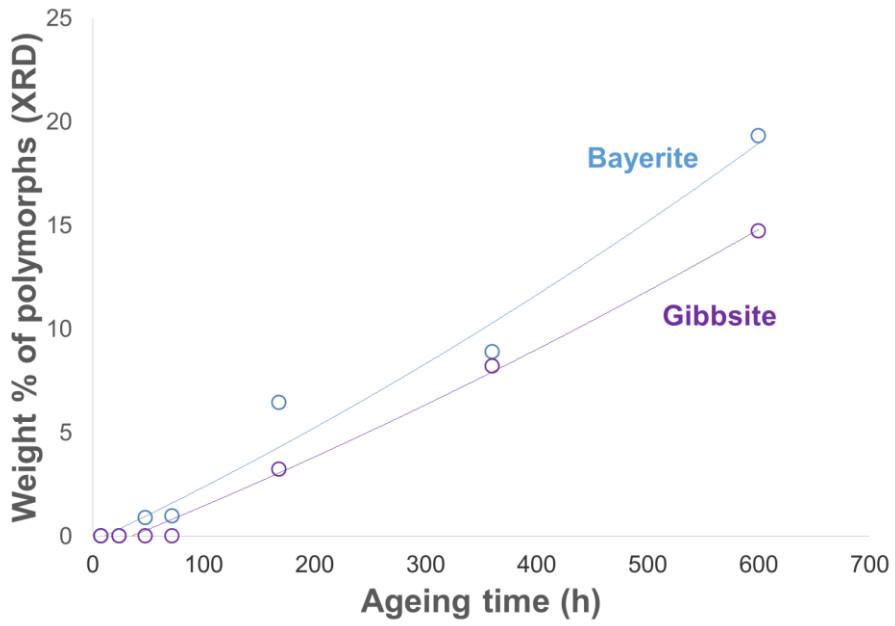

Figure S9. Variation of the amount of bayerite (blue) and gibbsite (purple) after ageing γ-Al_2O_3 in water under stirring at 25°C (0.6 g/30 mL, atm. pressure).

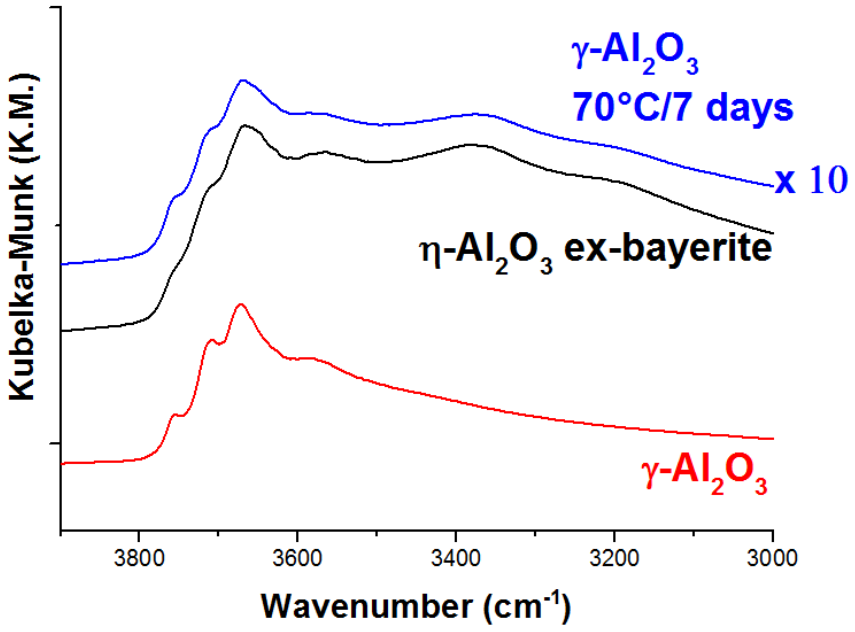

Figure S10. DRIFT spectra obtained after calcination at 500°C of γ-Al_2O_3 (red), bayerite (black) and γ-Al_2O_3 after being subjected to an ageing treatment in water at 70°C during 7 days (blue). Black spectrum shows the transformation of bayerite to η-Al_2O_3 (see Figure S1). Similarity of the black spectrum with the blue shows that the bayerite fraction of aged aluminas has also transformed into η-Al_2O_3, the thermal decomposition product of bayerite, which exhibit distinct surface hydroxyl groups as compared to the initial material (red).

(1) Wefers, K.; Misra, C. Oxides and Hydroxides of Aluminum; Alcoa Laboratories, 1987.

(2) Chen, Q.; Zeng, W.; Chen, X.; Gu, S.; Yang, G.; Zhou, H.; Yin, Z. Investigation of the Thermodynamic Properties of γ-Al2O3. Thermochim. Acta 1995, 253, 33–39.

(3) Verdes, G.; Gout, R.; Castet, S. Thermodynamic Properties of the Aluminate Ion and of Bayerite, Boehmite, Diaspore, and Gibbsite. Eur. J. Mineral. 1992, 4, 767–792.

(4) Castet, S.; Dandurand, J. L.; Schott, J.; Gout, R. Boehmite Solubility and Aqueous Aluminum Speciation in Hydrothermal Solutions (90-350°C): Experimental Study and Modeling. Geochim. Cosmochim. Acta 1993, 57, 4869–4884.

(5) Martell, A. E.; Smith, R. M. Critical Stability Constants. 4. Inorganic Complexes; Plenum Press, 1976.

(6) Stumm, W.; Morgan, J. J. Aquatic Chemistry: Chemical Equilibria and Rates in Natural Waters; Environmental Science and Technology: A Wiley-Interscience Series of Texts and Monographs; Wiley, 1996.

(7) Carrier, X.; Marceau, E.; Lambert, J.-F.; Che, M. Transformations of γ-Alumina in Aqueous Suspensions. J. Colloid Interface Sci. 2007, 308, 429–437.

(8) Euzen, P.; Raybaud, P.; Krokidis, X.; Toulhoat, H.; Le Loarer, J.-L.; Jolivet, J.-P.; Froidefond, C. Alumina. In Handbook of Porous Solids; Schüth, F., Kenneth, Weitkamp, J., Eds.; Wiley-VCH Verlag GmbH, 2008; pp 1591–1677.

(9) Saalfeld, H.; Jarchow, O. Crystal Structure of Nordstrandite, Aluminum Hydroxide. Neues Jahrb. Fuer Mineral. Abh. 1968, 109, 185–191.

II.8. Annex – Acidic medium

Fischer-Tropsch synthesis leads to the formation of small quantities (<1%wt) of carboxylic acids as by-products, and the catalyst is in contact with an acidic aqueous phase during the reaction. Hence, it is of prime interest for the present work to study alumina hydration, not only in pure water, but also when it is subjected to acidic conditions. Two acids were chosen for this aim: nitric acid (non-complexing, 65%, Prolabo, 1.40 $kg.L^{-1}$) and acetic acid (a carboxylic acid whose anion exhibits complexing properties, 99-100%, Prolabo, 1.05 $kg.L^{-1}$).

Two transition aluminas only were chosen for this part of the work, γ-Al_2O_3 and δ/θ-Al_2O_3 since they are largely differing by their crystallinity and specific surface area. These solids were subjected to ageing treatments under stirring similar to the ones described in Chapter II:

- 25°C, 11 days
- 70°C, 7 days

II.8.1. Nitric acid

In an Al_2O_3/water suspension adjusted to pH=3 by nitric acid and aged at 25°C or 70°C, only gibbsite was formed. This can be seen on the XRD patterns of the aged solids on Figure 1 where none of the peaks characteristics of bayerite could be observed. Results for γ-Al_2O_3 aged at 70°C are not shown due to a lack in experiments of reproducibility.

The formation of gibbsite in acidic medium is in perfect agreement with the phase diagram of aluminum (oxy)hydroxides in Figure 5 of Chapter I and with the literature (Section I, Chapter I).

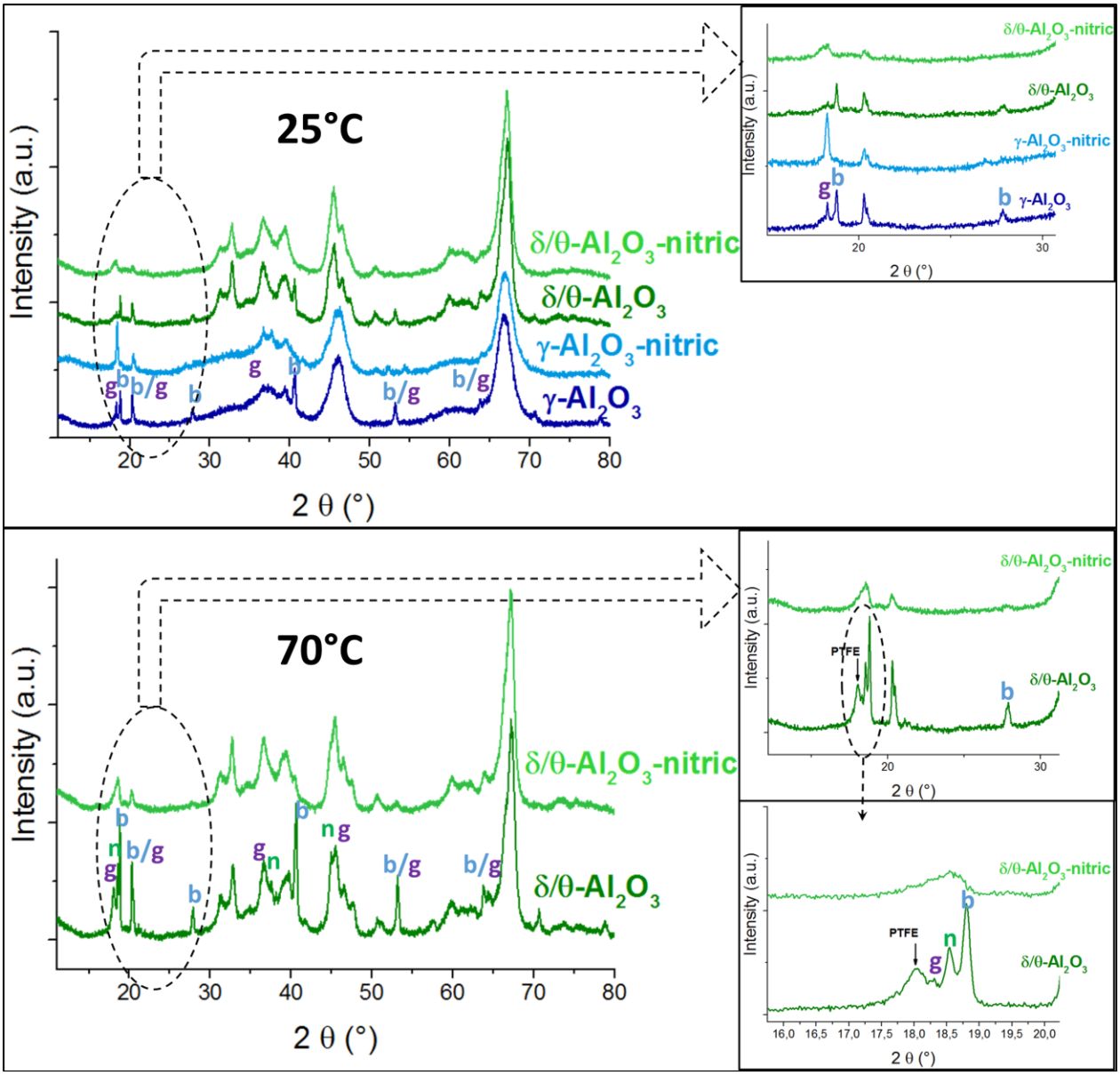

Figure 1. XRD patterns of γ-Al_2O_3 (blue) and δ/θ-Al_2O_3 (green) subjected to ageing treatment at 25°C during 11 days (A) and 70°C during 7 days (B) in water only (dark blue and dark green) and with nitric acid (light blue and light green). The pH of the suspensions was adjusted to 3. g: gibbsite, n: nordstrandite and b: bayerite. (0.6 g/ 30 mL, atm. pressure).

II.8.2. Acetic acid

In presence of acetic acid (pH=3), crystallized hydroxides were not detected by XRD whatever the alumina polymorph and the temperature (Figure 2).

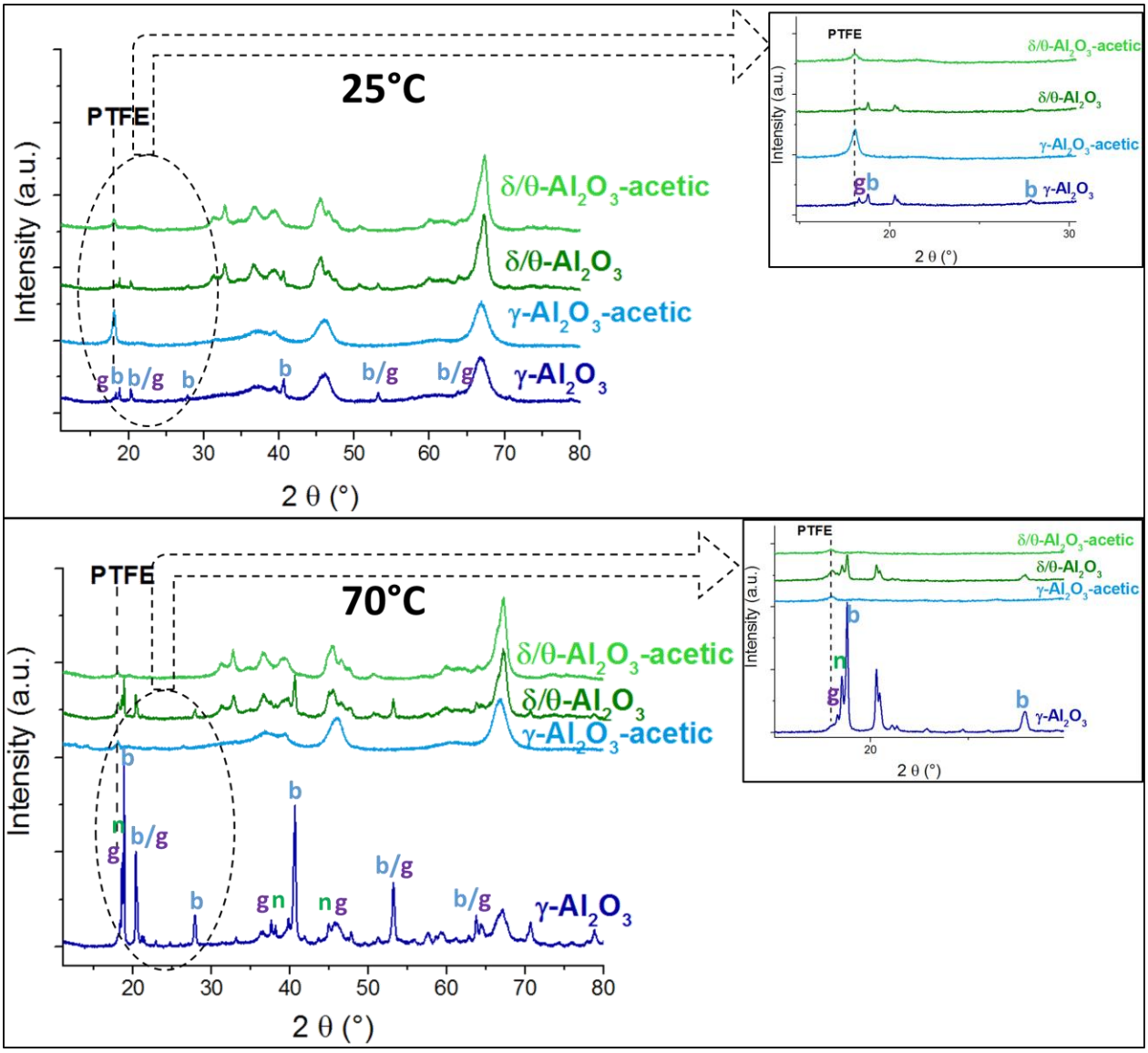

Figure 2. XRD patterns of γ-Al_2O_3 (blue) and δ/θ-Al_2O_3 (green) subjected to ageing treatment at 25°C during 11 days (A) and 70°C during 7 days (B) in water only (dark blue and dark green) and with acetic acid (light blue and light green). The pH of the suspensions was adjusted to 3. g: gibbsite, n: nordstrandite and b: bayerite. (0.6 g/ 30 mL, atm. pressure).

The TGA for the γ-Al_2O_3 aged at 25°C in presence of acetic acid confirmed the absence of hydroxides formation while that of the solid aged at 70°C showed a weight loss at about 250°C corresponding to hydroxides dehydration. Hence, either an aluminum hydroxide is probably

formed but as an amorphous compound not detectable by XRD, or small seeds of $Al(OH)_3$, mainly gibbsite, are formed and their growth was inhibited by the presence of acetic acid.

a) Liquid-phase aluminum concentration

Liquid-phase Al(III) concentrations were analyzed in the solutions obtained after filtration of the γ-Al_2O_3- or δ/θ-Al_2O_3-water suspensions aged at 25°C and 70°C. Al(III) concentrations were determined by ICP-OES. Results are reported on Figure 3 along with the solubility curves of γ-Al_2O_3, bayerite and gibbsite (see Chapter II for the calculation of these curves).

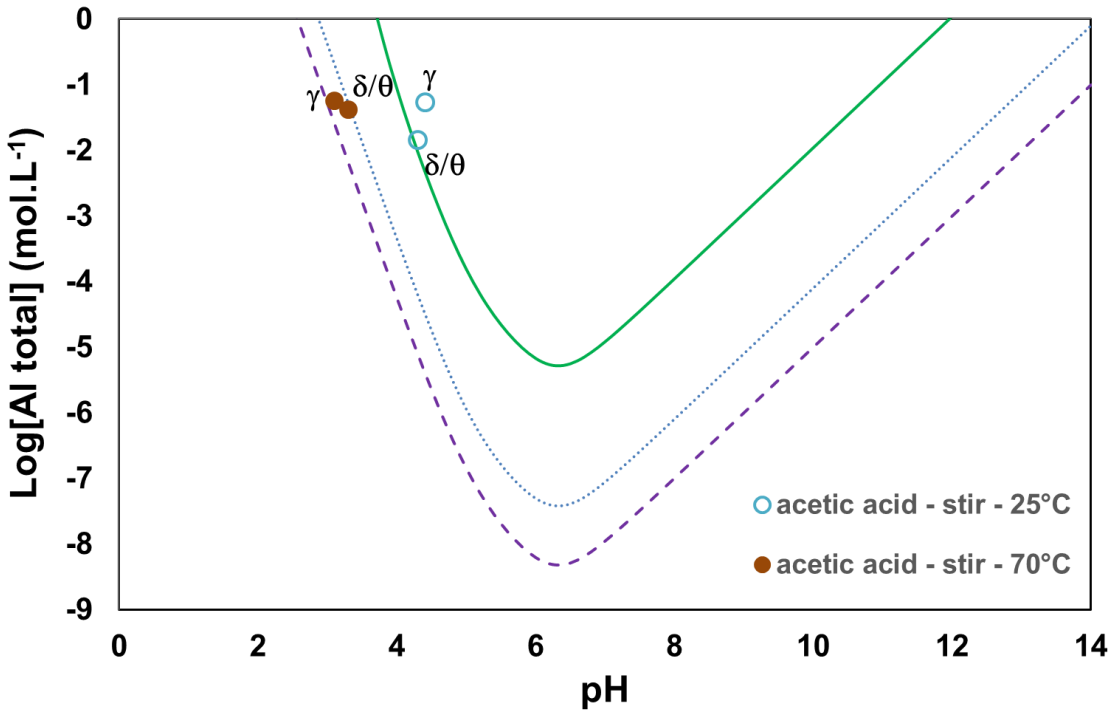

Figure 3. Calculated concentrations of Al(III) in solution (log scale) as a function of pH for γ-Al_2O_3 (solid green line), bayerite (dotted blue line), and gibbsite (dashed purple line). Experimental data points are shown as empty and filled circles for suspensions of γ-Al_2O_3 and δ/θ-Al_2O_3 aged in presence of acetic acid at 25°C and 70°C respectively (0.6 g/30 mL for distilled water, atm. pressure).

For values obtained in presence of acetic acid at 25°C, there is a consistency with γ-Al_2O_3 solubility (the curve of the solubility of δ/θ–Al_2O_3 should be below the one of γ-Al_2O_3 which confirms the

consistency for this polymorph also) and supernatant liquors are supersaturated with respect to $Al(OH)_3$ precipitation. This indicates that alumina is dissolved and explain the absence of aluminum hydroxides formation. Values at 70°C are consistent with $Al(OH)_3$ precipitation and thus does not rule out the hypothesis of a possible formation of small $Al(OH)_3$ particles. Hydroxides precipitation occurred at 70°C in a shorter time compared to 25°C (7 days vs 11 days respectively) probably due to a temperature effect which influence the kinetics of hydration (dissolution/hydroxides precipitation, Chapter II).

b) Evidence for $Al(OH)_3$ formation

SEM images of γ-Al_2O_3 aged at 70°C in presence of acetic acid (Figure 4) shows small crystallized particles whose size varies approximately between 1 and 3 µm. This result is in agreement with the concentration of Al(III) in the solution indicating the precipitation of hydroxides (paragraph (a)). In correlation with the acidic medium, these phases are probably gibbsite whose thin platelet-like shape looks like the one obtained in the work of Watling *et al.*[1] where they synthesized gibbsite in presence of 4 $mmol.L^{-1}$ of threonic acid. The effect of the latter, according to the authors, was to change the morphology and growth of gibbsite by adsorbing on the basal face at specific sites. Hence, acetic acid probably influenced the growth of $Al(OH)_3$ particles since the acetate anion exhibits complexing properties.

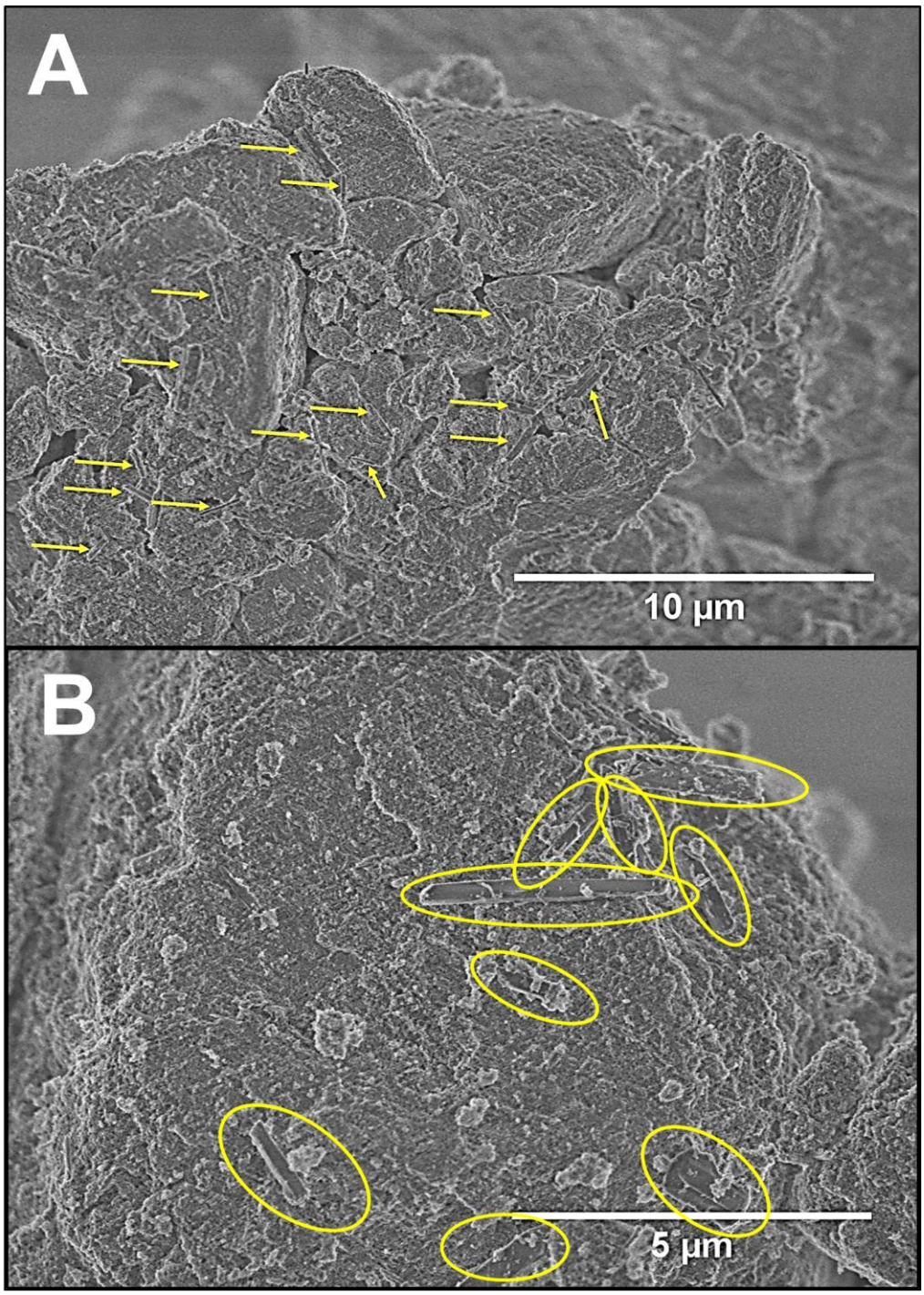

Figure 4. SEM images of γ-Al_2O_3 subjected to ageing treatment at 70°C during 7 days in presence of acetic acid. The pH of the suspensions was adjusted and the total weight percentage of the acid relative to the amount of water was 37% (0.6 g/ 30 mL, atm. pressure).

II.8.3. Conclusion

The effect of nitric and acetic acids on γ-Al_2O_3 chemical weathering was studied under atmospheric pressure.

Gibbsite formation was detected by XRD in presence of nitric acid. However, more studies should be completed especially concerning the ageing of γ-Al_2O_3 at 70°C and quantification of Al(III) in the liquid-phase in order to explore a possible effect of the nitric acid on increasing the dissolution of alumina.

In presence of acetic acid and for treatments at 25°C *alumina dissolution* is the predominant phenomenon at 11 days of ageing while at 70°C *hydroxides precipitation* occurs at 7 days of test. Hence the effect of temperature in accelerating the two-step mechanism for γ-alumina hydration demonstrated in Chapter II, is emphasized. The hydroxides particles obtained at 70°C of ageing were not detected by XRD probably due to their low amount and small size that was influenced by the presence of acetic acid which has complexing properties.

II.8.4. References

(1) Watling, H. Gibbsite Crystallization Inhibition: 2. Comparative Effects of Selected Alditols and Hydroxycarboxylic Acids. *Hydrometallurgy* **2000**, *55*, 289–309.

Chapitre III

Chemical weathering of alumina in aqueous phase in hydrothermal conditions and influence of organic additives

III. Chemical weathering of alumina in aqueous phase in hydrothermal conditions and influence of organic additives 109

III.A. Chemical weathering of alumina in aqueous suspension in hydrothermal conditions... 109

III.A.1. Introduction 109

III.A.2. Materials and methods 110

III.A.3. Hydrothermal ageing of alumina polymorphs 112

III.A.4. Mechanism of hydration in hydrothermal conditions for γ-Al_2O_3 115

III.A.5. Conclusion 123

III.B. Influence of organic additives on alumina chemical weathering in aqueous phase under hydrothermal conditions 125

III.B.1. Introduction 125

III.B.2. Effect of organic molecules on boehmite formation 126

III.B.3. Interaction of sorbitol with γ-Al_2O_3 upon hydrothermal treatment 129

III.B.4. Evidence for a dissolution step and role of polyols 134

III.B.5. Conclusion 143

III.C. Conclusion 145

III.D. Annex to chapter III – part A 147

III.E. References 150

III. Chemical weathering of alumina in aqueous phase in hydrothermal conditions and influence of organic additives

In the previous chapter, the mechanism of hydration of various polymorphs of alumina was described through a qualitative as well as a quantitative study, by following the **ageing of the support under mild conditions (T ≤ 70°C) and at atmospheric pressure**. These results can now serve as rational guides to investigate the chemical degradation that occurs while alumina undergoes **ageing in hydrothermal conditions** (T > 100°C and P > 1 bar). For the sake of clarity, this chapter will fall into two parts. Part A will focus on the hydration of alumina in pure water, while part B will deal on the influence of organic molecules present in the aqueous medium.

III.A. Chemical weathering of alumina in aqueous suspension in hydrothermal conditions

III.A.1. Introduction

Analysis of the literature results (Chapter I) has shown that boehmite AlOOH should be the predominant oxyhydroxide polymorph in hydrothermal conditions. This section will confirm these results but will also give more insight into parameters relevant to boehmite formation: time, temperature and influence of the alumina polymorph.

In a first part, a description of the experimental set-up used for ageing alumina under hydrothermal conditions will be described, and the choice of the experimental parameters (time and temperature) will be explained. Then, a study of the hydration of different transition aluminas will be detailed. A more extensive account will be given on the hydration mechanism and evolution of the textural properties of γ-Al_2O_3 specifically. This polymorph is particularly studied for the reasons discussed earlier, in particular because it is the most used among transition aluminas as catalysts supports for the Fischer-Tropsch synthesis and for the conversion of biomass products.

III.A.2. Materials and methods

Experiments were conducted in a 100 mL Hastelloy C276 autoclave from Top Industrie (Figure 1-A) under continuous stirring at a rate of 1000 rpm using a propeller stirrer (Figure 1-B). The different transition aluminas used in the previous chapter were aged in distilled water in hydrothermal conditions at 150°C, up to 14 h, with an oxide/water content of 1.6 g/80 mL, which corresponds to the same ratio as under mild conditions. The pressure reached in these conditions only due to the vaporization of the water in the autoclave was 4.6 bar. The heating time before reaching 150°C was 30 min and the cooling time was about 2 h 30 min.

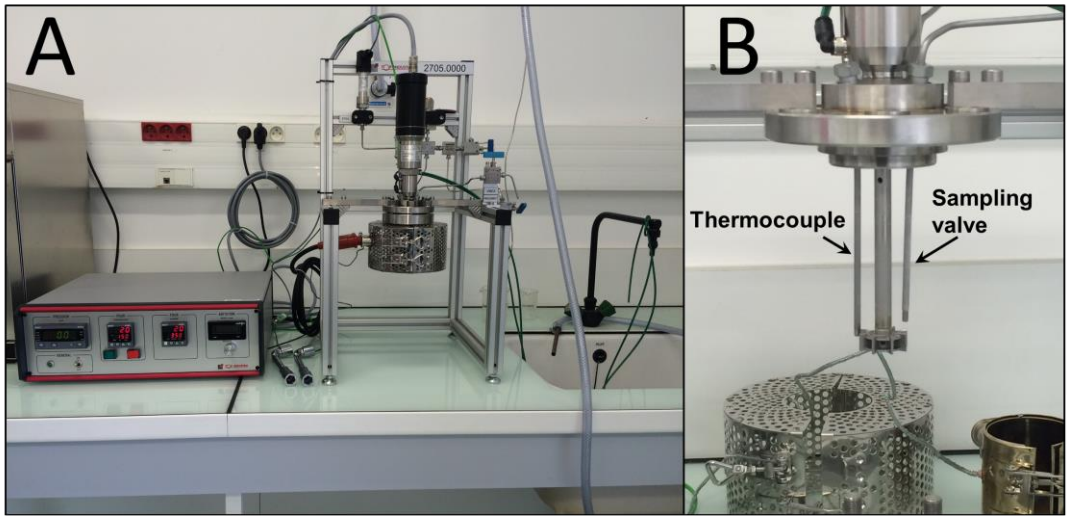

Figure 1. Autoclave (Top Industrie) used for alumina ageing in hydrothermal conditions (A) ; zoom on the propeller stirrer (B).

Experimental conditions had to be selected in order to hydrate aluminas only *partially*, which means to form boehmite but also to conserve a certain amount of alumina. A too severe treatment leading to a full conversion of alumina to boehmite would level off any differences among the different alumina polymorphs, mask the respective effects of the different experimental parameters, and prevent a comprehensive study of the hydration mechanism. The XRD patterns recorded after different tests on γ-Al_2O_3 are presented in Figure 2. Boehmite was detected through its main characteristic peaks at 2θ = 14.4° (020 (reflection)), 28.1° (021), 38.3° (130) and 49.28° (150) and

(002) (PDF No. 83-1505). It is shown that a good compromise between alumina conversion and boehmite detection is found at a temperature of 150°C and an ageing time of 4 h. These conditions will be chosen as the reference ones throughout this chapter and the following one.

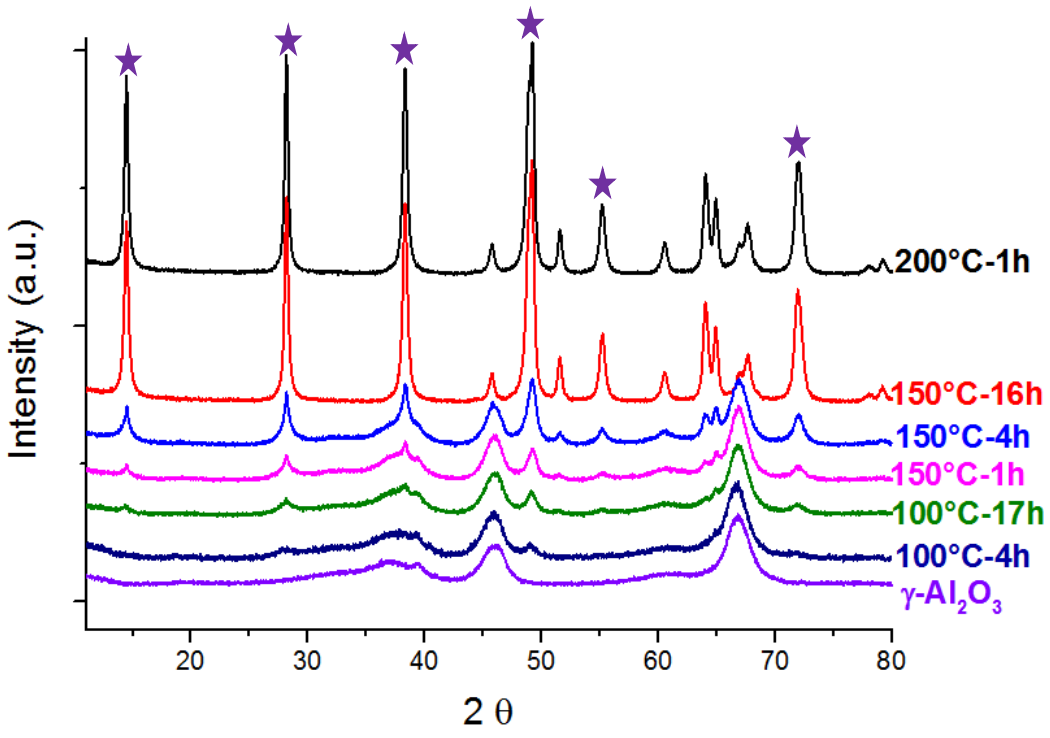

Figure 2. XRD patterns of γ-Al_2O_3 (purple), subjected to an ageing treatment in water under hydrothermal conditions at different temperatures/ageing times (1.6 g/80 mL). ★ : boehmite (PDF No. 83-1505).

The same characterization techniques (XRD, TGA-DTA, SEM-FEG, ICP-OES and N_2 adsorption and desorption) that have been described in Chapter II will be used in this part of the work.

III.A.3. Hydrothermal ageing of alumina polymorphs

Ageing of the different transition aluminas (γ, δ, θ and combinations of these) under hydrothermal conditions at 150°C during 4 h, leads to the formation of boehmite AlOOH as identified by XRD (PDF No. 83-1505), without any other (oxy)hydroxide crystalline phase being detected (Figure 3). The possible formation of an amorphous phase will be discussed below.

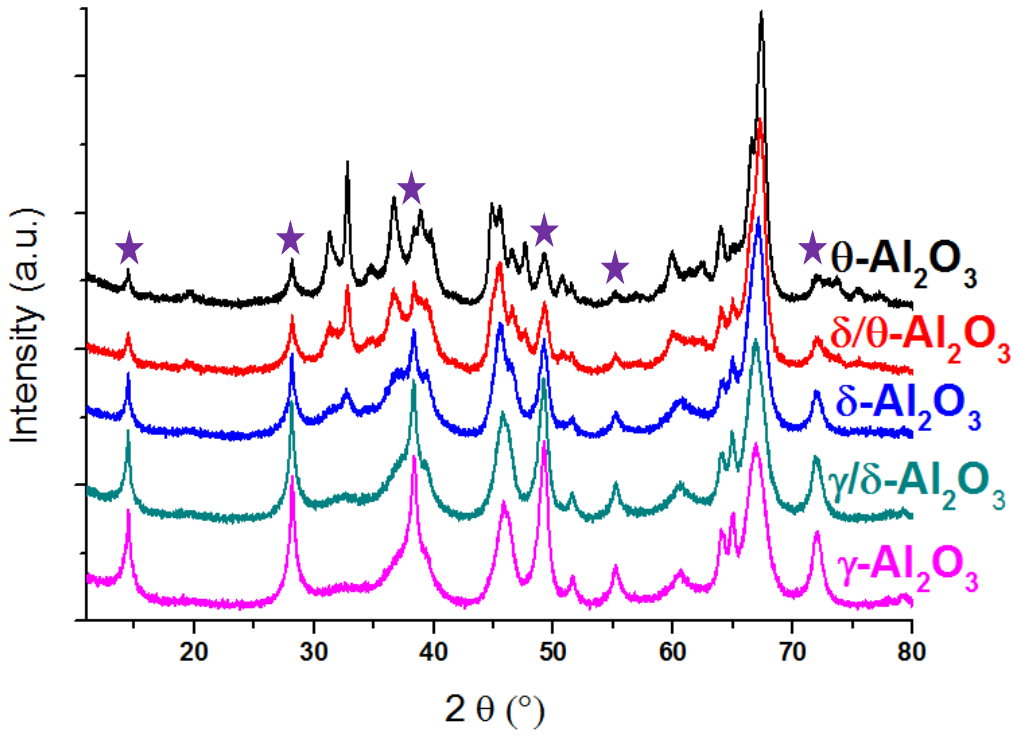

Figure 3. XRD patterns of various alumina polymorphs subjected to an ageing treatment in water at 150°C under stirring during 4 h (1.6 g/80 mL, hydrothermal conditions) : γ-Al_2O_3 (pink), γ/δ-Al_2O_3 (green), δ-Al_2O_3 (blue), δ/θ-Al_2O_3 (red) and θ-Al_2O_3 (black) ★ : boehmite (PDF No. 83-1505).

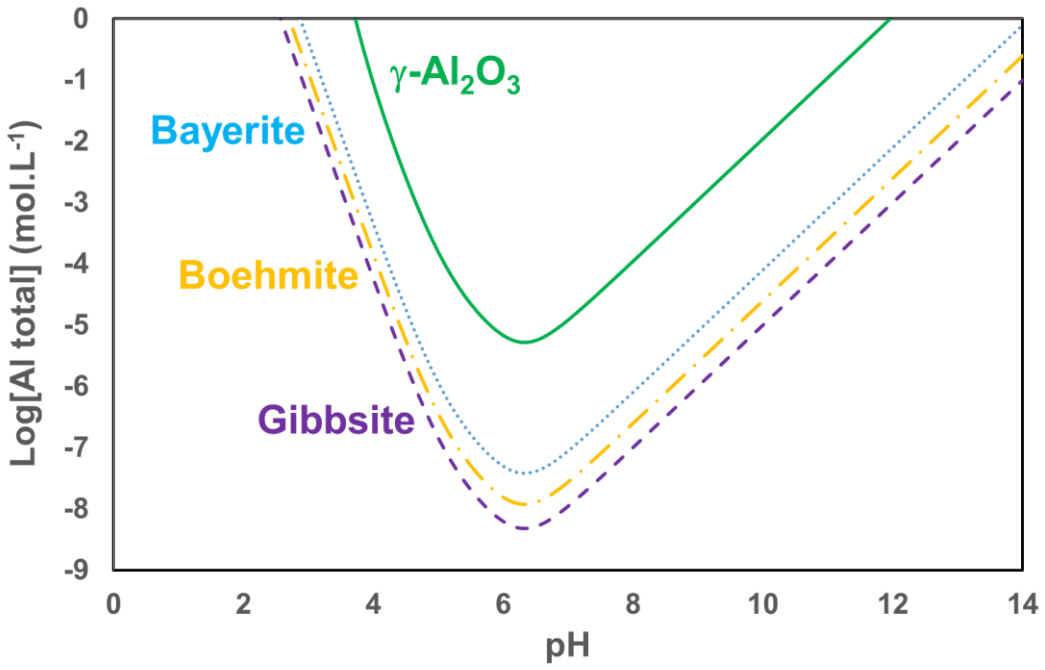

Figure 4. Calculated concentrations of Al[III] in solution (log scale) as a function of pH for γ-Al_2O_3 (solid green line), bayerite (dotted blue line), boehmite (dash-dotted yellow line) and gibbsite (dashed purple line).

The formation of AlOOH at 150°C under hydrothermal conditions is in perfect agreement with previous results from the literature[1–10] and with the thermodynamic instability of γ-Al_2O_3 with respect to the formation of boehmite in solution. This can be confirmed by comparing the solubility curves of the oxide and of the oxyhydroxide on Figure 4. The boehmite solubility curve is calculated using the Gibbs free energy of formation from Bénézeth *et al.*[11] ($\Delta_f G°$, 298 K = -917.82 kJ.mol^{-1}).

A quantitative analysis of the amount of boehmite formed upon ageing was performed by XRD in a similar way as under mild conditions (Chapter II, see supplementary section of this chapter for the method). It was cross-checked with TGA, thanks to which the amount of boehmite was evaluated from the amount of water evolved at 450°C (dehydration of boehmite, $\Delta m_{450°C}$, Figure 32-supplementary information) according to the reaction:

2 AlOOH → Al_2O_3 + H_2O

Following the method explained in the work of Carrier *et al.*[12] for evaluating the amount of $Al(OH)_3$, the boehmite content is thus calculated as:

$$\%AlOOH = \left[\frac{2 \times \Delta m_{450°C} / 18}{m_{700°C}} \times 60 \right] \times 100,$$

60 and 18 g.mol^{-1} being the molar masses of AlOOH and H_2O, respectively, and $m_{700°C}$ is the total weight of the sample at 700°C after boehmite dehydration.

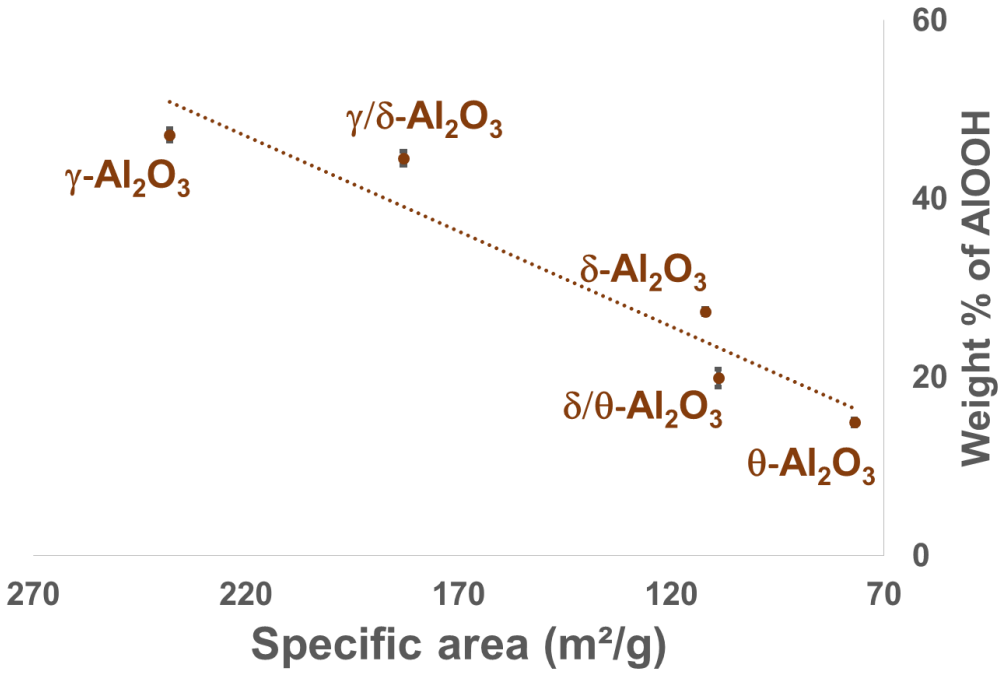

Figure 5. Variation of the total amount of boehmite formed for different transition Al_2O_3 subjected to an ageing treatment at 150°C during 4 h (1.6 g/80 mL of distilled water, hydrothermal conditions). Quantitative analysis was performed with XRD and TGA.

The average of the total amount of boehmite formed after ageing the different transition aluminas at 150°C for 4 h is plotted as a function of the specific surface area on Figure 5. Error bars are the standard deviation from both techniques. The very small error bars lead to reject the possibility of

the formation of an amorphous phase after 4 h of ageing. The absence of a baseline deformation or a broad diffraction halo on the XR diffractograms (Figure 3) is also consistent with this observation.

As was the case under mild conditions, a clear decrease of the total amount of boehmite is observed with a decrease of the specific surface area and increase of the crystallinity of the aluminas. This evolution can be tentatively analyzed through the same reasoning used to explain the results obtained at atmospheric pressure. An increase in crystallinity (from γ to θ) decreases the solubility of the oxide (thermodynamic effect). In parallel, a decrease in specific surface (from γ to θ) will diminish surface dissolution rates (kinetic effect) since both parameters are directly proportional.[13] Hence, increased crystallinity and decreased surface area should lead both to a lower dissolution of alumina and consequently a lower amount of boehmite. However, it is very difficult to discriminate between both effects since crystallinity and surface area are highly correlated. Moreover, at this stage, the possibility of a topotactic transformation of aluminas to boehmite without intermediate dissolution cannot be completely ruled out.

III.A.4. Mechanism of hydration in hydrothermal conditions for γ-Al_2O_3

a) Role of Attrition ?

The morphology of γ-Al_2O_3 particles aged in the autoclave (150°C/hydrothermal conditions) during different periods of time (30 min, 2 h, 4 h and 6 h) was observed by SEM (Figure 6). The images show that the grains maintain their mechanical integrity and do not burst as observed at ambient pressure when stirring was performed with a magnetic bar exerting friction toward the powder. Hence it can be concluded that: i) stirring with the propeller causes no mechanical degradation, even after 6 h of treatment, and attrition does not occur under these conditions and ii) attrition *is not necessarily a direct consequence of* weathering (chemical degradation).

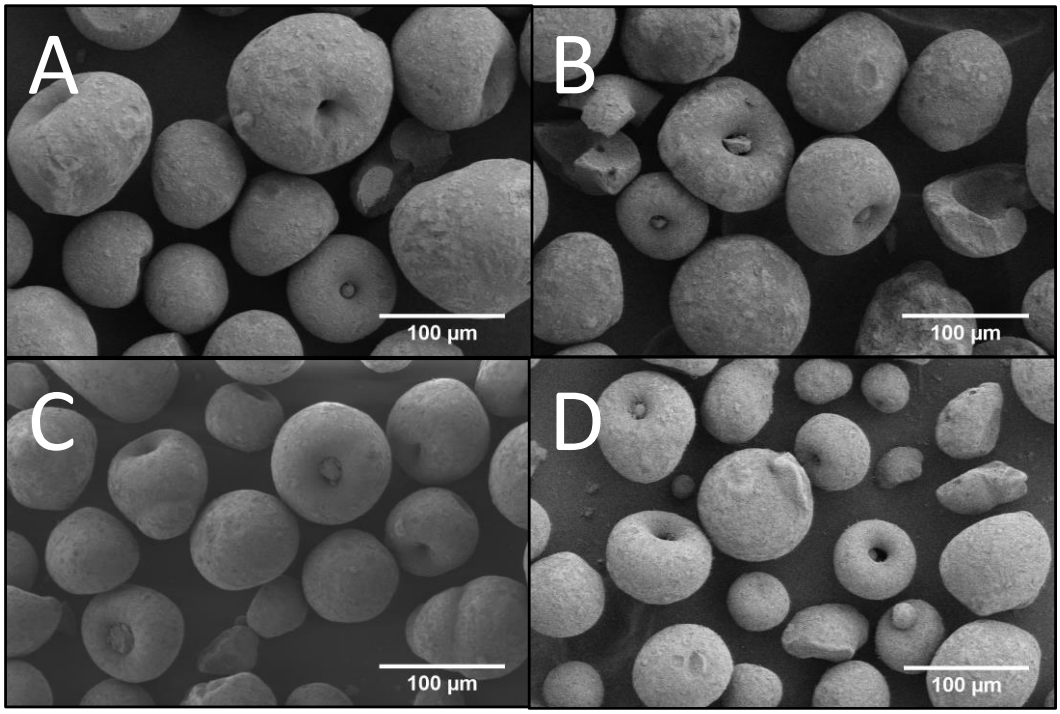

Figure 6. SEM images of γ-Al_2O_3 subjected to an ageing treatment at 150°C during 30 min (A), 2 h (B), 4 h (C) and 6 h (D).

b) Evidence for a dissolution-precipitation mechanism

Liquid-state Al(III) concentrations were measured by XRF and ICP-OES in the solutions obtained after filtration of the γ-Al_2O_3-water aged suspensions at 150°C/ hydrothermal conditions during various times. It has to be noted that these filtrates were acidified after filtration in order to prevent AlOOH precipitation from supersaturated solutions at room temperature. For all experiments, the concentrations of Al(III) released in the filtrates, for ageing times ranging from 30 min up to 14 h, were under the detection limit of both techniques ($3.7x10^{-6}$ $mol.L^{-1}$ for ICP).

If we suppose that under these severe conditions, as was the case at 70°C/atmospheric pressure, alumina *dissolution* is the first step of the weathering mechanism, it should thus occur very rapidly, leading to an immediate supersaturation followed by boehmite precipitation at much shorter times than for ageing at ambient pressure. Unlike for experiments described in Chapter II, for the

investigation of shorter times, we are intrinsically limited here by the duration of the cooling stage, which is unfortunately not less than 2 h 30 min approximately.

Following the same line, one may also contend that boehmite precipitation could occur not in hydrothermal conditions but during the cooling period, before the filtration of the suspension, due to a lower boehmite solubility at 25°C than at 150°C.[11,14] As a consequence, precipitation of boehmite during cooling could prevent the detection of aluminum that would be dissolved at 150°C. However, it will be shown after the next paragraph that this hypothesis is highly unlikely.

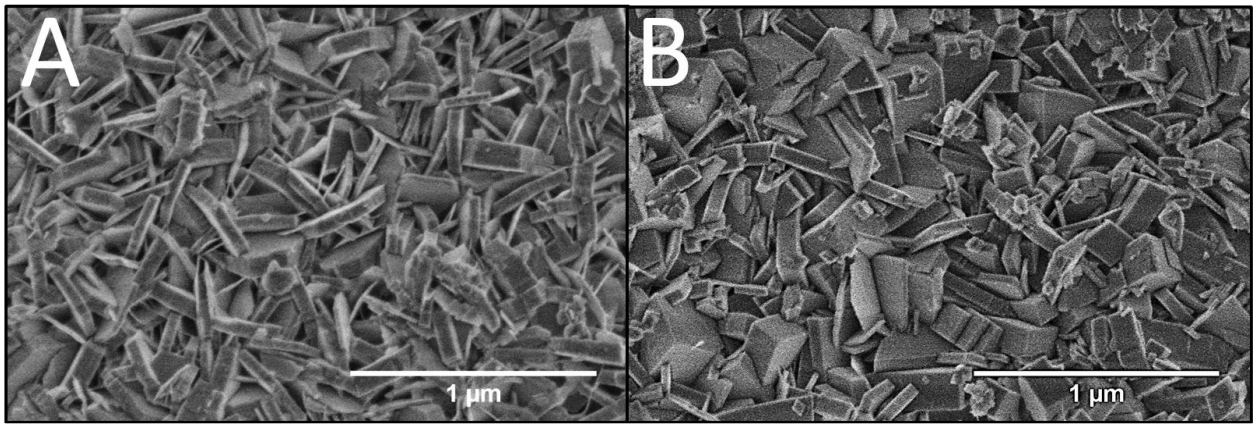

Figure 7. SEM images of γ-Al_2O_3 subjected to a hydrothermal treatment at 150°C during 30 min (A) and 6 h (B).

SEM images at high magnification show that platelet-like particles have covered the surface of the grains after hydrothermal ageing at 150°C during ageing periods of 30 min (Figure 7-A) and 6 h (Figure 7-B). This observation can be clearly associated with the detection of boehmite by XRD. Hence, this result reveals a *surface nucleation mechanism* of formation of boehmite particles on the alumina grains, in agreement with what has been demonstrated at 70°C. Additionally, observing an increase of their size vs ageing time, *crystal growth* is found as under milder conditions.

This result allows us to rule out the hypothesis that boehmite formation occurs during cooling after hydrothermal ageing. As a matter of fact, fast precipitation during cooling would most probably: 1) involve both homogeneous (in the solution) and heterogeneous (on the surface) precipitation and 2) could not involve particle growth with time, as cooling duration is always the same. On the

contrary, precipitation during cooling would arise from a supersaturation increasing with time, leading to a higher number of small particles forming during cooling after 6 h of ageing with respect to 30 min. Moreover, if precipitation was occurring during cooling (i.e. at low temperature), hydroxide (bayerite/gibbsite) formation would be favored instead of boehmite as in the case of ageing at 70°C. The observation of crystal growth with time is also against an alternative mechanism in which no dissolution would occur and that would involve a progressive topotactic transformation of the alumina individual particles back to the original boehmite.

Hence, despite the fact that aluminum cannot be quantified in solution, the parallelism between phenomena taking place at 70°C and under hydrothermal conditions allows us to conclude that the formation of boehmite as detected by XRD and SEM after hydrothermal treatment is probably a direct consequence of a dissolution-surface precipitation mechanism occurring during ageing at high temperature and pressure and starting in the very first minutes of treatment. Finally, no attrition is evidenced during alumina ageing in the autoclave set-up. As a consequence, it will not be possible to discuss the mechanical degradation of alumina in our conditions. We can nevertheless observe that attrition is not an inevitable consequence of alumina chemical weathering.

c) Kinetics of γ-Al_2O_3 Hydration in hydrothermal conditions

Figure 8 displays X-ray diffractograms of γ-Al_2O_3 aged under hydrothermal conditions during different periods of time. A qualitative analysis shows that the amount of boehmite increases with time.

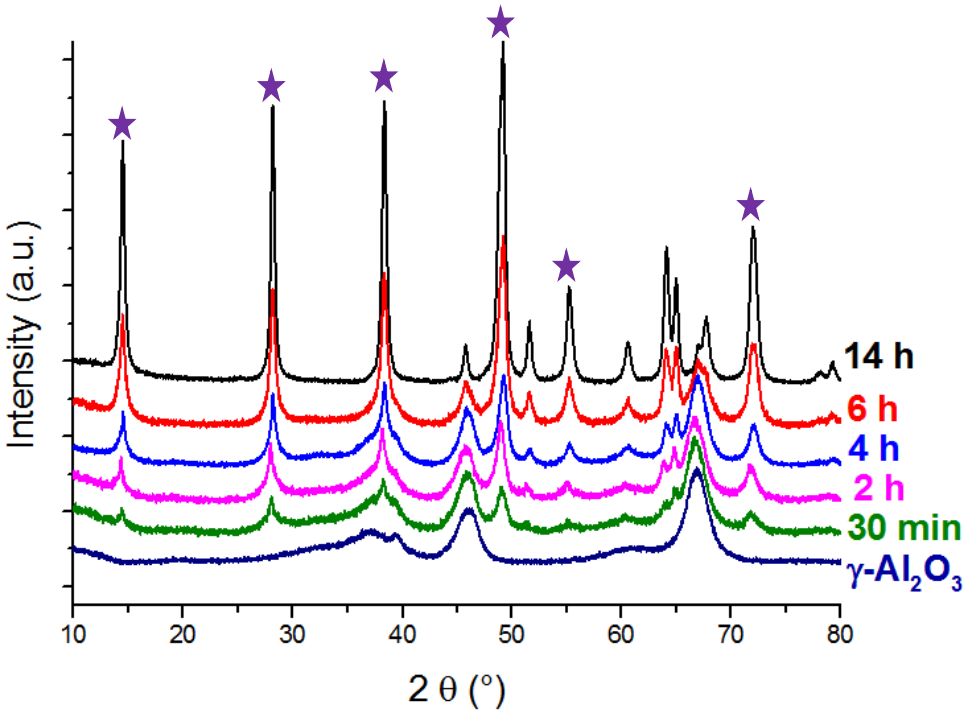

Figure 8. XRD patterns of γ-Al_2O_3 (dark blue, PDF No. 10-0425) subjected to an ageing treatment in water at 150°C under hydrothermal conditions during 30 min (green), 2 h (pink), 4 h (blue), 6 h (red) and 14 h (black) (1.6g/80 mL). ★: boehmite (PDF No. 83-1505).

Figure 9 shows the quantitative evaluation of the amount of boehmite visible in Figure 8 (ageing of γ-Al_2O_3 at 150°C/ hydrothermal conditions as a function of time). This evaluation was carried out with XRD (see supplementary section of this chapter) and cross-checked with TGA according to the same method as explained in III.A.3.

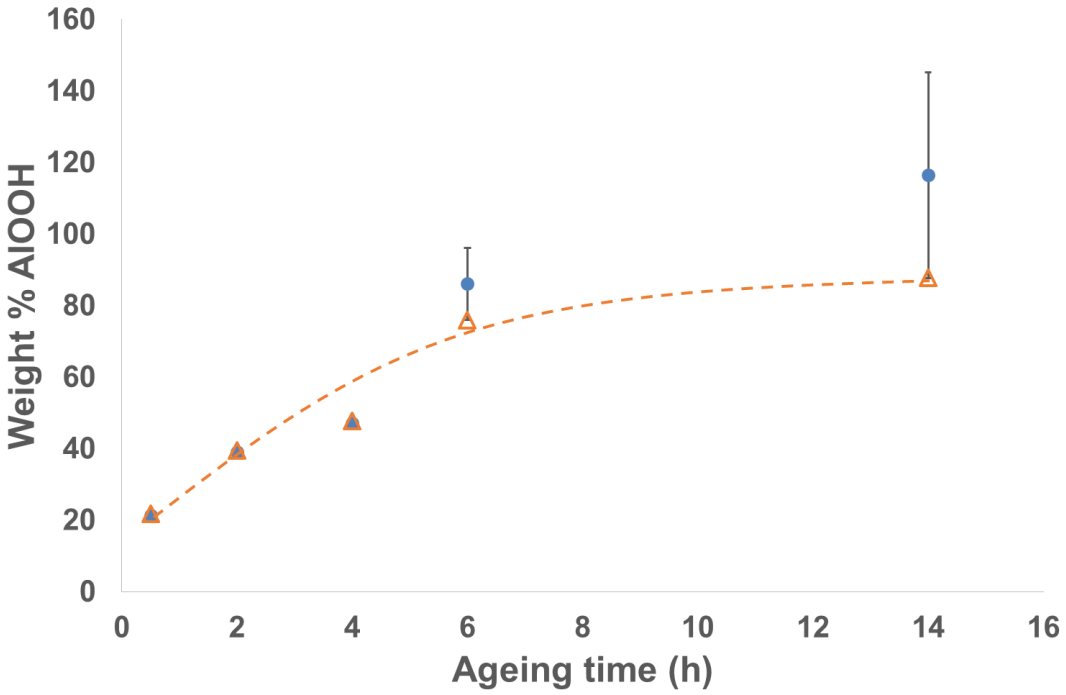

Figure 9. Variation of the amount of boehmite formed after ageing γ-Al_2O_3 in water for different times under stirring at 150°C (1.6 g/80 mL, hydrothermal conditions). Triangles correspond to the TGA analyses. Circles are the average of the XRD and TGA analyses and error bars are the standard deviation between both methods (see in the text).

Results shown with circles in Figure 9 are the average values of the quantifications resulting from XRD and TGA analyses, and error bars are the standard deviation from both techniques. The very small error bars at short ageing times demonstrate a good agreement between XRD and TGA and thus confirm the absence of a transient amorphous phase (at least after 30 min of treatment) that would be quantified by TGA but XRD-invisible. The absence of a transitory amorphous phase is in disagreement with the results of Lefèvre *et al.*[15] However, it has to be noted that these authors reported results of alumina hydration in very different conditions, i.e., atmospheric pressure. At longer ageing times (6 and 14 h), a larger standard deviation is obtained. There is clearly an overestimation of the amount of boehmite with XRD since a value of "143 %" is calculated after 14 h (looking at the diffractogram shows that the conversion is almost complete, 100%), while TGA underestimates boehmite, since it yields an amount of 88 %. First, it can be excluded that this difference arises from the presence of an amorphous phase since it would lead to higher AlOOH

quantification with TGA. Second, the XRD calibration curve shown in supplementary information (Figure 30) shows that a deviation from the linear correlation occurs at very high boehmite content (above 90%) casting some doubt on the reliability of the quantification for Al_2O_3/AlOOH mixture with boehmite amount above 90 %.

Hence for a more reliable quantification throughout the kinetic study from 30 min to 14 h, TGA results should be favored over XRD. The amount of boehmite increases with ageing time and reaches almost 100% after 14 h of hydrothermal treatment. This result correlates with previous works in hydrothermal conditions[4,10] and confirms that the rate of boehmite formation is higher at short ageing times, which implies that this rate depends, in line with Koichumanova et *al.*,[10] on the amount of available alumina. Moreover, it is confirmed that γ-Al_2O_3 hydration can lead within a few hours to the complete conversion of the initial solid even at moderate temperature (150°C) in hydrothermal conditions.

d) Effect of hydration in hydrothermal conditions on the textural properties of Al_2O_3

The specific surface areas of transition aluminas aged at 150°C during 4 h under hydrothermal conditions were compared to the corresponding untreated aluminas (Figure 10). A difference is visible for the different polymorphs. The specific surface areas (SSA) increased upon hydrothermal treatment and boehmite formation for the most crystalline ones: δ, δ/θ and θ. Conversely, the SSA remained constant for the γ/δ polymorph while it decreased for γ-Al_2O_3 as compared to the initial support.

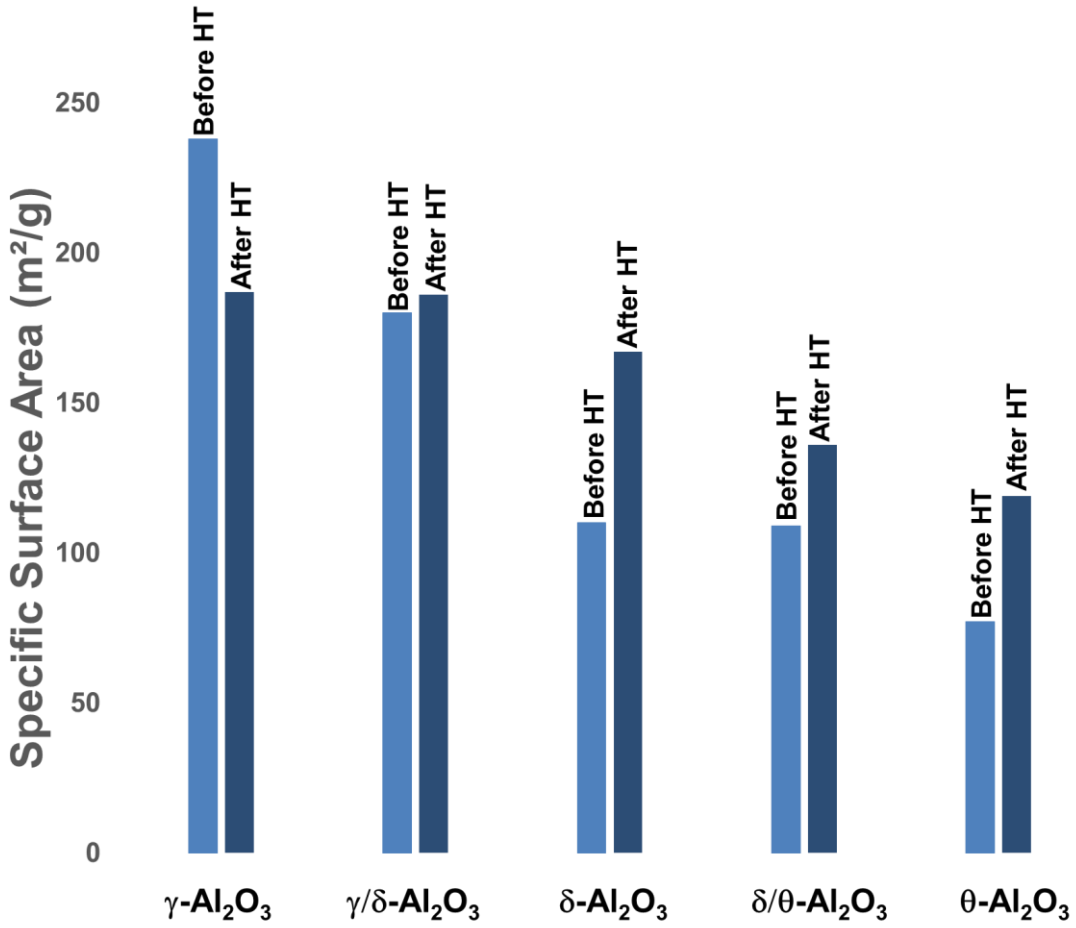

Figure 10. Specific surface areas of transition aluminas before (light blue) and after (dark blue) hydrothermal treatment (HT) in water at 150°C during 4 h (1.6 g/80 mL, hydrothermal conditions).

A closer look at the γ-Al_2O_3 case as a function of ageing time (Figure 11) shows that the specific surface area of this latter support increases at short ageing times (30 min) and then decreases. Such a behavior has already been described by Ravenelle *et al.*[4] and assigned to a two-stage process: first stage at short times, formation of small boehmite particles on the surface of alumina that create additional specific surface area; and second stage at longer ageing times, formation of a dense layer of boehmite that will block the porosity and hence, diminish the overall surface area.

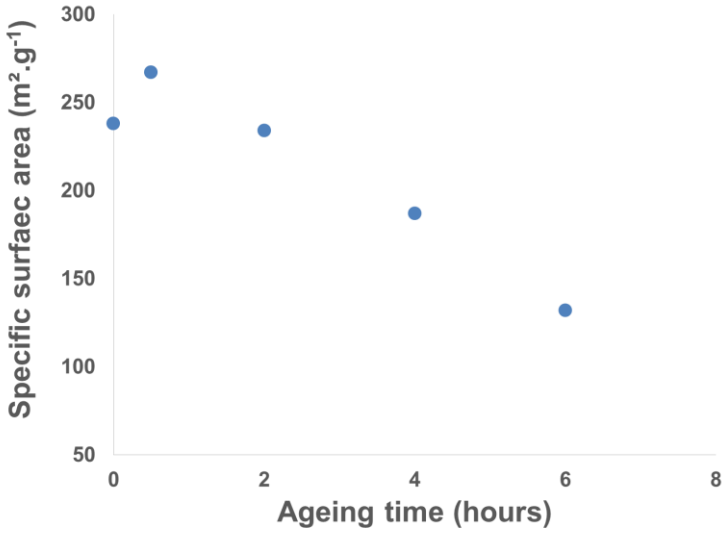

Figure 11. Variation of the specific surface area of γ-Al_2O_3 subjected to an ageing treatment at 150°C during different ageing times (1.6 g/80 mL, hydrothermal conditions).

This can explain the differences observed among the various alumina polymorphs (Figure 10) since we demonstrated in Figure 5 that the alumina reactivity is directly proportional to the surface area and crystallinity. Hence, after 4 h of ageing (conditions on Figure 10), the most reactive support (γ-Al_2O_3, 238 m^2/g) is already covered by a coating of boehmite (see Figure 7-B) explaining a lower surface area. It can be seen as a dilution of a porous solid (γ-Al_2O_3) with a non-porous one (boehmite). Inversely, for the less reactive supports (δ, δ/θ and θ), boehmite formation is slower and is only reaching the first stage of the textural modification under hydration (small boehmite particles) leading to an increased surface area. The γ/δ case is an intermediate one where the second stage has just begun leading to an identical specific surface area (equivalent to the third point on Figure 11).

III.A.5. Conclusion

Chemical weathering under hydrothermal conditions was studied as a function of time for a variety of transition aluminas. Experimental conditions (150°C/4 h, hydrothermal conditions) were chosen so as to limit the extent of hydration and to work below 100% conversion of the parent support, in order to compare the reactivity of the different alumina polymorphs. XRD results conclusively

showed that crystalline boehmite AlOOH was the only phase formed in these conditions. Going from γ to θ polymorphs, a clear decrease of the alumina reactivity was observed with a reduced amount of boehmite formed in parallel with a decrease of the specific surface area and increase of the crystallinity of the initial alumina.

Analysis of aluminum concentration in the filtrates, SEM imaging of alumina grains after ageing and boehmite quantification suggest the same conclusions obtained for hydroxide formation obtained under mild conditions: 1) here again, alumina *dissolution* is probably the key parameter for assessing the oxide reactivity, 2) dissolution is followed by AlOOH precipitation and crystal growth, 3) precipitation is exclusively a surface-induced process. It was shown also that supersaturation followed by precipitation probably occurs much more rapidly in hydrothermal conditions since no measurable Al^{3+} in solution was detected after 30 min of ageing.

However, in contrast to the results obtained under mild conditions, no attrition (mechanical degradation) was observed during ageing in the autoclave due to a more gentle stirring method.

A kinetic study showed that γ-Al_2O_3 hydration leads to the complete conversion of the initial solid to boehmite in a few hours at moderate temperature (150°C) in hydrothermal conditions.

Evolution of the specific surface area after hydrothermal ageing depends both on time and on the reactivity of the alumina: for the most reactive alumina (mostly γ), the fast formation of a layer of boehmite will decrease the overall surface area while for the less reactive ones (δ, δ/θ, θ) more limited formation of small boehmite particles will create additional surface area and lead to an increase of the specific surface area of the solid.

After this first investigation of the reactivity of alumina in pure water, the next part will focus on the influence of organic molecules (potential or model chemical reactants or products for biomass valorization or Fischer-Tropsch synthesis) on alumina hydration. Moreover, the presence of organic molecules will help to emphasize the various steps of alumina hydration mechanism.

III.B. Influence of organic additives on alumina chemical weathering in aqueous phase under hydrothermal conditions

III.B.1. Introduction

The results shown in part A illustrate the transformation of alumina into boehmite when subjected to an ageing treatment in presence of water only. It is of prime importance to study how the chemical weathering process of alumina may be altered in a reaction-like medium, since alumina, used as a catalyst carrier in hydrothermal conditions, will be in contact not only with pure water but also with organic molecules, as reactants or produced by the catalytic process.

Some authors reported a possible stabilization of the support by adding organic molecules to the medium, that were found to increase the hydrophobicity of alumina surface and therefore decreasing its weathering in aqueous phase (Chapter I, section I.3.3).[16–19]

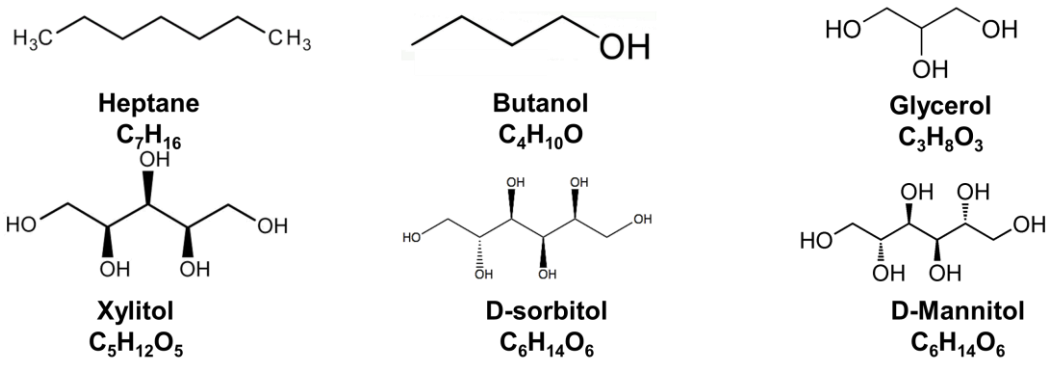

Figure 12. Organic molecules added to water throughout part B.

In part B, the effect of six organic molecules (Figure 12) on the chemical weathering of alumina in water will be studied: a C_7 alkane, heptane (VWR CHEMICALS, 99.3%) (selected for its lower toxicity compared to C_6 hexane and as a product of the Fischer-Tropsch syntheis); a C_4 alcohol, 1-butanol (Sigma-Aldrich, ≥99.4%) (selected as it is a byproduct of the Fischer-Tropsch synthesis); and four polyols, C_3 glycerol (Sigma-Aldrich, ≥99.5%), C_5 xylitol (Fluka, ≥99%), C_6 D(-)-sorbitol (Prolabo), C_6 D-mannitol (Sigma-Aldrich, 98%). These molecules were chosen in order to study the influence of i) the presence of hydroxyl groups (consider results obtained with heptane vs. the

other molecules; butanol vs. polyols); ii) the carbon chain length associated to the number of hydroxyl groups (glycerol vs. xylitol and sorbitol/mannitol); and iii) the stereochemistry of the polyols (sorbitol vs. mannitol).

In a first part, the effect of these three parameters on γ-Al_2O_3 weathering will be studied. Then, the interaction of sorbitol with γ-Al_2O_3 after the hydrothermal treatment will be more specifically detailed. In the last section, the various roles of polyols with respect to boehmite formation will also be investigated.

III.B.2. Effect of organic molecules on boehmite formation

Each organic compound was added to water at a concentration of 0.25 $mol.L^{-1}$ (same concentration as used in Ravenelle *et al*.[17] for their tests in the presence of sorbitol) before γ-Al_2O_3 was subjected to an ageing treatment at 150°C during 4 h. XRD patterns of the solids obtained after the different tests are compared to that of γ-Al_2O_3 treated in water (Figure 13).

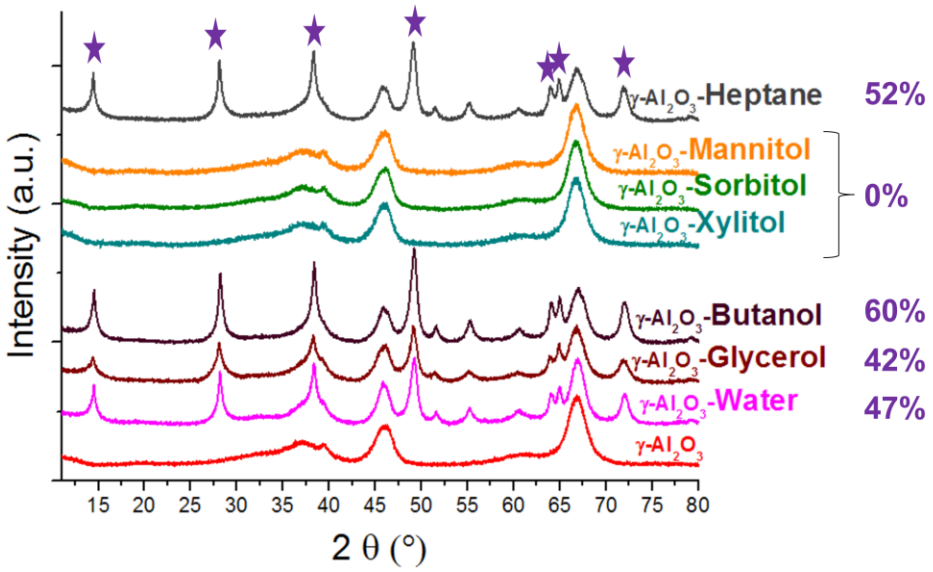

Figure 13. XRD patterns of γ-Al_2O_3 (red) subjected to an ageing treatment under hydrothermal conditions at 150°C under stirring during 4 h in presence of water (pink) and 0.25 $mol.L^{-1}$ glycerol (bordeaux), butanol (dark purple), xylitol (light blue), sorbitol (green), mannitol (orange) and heptane (dark grey) (1.6 g/80 mL). ★: boehmite (PDF No. 83-1505). The percentages indicate the amount of boehmite formed.

The amount of AlOOH detected in presence of heptane, which is an OH-free molecule, is not significantly different from that in water which indicates that the presence of hydroxyl groups could be a prerequisite for the decrease of boehmite formation. However, n-butanol does not inhibit alumina hydration either. The effect of OH number can be affirmed by comparing the amount of boehmite formed in presence of glycerol ($C_3H_8O_3$) vs. C_5- and C_6-polyols, xylitol ($C_5H_{12}O_5$), sorbitol ($C_6H_{14}O_6$) or mannitol ($C_6H_{14}O_6$) that all have a total inhibiting effect on boehmite formation. Jongerius *et al.*[18] showed that the inhibiting effect of boehmite formation on a Pt/γ-Al_2O_3 catalyst in presence of guaiacol (a natural aromatic compound present in guaiacum trees, $C_7H_8O_2$) is higher than ethanol (C_2H_6O) and according to the authors this was due to the higher number of oxygen functionalities. Results obtained by Ravenelle *et al.*[17] are in the same line and were attributed to the increase of the carbon chain length. On the other hand, no differences could be evidenced between sorbitol and mannitol that are stereoisomers. Hence, the effect of stereochemistry of polyols on γ-Al_2O_3 chemical weathering is difficult to emphasize under these experimental conditions since a total inhibition is observed for both stereoisomers.

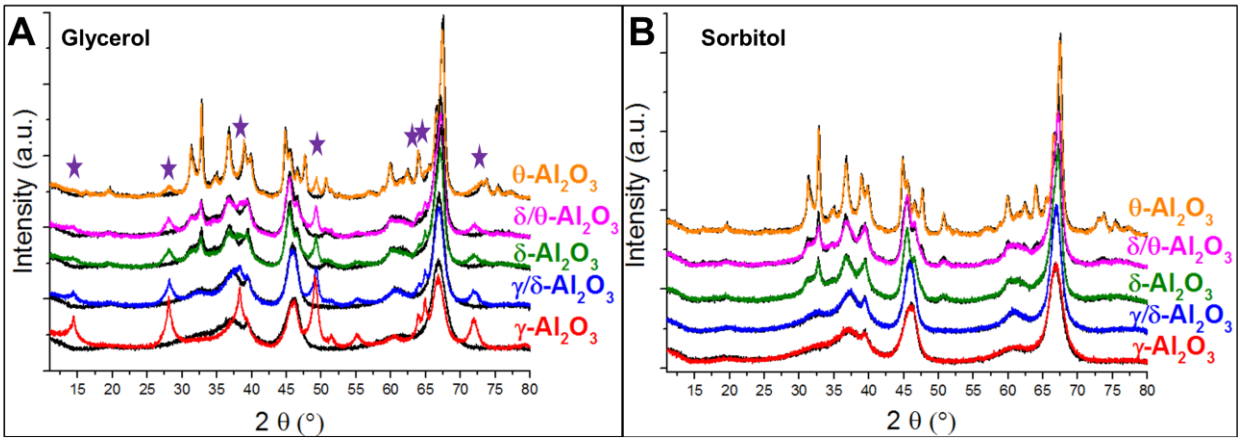

Figure 14. XRD patterns of γ-Al_2O_3 (red), γ/δ-Al_2O_3 (blue), δ-Al_2O_3 (green), δ/θ-Al_2O_3 (pink), θ-Al_2O_3 (orange), subjected to an ageing treatment under hydrothermal conditions in water in presence of 0.25 mol.L^{-1} glycerol (A) and sorbitol (B) at 150°C under stirring during 4 h (1.6 g/80 mL), and compared to the initial diffractograms (black).★ : boehmite (PDF No. 83-1505).

Tests in the presence of glycerol or sorbitol were carried out for all the transition aluminas. Boehmite was formed with glycerol and its amount decreased with the decrease of the specific

surface area (compare intensity of AlOOH peaks on Figure 14-A). Hence, the variation of boehmite amount formed follows the same tendency observed in water (Part A). No boehmite was detected with sorbitol (Figure 14-B) neither by XRD nor on SEM images (Figure 15). The same morphology of grains is retained from the non-treated γ-Al_2O_3 (Figure 15-A) and there is no other visible phase on the surface even at the higher magnifications (Figure 15-B, C and D) for which boehmite particles were clearly distinguished in pure water (Figure 7-A, Part III.A).

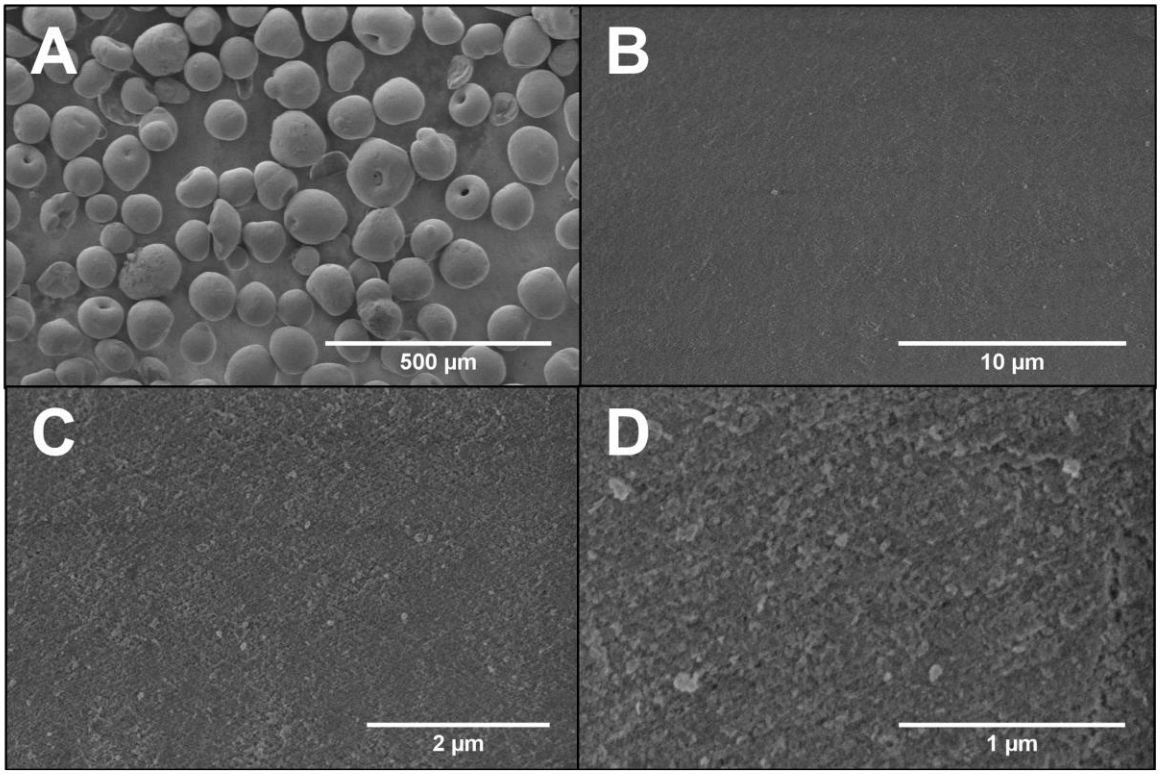

Figure 15. SEM images at different magnifications of γ-Al_2O_3 subjected to an ageing treatment at 150°C during 4 h in water with 0.25 mol.L^{-1} ***sorbitol****. (1.6 g/80 mL, hydrothermal conditions).*

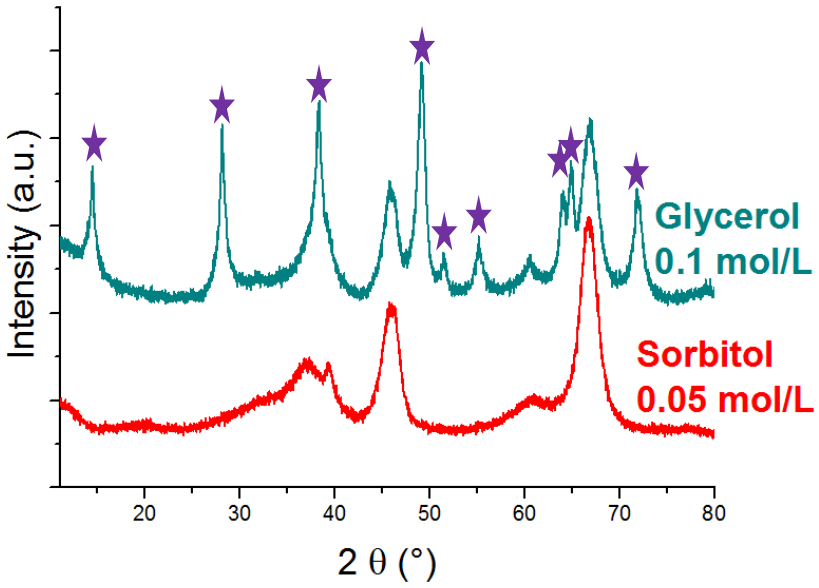

Figure 16. XRD patterns of γ-Al_2O_3 subjected to an ageing treatment at 150°C under stirring during 4 h in an aqueous solution of 0.05 mol.L^{-1} sorbitol (red) or 0.1 mol.L^{-1} glycerol (light blue) (1.6 g/80 mL, hydrothermal conditions). ★: boehmite (PDF No. 83-1505).

In order to decorrelate the effect of the OH number and of the carbon chain length, the concentration of C_3 glycerol was set to 0.1 mol.L^{-1}, that is twice that of C_6 sorbitol which is fixed here at 0.05 mol.L^{-1}. The number of OH functions in solution is thus identical. From the corresponding XRD patterns of γ-Al_2O_3 presented on Figure 16, it can be seen that in the presence of glycerol, peaks characteristic of boehmite are still detected. Hence, even when fixing the same number of OH groups, the effect of organic molecules on boehmite formation is not similar. Unlike the three other tested molecules, C_5- and C_6-polyols have a specific effect on alumina weathering that will be investigated in the next sections.

III.B.3. Interaction of sorbitol with γ-Al_2O_3 upon hydrothermal treatment

Since promising results were obtained with sorbitol, a more in-depth study of its effect on alumina hydration will be detailed in the section. Textural and structural analyses of γ-Al_2O_3 that was aged in presence of sorbitol will be shown and the interaction of sorbitol with alumina under these conditions will be investigated by spectroscopic methods.

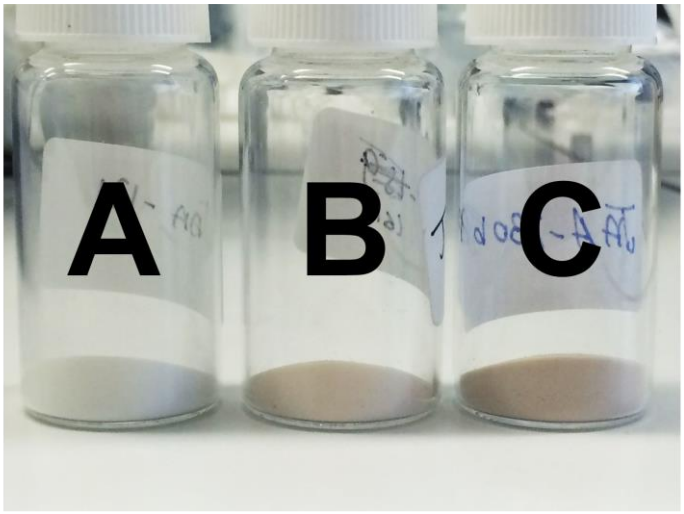

Figure 17. Photo of γ-Al_2O_3 samples subjected to an ageing treatment at 150°C under stirring: in presence of water during 4 h (A); in an aqueous solution of 0.25 mol.L^{-1} sorbitol during 4 h (B) and 14 h (C) (1.6 g/80 mL, hydrothermal conditions).

Only in presence of sorbitol, a very clear change of the color of the solids was observed after the ageing tests. It can be seen in Figure 17 that the color changed from white (Figure 17-A) to caramel (Figure 17-B), and became darker when the ageing treatment time was longer (from 4 h to 14 h, Figure 17-C) which indicates that organic species were deposited on γ-Al_2O_3.

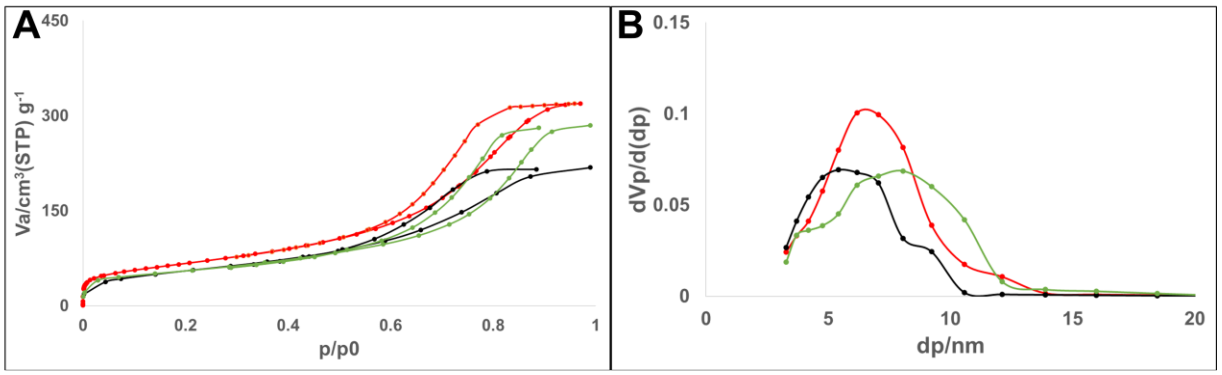

Figure 18. Adsorption desorption isotherms and BJH plot of γ-Al_2O_3 (red) and γ-Al_2O_3 subjected to an ageing treatment in water (green) and with 0.25 mol.L^{-1} sorbitol (black) at 150°C during 4 h (1.6 g/80 mL, hydrothermal conditions).

The specific surface area of γ-Al_2O_3 aged in presence of sorbitol during 4 h decreased from 238 $m^2.g^{-1}$ to 193 $m^2.g^{-1}$ which is similar to the case of the support aged in water only (S_s = 187 $m^2.g^{-1}$). This decrease was accompanied with a decrease in the total pore volume of the support from 0.49 to 0.33 $cm^3.g^{-1}$ resulting in a lower pore volume with sorbitol with respect to the ageing treatment in pure water (0.43 $cm^3.g^{-1}$) (Figure 18). Since there is no formation of boehmite in the case of sorbitol, one can deduce that the decrease in the total pore volume is due to the blockage of the pores by a coating of organic molecules. A first conclusion is that sorbitol did not help keeping the surface of γ-Al_2O_3 fully accessible.

A ^{13}C NMR study was done in order to verify the nature of the chemical species, if any, derived from sorbitol and deposited on the alumina surface. The experiments were performed using a 500 MHz Brucker AV III in cross polarization for solid state (relaxation time (D1) = 1 s, contact time = 1 ms, decoupling ^1H: spinal 64, spinning rate = 14 KHz and number of scans = 2464) and in zgpg 30° for liquid state (decoupling ^1H, D1 = 5 s, pulse duration = 14.5 µs and number of scans = 2048). The spectra were recorded on:

- (i) a solid obtained by adsorbing sorbitol on alumina in aqueous phase (used as reference). A mixture between γ-Al_2O_3, water and sorbitol respecting the same proportions used for the test (1.6 g of γ-Al_2O_3 + 80 mL of water + 0.25 $mol.L^{-1}$ of sorbitol) was stirred and the solid recovered by filtration. The solid was washed once to remove any physisorbed organic layer and then was dried at 90°C during one night. It has to be noted that the powder kept its white color contrary to the aged sample. The filtrate was retained for ^{13}C NMR analysis in liquid phase, which will be discussed below;
- (ii) γ-Al_2O_3 after being subjected to a hydrothermal treatment in presence of 0.25 $mol.L^{-1}$ sorbitol at 150°C during 4 h. The ^{13}C RMN spectrum recorded on the supernatant liquor will also be discussed in the next section;
- (iii) The solid obtained in (ii) after the ageing test in presence of sorbitol, but washed once in order to remove any physisorbed organic molecules. The solid obtained was still colored (caramel) which confirms the deposition of strongly adsorbed organic molecules on the surface of γ-alumina.

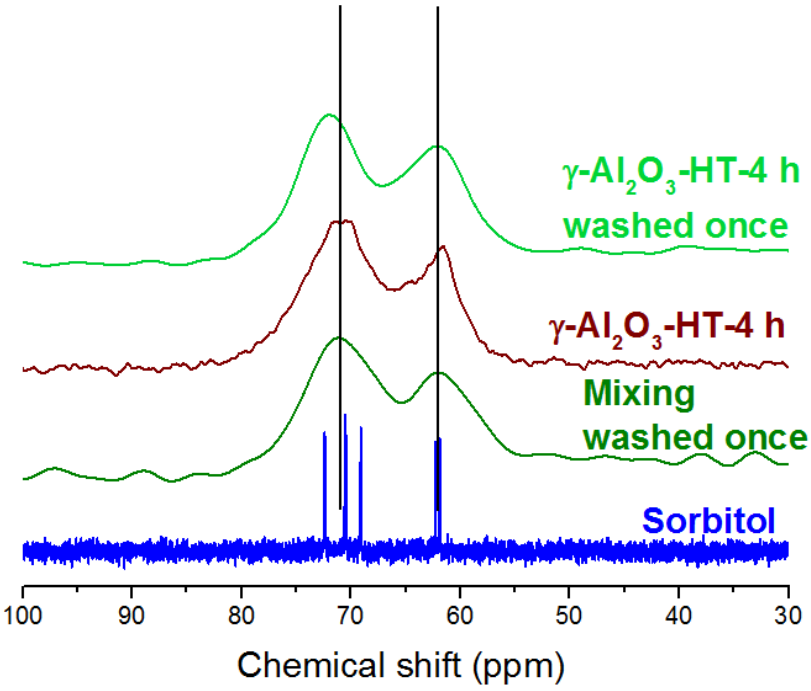

Figure 19. ^{13}C NMR spectra of sorbitol dissolved in water (0.55 mol.L^{-1}) (blue), mixing of γ-Al_2O_3 and sorbitol washed once (green), γ-Al_2O_3 subjected to an ageing treatment at 150°C during 4 h under hydrothermal conditions (brown) and washed once (light green).

These spectra were compared to the one of sorbitol dissolved in water at a concentration of 0.55 mol.L^{-1} and are represented in Figure 19. The spectrum of sorbitol in aqueous solution is in line with the one presented in the literature.[20] The attribution of the six peaks is summarized in Figure 20.

The NMR spectra of the three solids show two broad peaks, the first one at higher chemical shift that includes the four carbons in the middle of the chain, and the second one at lower chemical shift that includes the two carbons at the ends of the molecule. The similarities observed in Figure 19 for the first two spectra with the spectrum of sorbitol in aqueous solution suggest that the molecules adsorbed are chemically close to sorbitol even after hydrothermal treatment. The broadening indicates that these species are immobilized on the surface of alumina which prevents the detection of thinner peaks.

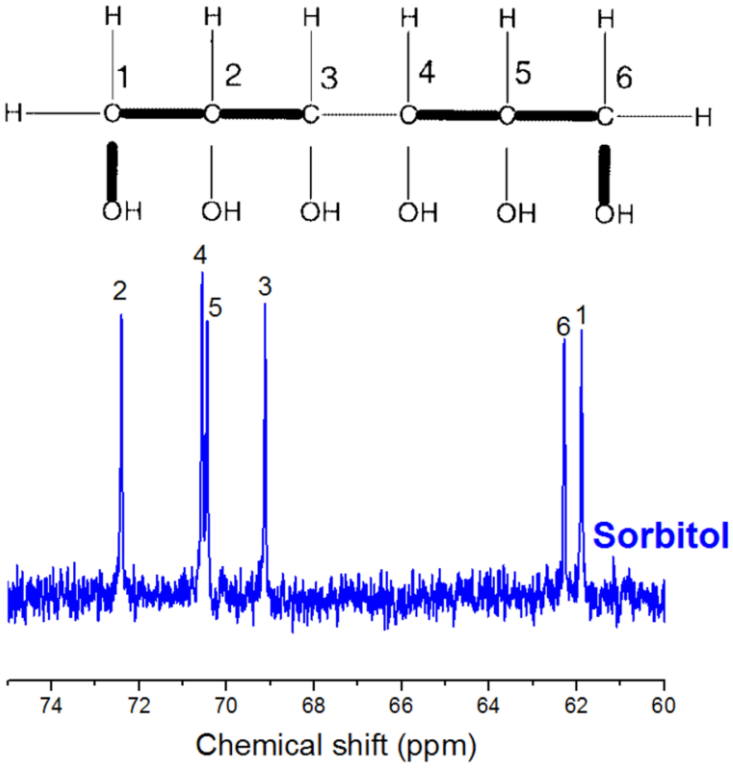

Figure 20. Chemical structure of sorbitol and numbering of their carbons in the Fischer representation.[20] ^{13}C NMR spectrum of sorbitol dissolved in water (0.55 mol.L^{-1}).

Nevertheless a small shift is observed only for the peak at about 70.45 ppm for the solid subjected to the ageing test and then washed, i.e. after removing loosely bound organic molecules. Hence, it can be concluded that some molecules are strongly adsorbed on the surface and are not fully chemically similar to the initial sorbitol species, and that these sorbitol-derived caramel-like molecules are responsible for the color change of the solid. As a matter of fact, the sample on which sorbitol was only adsorbed without hydrothermal treatment remained white. Since the 70 ppm peak includes the carbons in the middle of the sorbitol chain, one can suppose that the chemical changes affect these carbons. The deposition of a carbonaceous layer on the surface of γ-Al_2O_3 was observed in previous works in presence of organic compounds such as polyols (sorbitol, glycerol, ethylene glycol, guaïacol, lignin…) and simple sugars (like glucose).[16–18,21,22]

Hence, upon ageing γ-Al_2O_3 in a solution of sorbitol in hydrothermal conditions, a mixture of sorbitol and of strongly adsorbed caramel-like organic molecules derived from sorbitol remain on

its surface. Pore blockage and a decrease in the specific surface area of alumina consequently occur which lead to a reduced accessibility of γ-alumina surface.

III.B.4. Evidence for a dissolution step and role of polyols

We have shown previously that C_6 polyols clearly inhibit boehmite formation. However, we showed in the previous chapter that chemical weathering of γ-Al_2O_3 occurred through a two-step dissolution-precipitation mechanism. The aim of this part is to understand on which step polyols play a major role, the first step of the chemical degradation of γ-Al_2O_3, dissolution, the second one, oxyhydroxide precipitation, or even both.

γ-Al_2O_3 was subjected to an ageing treatment in water in presence of 0.25 mol.L^{-1} sorbitol at 150°C during different ageing times up to 38 h. No peaks characteristic of boehmite were visible on the XRD patterns of the solids after the tests (Figure 21). The second step of the hydration mechanism defined in chapter II, which is (oxy)hydroxides precipitation, is thus not evidenced in the presence of sorbitol, even for long ageing times. However, the possibility that the alumina surface dissolves (the first step of the mechanism) remains undetermined for the moment.

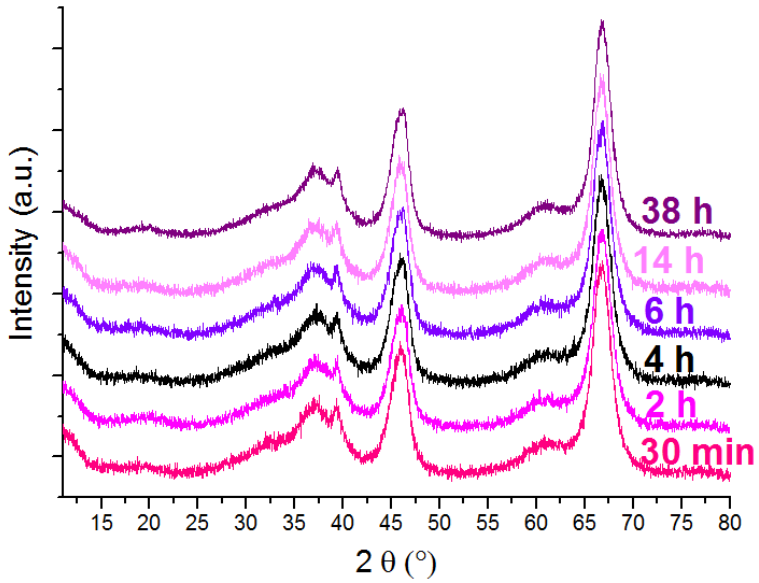

Figure 21. XRD patterns of γ-Al_2O_3 subjected to an ageing treatment in water with 0.25 mol.L^{-1} sorbitol at 150°C during different ageing times up to 38 h (1.6 g/80 mL, hydrothermal conditions).

Liquid-state Al(III) concentrations were measured by ICP-OES, with a SPECTRO ARCOS from SPECTRO AMETEK, in the solutions obtained after filtration of the six γ-Al_2O_3-water suspensions. It has to be noted that, as before, these filtrates were acidified after filtration in order to prevent AlOOH precipitation from supersaturated solutions at room temperature. Results obtained are presented on Figure 22 along with curves, showed in part A, of γ-Al_2O_3, bayerite, boehmite and gibbsite dissolution into Al(III) complexes.

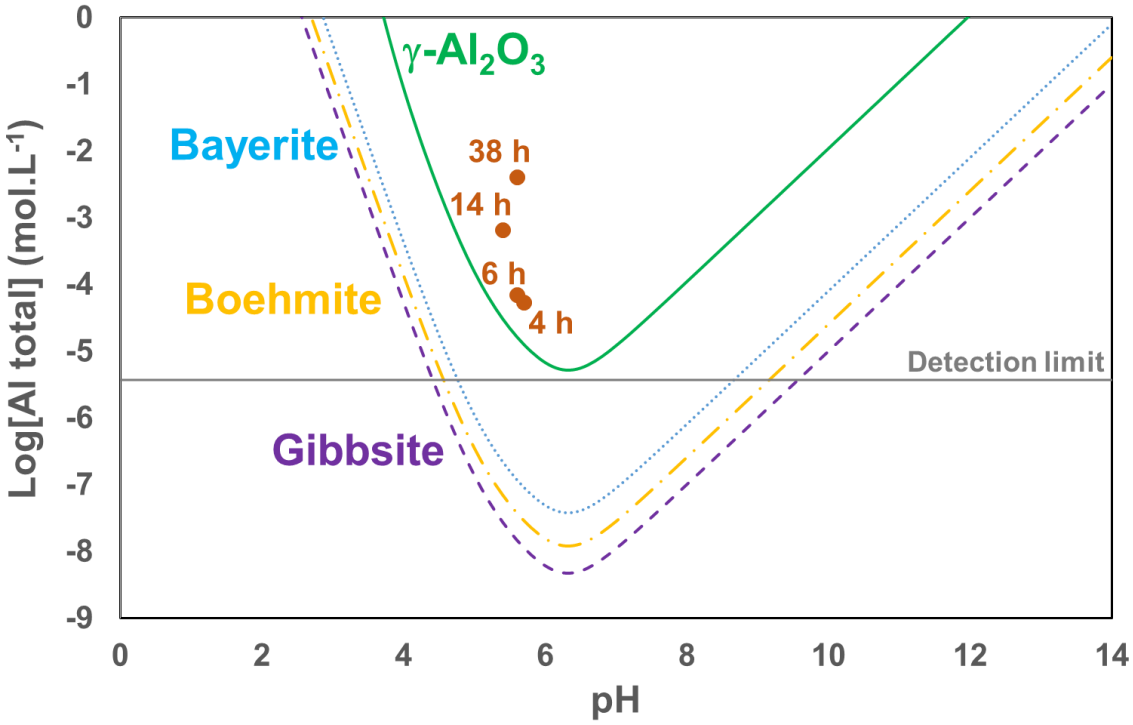

Figure 22. Concentrations of Al(III) in solution (log scale) as a function of pH for γ-Al_2O_3 (solid green line), bayerite (dotted blue line), boehmite (dash-dotted yellow line) and gibbsite (dashed purple line). Experimental data points are shown as filled circles for suspensions aged at 150°C in water with 0.25 mol.L^{-1} sorbitol during different ageing times up to 38 h (1.6 g/80 mL, hydrothermal conditions).

For experiments at 30 min and 2 h, the concentrations of Al(III) released in the filtrates were under the detection limit of the technique ($3.7x10^{-6}$ mol.L^{-1}). However, the concentrations increased from 4 h up to 38 h. Solutions are supersaturated with respect to AlOOH precipitation, though boehmite

is not seen to precipitate. Moreover, even if these concentrations are consistent with γ-alumina solubility, a steady-state is not reached up to 38 h, unlike what was evidenced in the absence of organic molecules, at milder temperatures in Chapter II and in hydrothermal conditions in part A of this chapter. This tends to indicate that in the presence of sorbitol, *alumina dissolution* is occurring and is even increasing with time, even though boehmite is not precipitating.

In the presence of sorbitol, the amount of dissolved alumina was 0.01% at 4 h of ageing and increased to 0.02, 0.18 and 1.17% at 6, 14 and 38 h respectively. In one occurrence, Ravenelle *et al.*[17] mentioned alumina dissolution in the presence of polyols (sorbitol or glycerol), with less than 0.1% of alumina dissolved at 10 h of ageing of Pt/γ-Al_2O_3 at 225°C. γ-Al_2O_3 surface undergoes a chemical weathering in the same order of magnitude, even in the absence of supported active phase. It can be reminded that the amount of boehmite formed in the absence of sorbitol (part A), which is equivalent to the alumina amount that dissolved before precipitating, was much higher, from 47% at 4 h to 76% at 6 h and to 88% at 14 h of ageing treatment. These amounts are summarized in Table 1.

Table 1. Amount of alumina dissolved for supports aged at 150°C during different ageing time with and without sorbitol.

Ageing Time	With Sorbitol (0.25 mol/L^{-1})	Without Sorbitol
4 h	0.01 %	47 %
6 h	0.02 %	76 %
14 h	0.18 %	88 %
38 h	1.17 %	Not done

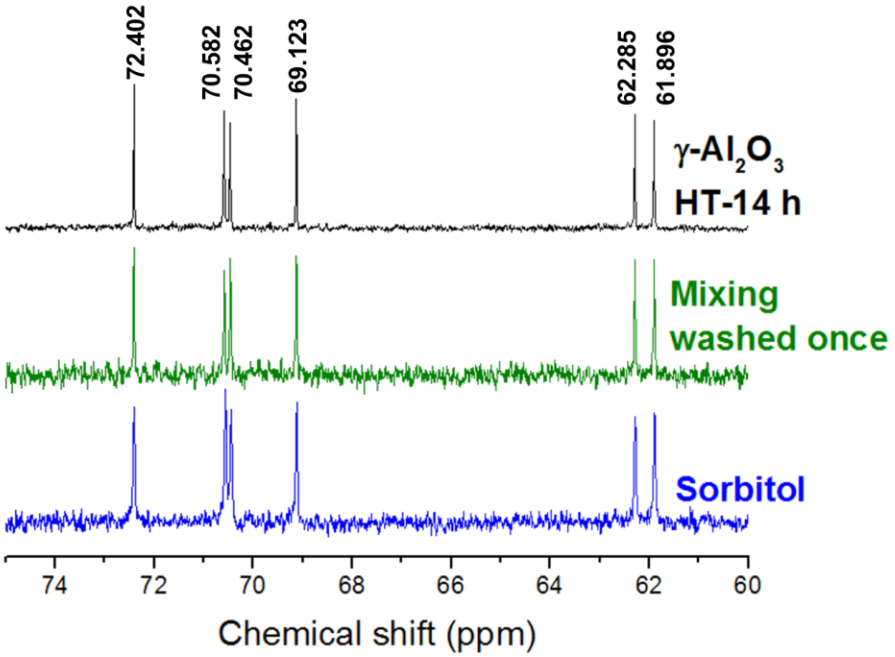

Figure 23. ^{13}C NMR spectra of sorbitol dissolved in water at a concentration of 0.55 mol.L^{-1} (blue), filtrate of a mixing between γ-Al_2O_3, sorbitol and water and that was washed once (green) and filtrate of the suspension of γ-Al_2O_3 subjected to an ageing treatment at 150°C during 14 h under hydrothermal conditions (black).

We have previously shown that sorbitol or derived molecules remain adsorbed on alumina after hydrothermal treatment. In order to rationalize our observations, we will determine by using ^{13}C NMR whether sorbitol or derived molecules are also present in the liquid phase containing the Al(III) ions, and if these molecules can influence Al(III) concentration in the solution and therefore alumina dissolution. Spectra were recorded on:

- (i) the filtrate of the mixture between sorbitol, γ-Al_2O_3 and water that was washed once (explained in section III.B.3, used as reference);
- (ii) the supernatant liquor obtained after recovering by centrifugation γ-Al_2O_3 submitted to a hydrothermal treatment in water at 150°C during 14 h with sorbitol.

Both spectra were compared to sorbitol dissolved in water at a concentration of 0.55 mol.L^{-1} (Figure 23). No modifications were detected in the spectra (attributions of the six peaks are shown

in Figure 20) indicating that there are no other sorbitol-derived molecules (like acids formed by oxidation of sorbitol) that, for instance, could interact by complexation with Al(III) in the solution.

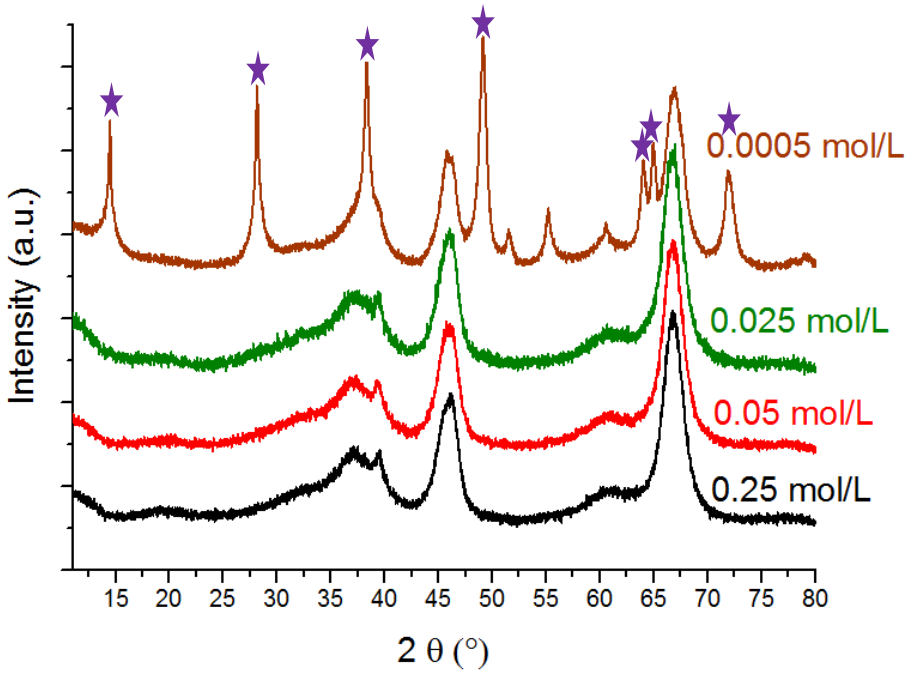

Figure 24. XRD patterns of γ-Al_2O_3 subjected to an ageing treatment in water with different concentrations of sorbitol at 150°C during 4 h (1.6 g/80 mL, hydrothermal conditions). ★ : boehmite (PDF No. 83-1505).

The effect of sorbitol concentration on boehmite formation was finally investigated. By decreasing the concentration of sorbitol from 0.25 to 0.025 mol.L^{-1}, no boehmite was detected by XRD. However, boehmite was detected when a very low concentration of sorbitol (0.0005 mol.L^{-1} or 0.5 mmol.L^{-1}) was used (Figure 24).

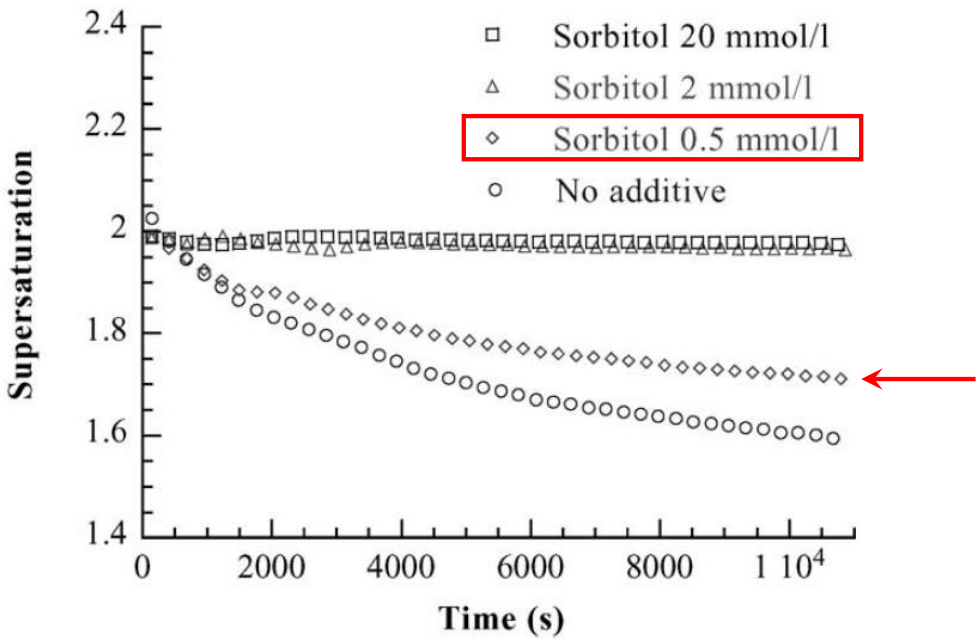

Figure 25. Effect of sorbitol concentration on gibbsite agglomeration. The term of agglomeration was explained by the authors as the mechanism by which particles existing in a suspension are linked by simultaneous aggregation and growth. It is a phenomenon that happens during the crystallization of gibbsite (a step of the Bayer process). The supersaturation is the concentration of aluminate ions and is measured by means of a conductivity regulation.[23]

These results can be compared with the work of Paulaime *et al.*[23] dealing with gibbsite agglomeration. The authors showed that when increasing sorbitol concentration from 0.5 to 20 mmol.L^{-1}, gibbsite crystals do not agglomerate and aluminum is maintained in solution despite the supersaturation (Figure 25). Similar observations with identical concentrations of polyols (from 20 to 0.5 mmol.L^{-1}) were found in the same work in presence of mannitol and xylitol. Similarly, Watling *et al.*[24] showed that by increasing the concentration of sorbitol, xylitol and mannitol from 2, 4 to 6 mmol.L^{-1} the growth of gibbsite particles also decreases (the growth of particles was calculated by weighting the amount of gibbsite precipitated as a function of time and validated by use of a particle size analyzer). We can conclude that sorbitol can limit the growth of boehmite nuclei formed in the solution and inhibit their precipitation. This effect increases with the polyol concentration.

We can thus suppose that in the presence of sorbitol, the hydration of alumina takes place in two steps similar to those evidenced in pure water, but with different intermediate species, *i.e.* $Al_x(OH)_y$ oligomeric species interacting with sorbitol. Reactions can be summarized as follows:

	Without sorbitol	With sorbitol
Dissolution	$Al_2O_{3\ (s)} \rightarrow Al_x(OH)_{y\ (aq)}$	$Al_2O_{3\ (s)} \rightarrow Al_x(OH)_y$-sorbitol $_{(aq)}$
Precipitation	$Al_x(OH)_{y\ (aq)} \rightarrow AlOOH_{\ (s)}$	$Al_x(OH)_y$-sorbitol $_{(aq)} \rightarrow AlOOH_{\ (s)}$ + sorbitol $_{(aq)}$

In the absence of sorbitol, as concentrations in solution (below the detection limit) are necessarily closer to the solubility of boehmite than to the solubility of alumina, it can be deduced that the precipitation step has rapidly tended towards equilibrium and the dissolution step is the rate-limiting one. The existence of the second step also draws the first reaction toward more dissolution, by removing the intermediate from the liquid phase.

It is difficult to discuss the concentration of $Al_x(OH)_y$ species interacting with sorbitol with respect to the solubility curve displayed on Figure 22 that was calculated for bare complexes $Al_x(OH)_y$. No steady-state is reached here, as Al(III) concentration continuously increases with time, despite the supersaturation with respect to boehmite precipitation. This suppression of boehmite precipitation tends to show that sorbitol stabilizes the intermediate. The comparison between the amount of Al(III) released by the first step, in the absence and in the presence of sorbitol, also indicates that the dissolution step is slowed down by sorbitol; otherwise, Al(III) would accumulate in solution and its concentration would be two to three orders of magnitude larger than measured. We thus conclude that sorbitol both *slows down the dissolution* of the support and *inhibits the growth* of hydroxy species that remain in suspension.

From our results, it can also be inferred that the formation of caramel-like molecules, detected when sorbitol is used, is not a prerequisite to inhibit the dissolution of alumina, since they do not appear to form with mannitol and xylitol. Measurements of aluminum dissolution in the presence of these two polyols should be done in complement to confirm this hypothesis.

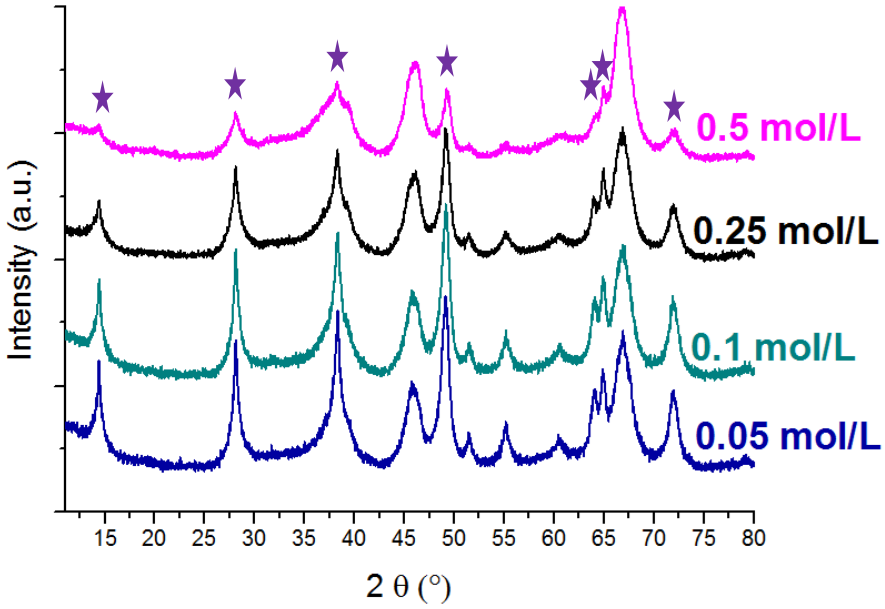

Figure 26. XRD patterns of γ-Al_2O_3 subjected to an ageing treatment in water with different concentrations of glycerol at 150°C during 4 h (1.6 g/80 mL, hydrothermal conditions). ★ : boehmite (PDF No. 83-1505).

It was shown before that glycerol was ineffective in preventing boehmite formation (Figure 13, Figure 14 and Figure 16) for a concentration of 0.25 M or below. An influence of the concentration of glycerol can be observed though, but at higher concentrations. Figure 26 shows that the amount of boehmite formed decreases (compare peaks intensities) at 0.5 M. The increased number of C-OH in the medium has thus an effect on decreasing boehmite formation, but this remains less efficient than with C_5 and C_6 polyols.

Several authors[23–25] showed that polyols prevent (oxy)hydroxides growth and this effect increases with the number of carbon atoms (hydroxyl groups). This can explain the formation of particles of boehmite detected by XRD in presence of glycerol ($C_3H_8O_3$) and not sorbitol ($C_6H_{14}O_6$) for the same concentration (0.25 M) (Figure 13). Moreover this strength of interaction between polyols and aluminum-containing compounds is reported to change according to the stereochemistry of the additive. Chiche *et al.*[25] showed that smaller particles of boehmite are formed in presence of polyols with higher complexing strength. This strength increases with the number of OH groups and when the polyol contains two successive OH threo sequence (i.e. three consecutive OH groups alternating

on each side of the Fischer projection of the molecule), as is found in xylitol and sorbitol. Of the two, xylitol had the lower effect due to a lower number of OH group. Mannitol exhibits a weaker effect as it lacks the two successive threo sequence. In our work, boehmite was not detected in presence of the three polyols cited above. The effect of stereochemistry (sorbitol vs mannitol) linked to a specific complexing effect is thus not as marked as in their work,[25] at least at the high concentrations we used. Hence, experiments with a lower concentration of sorbitol and mannitol should be performed in order to reveal a potential effect of the stereochemistry. Aluminum complexation was also proposed by Paulaime *et al*. (Figure 27).[23] However, their study was carried out at very high pH, at which polyols can be deprotonated, which is not the case of our work (pH ≤ 6). Moreover, according to our ^{13}C NMR results on the liquid phase (Figure 23), no other molecules that could complex Al (III) were detected. If polyols inhibit the growth of boehmite particles in our experimental conditions, it would rather be through physical interactions, rather than by specific adsorption or complexation.

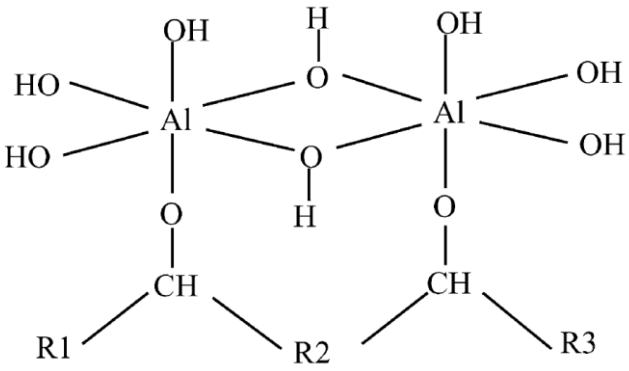

Figure 27. Molecular complex between gibbsite seed and a polyhydroxyl additive.[23]

The effect of polyols on γ-Al_2O_3 surface passivation can also be discussed at the molecular level. The carbonaceous layer (adsorbed species after hydrothermal treatment) that was shown to form on γ-alumina surface (section III.B.3) decreases the chemical weathering of alumina by increasing the hydrophobicity of its surface according to the literature.[16–19] A group of researchers[17,18,21,22] investigated the interactions of organic molecules with the surface of alumina in order to study

their stabilizing effect against alumina transformation to boehmite. They suggest that a strong interaction between a polyol and γ-Al_2O_3 surface is supposed to establish by forming multidentate alkoxy species when the carbon chain of the polyol is composed of a minimum of three carbons and a minimum of two hydroxyl groups positioned on the first and the last carbon (Figure 28). In our case, we have proved that molecules resembling polyols remain strongly adsorbed on the alumina surface and the proposed adsorption mode is plausible. However, we do not have evidence of an increase of hydrophobicity of the organic layer, and we can suppose that adsorbed organic molecules simply block access of the alumina surface and porosity to water, thus limiting its dissolution.

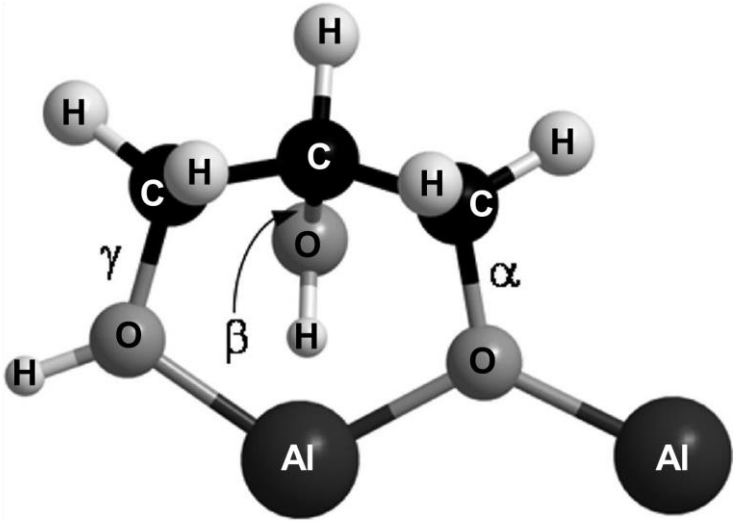

Figure 28. Conformation of glycerol adsorbed on γ-Al_2O_3.[22]

III.B.5. Conclusion

Chemical weathering of γ-alumina was studied in presence of organic molecules. Boehmite formation was observed to slightly decrease in presence of glycerol and to be completely inhibited when polyols with a larger carbon chain length were used (xylitol, sorbitol, mannitol).

It is demonstrated that polyols have two possible effects of the transformation of alumina to boehmite:

- Adsorbing as polyols or as polyol-derived caramel-like molecules on the alumina surface, forming a carbonaceous layer (evidenced by ^{13}C NMR in the case of sorbitol) that passivates alumina with respect to the reaction with water and significantly slows down its dissolution.
- Adsorbing on boehmite seeds formed in the liquid phase and inhibiting their growth. This effect was shown to increase with the concentration of the polyols.

Additionally, by studying the effect of organic molecules on alumina hydration, the *dissolution* step whose existence was suggested in part A is confirmed as part of alumina evolution under hydrothermal conditions. Therefore it is proved to be the key step in γ-alumina chemical weathering, on which one must act to inhibit the latter.

III.C. Conclusion

The degradation of γ-Al_2O_3 under hydrothermal conditions leads to the formation of boehmite through a two-step dissolution-precipitation mechanism, like under mild conditions (Chapter II), but with precipitation starting very early. The detection of aluminum in solution when ageing is performed in a solution of polyols and the growth of boehmite particles with ageing time favor this mechanism against a direct topotactic transformation of alumina particles into boehmite. Precipitation of boehmite is surface-induced and a growth of boehmite crystals occurs with ageing time. γ-Al_2O_3 thus undergoes weathering (chemical degradation) while attrition (physical degradation) was not observed in our experimental conditions due to a more gentle stirring method.

The amount of boehmite formed depends on the textural properties of the alumina. Boehmite content decreases with the decrease of the specific surface area of alumina and the increase of its crystallinity. Boehmite starts to form as small crystallites on the surface of alumina which lead to an increase in the specific surface area of the support and ultimately forms a dense layer at longer ageing time that decreases the specific surface area. This process occurs earlier when the specific surface area of the alumina is larger (i.e. when alumina is more reactive).

The chemical weathering of γ-Al_2O_3 was studied in a reaction-like medium. In the presence of polyols in the aqueous medium, a lower amount of boehmite was formed and its formation was even inhibited when C_5 and C_6 polyols were used. Two roles of polyols on γ-Al_2O_3 hydration were determined. The first role is due to the formation of a carbonaceous layer formed by adsorption of the polyols on γ-Al_2O_3 surface, that passivates the surface and slows down dissolution. The second one is, possibly, to adsorb on boehmite seeds formed in the aqueous phase and inhibit their growth, which leads to the formation of colloids that remain in solution.

In other terms, in order to prevent γ-Al_2O_3 degradation, it is required to stop its dissolution since in all cases this is the key parameter that triggers the formation of secondary phases. The different ways to stabilize alumina with respect to water and to inhibit alumina dissolution will be explored in next chapter (Chapter VI).

III.D. Annex to chapter III – part A

Quantitative analysis by XRD and TGA

The evaluation of the total amount of boehmite AlOOH formed after ageing of various Al_2O_3 polymorphs in water as shown in Figure 5 and Figure 9 of chapter III was performed by integration of the XRD peaks of AlOOH. A preliminary investigation was performed on reflections at 14.4°, 28.1° and 49.28° in 2θ (Figure 29). The integrated intensity was transposed to a weight percentage by using a calibration curve whose construction and validation is detailed below.

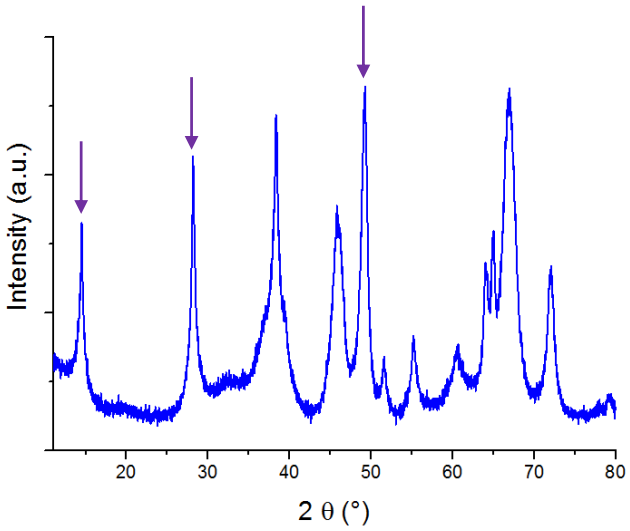

Figure 29. XRD pattern of γ-Al_2O_3 (PDF No. 10-0425) subjected to an ageing treatment in water at 150°C under hydrothermal conditions during 4 h (blue) (1.6 g/80 mL). ↓ : boehmite peaks used for the calibration method (PDF No. 83-1505).

The calibration curve was created by preparing mechanical mixtures between the boehmite used to obtain the aluminas (Sasol Pural SB3 SCCa), and γ-alumina with weight ratios varying between 10 and 90% (the total mass of the mixture was 0.6 g). The integrated areas calculated by WinPLOTR of the characteristic XRD peaks of boehmite (at 14.4°, (020), 28.1° (021) and 49.28° ((150) and (002)), PDF No. 83-1505) were then plotted as a function of the weight percentage of boehmite introduced in the mixture as shown on Figure 30 for the reflection at 49.28°. Three very close

correlation coefficients (R^2=0.94, 0.98 and 0.98 respectively) and three slopes (25.097, 29.684 and 44.494 respectively) were found for the three peaks.

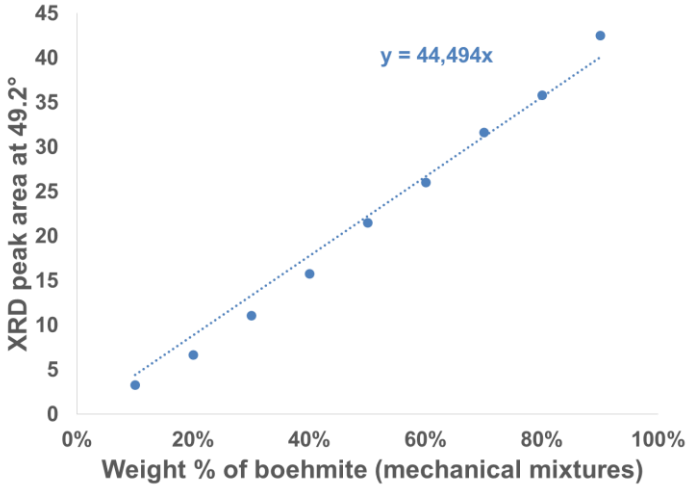

Figure 30. XRD peak integrated intensity at 2θ = 49.28° (boehmite) as a function of the weight % of boehmite in γ-Al_2O_3-boehmite mechanical mixtures.

Validation of this correlation was performed by comparing the XRD-derived AlOOH content with that obtained by TGA (quantification of the oxyhydroxide dehydration at about 450°C, see text in section A.4.3) for a series of transition aluminas aged at 150°C in water under hydrothermal conditions (Figure 5 in section A.3). XRD-derived boehmite content was evaluated using the calibration curve of 49.28° (weight percentage of oxyhydroxide = XRD area/44.494) since it yielded the best agreement with TGA results. Figure 31 shows the correlation between both quantifications. A very good agreement is found between both techniques with a slope of about 1 (R^2=0.99) for the linear correlation, which is validating the quantification by XRD even if the peak considered (49.28°) is actually made of two reflections ((150) and (002)).

Additionally, the linear correlation found in Figure 31 leads to conclude that the potential formation of an AlOOH amorphous phase is inexistent or very minor, since it would be undetected by XRD and quantified by TGA.

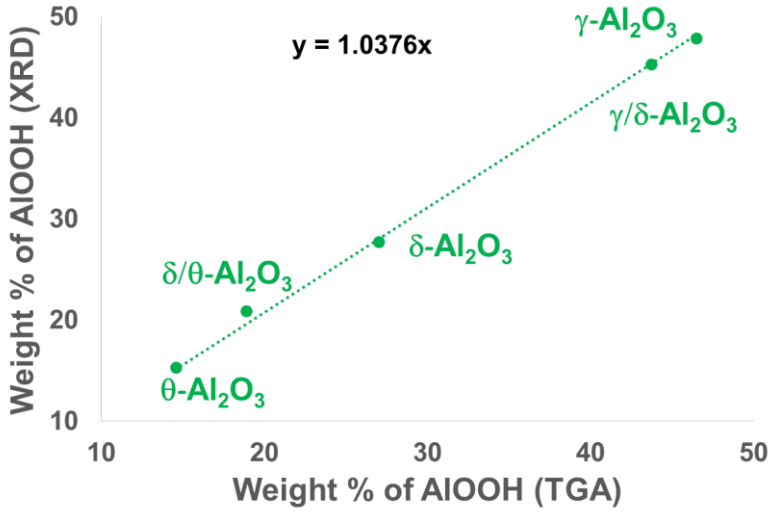

Figure 31. Weight percentages of boehmite determined by XRD as a function of those determined by TGA for a series of aluminas aged at 150°C in water during 4 h under hydrothermal conditions.

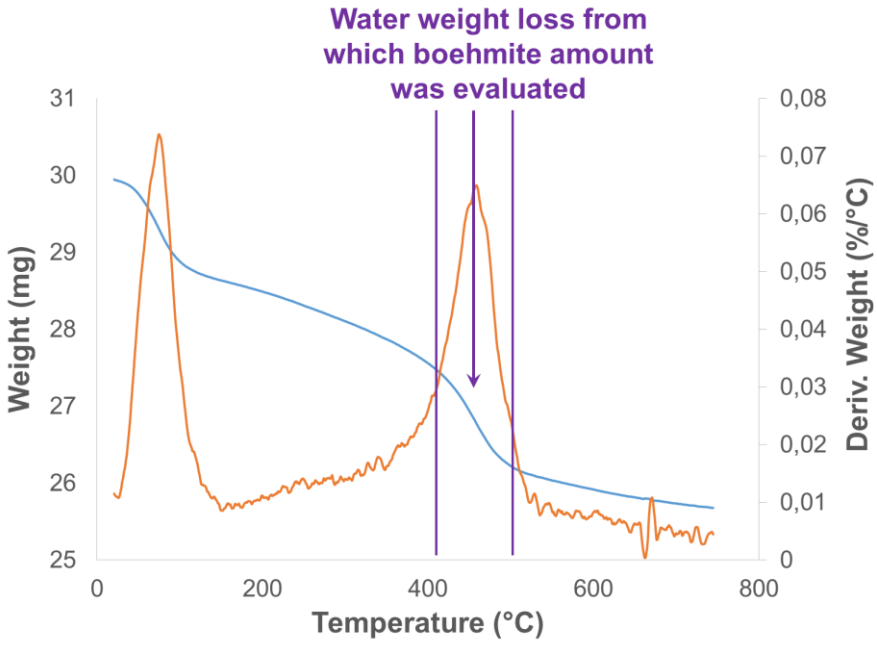

Figure 32. Thermogravimetric analysis of γ-Al_2O_3 aged at 150°C in water during 4 h under hydrothermal conditions (1.6 g/80 mL).

III.E. References

(1) Franck, J. P.; Freund, E.; Quéméré, E. Textural and Structural Changes in Transition Alumina Supports. *J. Chem. Soc., Chem. Commun.* **1984**, 629–630.

(2) Jun-Cheng, L.; Lan, X.; Feng, X.; Zhan-Wen, W.; Fei, W. Effect of Hydrothermal Treatment on the Acidity Distribution of γ-Al_2O_3 Support. *Appl. Surf. Sci.* **2006**, *253*, 766–770.

(3) Mironenko, R. M.; Belskaya, O. B.; Talsi, V. P.; Gulyaeva, T. I.; Kazakov, M. O.; Nizovskii, A. I.; Kalinkin, A. V.; Bukhtiyarov, V. I.; Lavrenov, A. V.; Likholobov, V. A. Effect of γ-Al_2O_3 Hydrothermal Treatment on the Formation and Properties of Platinum Sites in Pt/γ-Al_2O_3 Catalysts. *Appl. Catal. A Gen.* **2014**, *469*, 472–482.

(4) Ravenelle, R. M.; Copeland, J. R.; Kim, W.-G.; Crittenden, J. C.; Sievers, C. Structural Changes of γ-Al_2O_3-Supported Catalysts in Hot Liquid Water. *ACS Catal.* **2011**, *1*, 552–561.

(5) Zhang, J.; Chen, J.; Ren, J.; Sun, Y. Chemical Treatment of γ-Al_2O_3 and Its Influence on the Properties of Co-Based Catalysts for Fischer–Tropsch Synthesis. *Appl. Catal. A Gen.* **2003**, *243*, 121–133.

(6) Zhou, Y.; Fu, H.; Zheng, X.; Li, R.; Chen, H.; Li, X. Hydrogenation of Methyl Propionate over Ru–Pt/AlOOH Catalyst: Effect of Surface Hydroxyl Groups on Support and Solvent. *Catal. Commun.* **2009**, *11*, 137–141.

(7) De Vlieger, D. J. M.; Chakinala, A. G.; Lefferts, L.; Kersten, S. R. A.; Seshan, K.; Brilman, D. W. F. Hydrogen from Ethylene Glycol by Supercritical Water Reforming Using Noble and Base Metal Catalysts. *Appl. Catal. B Environ.* **2012**, *111-112*, 536–544.

(8) Elliott, D. C.; Sealock Jr, L. J.; Baker, E. G. Chemical Processing in High-Pressure Aqueous Environments. 2. Development of Catalysts for Gasification. *Ind. Eng. Chem. Res.* **1993**, *32*, 1542–1548.

(9) El Doukkali, M.; Iriondo, A.; Cambra, J. F.; Arias, P. L. Recent Improvement on H_2 Production by Liquid Phase Reforming of Glycerol: Catalytic Properties and Performance, and Deactivation Studies. *Top. Catal.* **2014**, *57*, 1066–1077.

(10) Koichumanova, K.; Sai Sankar Gupta, K. B.; Lefferts, L.; Mojet, B. L.; Seshan, K. An in Situ ATR-IR Spectroscopy Study of Aluminas under Aqueous Phase Reforming Conditions. *Phys. Chem. Chem. Phys.* **2015**, *17*, 23795–23804.

(11) Bénézeth, P.; Palmer, D. A.; Wesolowski, D. J. Aqueous High-Temperature Solubility Studies. II. The Solubility of Boehmite at 0.03 M Ionic Strength as a Function of

Temperature and pH as Determined by in Situ Measurements. *Geochim. Cosmochim. Acta* **2001**, *65*, 2097–2111.

(12) Carrier, X.; Marceau, E.; Lambert, J.-F.; Che, M. Transformations of γ-Alumina in Aqueous Suspensions. *J. Colloid Interface Sci.* **2007**, *308*, 429–437.

(13) Stumm, W. Reactivity at the Mineral-Water Interface: Dissolution and Inhibition. *Colloids Surf. Physicochem. Eng. Asp.* **1997**, *120*, 143–166.

(14) Castet, S.; Dandurand, J. L.; Schott, J.; Gout, R. Boehmite Solubility and Aqueous Aluminum Speciation in Hydrothermal Solutions (90-350°C): Experimental Study and Modeling. *Geochim. Cosmochim. Acta* **1993**, *57*, 4869–4884.

(15) Lefèvre, G.; Duc, M.; Lepeut, P.; Caplain, R.; Fédoroff, M. Hydration of γ-Alumina in Water and Its Effects on Surface Reactivity. *Langmuir* **2002**, *18*, 7530–7537.

(16) Pham, H. N.; Anderson, A. E.; Johnson, R. L.; Schmidt-Rohr, K.; Datye, A. K. Improved Hydrothermal Stability of Mesoporous Oxides for Reactions in the Aqueous Phase. *Angew. Chem. Int. Ed.* **2012**, *51*, 13163–13167.

(17) Ravenelle, R. M.; Copeland, J. R.; Pelt, A. H.; Crittenden, J. C.; Sievers, C. Stability of Pt/γ-Al_2O_3 Catalysts in Model Biomass Solutions. *Top. Catal.* **2012**, *55*, 162–174.

(18) Jongerius, A. L.; Copeland, J. R.; Foo, G. S.; Hofmann, J. P.; Bruijnincx, P. C. A.; Sievers, C.; Weckhuysen, B. M. Stability of Pt/γ-Al_2O_3 Catalysts in Lignin and Lignin Model Compound Solutions under Liquid Phase Reforming Reaction Conditions. *ACS Catal.* **2013**, *3*, 464–473.

(19) Massa, P.; Ivorra, F.; Haure, P.; Fenoglio, R. Optimized Wet-Proofed CuO/Al_2O_3 Catalysts for the Oxidation of Phenol Solutions: Enhancing Catalytic Stability. *Catal. Commun.* **2009**, *10*, 1706–1710.

(20) Margulies, M. M.; Sixou, B.; David, L.; Vigier, G.; Dolmazon, R.; Albrand, M. Molecular Mobility of Sorbitol and Maltitol: A 13C NMR and Molecular Dynamics Approach. *Eur. Phys. J. E* **2000**, *3*, 55–62.

(21) Copeland, J. R.; Shi, X.-R.; Sholl, D. S.; Sievers, C. Surface Interactions of C_2 and C_3 Polyols with γ-Al_2O_3 and the Role of Coadsorbed Water. *Langmuir* **2013**, *29*, 581–593.

(22) Copeland, J. R.; Santillan, I. A.; Schimming, S. M.; Ewbank, J. L.; Sievers, C. Surface Interactions of Glycerol with Acidic and Basic Metal Oxides. *J. Phys. Chem. C* **2013**, *117*, 21413–21425.

(23) Paulaime, A. M.; Seyssiecq, I.; Veesler, S. The Influence of Organic Additives on the Crystallization and Agglomeration of Gibbsite. **2003**, *130*, 345–351.

(24) Watling, H. Gibbsite Crystallization Inhibition: 2. Comparative Effects of Selected Alditols and Hydroxycarboxylic Acids. *Hydrometallurgy* **2000**, *55*, 289–309.

(25) Chiche, D.; Chanéac, C.; Revel, R.; Jolivet, J.-P. Use of Polyols as Particle Size and Shape Controllers: Application to Boehmite Synthesis from Sol–gel Routes. *Phys. Chem. Chem. Phys.* **2011**, *13*, 6241-6248.

Chapitre IV

Inhibition of chemical weathering of γ-Al_2O_3 by inorganic dopants in hydrothermal conditions

IV. Inhibition of chemical weathering of γ-Al_2O_3 by inorganic dopants in hydrothermal conditions 157

IV.1. Preamble 157

IV.2. Introduction 160

IV.3. Results and Discussion 161

IV.3.1. Effect of dopants and calcination temperature on chemical weathering of γ-Al_2O_3–isomolar systems 163

IV.3.2. Effect of calcination treatment: spinel and hydrotalcite formation 165

IV.3.3. Kinetic of boehmite formation 169

IV.3.4. Effect of calcination and weathering on specific surface area 170

IV.3.5. Effect of specific surface area on chemical weathering of γ-Al_2O_3 172

IV.3.6. Role of dopants – surface study 176

IV.3.7. Effect of dopant loadings on boehmite formation 181

IV.3.8. Role of dopants - Liquid-state aluminum concentration 182

IV.4. Conclusions 184

IV.5. Experimental section 185

IV.5.1. Sample preparation 185

IV.5.2. Ageing tests in hydrothermal conditions 186

IV.5.3. Characterization techniques 186

IV.6. Acknowledgments 187

IV.7. Keywords 187

IV.8. References 187

IV.9. Supplementary information 193

IV.9.1. Qualitative analysis by XRD and TGA 193

IV.9.2. Additional figures and tables mentioned in the text 197

IV.9.3. References 201

IV. Inhibition of chemical weathering of γ-Al_2O_3 by inorganic dopants in hydrothermal conditions

IV.1. Preamble

The mechanisms of chemical weathering and attrition of alumina were determined in Chapter II under mild conditions (ambient pressure, room temperature or 70°C) and confirmed in Chapter III in hydrothermal conditions (150°C, autoclave).

In order to prevent γ-Al_2O_3 degradation, four inorganic dopants have been introduced by incipient wetness impregnation (Mg, Zr, Ni) or by chemical grafting (Si), and their role has been studied in the same hydrothermal conditions as in Chapter III. Moreover, the effect of dopant loading and calcination temperature of the doped supports toward γ-Al_2O_3 hydration has been investigated.

The gain in hydrothermal stability and the comprehension of the protective role of dopants as a function of the calcination temperature were explored by quantitative and qualitative studies by different characterization techniques (XRD, TGA, XPS, DRIFTS, ICP-OES…).

These results are presented in the form of a scientific publication.

Inhibition of chemical weathering of γ-Al_2O_3 by inorganic dopants in hydrothermal conditions

J. Abi Aad,[a, b] M. Michau,[b] F. Diehl,[b] A. Berliet,[b] Ph. Courty,[b] X. Carrier,[a] E. Marceau,[a, c]

[a] Sorbonne Universités, UPMC Univ Paris 06, Laboratoire de Réactivité de Surface, F-75005, Paris, France

[b] IFP Energies nouvelles, Rond-point de l'échangeur de Solaize, 69360 Solaize

[c] Unité de Catalyse et Chimie du Solide (UMR 8181 CNRS), Université Lille 1, 59655, Villeneuve d'Ascq

Abstract:

Alumina is the predominant oxide support used in heterogeneous catalysis and its resistance toward degradation in aqueous-phase reactions under hydrothermal conditions (biomass processing) or under the severe reaction conditions of Fischer-Tropsch (FT) synthesis (exposure to high partial pressure of water) is of paramount importance at the industrial scale. Understanding the mechanism leading to the prevention of alumina degradation to an oxyhydroxide form (e.g. boehmite) in hydrothermal conditions is a key step to design more stable and more resistant FT catalysts. We examine here the effect of four inorganic dopants on the inhibition of alumina degradation in water under a total pressure of 4.6 bar: three metal ions: Mg, Zr, Ni (introduced by incipient wetness impregnation at 3, 11 and 7 wt% loading, respectively) and a heteroatom Si (introduced by chemical grafting). The quantification of boehmite formed by dissolution-precipitation shows a significant decrease of alumina weathering in all cases. This reduced degradation is not strongly dependent on the chemical nature of the dopant in the case of metal ions. However, with Si, alumina degradation is fully inhibited. Analysis of Al(III) concentration in the aqueous phase shows that metal ions slow down the dissolution of the support. IR measurements in the OH stretching region point out to a particular reactivity toward chemical weathering of γ-alumina, of selective Al-OH sites that are located on alumina lateral facets. These most reactive sites are blocked by the addition

of dopants. Full inhibition of γ-alumina chemical weathering with Si suggests a very specific grafting of this dopant on the reactive surface sites.

IV.2. Introduction

The production of biofuels through the conversion of renewable feedstocks to replace fossil-fuels has witnessed an impressive widening in the last 10 years as discussed in many reviews.[1–8] Among the different processes involved, Fischer-Tropsch (FT) is a key player since it can convert syngas issued from biomass into clean fuels through Biomass to Liquids (BTL) technologies.[9–12] Indeed, the FT process, developed in Germany in 1923 by Frantz Fischer and Hans Tropsch, involves a set of catalytic reactions for obtaining a wide range of hydrocarbon molecules (paraffins, olefins, oxygenated derivatives…) from CO/H_2 [13,14] leading to middle distillates that give alternatives to conventional oil.[14,15] Moreover, one of the major advantage of this process is that a variety of raw materials from natural gas to coal and biomass can be used.[16] This process has regained interest in the last two decades because it is an economical viable process compared to petroleum refining and provides clean products (free of sulfur and aromatic molecules) and highly valuable.[16] The FT process occurs in a slurry bubble column reactor (SBCR) in tri-phasic conditions (gas-liquid-solid) where the catalyst (most often Co-based), and namely γ-Al_2O_3 as catalyst support, is subjected to severe reaction conditions: high temperature and pressure, high particle velocity, high water partial pressure (water is the main product in FT synthesis), presence of acidic oxygenates, etc… that are detrimental to the mechanical and chemical properties of the oxide support. As a consequence, γ-Al_2O_3 undergoes a mechanical attrition and a chemical degradation leading to the formation of boehmite in presence of water at elevated temperatures and pressures which produces fines that block the reactor.[17–26] Hence, a particular emphasis is currently placed on the development of more mechanically and chemically resistant alumina supports for this demanding process. However, chemical degradation of γ-Al_2O_3 is also a major issue in aqueous-phase biomass processing that occurs most often in hydrothermal conditions.[27,28]

Hence, inhibition of the chemical degradation of γ-Al_2O_3 is a major industrial concern for improving catalytic formulations in FT processes, hydrothermal biomass processing and a large number of applications in heterogeneous catalysis.[27–29] As a matter of fact, some authors showed

that the supported active phase may play a role in increasing the hydrothermal stability of the catalyst.[20,26,30] Other works claimed that the support can be stabilized by adding non-catalytically active metal ions or heteroatoms.[20,25,31–40] However, there is still little fundamental understanding on the role played by these inhibitors at the molecular level. Ravenelle *et al.*[20] studied the effect of supported metals (Ni and Pt) on reducing chemical weathering of alumina and suggested that the most basic alumina surface hydroxyl groups (singly coordinated hydroxyl groups, to which are bounded Ni and Pt), are playing a key role in the degradation of alumina to boehmite.

The present study builds on our previous works[41,42] dedicated to the investigation of the chemical weathering of pure γ-Al_2O_3 in model conditions (ambient pressure) that showed that alumina hydration occurs through a dissolution-surface nucleation mechanism. The role of some surface-dopants (Mg, Zr, Ni and Si) in improving γ-Al_2O_3 hydrothermal stability is discussed with reference to the previous mechanism. The stabilized aluminas have been subjected to an ageing treatment at 150°C under hydrothermal conditions after which the liquid and solid phases were analyzed. Quantification of boehmite formed through XRD and TGA and analysis of dissolved Al(III) has allowed us to investigate the gain in hydrothermal stability with dopants while IR spectroscopy has been used for a molecular-scale investigation of the role of dopants.

IV.3. Results and Discussion

A summary of the main materials used in this study (pure and doped supports) and their characteristics are given in Table 1 and preparation details are given in the experimental section. A post-calcination at 750°C or 900°C in static air in a muffle furnace during 12 h was performed on some samples in order to study the effect of high-temperature calcination and potential insertion of the dopant into the alumina structure.

Table 1. Main characteristics of γ-Al_2O_3 and stabilized-γ-Al_2O_3

Sample name	**Weight % of stabilizer**	**S_{BET} ($m^2.g^{-1}$)**	**Synthesis technique – calcination temperature**	**Post-calcination[d]**
γ-Al_2O_3	-	238	Boehmite calcination-500°C/12 h	-
3%Mg/γ-Al_2O_3-500°C	3	220	I.W.I.[a]-500°C/4 h	-
3%Mg/γ-Al_2O_3-750°C	3	158	I.W.I.[a]-500°C/4 h	750°C/12 h
3%Mg/γ-Al_2O_3-900°C	3	115	I.W.I.[a]-500°C/4 h	900°C/12 h
11%Zr/γ-Al_2O_3-500°C	11	200	I.W.I.[a]-500°C/4 h	-
11%Zr/γ-Al_2O_3-750°C	11	139	I.W.I.[a]-500°C/4 h	750°C/12 h
11%Zr/γ-Al_2O_3-900°C	11	116	I.W.I.[a]-500°C/4 h	900°C/12 h
7%Ni/γ-Al_2O_3-500°C	7	187	I.W.I.[a]-500°C/4 h	-
7%Ni/γ-Al_2O_3-750°C	7	162	I.W.I.[a]-500°C/4 h	750°C/12 h
7%Ni/γ-Al_2O_3-900°C	7	134	I.W.I.[a]-500°C/4 h	900°C/12 h
3.5%Si/γ-Al_2O_3	3.5	212	CLD[b]-500°C/4 h	-
7%Si/γ-Al_2O_3	7	203	CVD[c]-500°C/4 h	-
[a] I.W.I.: Incipient Wetness Impregnation, [b] Chemical Liquid Deposition, [c] Chemical Vapor Deposition, [d] in static air in a muffle furnace at a heating rate of 10°C/min				

After ageing most of the different supports at 150°C under hydrothermal conditions (4.6 bar), boehmite (AlOOH) is formed and detected by XRD with characteristic reflections at 14.4° (020), 28.1° (021), 38.3° (130) and 49.28° (150) and (002) in good agreement with results obtained in the literature.[17–26] An example is shown on Figure 1. The following sections will give a more detailed description on results obtained on doped-γ-Al_2O_3 and they will be compared to non-doped γ-Al_2O_3.

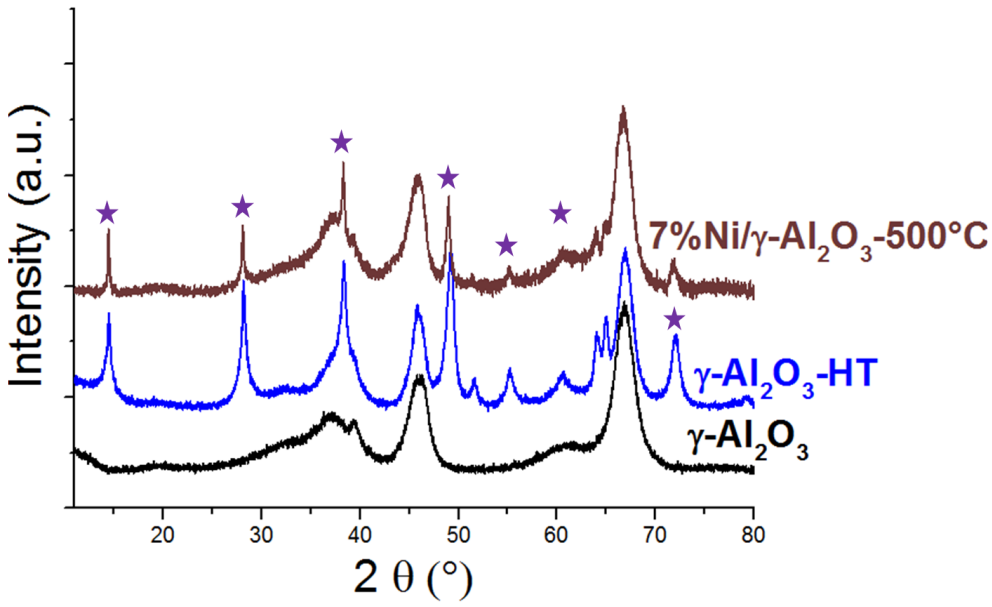

Figure 1. XRD patterns of γ-Al_2O_3 (black, PDF No. 10-0425) and γ-Al_2O_3-HT (blue) and 7%Ni/γ-Al_2O_3 (brown) subjected to an ageing treatment in water at 150°C under hydrothermal conditions (HT) during 4 h (1.6 g/80 mL). ★: boehmite (PDF No. 83-1505).

IV.3.1. Effect of dopants and calcination temperature on chemical weathering of γ-Al_2O_3–isomolar systems

The following weight loadings of the different dopants 3% Mg, 11% Zr, 7% Ni and 3.5% Si were chosen in a first step in order to keep the same surface loading (i.e. 3,0-3,2 at.nm^{-2}) for all dopants.

The total amount of boehmite formed after ageing γ-Al_2O_3 or doped-γ-Al_2O_3 at 150°C during 4 h under hydrothermal conditions is presented in Figure 2 (7% Si doping is also included for comparison). This total amount was evaluated following a quantitative XRD analysis based on the area of a characteristic peak of boehmite at 49.28° in 2θ (see supplementary information). This evaluation was cross-checked with TGA where the amount of boehmite was evaluated from the loss of water at 450°C according to the reaction:

2 AlOOH → Al_2O_3 + H_2O.

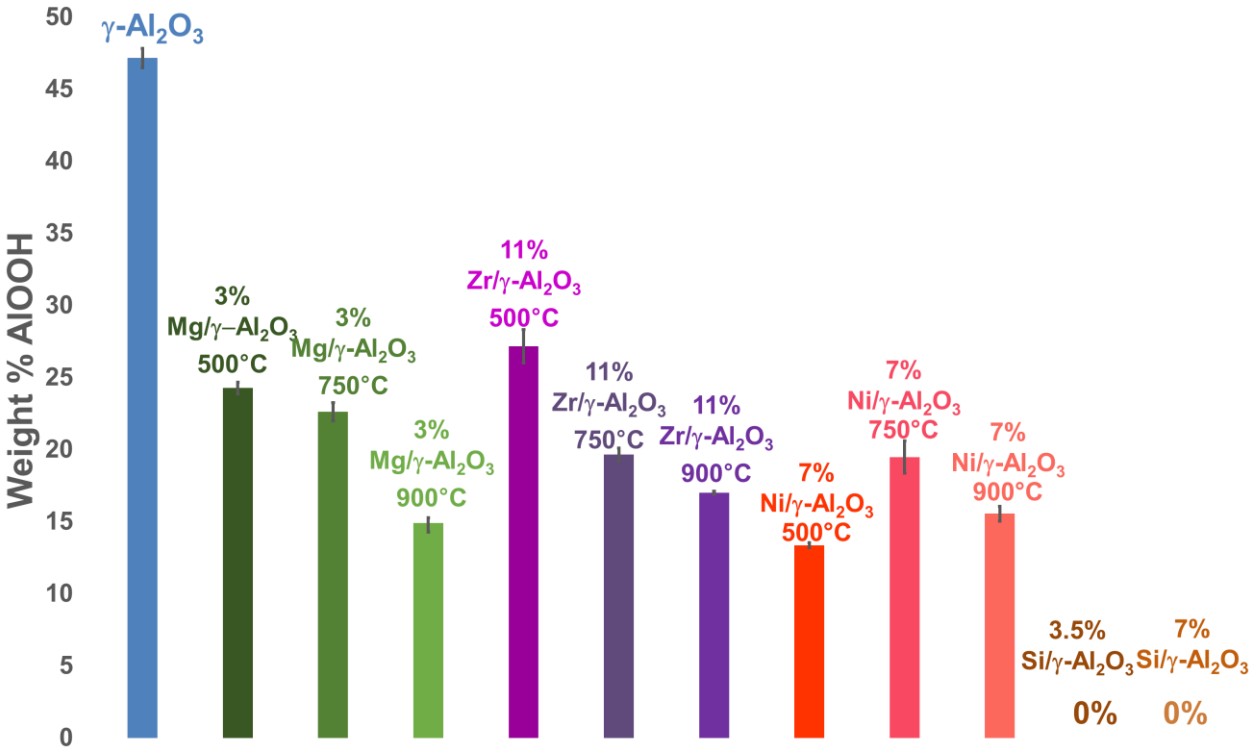

Figure 2. Weight percentage of boehmite formed after ageing γ-Al₂O₃ doped with 3% Mg (green),11% Zr (purple), 7% Ni (red) and (3.7 or 7%) Si (brown) in water at 150°C during 4 h (1.6 g/80 mL, hydrothermal conditions). 500°C, 750°C and 900°C refer to the calcination temperature of each doped supports.

Following the method explained in the work of Carrier *et al.*[41] for evaluating the amount of $Al(OH)_3$, the boehmite content is thus calculated as:

$$\%AlOOH = \left[\frac{2 \times \Delta m_{450°C} / 18}{m_{700°C}} \times 60 \right] \times 100$$

60 and 18 g.mol^{-1} being the molecular weight of AlOOH and H_2O, respectively and $m_{700°C}$ is the total weight of the sample at 700°C after boehmite dehydration. More information is provided in supplementary information.

The average of the values resulting from XRD and TGA analysis are plotted on Figure 2 and error bars are the standard deviation from both techniques. The very small error bars demonstrate a good

agreement between XRD and TGA and thus, confirm the absence of an amorphous phase that would be quantified by TGA but XRD-invisible.

These results confirm the effect of metal ions (Mg^{II}, Zr^{IV} and Ni^{II}) on reducing boehmite formation with respect to non-doped γ-Al_2O_3.

A larger inhibition of boehmite formation was observed with an increase of the calcination temperature of the doped-support at 750°C and 900°C. The only exception comes from the Ni case where the lowest extent of boehmite formation was observed for the lowest calcination temperature at 500°C.

These observations are in line with other works like Wang *et al.*[38] who showed that the incorporation of Zr^{IV} improves the hydrothermal stability of mesoporous alumina. An increase of the stability of alumina with an increase of the calcination temperature was also reported in the literature in presence of zirconia but under different "hydrothermal" conditions, i.e. under water vapor (230°C during 24 h under steam).[40] Enache *et al.*[40] explained this effect by a "stronger" interaction between zirconia and the support after calcination without a more detailed discussion.

It has to be mentioned here that ICP-OES analysis showed that a small fraction of Mg and Ni are leached in solution after hydrothermal ageing at 150°C during 4 h for the doped supports calcined at the three calcination temperatures (Table S1, supplementary information). Hence, dopant leaching is a minor issue in the present experimental conditions.

Hence, the combined effect of dopants and calcination temperature is shown to reduce boehmite formation but the role of these two parameters is not well understood in the literature. In the following, detailed studies will thus be shown in order to gain more insight into the specific role of dopants and the role of the calcination temperature.

IV.3.2. Effect of calcination treatment: spinel and hydrotalcite formation

XRD analysis of the doped supports 3%Mg/γ-Al_2O_3 and 7%Ni/γ-Al_2O_3 calcined at 750°C and 900°C, before any hydrothermal treatment, shows the formation of a spinel phase ($MgAl_2O_4$ and $NiAl_2O_4$ respectively) (Figure 3) with characteristic peaks at 19.26° (111), 31.7° (220), 37.4° (311),

45.4° (400), and 66.3° (440) for $MgAl_2O_4$ and 19.1° (111), 31.5° (220), 37° (311), 45° (400) and 66° (440) for $NiAl_2O_4$. Formation of nickel aluminate was also verified by TPR[43–46] through the detection of a high temperature reduction peak (at or above 900°C for the 750°C and 900°C-calcined support respectively) (Figure S5, supplementary information). The extent of spinel formation is depending on the calcination temperature with an increased formation of spinel with temperature (Figure 3) and a concomitant decrease of boehmite formation (Figure 2).

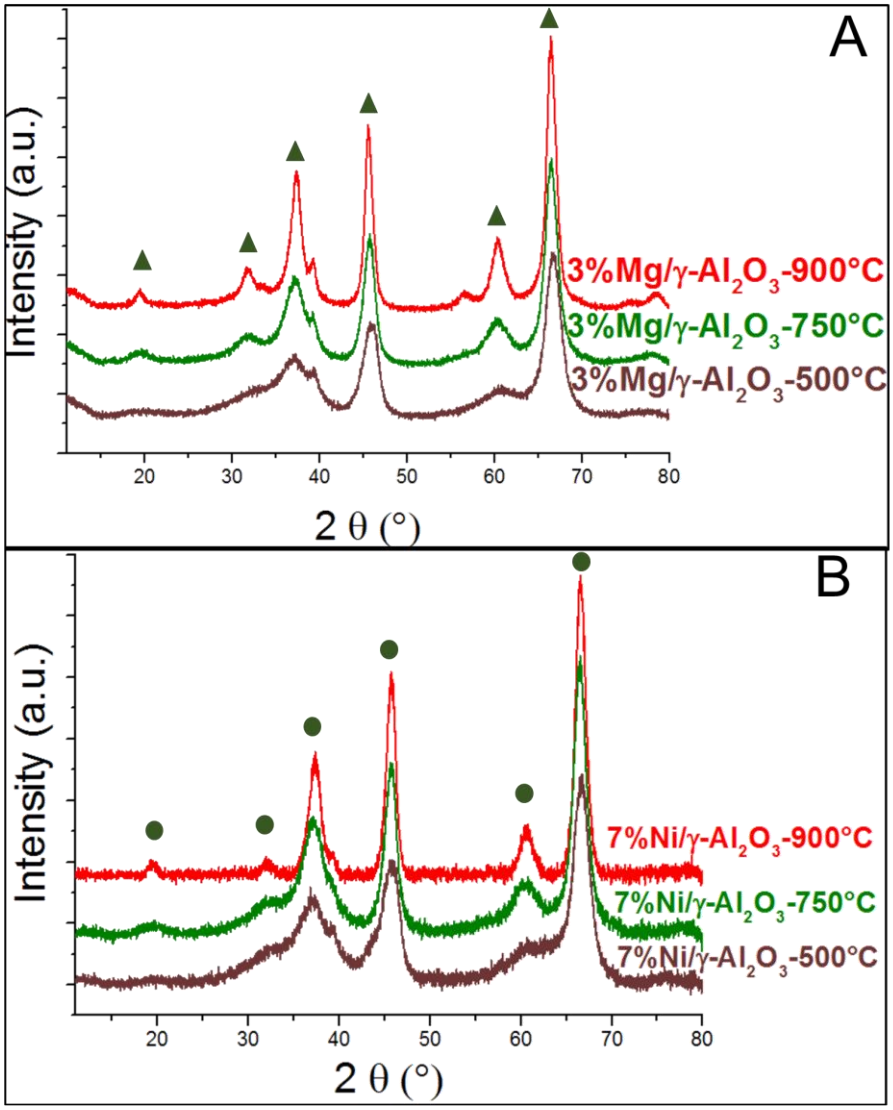

Figure 3. XRD patterns of γ-Al_2O_3 doped by Mg^{II} (A) and Ni^{II} (B) and calcined at 500°C, 750°C and 900°C. ▲: $MgAl_2O_4$ (PDF No. 87-0340),●:$NiAl_2O_4$ (PDF No. 10-0339).

The Ni case after a 500°C calcination is a peculiar one since the lowest amount of boehmite is observed after treatment under hydrothermal conditions (150°C) (Figure 2). TPR results (Figure S5, supplementary information) show that 7%Ni/γ-Al_2O_3-500°C contains small particles of NiO (peak below 750°C) that are strongly interacting with the alumina surface, and surface $NiAl_2O_4$ spinel (peak above 750°C). [43–46] Conversely for the two other doped supports calcined at 750°C and 900°C, only one TPR peak was observed at high temperature (above 850°C) indicating the presence of less reducible spinel phase. Hence, it can be suggested that Ni migrates more deeply into the alumina structure after 750 and 900°C calcination forming a bulk-like spinel aluminate leading to a less efficient protection of the alumina surface toward chemical weathering (Figure 2) with respect to 500°C-calcined support where a more surface spinel is obtained. As a matter of fact, XPS analysis (Table S2, supplementary information) shows a very slight decrease of Ni/Al with calcination temperature (from 0.04 to 0.03). However, XPS is not fully conclusive in this case since a mixture of surface spinel and NiO particles are present at 500°C.

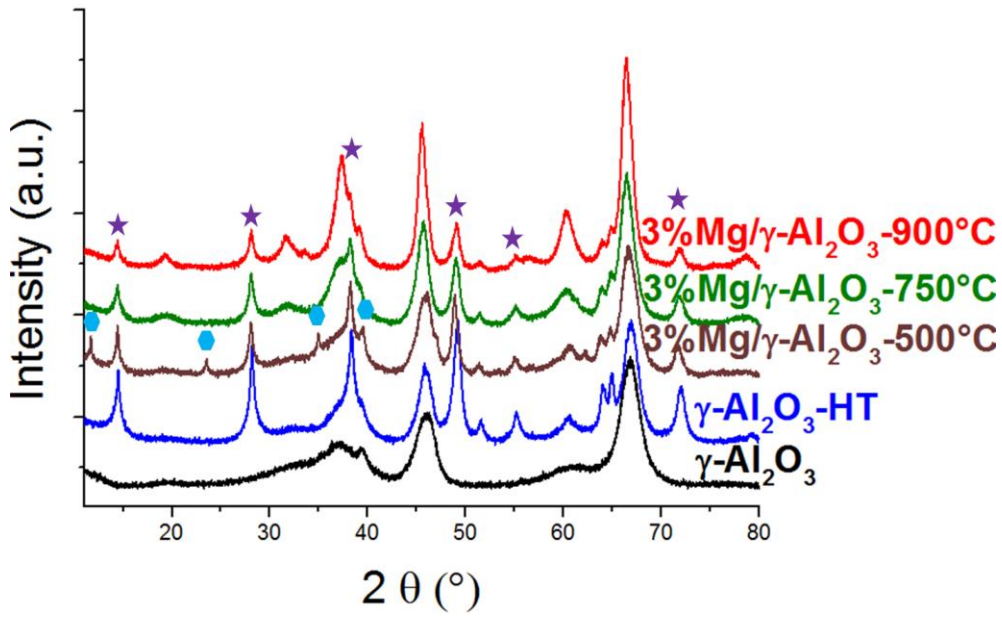

Figure 4. XRD patterns of γ-Al_2O_3 (black) and γ-Al_2O_3-HT (blue) and 3%Mg/γ-Al_2O_3 calcined at 500°C (brown), 750°C (green) and 900°C (red) and subjected to hydrothermal treatment at 150°C during 4 h (1.6 g/80 mL, hydrothermal conditions) (B). ★: boehmite (PDF No. 83-1505) and ⬣: hydrotalcite (PDF No. 89-0460)

After ageing 3%Mg/γ-Al_2O_3-500°C at 150°C under hydrothermal conditions, not only boehmite was observed but also an hydrotalcite phase (Figure 4, ideal formula: $(Mg_{0.667}Al_{0.333})(OH)_2(CO_3)_{0.167}(H_2O)_{0.5}$). It was checked that hydrotalcite did not form during impregnation of Mg (Figure S6, supplementary information), but only after hydrothermal treatment. This phase does not form when the aged supports have undergone a post-calcination at higher temperatures (750°C and 900°C). SEM micrographs of the supports 3%Mg/γ–Al_2O_3-500°C and 3%Mg/γ-Al_2O_3-900°C hydrothermally treated at 150°C during 4 and 14 h (Figure S7, supplementary information) do not allow to distinguish boehmite from hydrotalcite which is supposed to have also a platelet-like morphology. The absence of these platelets could also be due to the small amount of hydrotalcite, which is much lower than boehmite (compare corresponding peak intensities in Figure 4). One can also imagine that hydrotalcite platelets are not stable under the electron beam in the SEM analysis. As a matter of fact, formation of hydrotalcite is not surprising in the experimental conditions of this work since Roy *et al*.[47] and Pausch *et al*.[48] reported the formation of a hydrotalcite-like compound by subjecting a mixture of MgO and Al_2O_3 to a hydrothermal treatment in an autoclave at high temperature (> 100°C) and high water partial pressure (> 6.7 MPa).

Two mechanisms could account for the formation of a hydrotalcite phase in our case:

- Dissolution of alumina, concomitant leaching of Mg(II), and subsequent precipitation of Al(III) and Mg(II) released in solution. However, analysis of the concentration of dissolved Mg(II) after hydrothermal treatment (Table S1) shows that the amount of Mg(II) leached in aqueous phase does not significantly change for the doped supports calcined at 500, 750 and 900°C which is not in favor of an exclusive formation of hydrotalcite for 3%Mg/γ-Al_2O_3-500°C.
- Hydration of a spinel phase formed on the support calcined at 500°C that could be undetectable by XRD, due to its amorphous structure or small size. Such a reversible hydration of a spinel magnesium aluminate toward a hydrotalcite phase is well-known in the literature.[49–51] The $MgAl_2O_4$ spinel formed in the case of the supports calcined at higher temperature (750 and 900°C) is probably less prone to hydration since Mg(II)

species are more deeply buried into the surface which might explains the absence of formation of a hydrotalcite phase for these latter species.

IV.3.3. Kinetic of boehmite formation

A series of hydrothermal tests was performed for the Mg-doped supports 3%Mg/γ-Al_2O_3-500°C, 3%Mg/γ-Al_2O_3-750°C and 3%Mg/γ-Al_2O_3-900°C during different hydration times.

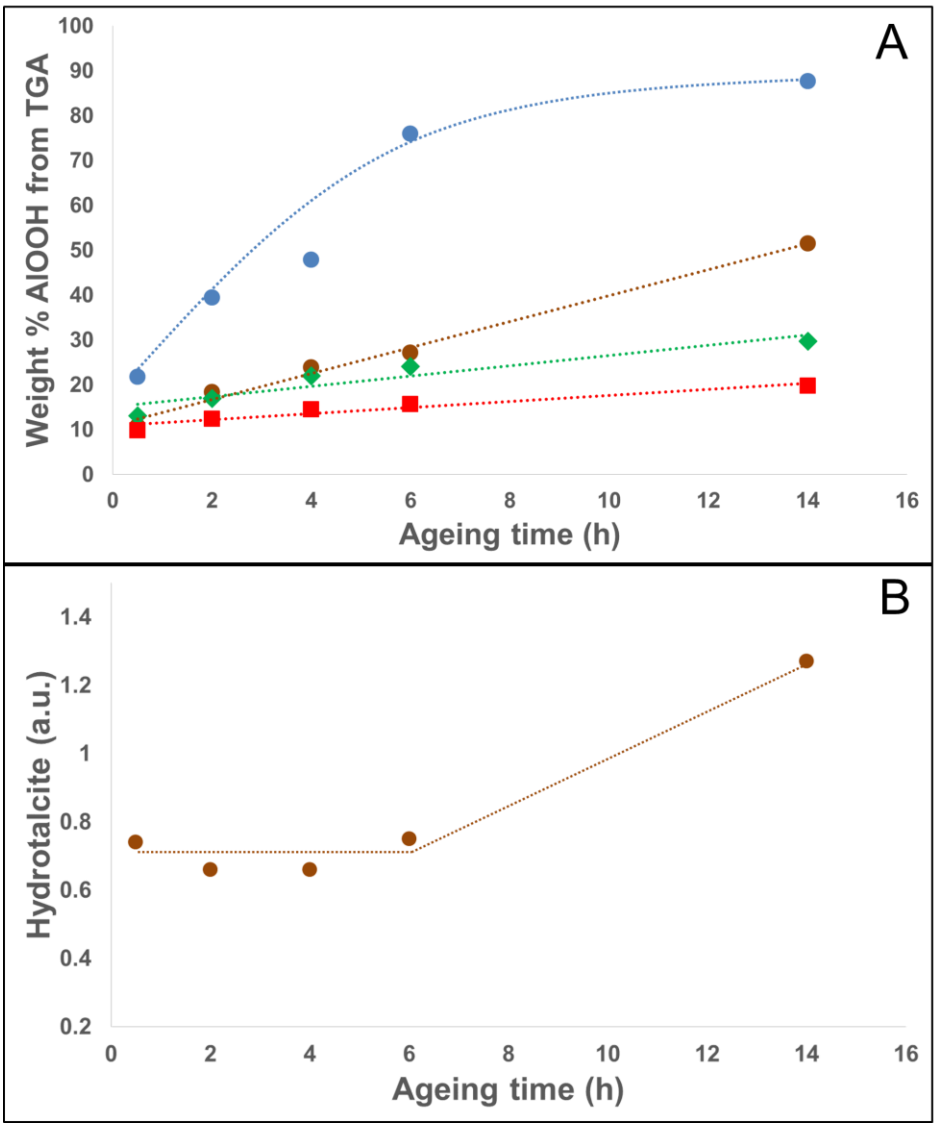

Figure 5. (A) Amount of boehmite formed after ageing γ-Al_2O_3 (blue circles), 3%Mg/γ-Al_2O_3-500°C (brown circles), 3%Mg/γ-Al_2O_3-750°C (green diamonds) and 3%Mg/γ-Al_2O_3-900°C (red squares) in water at 150°C during different ageing times (1.6 g/80 mL, hydrothermal conditions).

(B) Variation of the area of the XRD peak at 11.69° corresponding to hydrotalcite as a function of ageing time for 3%Mg/γ-Al_2O_3-500°C.

The amount of oxyhydroxide formed is plotted as a function of ageing times (Figure 5-A). It is shown that the kinetic of boehmite formation is decreasing with an increase in the calcination temperature of the doped support. Hence, these results confirm those shown on Figure 2: chemical weathering of γ-Al_2O_3 is reduced both with the addition of Mg and increase of calcination temperature.

Figure 5-B shows the evolution of hydrotalcite formed with time for the 500°C-calcined support. The amount is fairly constant during the first ageing times (up to 6 h) and increases afterwards while there is a continuous increase of the amount of boehmite. These results suggest 1) that hydrotalcite does not have a specific role in protecting the surface of γ-Al_2O_3 from hydration and 2) there is no direct link between hydrotalcite and boehmite formations since their evolution are not correlated. Hence, it can be concluded that only a fraction of Mg, not involved in hydrotalcite formation, is playing a role on the inhibition of the chemical weathering of γ-Al_2O_3. Hydrotalcite formation appears to be a second order process.

IV.3.4. Effect of calcination and weathering on specific surface area

Figure 6 shows the variation of the specific surface area (SSA) of γ-Al_2O_3 and of the doped supports calculated per m² of the support only, before and after hydrothermal treatment at 150°C during 4 h. Before hydrothermal ageing, there is a clear decrease of SSA after calcination at 750°C or 900°C which can easily be explained by the sintering and crystallization of alumina[52] along with the formation of a spinel phase ($MgAl_2O_4$ in the case of Mg-doped supports and $NiAl_2O_4$ in the case of Ni-doped supports, Figure 3). In the case of Zr, the additional formation of ZrO_2 particles is also observed by XRD (Figure S8, supplementary information).

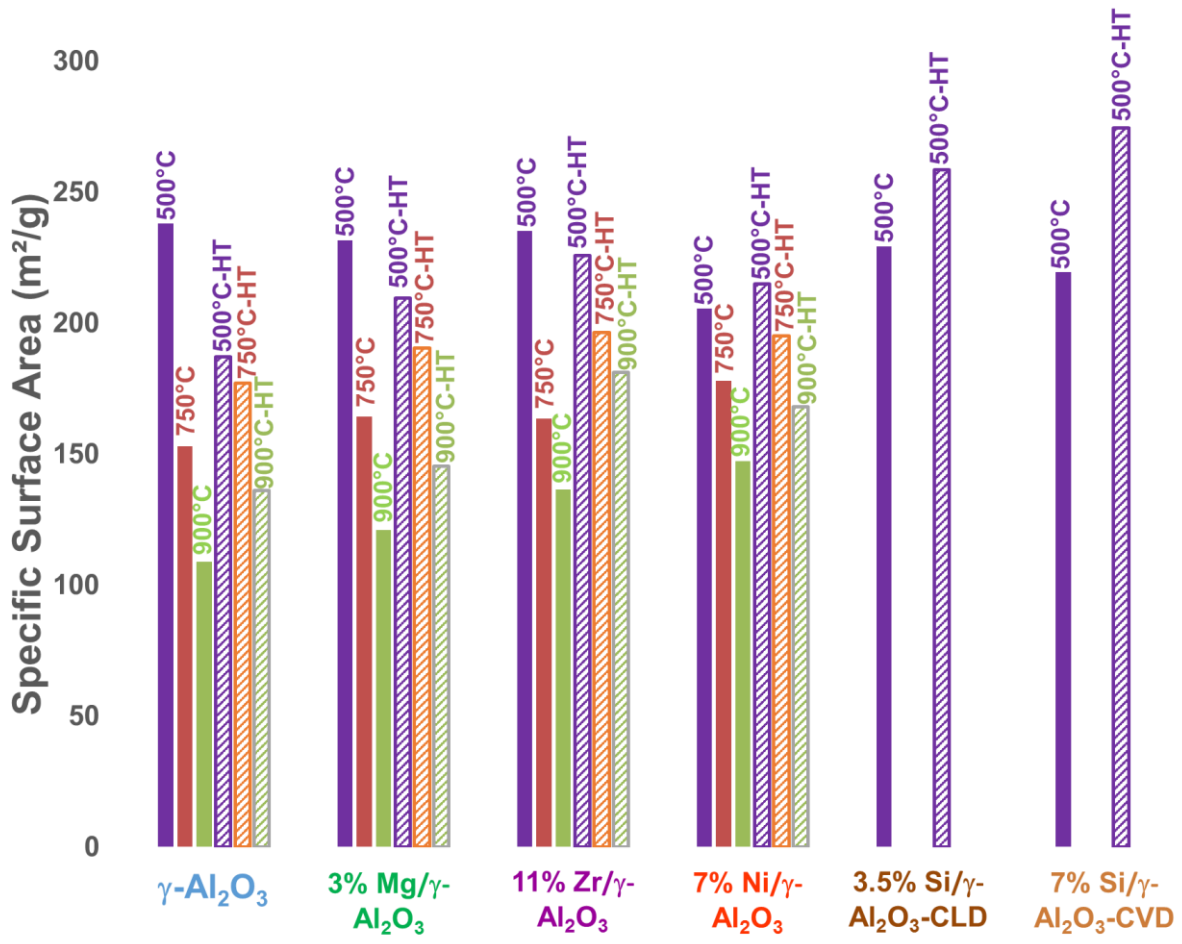

Figure 6. Specific surface areas of γ-Al_2O_3, 3%Mg/γ-Al_2O_3, 11%Zr/γ -Al_2O_3; 7%Ni/γ-Al_2O_3, 3.5%Si/γ -Al_2O_3-CLD and 7%Si/γ -Al_2O_3-CVD calcined at 500°C (purple), 750°C (red) and 900°C (green) and subjected to a hydrothermal treatment (HT, hatched histograms) at 150°C during 4 (1.6 g/80 mL).

After hydrothermal ageing, the SSAs of the supports calcined at 750 and 900°C increase compared to non-aged solids. This effect was already discussed in Chapter 3 (paragraph III.A.4.d). It can be explained by the formation of small boehmite particles on the surface of alumina that creates an additional surface to Al_2O_3 in agreement with literature results.[20,21,53]

A different situation is observed for the supports calcined at 500°C which are more reactive, mainly γ-Al_2O_3, 3%Mg/γ-Al_2O_3-500°C and 11%Zr/γ-Al_2O_3-500°C. In these samples, the specific surface area of the hydrothermally aged samples decreases with respect to calcined solids. This effect was already discussed in Chapter 3 (paragraph III.A.4.d) by studying the evolution of the SSA of γ-

Al_2O_3 as a function of ageing time. It was shown that the SSA increases in the first 30 min and then starts decreasing with time (Figure 11, Chapter III). This effect was explained by the formation of a coating of boehmite blocking the porosity of the alumina and/or dilution of a porous support (γ-Al_2O_3) with a non-porous one (boehmite). Similarly, in the present case, after 4 h of ageing, it is suggested that for the most reactive supports (3%Mg/γ-Al_2O_3-500°C and 11%Zr/γ-Al_2O_3-500°C), the amount of boehmite formed, is sufficient to partially block the porosity of the support or just diluting the porous support, both phenomena leading to a lower surface area.

The Si case is different since it is shown on Figure 6 that the specific surface area of 3,5%Si/γ-Al_2O_3-CLD and 7%Si/γ-Al_2O_3-CVD increases after hydrothermal treatment while no boehmite is formed with this dopant (Figure 2, the results are also confirmed by TGA). Hence, these results show that the textural evolution of γ-Al_2O_3 after hydrothermal treatment cannot only be explained by AlOOH formation. The pore network of the solid is most probably modified in hydrothermal conditions through modification of inter-particular organization.

IV.3.5. Effect of specific surface area on chemical weathering of γ-Al_2O_3

The amount of boehmite formed after ageing various transition aluminas in hydrothermal condition at 150°C during 4 h is compared to the doped supports (Figure 7) as a function of the specific surface area *calculated per m² of the corresponding support*.

It was already shown in Chapter 3 that for pure aluminas, the total amount of boehmite clearly decreases with the decrease of the specific surface area and the concomitant increase in alumina crystallinity. It is very interesting to note in Figure 7 that the variation of the amount of boehmite follows the same trend for the doped supports.

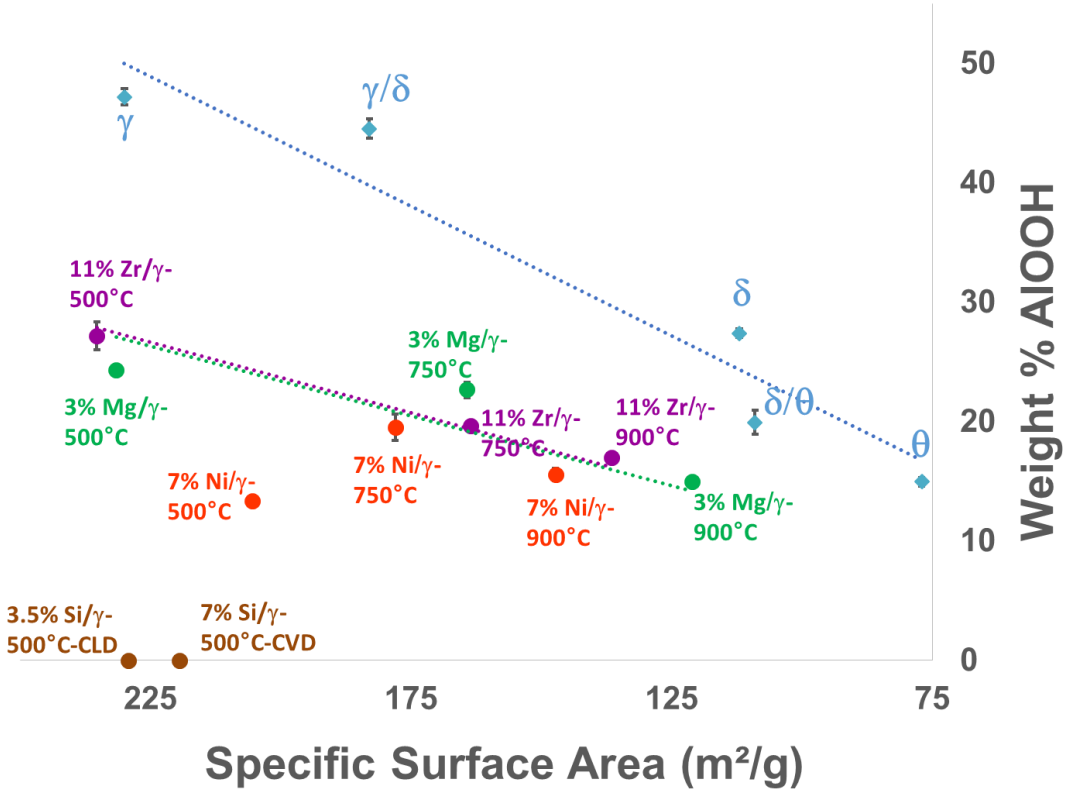

Figure 7. Amount of boehmite formed after hydrothermal treatment at 150°C during 4 h of various solids: transitions aluminas (blue), 3%Mg/γ-Al_2O_3 (green), 11%Zr/γ-Al_2O_3 (purple), 7%Ni/γ-Al_2O_3 (red), 3.5%Si/γ-Al_2O_3 and 7%Si/γ-Al_2O_3 (brown) as a function of specific surface area calculated per m² of the corresponding support. 500°C, 750°C and 900°C are the calcination temperature of each doped support.

Several conclusions can be drawn from examination of Figure 7:

- The common trend observed between pure aluminas of various crystallinity and doped γ-Al_2O_3 shows that the main descriptor for a predictive evaluation of the hydrothermal resistance of alumina is the specific surface area.
- For the same specific surface area, the addition of dopants has a clear positive effect for enhancing the resistance of aluminas toward chemical weathering. This effect is more pronounced for the lowest calcination temperature. It can be estimated that doped-supports are twice more resistant than pure transition aluminas.

- For most of the samples, the amount of boehmite formed for the doped supports follows a decreasing straight line which means that there is no specificity of the different dopants (i.e. dependence on its chemical nature) for inhibiting the chemical weathering of alumina.

Hence, it is shown that reduced boehmite formation with calcination temperature is mainly governed by textural effects.

It was demonstrated above (section 2.2) that with increasing calcination temperatures for Mg- and Ni-doped supports there was a modification of the surface layers of alumina with the formation of a spinel phase (Figure 3). Previous literature results suggested that formation of such surface spinels could result in an improvement of the hydrothermal stability of doped-γ-alumina. For example, Liu *et al.*[54]. postulated that the formation of $NiAl_2O_3$ spinel was responsible of the stabilization of a Pd/Al_2O_3 catalyst doped with Ni, under steam at 600°C. However, the common trend observed on Figure 7 for most of the doped supports including Zr-doped aluminas where no spinels are identified leads to reject this hypothesis. Spinel formation appears to be a second order effect with no direct influence on the hydrothermal stabilization.

However, there are two exceptions to the preceding conclusion: the $7\%Ni/\gamma\text{-}Al_2O_3$-500°C sample and the silicon-doped supports (prepared both by CLV and CVD).

For Si-doped aluminas, boehmite formation is completely suppressed while their specific surface areas are in the range of the 500°C-calcined supports (Figure 7). The improvement of γ-alumina hydrothermal stability in presence of silicon has also been found by other authors.[32,55] Ravenelle showed a full inhibition of boehmite formation for the same amounts of Si added here (3.5% and 7%).[55] Li *et al.*[34] observed that under mild treatment conditions (8 h at 90°C), the addition of SiO_2 to a Ni/Al_2O_3 catalyst inhibited the hydration of Al_2O_3 and therefore prevented the formation of $Al(OH)_3$.

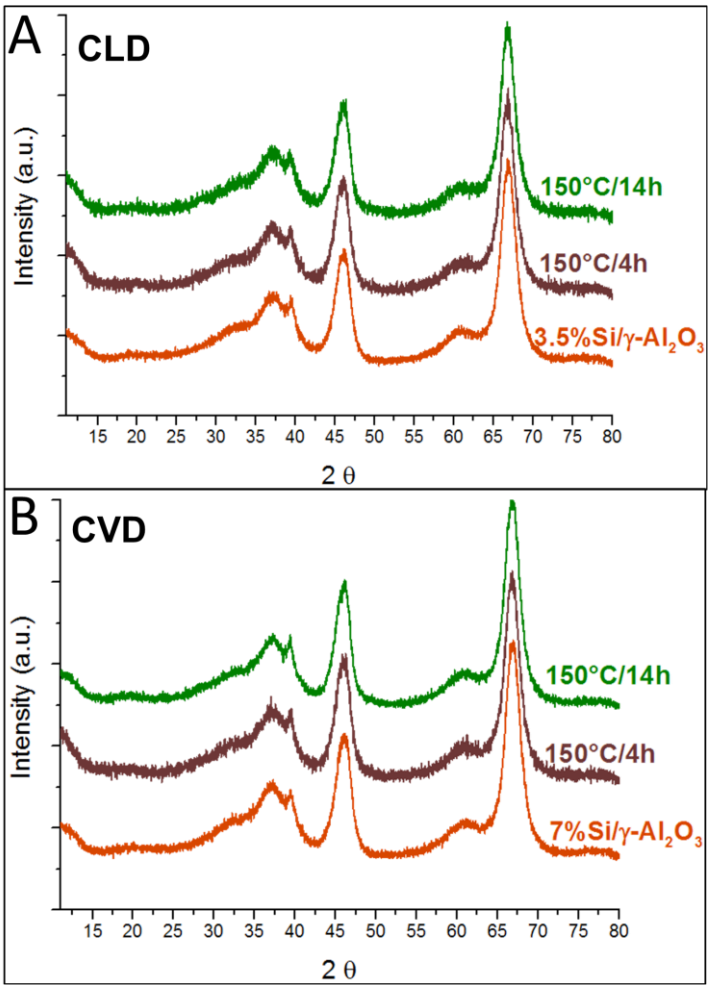

Figure 2. XRD patterns of 3.5%Si/γ-Al_2O_3-CLD and 7%Si/γ-Al_2O_3-CVD (orange) subjected to an ageing treatment at 150°C during 4 h (brown) and 14 h (green) (1.6 g/80 mL, hydrothermal conditions).

Confirmation of the very peculiar behaviour of Si-doped aluminas was obtained by performing an hydrothermal treatment during 14 h. XRD patterns of the solids are presented on Figure 8. No boehmite-characteristic peaks are detected which shows that AlOOH formation is also fully inhibited in Si-doped aluminas even during a long hydrothermal ageing time. Some authors related the increased hydrothermal stability of alumina to the formation of Si-O-Si and Si-O-Al bonds[33,56] that are known to be resistant to cleavage.[57,58]

Hence, these experimental results suggest that Si specifically blocks the most reactive sites of γ-Al_2O_3 and the deposition mode of Si is most probably a key parameter for the selective consumption

of these reactive sites. As a matter of fact, previous literature results[59] demonstrated that CLD and CVD from TEOS leads to a specific grafting of silicon on defined γ-Al_2O_3 surfaces. Other literature results showed that selective and controlled deposition of the dopant is a key parameter for improved alumina resistance. Enache *et al*.[40] showed that when Zr-doping is carried out from an alkoxide precursor the hydrothermal stability of alumina is higher than when using a colloidal solution. Similarly, Ravenelle *et al*. demonstrated that by changing the precursor of the dopant (from H_2PtCl_6 to $H_2Pt(OH)_6$ in one case[60] and from poly-dimethylsiloxane to TEOS in another case[55]), the stability of alumina could be improved.

For 7%Ni/γ-Al_2O_3-500°C, TPR results (section IV.2.2) showed that NiO particles are present along with a surface spinel phase. Conversely, for Ni-doped supports calcined at higher temperatures, NiO particles are no longer present and the amount of boehmite is increasing (Figure 7). Hence, similarly to the Si case, it can be suggested that NiO particles selectively blocks the most reactive surface alumina sites.

A more detailed discussion will follow supported by DRIFTS results.

IV.3.6. Role of dopants – surface study

Investigation of the role of dopants was carried out with IR spectroscopy in the diffuse reflectance mode (DRIFTS) in order to probe the evolution of surface OHs with doping. IR spectra in the ν_{OH} region of the doped-supports are compared to γ-Al_2O_3 and δ-Al_2O_3 on Figure 9. It can be clearly seen that when adding dopants to alumina, the shape of the IR spectra is modified with a preferential decrease of the 3672 cm^{-1} band along with that at 3757 cm^{-1} at the expense of the 3715 cm^{-1} peak. Moreover, Figure 9 shows that the spectra of the doped supports are similar to that of δ-Al_2O_3.

A first qualitative conclusion can be drawn from this correspondence. It is known that the transformation from γ-Al_2O_3 to δ-Al_2O_3 is accompanied by the consumption of lateral facets through the formation of Al-O-Al bridges (Figure S9, supplementary information).[52] Hence, the similarity between doped-supports and δ-Al_2O_3 suggests a preferential consumption of surface OH located on lateral facets of alumina after doping.

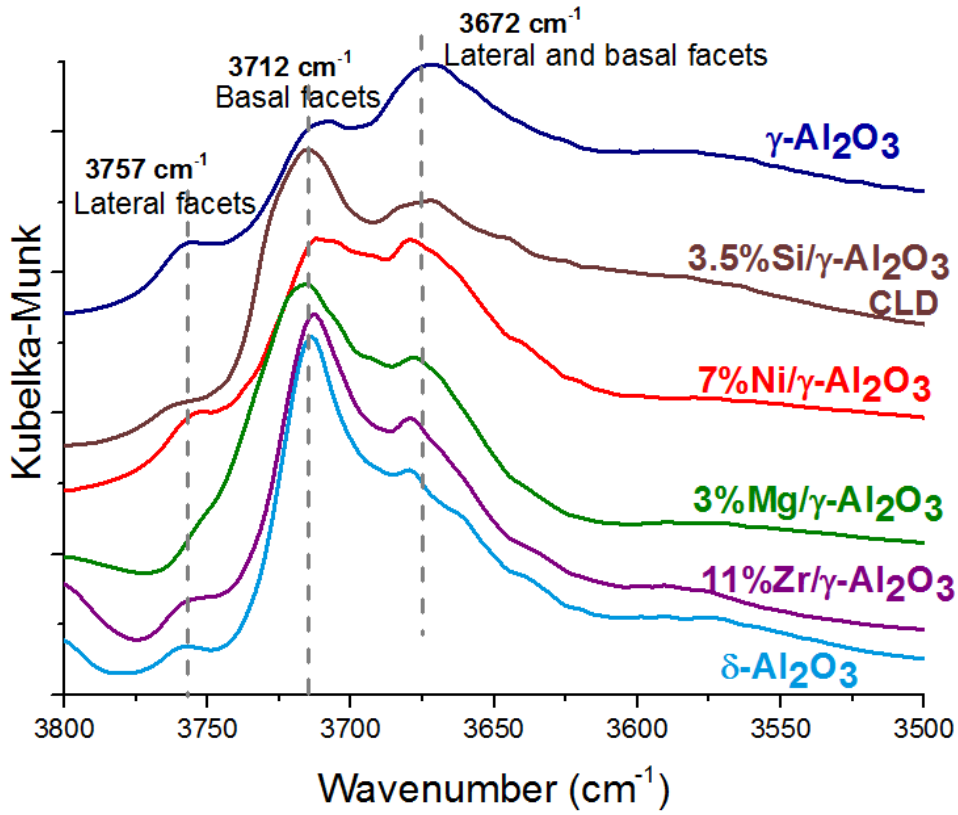

*Figure 9. DRIFTS spectra **recorded at 500°C** of γ-Al_2O_3 (blue), 3.5%Si/γ-Al_2O_3-CLD (dark brown), 7%Ni/γ-Al_2O_3-500°C (red), 3%Mg/γ-Al_2O_3-500°C (green), 11%Zr/γ-Al_2O_3-500°C (purple) and δ-Al_2O_3 (light blue).*

Assignment of the different ν_{OH} bands from literature results is also in line with the preceding qualitative conclusion and will be detailed below.

Three main bands for γ and δ-Al_2O_3 as well as the doped supports are detected on the corresponding IR spectra at: 3672, 3712 and 3757 cm^{-1} (Figure 9). First, it has to be emphasized that these spectra were recorded at 500°C in order to prevent any rehydration in the DRIFTS cell. Hence, in order to permit a full comparison with literature results, the spectrum of γ-Al_2O_3 recorded in the present work (DRIFTS, 500°C) was compared with the spectrum of the same alumina recorded in the transmission mode at room-temperature (FTIR, RT) (Figure S10, supplementary information). A difference of 8 to 13 cm^{-1} in the peak positions is observed between DRIFTS and FTIR spectra that can be explained by a temperature effect (the higher the temperature, the lower the OH force constant).

Many assignments for the surface hydroxyls of alumina have been proposed and discussed in the literature. Table 2 summarizes three well-known and comprehensive models (Knözinger and Ratnasamy[61], Busca et al.[62] and Digne et al.[63]) and a fourth very recent account (Koerin[64]) that has revisited the preceding assignments. Peak positions reported in the first column are those found at 500°C (Figure 9, DRIFTS) while those mentioned in brackets correspond to their conversion to room-temperature values following Figure S10 (supplementary information) since they are more directly comparable to literature results.

Table 1. Assignments of the vOH vibrations for γ-Al_2O_3 according to four reports.

Models / νOH DRIFTS, 500°C (FTIR, RT)	**Knözinger and Ratnasamy**[61]	**Busca *et al.***[62]	**Digne *et al.***[63]	**Koerin**[64]
3757 (3770) cm^{-1}	HO–μ_1–Al_{IV}	I (tetr-vac)	HO–μ_1–Al_{VI} (100)	Unresolved assignment but OH located on (111)
3712 (3720) cm^{-1}	HO–μ_2–(Al_{VI},Al_{IV})	I (oct)	HO–μ_1–Al_V (110)	OH-μ_1-Al_V-(110) + OH-μ_1-Al_V mainly on junction (110)/(100)
3672 (3680) cm^{-1}	HO–μ_3-Al_{VI}	II	HO–μ_2–Al_{VI} (111)	OH-μ_2-Al_{VI}-Al_{VI} located on all the particle
μ1 and I: singly coordinated OH; μ2 and II: doubly coordinated OH; μ3: triply coordinated OH (tetr-vac): tetrahedrally coordinated Al ion near a cation vacancy, (oct): octahedrally coordinated Al ion				

Table 2 shows that there is some disagreement among the different proposals. Digne *et al*.[63] suggested (from a combined DFT and experimental approach) that these discrepancies could be explained by the predominant influence of hydrogen bonding among surface OHs that was not properly taken into account in the models of Knözinger and Ratnasamy[61] and Busca *et al*.[62] However, without focusing on the assignment of vibrations to a specific type of surface OH, table 2 shows that the different ν_{OH} peaks can be attributed to different types of facets : lateral (100) or (111) and basal (110) (see Figure 10). The most recent models of Digne *et al*.[63] and Koerin[64]

converge to show that the band at 3757 cm^{-1} can be assigned to a lateral facet : (100) or (111). Conversely, the band at 3712 cm^{-1} is assigned to the predominant basal plane (110). The situation is less straightforward for the 3672 cm^{-1} vibration that is assigned either to a lateral facet (Digne *et al*.[63]) or that arises from the whole particle (Koerin[64]). Nevertheless, in both cases this band involves vibrations from OH located on lateral facets even if it is not exclusive.

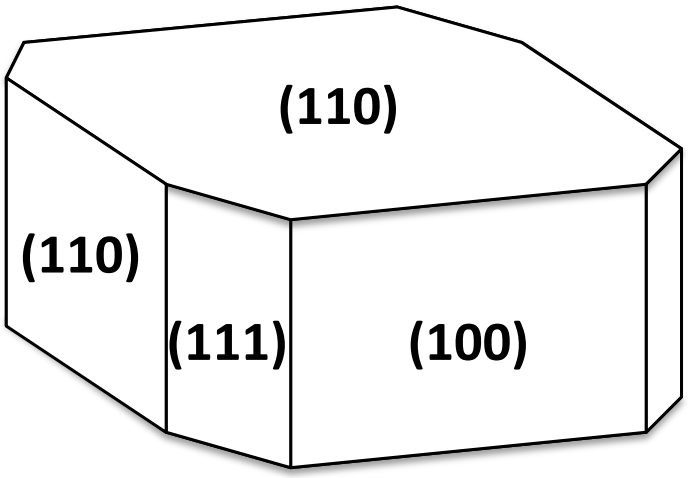

Figure 10. γ-alumina nanoparticle with the corresponding surface orientations.[63]

Keeping these assignments in mind, the comparison of IR spectra obtained for γ-Al_2O_3 and the doped supports (Figure 9) show that a predominant intensity decrease is observed for bands arising (at least in part) from lateral facets (3757 and 3672 cm^{-1}) at the expense of the band assigned to the basal plane (3712 cm^{-1}). These results allow us to conclude that dopants are predominantly deposited on these lateral facets in line with the close similarity of the spectra obtained for doped-supports and for δ-Al_2O_3 discussed above.

Hence, the stabilizing role of dopants toward boehmite formation also suggests that these dopants will deposit on (and block) the most reactive Al-OH surface sites toward dissolution that are most probably located on these lateral facets.

.

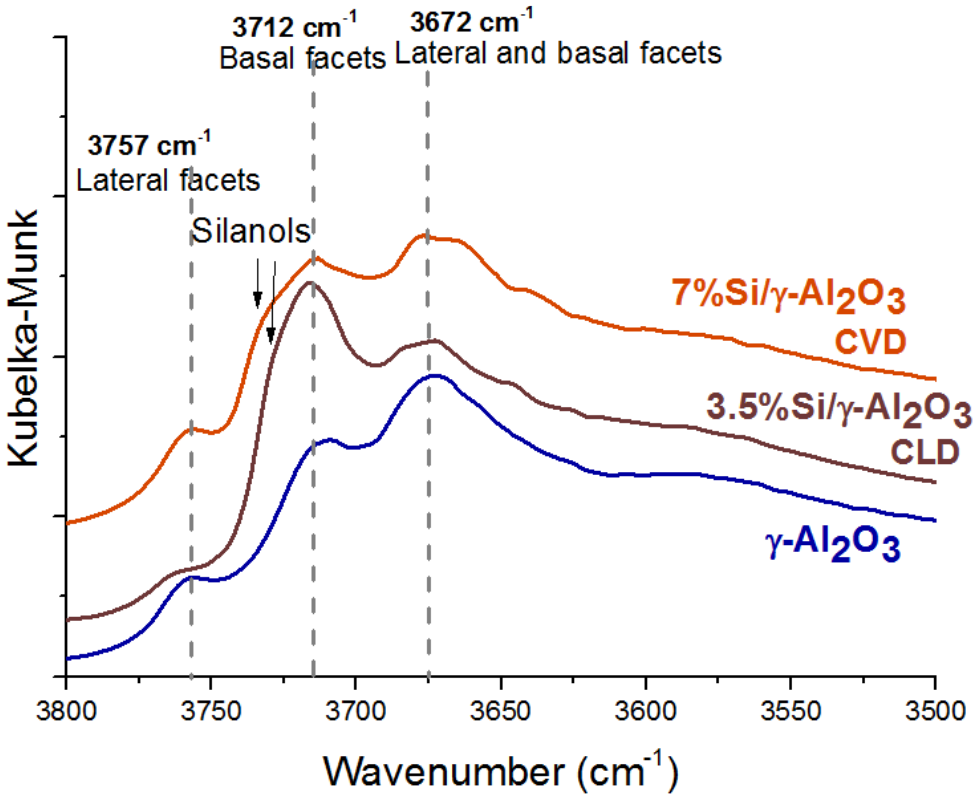

*Figure 11. DRIFTS spectra **recorded at 500°C** of γ-Al_2O_3 (blue) and 3.5%Si/γ-Al_2O_3-CLD (dark brown) and 7%Si/γ-Al_2O_3-CVD (light brown).*

The same behavior is observed for the Si-doped supports (Figure 11), i.e., a decreased intensity of bands assigned to lateral facets (3757 and 3672 cm^{-1}). However, in this case, an extra shoulder is observed at 3725 cm^{-1} that may correspond to the formation of isolated silanol groups.

Theses DRIFTS results are actually in good agreement with the work of Caillot *et al.*[59] who investigated with IR spectroscopy the specific grafting of Si with CLD and CVD deposition methods used in the present work. It was shown that for low amount of Si (i.e. 2.8%) deposited under mild conditions, grafting takes place preferentially on (100) facet (lateral). However, when increasing the Si loading to 5.6%, grafting partially occurs on the basal (110) facet once the whole (100) facet is covered. For high loadings (i.e. 8,4%), Si is grafted on the entire particle.

Hence, for 3.5%Si/γ-Al_2O_3-CLD, both DRIFTS results and literature data converge to show that Si is selectively grafted on a lateral facet. However, the discrepancies in the detailed assignment of ν_{OH} vibrations reported in Table 2 does not allow us to be more specific on the type of lateral facets

involved : (110), (111) or both and on the specific type of surface OH. For 7%Si/γ-Al_2O_3-CVD, the DRIFTS spectrum is more similar to that of γ-Al_2O_3. It can be explained by the higher amount of Si that will cover most of the γ-Al_2O_3 planes leading to a broad coverage of the support (including obviously the reactive lateral facets).

Nevertheless, the full inhibition of boehmite formation observed with Si (Figure 2 and Figure 7) shows that Si grafting is probably much more specific than for any of the other dopants where only a partial inhibition was observed. As a matter of fact, all dopants (3% Mg, 11% Zr, 7% Ni and 3.5% Si) are impregnated with a similar surface loading (i.e. 3,0-3,2 at.nm^{-2}). For low Si loading (ca. 3 wt%) there is probably exclusive deposition on lateral facets which leads to a selective blocking of all reactive surface sites while for other metal dopants (Mg, Zr and Ni), deposition is probably less selective. For 7%Si/γ-Al_2O_3-CVD, there is also presumably selective deposition of Si up to 3 wt% leading to a full inhibition of boehmite formation while the excess of Si will spread on the entire surface of the particle.

IV.3.7. Effect of dopant loadings on boehmite formation

The amount of boehmite formed after hydrothermal ageing at 150°C during 4 h of Mg/γ-Al_2O_3 and Zr/γ-Al_2O_3 with different loadings are plotted in Figure 12 and compared to γ-Al_2O_3. There is no significant change in the extent of AlOOH formation while increasing the amount of dopant. Hence, these results suggest that there is a saturation limit for selective blocking of reactive surface Al-OH sites on alumina by Mg or Zr. Excess dopants will most probably spread on the entire surface of γ-Al_2O_3.

On a more applied point of view, it has been recently shown that Mg-doping is not affecting the FT-synthesis (mainly C_{5+} selectivity) as long as the Mg loading is less than 10 wt%,[66] which is the case of the present work (3 wt% of Mg). Stabilizing γ-Al_2O_3 with Mg can thus be an interesting way for FT application.

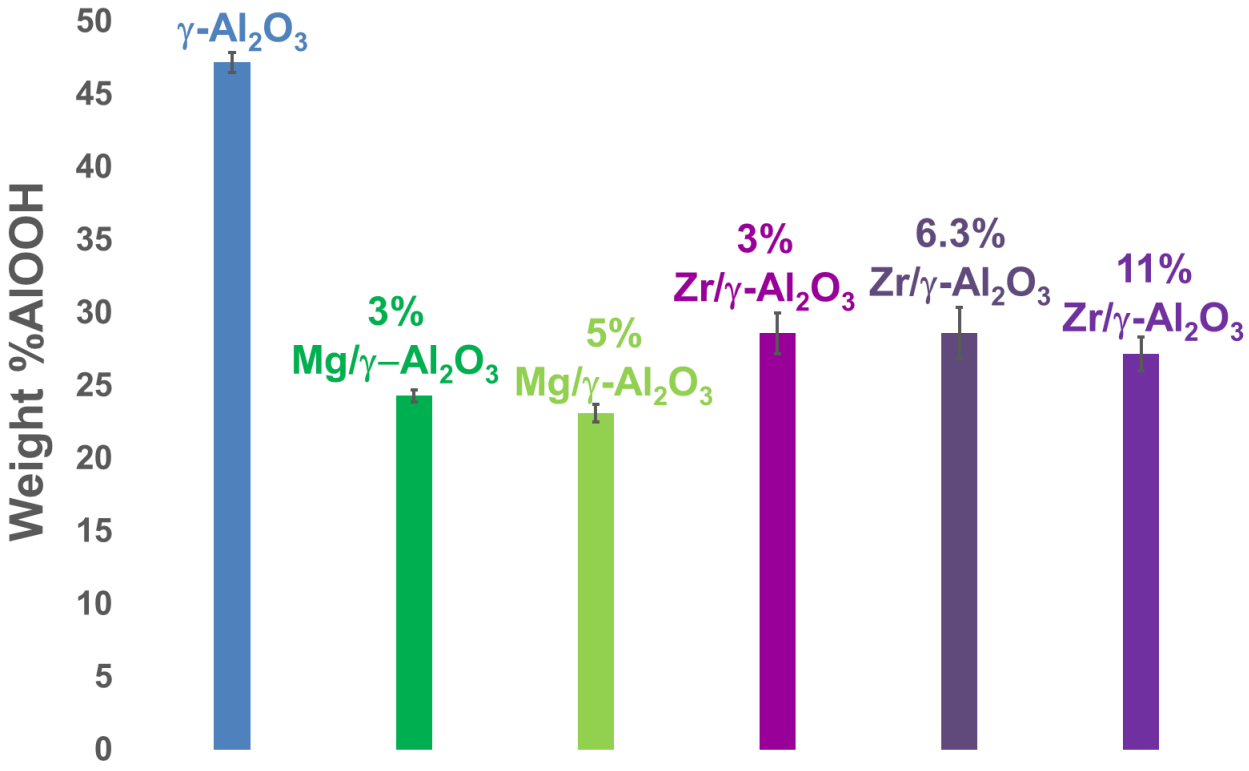

Figure 12. Amount of boehmite formed after ageing γ-Al_2O_3 in water at 150°C during 4 h after doping with Mg (green) and Zr (purple) and calcination at 500°C, (1.6 g/80 mL, hydrothermal conditions).

IV.3.8. Role of dopants - Liquid-state aluminum concentration

Liquid-state Al(III) concentrations were analyzed in the supernatants obtained after filtration of doped γ-Al_2O_3-water suspensions aged at 150°C during various times (Table 3). As in Chapter II, these filtrates were acidified after cooling in order to prevent AlOOH precipitation from supersaturated solutions. Al(III) concentrations were determined by ICP-OES and results are reported in Table 3.

Table 3. Concentrations of Al(III) in solution after hydrothermal ageing of γ-Al_2O_3, 3%Mg/γ-Al_2O_3-500°C, -750°C and -900°C. Ageing was carried out at 150°C during different ageing times from 30 minutes to 4 h. (1.6 g/80 mL, hydrothermal conditions).

Samples	**Aluminum concentration (mol.L^{-1})**		
	30 min	**2 h**	**4 h**
γ-Al_2O_3	< DL	< DL	< DL
3% Mg/γ-Al_2O_3-500°C	4.1 x 10^{-5}	3.2 x 10^{-5}	2.5 x 10^{-5}
3% Mg/γ-Al_2O_3-750°C	2.2 x 10^{-5}	1.4 x 10^{-5}	< DL
3% Mg/γ-Al_2O_3-900°C	1.7 x 10^{-5}	6.3 x 10^{-6}	< DL
DL: detection limit (3.7x10^{-6} mol.L^{-1})			

First, one has to note that the concentration of dissolved Al(III) after hydrothermal ageing of pure γ-Al_2O_3 is under the detection limit of the technique which is in line with the massive precipitation of boehmite observed for short ageing times (Figure 5, 20% of AlOOH at 30 min) via dissolution-precipitation (Chapter II).[41,42] Conversely, for the three doped supports 3%Mg/γ-Al_2O_3 -500, -750 and -900°C, the dissolution step is evidenced by the detection of dissolved Al(III) (Table 3). No attempt will be made to compare these Al(III) concentrations with the thermodynamic solubility of pure γ-Al_2O_3 (Figure 4, Chapter III-A) since the surface of the doped support is partly made of a spinel phase (Figure 3) inducing obvious modifications on the thermodynamic solubility of the support. The higher amount of dissolved Al(III) between doped- and pure-γ-Al_2O_3 can be explained by a slower dissolution rate for γ-Al_2O_3 after doping. It will thus lead to a lower supersaturation of Al(III) and thus to a less explosive nucleation-growth process maintaining dissolved Al(III) in solution and giving smaller amount of boehmite (Figure 5, 10% at 30 min) compared to non-doped support.

Nonetheless, after 4h of ageing for 3%Mg/γ-Al_2O_3-750 and 900°C, nucleation-growth of boehmite becomes again predominant (about 20% of boehmite is obtained) as for pure γ-Al_2O_3 and the concentration of dissolved Al(III) goes under the detection limit.

These results confirm the protecting role of the different dopants toward alumina dissolution. However, an exception is observed for 3%Mg/γ-Al_2O_3-500°C for which Al(III) is still detected even after 4 h of ageing. However, in this case, hydrotalcite was identified (Figure 4) and nucleation-growth processes are probably more complex.

IV.4. Conclusions

The effect of dopants (Mg^{II}, Zr^{IV}, Ni^{II} and Si^{IV}) on mitigating the chemical weathering of γ-Al_2O_3 toward boehmite under hydrothermal conditions (water, 150°C, 4.6 bar) was studied. Their specific role and that of the calcination temperature of the doped-supports on hydrothermal resistance of γ-Al_2O_3 were investigated with both macroscopic (XRD, SEM) and molecular-scale (DRIFTS) techniques.

In presence of metal ions (Mg^{II}, Zr^{IV} and Ni^{II}), the degradation of γ-alumina is clearly attenuated, but not suppressed, and there is little dependence on the chemical nature of the dopant. Formation of surface spinels after doping (Mg^{II}, and Ni^{II}) or hydrotalcite during ageing (Mg^{II}) appear as second-order processes with no direct influence on the inhibition of chemical weathering. As for pure alumina, the enhancement of alumina resistance toward chemical weathering increases with the calcination temperature of the stabilized support and it is confirmed that it is strongly related to a decrease in the specific surface area of the doped-support. Nonetheless, for a given surface area, doped-supports are twice more resistant than pure transition aluminas. A peculiar behaviour is observed with 7%Ni/γ-Al_2O_3 calcined at 500°C which showed a greater inhibition of boehmite formation than the other doped supports. This comportment is related to the formation of small NiO particles on the surface.

Silicon doping appears much more specific since a complete suppression of boehmite formation is shown, even after a long hydrothermal ageing time (14 h). This full inhibition is related to the formation of highly resistant Si-O-Al bonds on specific surface sites.

The specificity of reactive alumina surface sites was further investigated with DRIFTS in the ν_{OH} region. It is suggested that the role of the dopants is to block the most reactive surface Al-OH sites located on lateral facets, (100) and/or (111), of γ-Al_2O_3. Analysis of dissolved Al^{III} confirms that dopants decrease the dissolution kinetics of alumina. The high hydrothermal resistance observed with Si indicates that this dopant will selectively and fully consume these reactive surface sites. Conversely, in the case of Mg^{II} and Zr^{IV}, a saturation loading is observed above which a further addition of dopants will not lead to any gain in hydrothermal resistance indicating that these dopants are less selective.

IV.5. Experimental section

IV.5.1. Sample preparation

A commercial boehmite (Sasol Pural SB3 SCCa) was calcined in static air in a muffle furnace at different calcination temperatures with a heating rate of 10°C/min and a plateau of 12 h in order to obtain five different transition aluminas :[42,52,67]

- 500°C: γ-Al_2O_3 (238 m²/g)
- 700°C: γ/δ-Al_2O_3 (183 m²/g)
- 850°C: δ-Al_2O_3 (110 m²/g)
- 900°C: δ/θ-Al_2O_3 (109 m²/g)
- 1000°C: θ-Al_2O_3 (77 m²/g)

Incipient wetness impregnation of Mg^{II}, Zr^{IV} and Ni^{II} salts on γ-Al_2O_3 (pore volume = 0.42 $cm^3.g^{-1}$) was then performed in order to obtain various doped supports: 3% Mg/γ-Al_2O_3 (3.2 at/nm²), 5% Mg/γ-Al_2O_3 (5.3 at/nm²), 3% Zr/γ-Al_2O_3 (0.8 at/nm²), 6.3% Zr/γ-Al_2O_3 (1.7 at/nm²), 11% Zr/γ-Al_2O_3 (3.1 at/nm²) and 7% Ni (3.0 at/nm²) using magnesium nitrate hexahydrate ($Mg(NO_3)_2.6H_2O$, Sigma-Aldrich), zirconyle nitrate ($ZrO(NO_3)_2$, Prolabo) and nickel(II) nitrate hexahydrate ($Ni(NO_3)_2.6H_2O$, Sigma-Aldrich). The weight loadings refer to the relative weight of the metal to the oxide. After impregnation, the powders were dried in an oven at 120°C for 12 h and then calcined under dried air at 500°C during 4 h at a heating rate of 10°C/min. Some of the samples underwent a further calcination at higher temperature (750 or 900°C) during 12 h.

Chemical liquid deposition in organic solvent and chemical vapor deposition were performed for Si^{IV} doping following a method described in Ref [68]. The synthesis conditions are below:

Sample name	**Si [wt %]**	**Synthesis technique**	**Conditions (T[°C])**	
			Pretreatment	**Synthesis**
3.5% Si/γ-Al_2O_3-CLD	3.5	CLD anhydrous	40°C, vacuum	140°C, toluene
7%Si /γ-Al_2O_3-CVD	7	CVD	250°C, N_2 flow	400°C, N_2

IV.5.2. Ageing tests in hydrothermal conditions

Ageing tests were conducted in a 100 mL Hastelloy C276 autoclave from Top Industrie under continuous stirring by a propeller stirrer at a rate of 1000 rpm. The various transition aluminas and stabilized supports were suspended in distilled water with an oxide/water ratio of 1.6 g/80 mL and aged at 150°C under hydrothermal conditions (4.6 bar) during different ageing times. After the autoclave had been cooled down, the filtrate was separated from the solid by centrifugation. An additional filtration of the supernatant was performed, using a syringe equipped with a filter of 0.2 µm porosity. The supernatant was then acidified by nitric acid in order to prevent hydroxide/oxyhydroxide precipitation before performing elemental analysis of aluminum. The solid was dried in an oven at 90°C during 12 h.

IV.5.3. Characterization techniques

X-Ray diffraction patterns were recorded with a Bruker D8 Advanced diffractometer operated at 30 kV and 5 mA in the θ–2θ mode with Bragg–Brentano geometry using CuKα radiation (λ = 1.5418 Å). The diffractometer is equipped with a back monochromator and a scintillation detector. A scan rate of 0.5 step per second was used from 2θ = 10° to 80°.

Specific surface areas were determined by nitrogen physisorption (Brunauer-Emmett-Teller model (BET)), performed with a BELSORP-max analyzer from BelJapan, after degassing the samples for 1 night at 150°C.

Combined thermogravimetric and differential thermal analyses (TGA-DTA) were performed with a SDT Q600 TA instrument. The samples were heated in a flow of nitrogen (100 mL/min) at a heating rate of 10 °C/min.

Temperature-programmed reductions (TPR) were carried out on calcined catalysts, using an Autochem 2910 apparatus (Micromeritics), under 5% H_2/Ar (ramp rate 7.5°C min^{-1} up to 950°C).

XPS spectra were recorded with an Omicron (ESCA+) instrument using a monochromatic Al X-ray source (hν = 1486.6 eV) with an accelerating voltage of 14 kV and a current intensity of 20 mA (overall energy resolution was about 0.8 eV).

SEM-FEG images were recorded with a Hitachi SU-70 Field Emission Gun Scanning Electron Microscope. The powder samples were fixed on an alumina SEM support with a carbon adhesive tape and observed without any metallization. Low accelerating voltage (1 kV) was used and the working distance was either about 3 mm or 15 mm. According to these experimental conditions, images were obtained by an "in Lens" secondary electron detector (SE-Upper).

Liquid-phase elemental analysis of dissolved Al and dopants was performed by ICP-OES with a SPECTRO ARCOS from SPECTRO AMETEK.

Infrared DRIFTS spectroscopy was carried out on a Bruker Vector 22 spectrometer under Ar with a flow rate equal to 50 mL/min. The spectra were normalized with respect to KBr and converted using OPUS software, according to the Kubelka-Munk equation below:

$$f(R) = \frac{(1-R)^2}{2R} = \frac{k}{s}$$

R is the absolute reflectance of the sampled layer, k is the molar absorption coefficient and s is the scattering coefficient. DRIFTS spectra were recorded at 500°C.

IV.6. Acknowledgments

SEM-FEG instrumentation was financially supported by the C'Nano projects of the Région Ile-de-France and IMPC FR2482 (Institut des Matériaux de Paris Centre).

IV.7. Keywords

Alumina, hydrothermal stability, chemical weathering, boehmite, dopants, magnesium, zirconium, nickel, silicon, organic additives, sorbitol, Fischer-Trospch.

IV.8. References

[1] J.-P. Lange, *Biofuels Bioprod. Biorefining* **2007**, *1*, 39–48.

[2] K. Wu, Y. Wu, Y. Chen, H. Chen, J. Wang, M. Yang, *ChemSusChem* **2016**, *9*, 1355–1385.

[3] M. Dusselier, M. Mascal, B. F. Sels, *Top. Curr. Chem.* **2014**, *353*, 1–40.

[4] J. S. Luterbacher, D. Martin Alonso, J. A. Dumesic, *Green Chem.* **2014**, *16*, 4816–4838.

[5] P. N. R. Vennestrom, C. M. Osmundsen, C. H. Christensen, E. Taarning, *Angew. Chem. Int. Ed.* **2011**, *50*, 10502–10509.

[6] G. W. Huber, S. Iborra, A. Corma, *Chem. Rev.* **2006**, *106*, 4044–4098.

[7] A. Corma, S. Iborra, A. Velty, *Chem. Rev.* **2007**, *107*, 2411–2502.

[8] X. Yan, O. R. Inderwildi, D. A. King, *Energy Environ. Sci.* **2010**, *3*, 190–197.

[9] H. Boerrigter, H. Den Uil, H.-P. Calis, *Green Diesel from Biomass via Fischer-Tropsch Synthesis: New Insights in Gas Cleaning and Process Design*, Citeseer, **2003**.

[10] J. Hu, F. Yu, Y. Lu, *Catalysts* **2012**, *2*, 303–326.

[11] T. G. Kreutz, E. D. Larson, G. Liu, R. H. Williams, in *25th Annu. Int. Pittsburgh Coal Conf.*, **2008**.

[12] E. van Steen, M. Claeys, *Chem. Eng. Technol.* **2008**, *31*, 655–666.

[13] O. R. Inderwildi, S. J. Jenkins, D. A. King, *J. Phys. Chem. C* **2008**, *112*, 1305–1307.

[14] R. C. Brady III, R. Pettit, *J. Am. Chem. Soc.* **1981**, *103*, 1287–9.

[15] P. Biloen, J. N. Helle, W. M. H. Sachtler, *J. Catal.* **1979**, *58*, 95–107.

[16] H. Schulz, *Appl. Catal. A Gen.* **1999**, *186*, 3–12.

[17] J. P. Franck, E. Freund, E. Quéméré, *J. Chem. Soc. Chem. Commun.* **1984**, 629–630.

[18] L. Jun-Cheng, X. Lan, X. Feng, W. Zhan-Wen, W. Fei, *Appl. Surf. Sci.* **2006**, *253*, 766–770.

[19] R. M. Mironenko, O. B. Belskaya, V. P. Talsi, T. I. Gulyaeva, M. O. Kazakov, A. I. Nizovskii, A. V. Kalinkin, V. I. Bukhtiyarov, A. V. Lavrenov, V. A. Likholobov, *Appl. Catal. A Gen.* **2014**, *469*, 472–482.

[20] R. M. Ravenelle, J. R. Copeland, W.-G. Kim, J. C. Crittenden, C. Sievers, *ACS Catal.* **2011**, *1*, 552–561.

[21] J. Zhang, J. Chen, J. Ren, Y. Sun, *Appl. Catal. A Gen.* **2003**, *243*, 121–133.

[22] Y. Zhou, H. Fu, X. Zheng, R. Li, H. Chen, X. Li, *Catal. Commun.* **2009**, *11*, 137–141.

[23] D. J. M. de Vlieger, A. G. Chakinala, L. Lefferts, S. R. A. Kersten, K. Seshan, D. W. F. Brilman, *Appl. Catal. B Environ.* **2012**, *111-112*, 536–544.

[24] D. C. Elliott, L. J. Sealock Jr, E. G. Baker, *Ind. Eng. Chem. Res.* **1993**, *32*, 1542–1548.

[25] M. El Doukkali, A. Iriondo, J. F. Cambra, P. L. Arias, *Top. Catal.* **2014**, *57*, 1066–1077.

[26] K. Koichumanova, K. B. Sai Sankar Gupta, L. Lefferts, B. L. Mojet, K. Seshan, *Phys. Chem. Chem. Phys.* **2015**, *17*, 23795–23804.

[27] J.-P. Lange, *Angew. Chem. Int. Ed.* **2015**, *54*, 13186–13197.

[28] H. Xiong, H. N. Pham, A. K. Datye, *Green Chem* **2014**, *16*, 4627–4643.

[29] I. Sádaba, M. López Granados, A. Riisager, E. Taarning, *Green Chem* **2015**, *17*, 4133–4145.

[30] W. C. Ketchie, E. P. Maris, R. J. Davis, *Chem. Mater.* **2007**, *19*, 3406–3411.

[31] J. Tan, J. Cui, G. Ding, T. Deng, Y. Zhu, Y. Li, *Catal Sci Technol* **2016**, *6*, 1469–1475.

[32] J. van de Loosdrecht, S. Barradas, E. A. Caricato, P. J. Van Berge, J. L. Visagie, *Prepr. Symp. - Am. Chem. Soc. Div. Fuel Chem.* **2000**, *45*, 587–591.

[33] K. Keyvanloo, W. C. Hecker, B. F. Woodfield, C. H. Bartholomew, *J. Catal.* **2014**, *319*, 220–231.

[34] S. Li, H. Chen, J. Shen, *J. Colloid Interface Sci.* **2015**, *447*, 68–76.

[35] K. Jothimurugesan, *Support For Fischer-Tropsch Catalyst Having Improved Activity*, **2016**, Brevet US 9,233,358 BI.

[36] K. Jothimurugesan, *Stable Support for Fischer-Tropsch Catalyst*, **2016**, Brevet WO 2016/039861 Al.

[37] K. Jothimurugesan, M. Muraoka, *Support For Fischer-Tropsch Catalyst Having Improved Activity*, **2016**, Brevet WO 2016/039862 Al.

[38] X. Wang, D. Pan, M. Guo, M. He, P. Niu, R. Li, *Mater. Lett.* **2013**, *97*, 27–30.

[39] D. Wei, J. G. Goodwin, R. Oukaci, A. H. Singleton, *Appl. Catal. A Gen.* **2001**, *210*, 137–150.

[40] D. Enache, M. Roy-Auberger, K. Esterle, R. Revel, *Colloids Surf. Physicochem. Eng. Asp.* **2003**, *220*, 223–233.

[41] X. Carrier, E. Marceau, J.-F. Lambert, M. Che, *J. Colloid Interface Sci.* **2007**, *308*, 429–437.

[42] J. Abi Aad, S. Casale, P. Courty, M. Michau, F. Diehl, E. Marceau, X. Carrier, *Submitted*

[43] C. Li, Y.-W. Chen, *Thermochim. Acta* **1995**, *256*, 457–465.

[44] L. F. Lundegaard, R. R. Tiruvalam, C. Tyrsted, A. Carlsson, F. Morales-Cano, C. V. Ovesen, *Catal. Today* **2016**, *272*, 25–31.

[45] J. L. Ewbank, L. Kovarik, F. Z. Diallo, C. Sievers, *Appl. Catal. A Gen.* **2015**, *494*, 57–67.

[46] F. Bentaleb, M. Che, A.-C. Dubreuil, C. Thomazeau, E. Marceau, *Catal. Today* **2014**, *235*, 250–255.

[47] D. M. Roy, R. Roy, E. F. Osborn, *Am. J. Sci.* **1953**, *251*, 337–361.

[48] I. Pausch, H. H. Lohse, K. Schurmann, R. Allmann, *Clays Clay Miner.* **1986**, *34*, 507–510.

[49] F. Cavani, F. Trifirò, A. Vaccari, *Catal. Today* **1991**, *11*, 173–301.

[50] J. A. van Bokhoven, J. C. Roelofs, K. P. de Jong, D. C. Koningsberger, *Chem. Eur. J.* **2001**, *7*, 1258–1265.

[51] M. Rajamathi, G. D. Nataraja, S. Ananthamurthy, P. V. Kamath, *J. Mater. Chem.* **2000**, *10*, 2754–2753.

[52] P. Euzen, P. Raybaud, X. Krokidis, H. Toulhoat, J.-L. Le Loarer, J.-P. Jolivet, C. Froidefond, in *Handb. Porous Solids*, Wiley-VCH Verlag GmbH, **2008**, pp. 1591–1677.

[53] F. Roelofs, W. Vogelsberger, *J. Colloid Interface Sci.* **2006**, *303*, 450–459.

[54] Y. Liu, S. Wang, T. Sun, D. Gao, C. Zhang, S. Wang, *Appl. Catal. B Environ.* **2012**, *119-120*, 321–328.

[55] R. M. Ravenelle, Heterogeneous Catalysts in Aqueous Phase Reforming Environments: An Investigation of Material Stability, Georgia Institute of Technology, Thèse **2011**.

[56] M. W. Hahn, J. R. Copeland, A. H. van Pelt, C. Sievers, *ChemSusChem* **2013**, *6*, 2304–2315.

[57] W. Lutz, H. Toufar, R. Kurzhals, M. Suckow, *Adsorption* **2005**, *11*, 405–413.

[58] R. M. Ravenelle, F. Schüβler, A. D'Amico, N. Danilina, J. A. van Bokhoven, J. A. Lercher, C. W. Jones, C. Sievers, *J. Phys. Chem. C* **2010**, *114*, 19582–19595.

[59] M. Caillot, A. Chaumonnot, M. Digne, J. A. V. Bokhoven, *ChemCatChem* **2013**, *5*, 3644–3656.

[60] R. M. Ravenelle, F. Z. Diallo, J. C. Crittenden, C. Sievers, *ChemCatChem* **2012**, *4*, 492–494.

[61] H. Knözinger, P. Ratnasamy, *Catal. Rev.* **1978**, *17*, 31–70.

[62] G. Busca, V. Lorenzelli, G. Ramis, R. J. Willey, *Langmuir* **1993**, *9*, 1492–1499.

[63] M. Digne, P. Sautet, P. Raybaud, P. Euzen, H. Toulhoat, *J. Catal.* **2004**, *226*, 54–68.

[64] R. Koerin, Influence Du Mode de Synthèse de La Boehmite Sur L'état de Surface de L'alumine-γ Mise En Forme ; Application Au Reformage Catalytique, Université de Caen Basse-Normandie, Thèse **2014**.

[65] V. Bolis, B. Fubini, L. Marchese, G. Martra, D. Costa, *J. Chem. Soc. Faraday Trans.* **1991**, *87*, 497–505.

[66] E. Rytter, A. Holmen, *Catal. Today* **2016**, *275*, 11–19.

[67] K. Wefers, C. Misra, *Oxides and Hydroxides of Aluminum*, Alcoa Laboratories, **1987**.

[68] M. Caillot, A. Chaumonnot, M. Digne, C. Poleunis, D. P. Debecker, J. A. van Bokhoven, *Microporous Mesoporous Mater.* **2014**, *185*, 179–189.

IV.9. Supplementary information

Inhibition of chemical weathering of γ-Al_2O_3 by inorganic dopants in hydrothermal conditions

J. Abi Aad,[a, b] M. Michau,[b] F. Diehl,[b] A. Berliet,[b] Ph. Courty,[b] X. Carrier,[a] E. Marceau,[a, c]

[1] Sorbonne Universités, UPMC Univ Paris 06, Laboratoire de Réactivité de Surface, F-75005, Paris, France

[2] IFP Energies nouvelles, Rond-point de l'échangeur de Solaize, 69360 Solaize

[3]Unité de Catalyse et Chimie du Solide (UMR 8181 CNRS), Université Lille 1, 59655 Villeneuve d'Ascq

IV.9.1. Qualitative analysis by XRD and TGA

The evaluation of the total amount of boehmite AlOOH formed after ageing of various Al_2O_3 polymorphs in water was performed with XRD and TGA.

Quantitative analysis with XRD was carried out by integration of the XRD peaks of AlOOH. A preliminary investigation was performed on reflections at 14.4°, 28.1° and 49.28° in 2θ (Figure S1). The integrated intensity was transposed to a weight percentage by using a calibration curve whose construction and validation is detailed below.

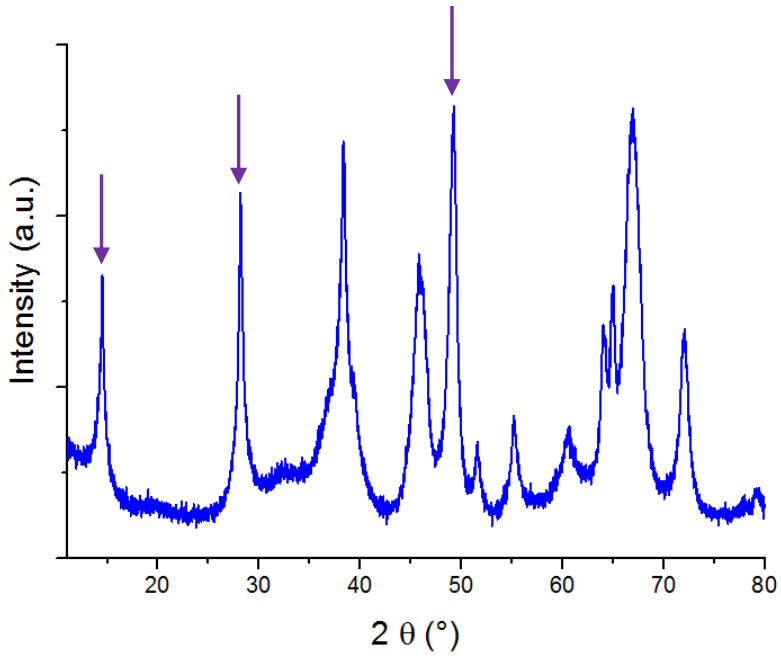

Figure S1. XRD pattern of γ-Al_2O_3 (PDF No. 10-0425) subjected to an ageing treatment in water at 150°C under hydrothermal conditions during 4 h (1.6g/80 mL). ↓ *: boehmite peaks used for the calibration method (PDF No. 83-1505).*

The calibration curve was created by preparing mechanical mixtures between the boehmite used to obtain the aluminas (Sasol Pural SB3 SCCa), and γ-alumina with weight ratios varying between 10 and 90% (the total mass of the mixture was 0.6 g). The integrated areas calculated by WinPLOTR of the characteristic XRD peaks of boehmite (at 14.4°, (020), 28.1° (021) and 49.28° ((150) and (002)), PDF No. 83-1505) were then plotted as a function of the weight percentage of boehmite introduced in the mixture as shown on Figure S2 for the reflection at 49.28°. Three very close correlation coefficients (R^2=0.94, 0.98 and 0.98 respectively) were found for the three peaks.

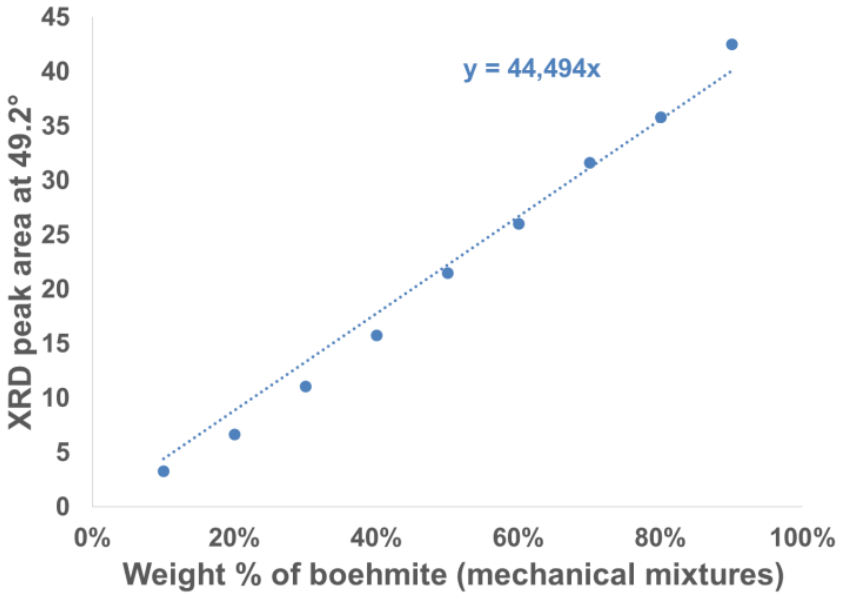

Figure S2. XRD peak integrated intensity at $2\theta = 49.28°$ (boehmite) as a function of the weight % of boehmite in γ-Al_2O_3-boehmite mechanical mixtures.

Validation of this correlation was performed by comparing the XRD-derived AlOOH content with that obtained by TGA (quantification of the oxyhydroxide dehydration at about 450°C, see Figure S4 and text in section Results and Discussions) for a series of transition aluminas aged at 150°C in water in hydrothermal conditions. XRD-derived boehmite content was evaluated using the calibration curve of the reflection at 49.28° (weight percentage of oxyhydroxide = XRD area/44.494) since it yielded the best agreement with TGA results. Figure S3 shows the correlation between both quantifications. A very good agreement is found between both techniques with a slope of about 1 (R^2=0.99) for the linear correlation, which is validating the quantification by XRD even if the peak considered (49.28°) is actually made of two reflections ((150) and (002)).

Additionally, the linear correlation found in Figure S3 leads to conclude that the potential formation of an AlOOH amorphous phase is inexistent or very minor, since it would be undetected by XRD and quantified by TGA.

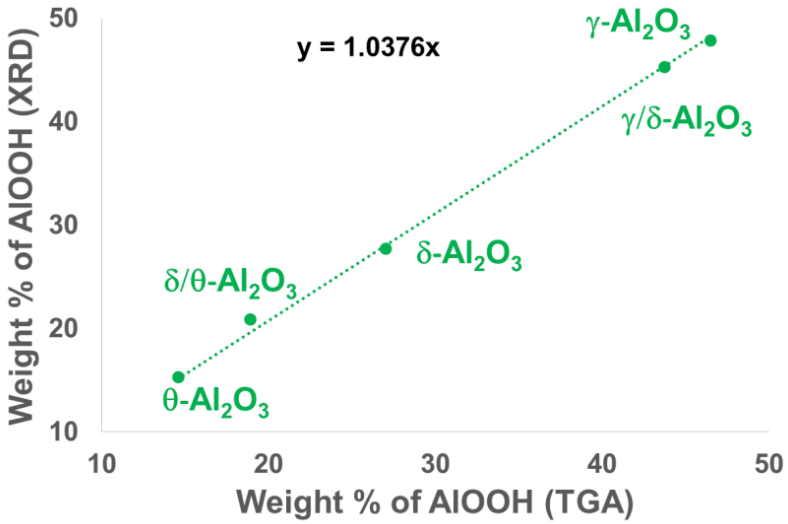

Figure S3. Weight percentages of boehmite determined by XRD as a function of those determined by TGA for a series of aluminas aged at 150°C in water during 4 h in hydrothermal conditions.

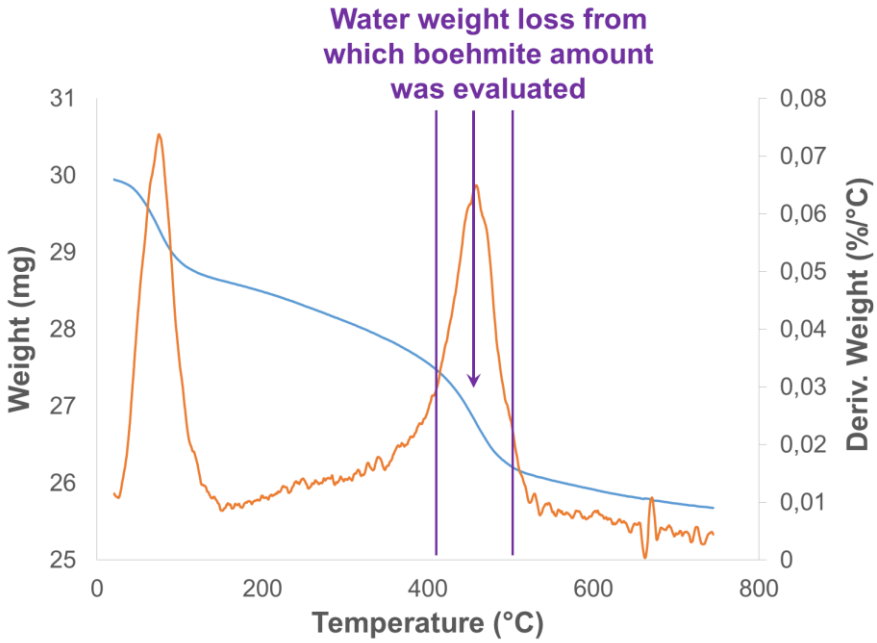

Figure S4. Thermogravimetric analysis of γ-Al_2O_3 aged at 150°C in water during 4 h in hydrothermal conditions (1.6 g/80 mL).

IV.9.2. Additional figures and tables mentioned in the text

Table S1. Concentration of dopants released in suspension for 3%Mg/γ-Al_2O_3 and 7%Ni/γ-Al_2O_3 calcined at 500°C, 750°C and 900°C after hydrothermal treatment at 150°C during 4 h (1.6 g/80 mL, autogenous pressure). Initial concentration of dopants added to the support is 2.4x10^{-2} mol.L^{-1} (i.e. 3 at.nm^{-2}). The weight loading of dopants released in solution is indicated in brackets.

Calcination temperature	[Mg] mol/L (weight %)	[Ni] mol/L (weight %)
500°C	3.4x10^{-4} (0.04)	4.4x10^{-5} (0.01)
750°C	3.3x10^{-4} (0.04)	1.1x10^{-5} (0.003)
900°C	5.4x10^{-4} (0.06)	8x10^{-5} (0.02)

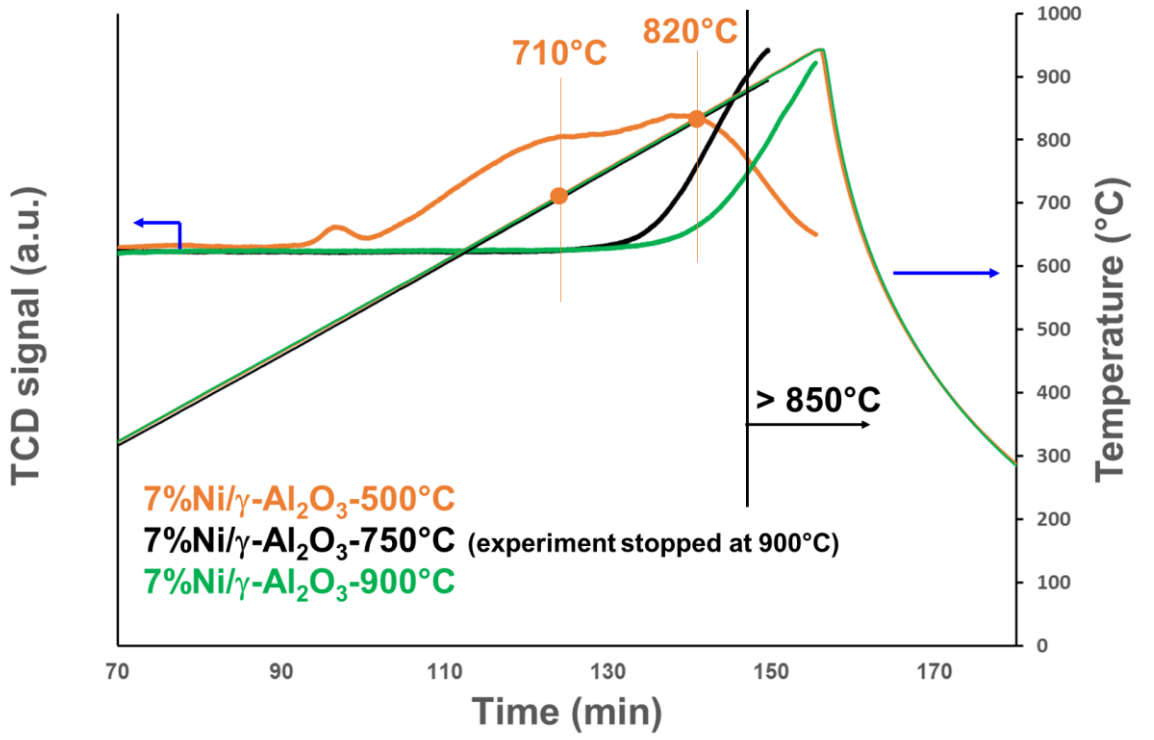

Figure S5. TPR profiles for: 7%Ni/γ-Al_2O_3-500°C (orange), 7%Ni/γ-Al_2O_3-750°C (black) and 7%Ni/γ-Al_2O_3-900°C (green). Peaks for 500°C-calcined support indicate the presence of small particles of NiO that strongly interact with the surface (part below 750°C) and surface nickel aluminate (part above 750°C). For 750 and 900°C-calcined supports, a peak at high temperature (above 900°C) identifies bulk $NiAl_2O_4$ species.[1–4]

Table S2. XPS analysis for 3%Mg/γ-Al_2O_3 and 7%Ni/γ-Al_2O_3.

Sample	Mg/Al	Ni/Al
x%M/γ-Al_2O_3-500°C	0.12	0.04
x%M/γ-Al_2O_3-500°C-HT	0.10	0.02
x%M/γ-Al_2O_3-750°C	0.09	0.03
x%M/γ-Al_2O_3-750°C-HT	0.07	0.01
x%M/γ-Al_2O_3-900°C	0.09	0.03
x%M/γ-Al_2O_3-900°C-HT	0.08	0.01
x%: weight percentage (3 or 7%), M: dopant (Mg or Ni), 500°C, 750°C and 900°C are the calcination temperatures of the supports (see experimental section in the article), HT: hydrothermal treatment in water at 150°C during 4 h.		

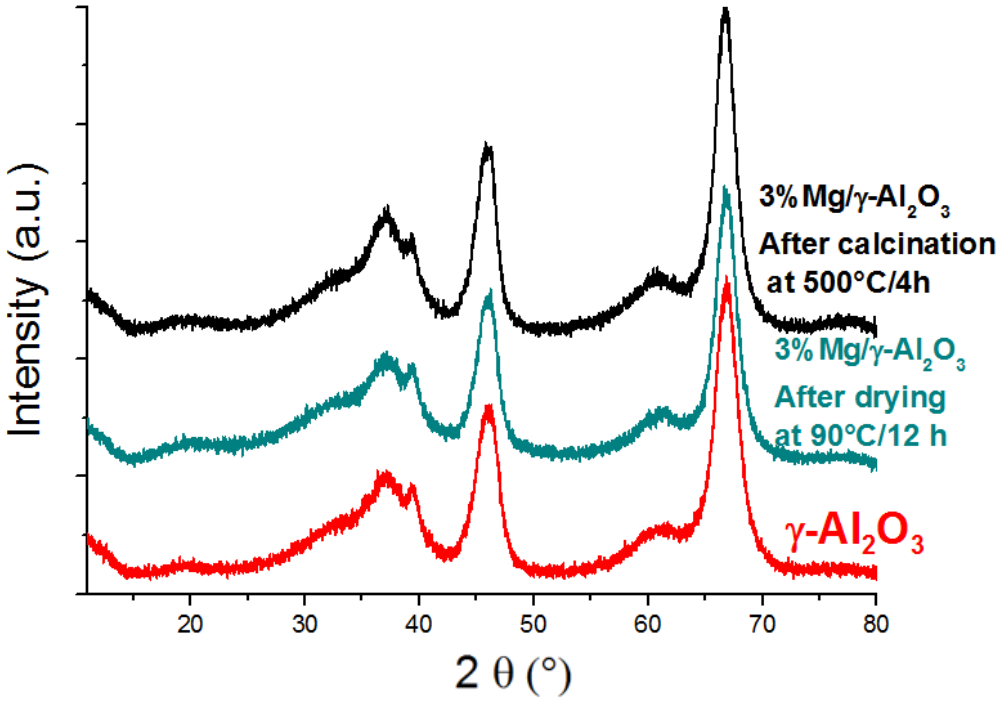

Figure S6. XRD patterns of γ-Al_2O_3 (red) and 3%Mg/γ-Al_2O_3 after impregnation of Mg and drying at 90°C during 12 h (cyan) and after calcination at 500°C during 4 h (black).

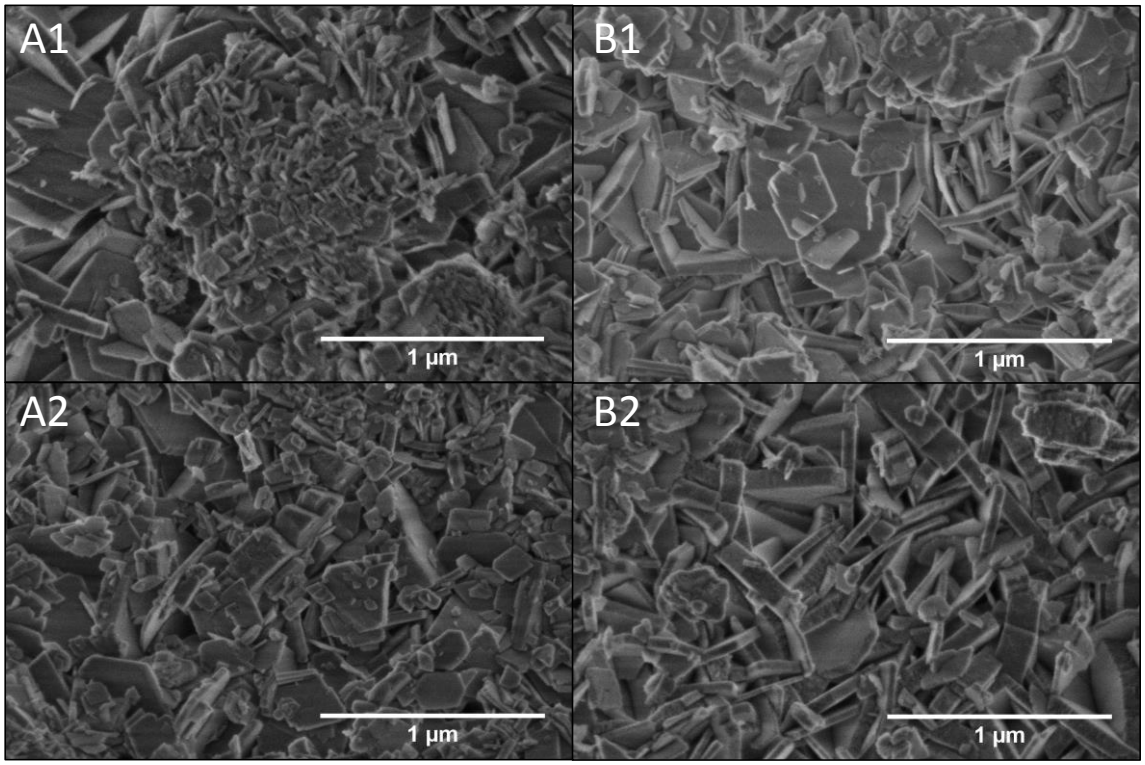

Figure S7. SEM images of 3%Mg/γ-Al_2O_3 calcined at 500°C (A series) and at 750°C (B series) subjected to an ageing treatment at 150°C during 4 h (1 series) and 14 h (2 series) under hydrothermal conditions (1.6 g/80 mL).

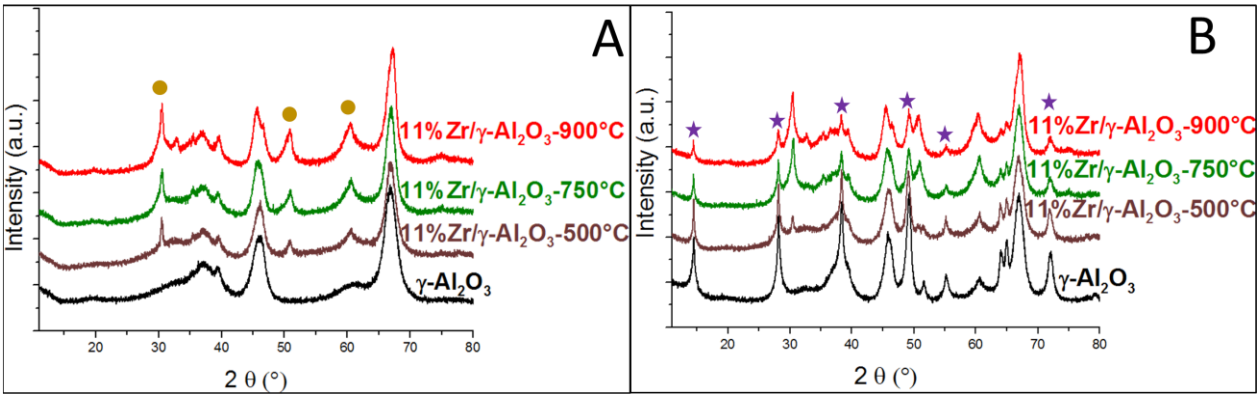

Figure S8. XRD patterns of (A) γ-Al_2O_3 (black) and 11% Zr/γ-Al_2O_3 calcined at 500°C (brown), 750°C (green,) and 900°C (red) and (B) after ageing at 150°C during 4 h (1.6 g/80 mL). ● ZrO_2 (PDF No 37-1413) ★: boehmite (PDF No. 83-1505).

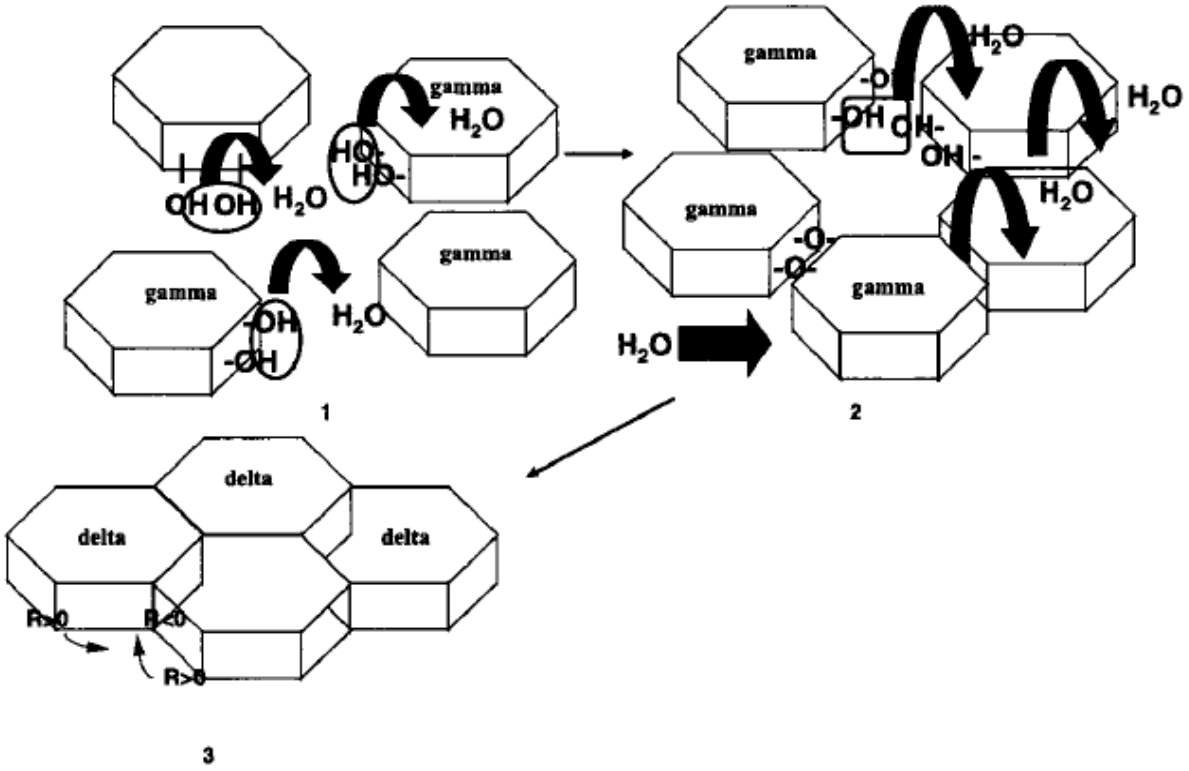

Figure S9. Simplified Scheme of the transition $\gamma \rightarrow \delta \rightarrow \theta \rightarrow \alpha$: 1: dehydroxylation of γ-Al_2O_3 ; 2 : formation of Al-O-Al bridges between platelets ; 3: $\gamma \rightarrow \delta$-$Al_2O_3$ transition.

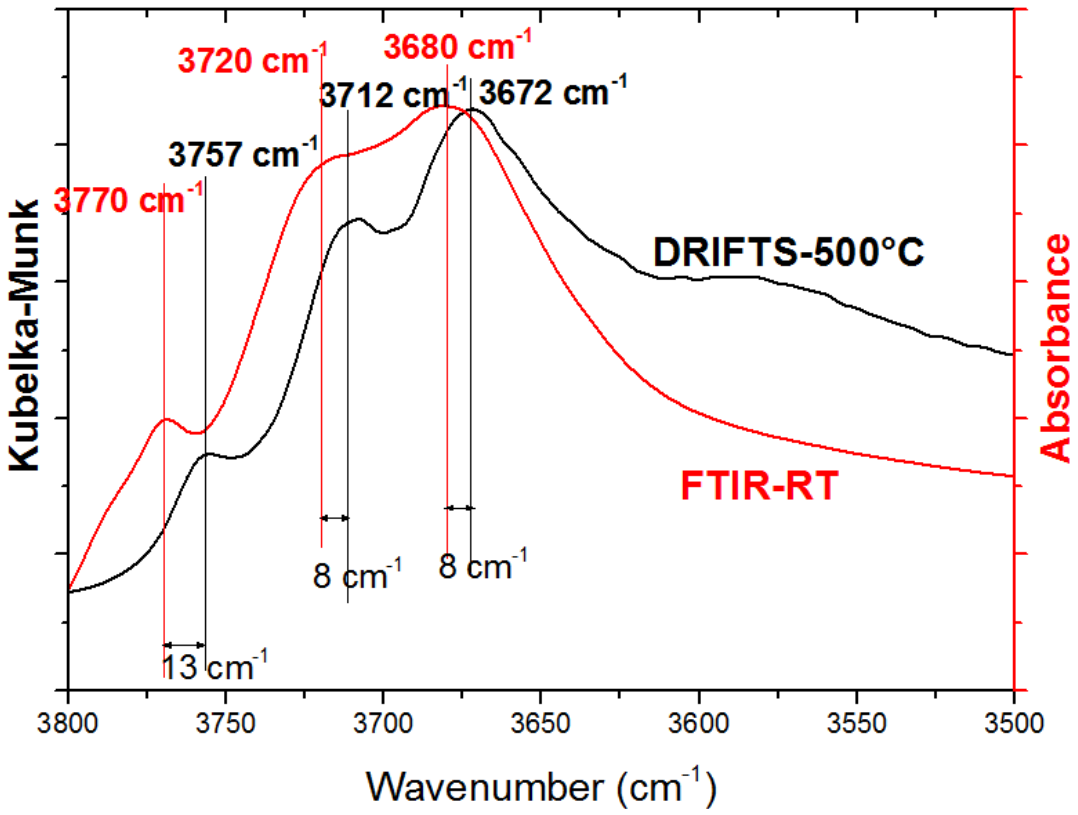

*Figure S10. Infrared spectra of γ-Al_2O_3 in the υ_{OH} region: in black, spectrum recorded in in the diffuse reflectance mode (DRIFTS**) at 500°C**; in red spectrum recorded in the transmission mode (FTIR) **at room temperature**.*

IV.9.3. References

[1] C. Li, Y.-W. Chen, *Thermochim. Acta* **1995**, *256*, 457–465.

[2] L. F. Lundegaard, R. R. Tiruvalam, C. Tyrsted, A. Carlsson, F. Morales-Cano, C. V. Ovesen, *Catal. Today* **2016**, *272*, 25–31.

[3] J. L. Ewbank, L. Kovarik, F. Z. Diallo, C. Sievers, *Appl. Catal. A Gen.* **2015**, *494*, 57–67.

[4] F. Bentaleb, M. Che, A.-C. Dubreuil, C. Thomazeau, E. Marceau, *Catal. Today* **2014**, *235*, 250–255.

Conclusion

Conclusion générale

Les alumines de transition, en particulier l'alumine γ, sont des supports oxydes couramment utilisés en catalyse hétérogène, en particulier pour des procédés catalytiques mis en œuvre dans des conditions relativement sévères qui peuvent conduire à une dégradation du support préjudiciable à la stabilité du système. On peut notamment citer les procédés qui impliquent la présence d'eau à haute température (>100°C) comme la synthèse Fischer-Tropsch ou la conversion de biomasse. Dans ces conditions, l'alumine γ subit une dégradation chimique, *érosion*, en se transformant en phases dites hydratées (hydroxydes $Al(OH)_3$, oxyhydroxyde AlOOH), et une dégradation physique, *attrition*, en produisant des fines suite aux chocs que subissent les grains de catalyseurs dans le réacteur. Des études ont été publiées pour déterminer dans quelle mesure la résistance à la dégradation chimique et mécanique des alumines en phase aqueuse peut être améliorée par dopage au moyen d'ions métalliques ou d'hétéroatomes. Néanmoins, la compréhension mécanistique à l'échelle moléculaire des phénomènes de dégradation et d'inhibition par les dopants est encore largement balbutiante. L'objectif de ce travail de thèse a donc été de déterminer les mécanismes d'hydratation de l'alumine et de préciser le rôle des dopants en identifiant les sites de surface de l'alumine par où commence le processus de dégradation.

Nous avons tout d'abord défini des conditions modèles permettant de suivre l'évolution du support au cours du temps en milieu aqueux :

- Sous pression atmosphérique à 70°C : les mécanismes d'érosion (dégradation chimique) et d'attrition (dégradation physique) ont été mis en évidence et explicités. Ces résultats ont servi de base pour interpréter les transformations ayant lieu en conditions plus sévères.
- Sous conditions hydrothermales à 150°C dans un autoclave sous pression : l'influence de différents milieux et de différentes compositions chimiques des matériaux a été explorée : eau pure, et présence de molécules organiques dans la phase aqueuse (choisies comme typiques de réactifs ou de produits relatifs à la transformation de molécules biosourcées ou à la synthèse Fischer-Tropsch) ; alumines pures, ou dopées par des ions métalliques ou par des hétéroatomes.

Mécanismes d'érosion et d'attrition à pression atmosphérique

L'étape clé de la dégradation de l'alumine γ en phase aqueuse est sa dissolution qui se produit à des temps de vieillissement courts (≤ 2 h). Cette dissolution est suivie par une précipitation d'hydroxydes ($Al(OH)_3$) par nucléation sur la surface de l'alumine et par une croissance des cristaux à des temps de traitements longs (≥ 8h). La dégradation physique (attrition), due en partie à l'affaiblissement des propriétés mécaniques de l'alumine par l'érosion, amplifie l'hydratation du support. Ces résultats contredisent l'hypothèse avancée dans la littérature d'une transformation topotactique de surface de l'alumine en hydroxydes d'aluminium.

La formation d'hydroxydes durant les premiers temps de vieillissement est sous contrôle cinétique. La bayerite est ainsi favorisée à temps courts, en raison de la vitesse de dissolution élevée de l'alumine conduisant à une sursaturation en ions aluminium dans la phase aqueuse. Un contrôle thermodynamique est suggéré à des temps de traitements plus longs pour lesquels la quantité de nordstrandite et de gibbsite (produit thermodynamique) augmente au détriment de la bayerite.

Toutes les alumines de transitions, de γ à θ, subissent cette dégradation. Cette dernière augmente avec la diminution de la cristallinité du polymorphe, la diminution de la taille des nanoparticules et l'augmentation de la surface spécifique. Ceci favorise la dissolution qui est donc régie par la thermodynamique (instabilité de l'alumine par rapport à l'eau) et la cinétique (conditionnée par la taille des particules et leur surface spécifique).

Mécanismes d'érosion en conditions hydrothermales

Un mécanisme similaire à celui trouvé sous pression atmosphérique a été proposé en conditions hydrothermales, mais avec une précipitation qui se produit à des temps encore plus courts (< 30 min) et qui conduit à la formation d'oxyhydroxyde (boehmite AlOOH). La formation de boehmite a la même dépendance envers les propriétés texturales et structurales de l'alumine que la formation d'hydroxydes d'aluminium dans l'eau chaude : la quantité de boehmite est maximisée pour l'alumine γ, oxyde le moins cristallin des alumines de transition. L'attrition n'a pas été observée dans l'autoclave en raison d'une méthode d'agitation plus douce et la dégradation mécanique des grains d'alumines n'a donc pas pu être discutée.

Influence de la présence de molécules organiques dans le milieu réactionnel

L'effet de six molécules organiques sur l'hydratation de l'alumine γ a été étudié (un alcane en C_7 : heptane; 1 alcool en C_4 : 1-butanol; et 4 polyols en C_3 : glycérol, C_5 : xylitol et C_6 : D(-)-sorbitol et D-mannitol). Seuls les polyols conduisent à une diminution significative de la quantité de boehmite formée. L'effet inhibiteur augmente avec la longueur de la chaîne carbonée et le nombre de groupes –OH, jusqu'à une complète inhibition pour les polyols en C_5 et C_6. En s'adsorbant fortement sur la surface de l'alumine, les polyols ou des molécules dérivées jouent un rôle de passivation de la surface de l'oxyde vis-à-vis de l'eau. Un second rôle mis en évidence est d'inhiber la croissance des germes de boehmite en s'adsorbant à leur surface.

Rôle des dopants

L'effet de quatre dopants sur la dégradation de l'alumine γ dans l'eau a été étudié : trois ions métalliques (Mg^{2+}, Zr^{4+} et Ni^{2+}, introduits par imprégnation) et un hétéroatome (Si déposé en phase vapeur ou liquide à partir du TEOS $Si(OEt)_4$).

Comme en l'absence de dopant, la quantité de boehmite formée diminue avec la température de calcination des supports dopés et avec leur surface spécifique. Se superposant à ce premier effet, à surface spécifique équivalente, il existe un deuxième effet inhibiteur général commun aux ions métalliques introduits au sein de l'alumine. Par ailleurs, une diminution encore plus importante de la formation de boehmite est observée lorsque des particules de NiO et une phase spinelle de surface sont présentes en surface de l'alumine. Le silicium, quant à lui, montre un rôle totalement spécifique puisque la formation de boehmite est complètement inhibée quel que soit le mode d'introduction de Si.

Les spectres DRIFT dans la région des OH de surface enregistrés avant et après introduction des dopants suggèrent que l'introduction de dopants métalliques est corrélée à une diminution des sites de surface (hydroxyles) situés sur les faces latérales de l'alumine, et supposés les plus réactifs. Le greffage de silicium montrerait une plus grande sélectivité pour le blocage de ces sites les plus réactifs.

Ce travail met donc en avant le rôle clé de l'étape de dissolution des alumines de transition dans leurs transformations en phases hydratées en milieu aqueux, à pression atmosphérique comme en conditions hydrothermales. Même si son intensité dépend fortement des propriétés texturales de l'alumine, ce processus apparaît inévitable, sauf si la surface de l'alumine est protégée par modification chimique. Par ailleurs, sous contrainte mécanique, l'érosion chimique de l'alumine amplifie les phénomènes d'attrition. Nous proposons que les sites les plus réactifs vis-à-vis de la dissolution sont semblables à ceux figurant sur les faces latérales de l'alumine γ. Nous avons identifié des moyens spécifiques (greffage de Si) ou non spécifiques (dopants métalliques, présence de molécules organiques adsorbées dérivées de polyols à chaîne longue) pour limiter cette dissolution.

Il est maintenant possible d'envisager des perspectives à ces travaux selon les trois axes de ce travail : mécanisme de dégradation, effet/rôle des molécules organiques et effet/rôle des dopants sur l'érosion de l'alumine.

<u>Mécanisme de dégradation</u>

- En partant de boehmites différentes de celle utilisée ici pour la synthèse de l'alumine, il serait possible de déterminer si l'histoire du matériau (méthode de préparation, traitement (autoclavage…), pureté…) peut influencer la dissolution future de l'alumine, et voir si un lien peut-être fait avec la concentration de surface en sites les plus réactifs.
- Une étude de l'érosion de l'alumine en utilisant deux polymorphes de surfaces spécifiques similaires mais de morphologies différentes (plaquettaires ou granulaires) a été initiée. Il serait intéressant de continuer cette étude en conservant identiques les autres paramètres du support (surface spécifique, granulométrie, état d'hydratation de surface…) pour pouvoir isoler l'effet de morphologie sur l'hydratation de l'alumine et relier ceci à la présence de sites réactifs sur les faces latérales.

<u>Molécules organiques :</u>

- Il a été montré qu'en présence de glycérol (C_3) la formation de boehmite est peu inhibée, alors qu'elle l'est totalement avec le sorbitol (C_6). Il serait intéressant d'étudier l'effet d'un

polyol contenant 4 OH (C_4) comme l'érythritol pour définir plus finement le rôle du nombre de groupes -OH et de la longueur de la chaîne carbonée sur l'inhibition de la formation de boehmite.

- Aucun effet de stéréoisomérie n'a été mis en évidence avec les polyols. Ceci peut s'expliquer par un effet nivelant pour les fortes concentrations en polyol utilisées (0,25 M). Il apparait donc nécessaire de reproduire cette étude pour de plus faibles concentrations en ajoutant à la liste un polyol eryhtro-eryhtro.

Dopants :

- En présence du silicium, une inhibition de la formation de boehmite a été observée. Contrairement aux ions métalliques qui étaient ajoutés par imprégnation simple de précurseurs à base de nitrates, cet hétéroatome a été inséré à partir de TEOS, ce qui conduit probablement à un greffage plus sélectif sur les hydroxyles de surface (notamment les plus réactifs). Il serait donc intéressant de reproduire le dopage par les ions métalliques en utilisant des précurseurs alcoxydes (notamment de Zr) pour favoriser un greffage plus sélectif.
- Il serait aussi nécessaire de compléter l'étude du dopage en évaluant l'acido-basicité de surface de l'alumine en présence des différents dopants utilisés afin de déterminer si ce dopage chimique modifie de manière significative les propriétés de surface, et donc catalytiques, du support.
- Enfin, des tests catalytiques en synthèse Fischer-Tropsch ont été initiés par l'IFPEN sur des catalyseurs au cobalt préparés à partir de supports dopés au silicium, au magnésium et au nickel, afin d'étudier l'effet du dopage sur l'activité catalytique.